2021

Nucleic acid sample preparation using magnetic ionic liquids as cell lysis and DNA extraction solvents

Miranda N. Emaus
Iowa State University

Nucleic acid sample preparation using magnetic ionic liquids as cell lysis and DNA extraction solvents

by

Miranda N. Emaus

A dissertation submitted to the graduate faculty

in partial fulfillment of the requirements for the degree of

DOCTOR OF PHILOSOPHY

Major: Analytical Chemistry

Program of Study Committee:
Jared L. Anderson, Major Professor
Robbyn K. Anand
Young Jin-Lee
Marit Nilsen-Hamilton
Jacob W. Petrich

The student author, whose presentation of the scholarship herein was approved by the program of study committee, is solely responsible for the content of this dissertation. The Graduate College will ensure this dissertation is globally accessible and will not permit alterations after a degree is conferred.

Iowa State University

Ames, Iowa

2021

DEDICATION

This dissertation is dedicated to my family who supported me throughout the past five years. It is also written in memory of my father, Paul Emaus. I hope I can make you proud.

TABLE OF CONTENTS

Page

ACKNOWLEDGMENTS

I would like to thank Dr. Jared Anderson for his guidance. In addition, I would like to thank my current and former lab mates at Iowa State University. I would also like to thank my friends and teammates on the Iowa State University Swim Club. Each of you has made my experience at Iowa State University a joy and brought a smile to my face every day. You pushed me to be the best I can be and gave me more opportunities than I could have dreamed of.

Finally, I would like to thank my family for their love and support. I would not have made it without you.

ABSTRACT

Sample preparation is vital in nucleic acid analysis. Cell lysis is generally the first step in DNA sample preparation where the cell membrane is disrupted to release intracellular components such as DNA. Moreover, the isolation and enrichment of nucleic acids is essential to prevent false negative results from enzymatic detection methods that are sensitive to impurities. Conventional nucleic acid sample preparation methods are tedious and time-consuming, limiting sample throughputs and the ability for automation and point-of-care diagnostics. Given the drawbacks of conventional methods and the need to provide rapid results, innovative cell lysis and DNA purification procedures should be investigated to improve sample throughputs while ensuring sample purity.

Magnetic ionic liquids (MILs) are molten salts that exhibit magnetic susceptibility due to a paramagnetic component within the chemical structure of the anion or cation. As a subclass of ionic liquids (ILs), MILs exhibit similar advantageous physicochemical properties to ILs, such as negligible vapor pressure and tunable viscosity. The paramagnetic nature of MILs has attracted substantial interest in sample preparation technologies as the solvent can be rapidly collected using a magnet avoiding traditional centrifugation steps required to collect the analyte-enriched extraction solvent.

Nucleic acid analysis can be broken into three distant steps, including 1) cell lysis, 2) DNA extraction, and 3) detection. DNA sample preparation is essential to remove cellular debris and impurities to permit enzymatic detection (i.e., polymerase chain reaction (PCR) and sequencing). Therefore, hexafluoroacetylactonate-based MILs were investigated as DNA extraction solvents to preconcentrate nucleic acids from complex matrices such as plasma, blood, and artificial sputum. The DNA-enriched MIL was collected on a rod magnet and directly

integrated into quantitative PCR (qPCR) and multiplex-qPCR assays with SYBR green and Taqman probe detection. Adding the DNA-enriched MIL into the reaction buffer drastically reduced the sample preparation time improving sample throughputs without inhibiting PCR efficiency.

A sequence-specific preconcentration step may be required to prevent low abundance nucleic acids from being masked by background DNA. Wild-type DNA sometimes differs by a single nucleotide, making it challenging to preconcentrate only the mutant target. Therefore, ion-tagged oligonucleotides (ITOs) were previously designed to capitalize on Watson-Crick base pairing to selectively anneal to DNA sequences. An ITO probe contains an imidazolium-based tag that allows the probe to be captured by a hydrophobic MIL that poorly extracts nucleic acids. A rapid sequence-specific DNA extraction (i.e., 11 min) to preconcentrate target nucleic acids was developed by dispersing a manganese(II)-based MIL in the sample after the ITO probe annealed to the target DNA. The DNA-enriched MIL was then integrated into the qPCR assay for analysis. The dispersive ITO-MIL sequence-specific extraction method could selectively extract nucleic acids from plasma, artificial sputum, and artificial urine. With the ITO-MIL extraction, 0.1% *BRAF* V600E (99.9% wild-type *BRAF*) could be discriminated from a 100% wild-type BRAF standard. In comparison, without the sequence-specific extraction, the 9% *BRAF* V600E could not be differentiated from the 100% wild-type *BRAF* standard. Commercial streptavidin-coated magnetic beads with biotin-modified oligonucleotides were unable to selectively extract target nucleic acids from plasma. This suggests that a total DNA extraction should be performed prior to a sequence-specific extraction using the commercial beads, which would drastically limit sample throughputs.

Cell lysis is the vital first step in DNA analysis. The cell membrane is either solubilized by a lysis reagent or disrupted by physical stress. However, conventional chemical cell lysis methods often inhibit downstream bioanalytical detection requiring substantial purification. In comparison, mechanical lysis methods need to be strong enough to break the cells. However, if the shear and friction forces are too strong genomic DNA can be damaged. To overcome the limitations of conventional cell lysis methods, MILs were investigated as lysis reagents. A hydrophobic MIL was dispersed in a blood sample and recovered with a magnet. The MIL simultaneously lysed blood cells and extracted DNA during the dispersion step. The 1 min sample preparation method using MILs captured picogram levels of genomic DNA without inhibiting the qPCR reaction. The metal ion incorporated within the MIL (i.e., Ni(II), Co(II), Dy(III), and Gd(III)) appears to cause hemolysis, while the cationic component reduces the cell's integrity by interacting with the cell membrane.

CHAPTER 1.

INTRODUCTION

1.1 Introduction to ionic liquids and magnetic ionic liquids

Ionic liquids (ILs) are molten salts that possess melting temperatures at or below 100°C. Since their discovery in 1914, ILs have been applied in separation, electrochemical, biomass conversion, synthesis, and catalysis technologies.[1,2] Furthermore, ILs have been shown to have several unique physicochemical properties, such as negligible vapor pressures at ambient temperatures, high conductivity, and tunable viscosity. It has been estimated that over 10^{18} unique ILs can be produced[3], and the differences in chemical structure can provide a multitude of interactions with analytes.

Magnetic ionic liquids (MILs) are a subclass of ILs that possess a paramagnetic component within the chemical structure, allowing the solvent to respond to an external magnetic field. Moreover, MILs possess similar physiochemical properties to ILs.[4] In 2004, Hayashi and co-workers reported the first MIL, 1-butyl-3-methylimidazolium tetrachloroferrate(III) ($[BMIM^+][FeCl_4^-]$), and described the solvent's magnetic suseptability[5]. The initially reported $[FeCl_4^-]$-based MILs suffer from high viscosities and hydrolyzed in water, limiting their application in sample preparation.[6,7] Therefore, new MIL structures have been explored to reduce the drawbacks of Fe(III)-based MILs, and some of the common cation and anion structures are illustrated in Table 1-1. The viscosity of MILs can be lowered by utilizing weakly coordinating metal complexes using hexafluoroacetylacetonate and imidazolium ligands, and transition and lanthanide metals (i.e., Ni(II), Co(II), Mn(II), Dy(III), Gd(III), or Nd(III)) have been examined as paramagnetic components.[6,8,9] In particular, incorporating a lanthanide metal into the MIL

structure is highly attractive as rare Earth metals possess higher magnetic moments compared to transition metals.[10]

Table 1-1 Common chemical structures used in MILs.

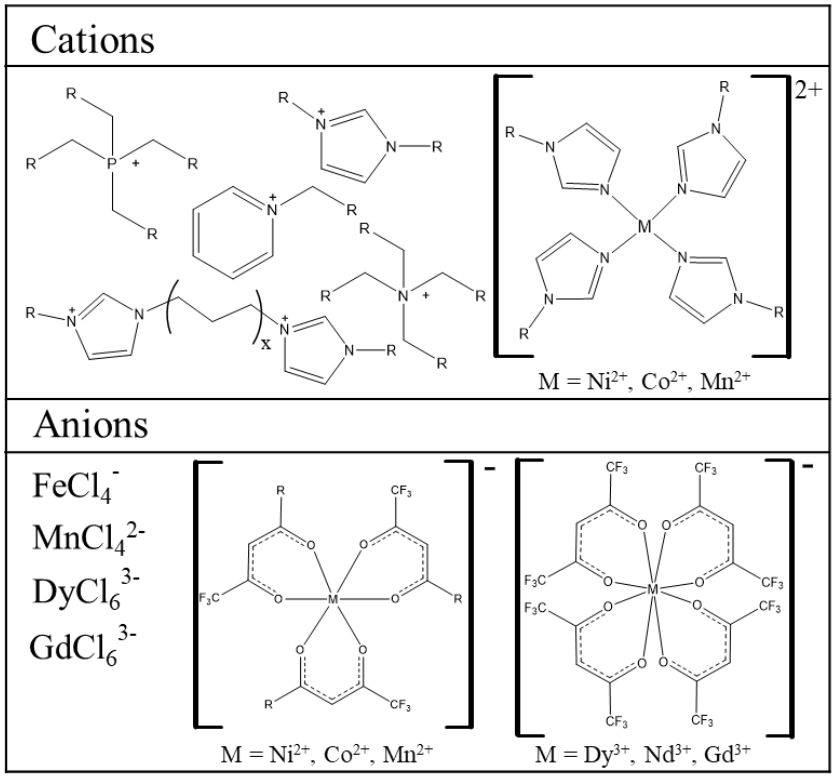

Recently, MILs have been the subject of interest in analytical chemistry as extraction solvents.[11–13] Traditional liquid-liquid extractions (LLE) utilize centrifugation to isolate analyte-enriched extraction media (i.e., 1-octanol, cyclohexane, chloroform, hexylmethylimidazolium hexafluorophosphate ($[C_6MIM^+][PF_6^-]$).[14] Analyte-enriched MIL droplets can be rapidly collected using an external magnet removing the need for tedious centrifugation steps.[4,15] However, MILs need to be insoluble in the sample matrix for droplets to exhibit magnetic susceptibility.[16] Therefore, a hydrophobic MIL is required to perform extractions from aqueous samples containing analytes such as environmental contaminants or biological molecules. Designing the MIL structure to contain long alkyl chains, perfluoroalkyl groups, fluorene-rich

ligands, or aromatic groups within the chemical structure can result in MILs immiscible in water down to 0.01% (w/v).[6,17–19]

1.2 Overview of cell lysis methods

Cell lysis is the process of disrupting cell membranes to access intracellular components such as DNA, RNA, and proteins. A cell lysis procedure is often the vital first step in analyzing intracellular components as a poor lysis efficiency will limit the amount of free analytes available for detection.[20] There are numerous lysis procedures that can be broadly categorized as chemical or mechanical lysis methods. Different approaches to cell lysis offer unique advantages and disadvantages that can affect the quantity, purity, and integrity of analytes.

Mechanical lysis methods include bead beating, grinding, freeze-thaw, surface acoustic wave (SAW) agitation, and sonication.[21] These procedures physically penetrate the cell membrane through shear stress, friction forces, and compressive stress to release cellular components.[22] Additional purification steps may not be required with mechanical lysis methods since they do not require chemical lysis reagents that inhibit downstream bioanalytical analysis. Mechanical lysis approaches need to be of sufficient strength to lyse the cells, as methods like SAW agitation often produce low lysis efficiencies.[23] However, the physical stress placed on the cells can damage nucleic acids. Mechanical lysis methods also may require instrumentation such as a sonicator or SAW device that may limit their use in point-of-care applications.

Surfactants such as sodium dodecyl sulfate (SDS), cetrimonium bromide (CTAB), Triton x-100 are some of the most common approaches to chemical cell lysis.[21] These reagents can solubilize the cell membrane to release intracellular components. Although effective at lysing cells without instrumentation, these surfactants generally inhibit downstream biological detection methods such as sequencing, polymerase chain reaction (PCR), and membrane sensors.[24,25] To

overcome this limitation, additional purification steps maybe be required to remove the lysis reagent.

The ability of ILs to disrupt muscle tissue cells[26], viruses[27], gram-positive[28,29], and gram-negative cells[28,29] have been investigated. In these methods, the cells were incubated with the IL at elevated temperatures to effectively lyse cells. Hydrophilic ILs are effective at lysing various cell types, while hydrophobic ILs struggle to lyse gram-positive cells, due to the cell's thick peptidoglycan layer. However, like most surfactant-based lysis methods, ILs can inhibit downstream bioanalytical detection and require the sample to be diluted or a subsequent purification step to remove the IL.[28]

1.3 Overview of nucleic acid extraction methods

DNA analysis has become the cornerstone of forensic analysis, clinical diagnostics, environmental analysis, and food safety. The speed of DNA analysis has improved over time by developing thermocyclers capable of rapidly cycling between temperatures.[30] Nucleic acid sample preparation is vital since bioassays such as PCR and DNA sequencing are sensitive to inhibitors present in biological and environmental matrices. However, sample preparation has become an overlooked bottleneck in nucleic acid analysis as conventional extraction methods are tedious and time-consuming.

Phenol-chloroform-based extractions are some of the most common nucleic acid purification methods.[31–34] In this biphasic extraction method, proteins and lipids partition to the denser phenol-chloroform phase while DNA remains in the aqueous phase. Nucleic acids can be further purified via ethanol or isopropanol precipitation. Although effective phenol-chloroform-based extractions often require several time consuming separation and washing steps to sufficiently purify nucleic acids for bioanalytical analysis. Furthermore, large volumes of toxic

organic solvents are required for phenol-chloroform-based extractions that have raised health and environmental concerns.

Silica-based solid-phase extractions (SPE) have been developed to limit the use of toxic organic solvents used in nucleic acid extractions. In these procedures, the nucleic acid is dehydrated using a chaotropic salt and reversibly bound to the silica sorbent through hydrogen bond interactions. The sorbent is then washed with ethanol or isopropanol to remove impurities, and nucleic acids are eluted with a low ionic strength solvent. SPE methods often utilize proteinase K or RNase prior to degrade protein and RNA interferences, respectively. Although SPE methods are widely utilized in forensic[35], environmental[36], archaeological[37], and clinical applications[38], SPE nucleic acid extractions require centrifugation or vacuum-assisted flow that limit automation and point-of-care applications.

To reduce the limitations of conventional nucleic extraction methods, Wang and co-workers first investigated using ILs as DNA extraction solvents.[39] Using an oscillator to disperse the 1-butyl-3-methylimidazolium hexafluorophosphate ([BMIM+][PF6-]) IL, a 99% extraction efficiency was achieved, and 30% of the DNA was recovered from the IL phase. FTIR and ^{31}P NMR analysis demonstrated that electrostatic interactions between the IL's cation and the phosphate backbone of the DNA strand primarily facilitated the extraction. Subsequent studies have also shown that dispersion forces, hydrogen bonding, and π-π interactions aid in the extraction of DNA by ILs.[40] Fe(III)-based MILs were first applied as DNA extraction solvents in Clark et al.[41] Extraction efficiencies over 90% were achieved, and DNA of sufficient quality and quantity was recovered from the MIL for PCR detection. In a subsequent study, DNA-enriched MILs were added directly into a PCR buffer designed to alleviate inhibition caused by the

Fe(III)-based MILs.[7] DNA was desorbed from the MIL during the reaction, which reduced the amount of time required for sample preparation.

Silica-based SPE and phenol-chloroform LLE methods are utilized for total nucleic acid extractions. However, the sorbent or solvent provides limited selectivity towards specific nucleic acids. In applications involving low abundance mutations, a sequence-specific preconcentration step may be required to prevent the desired sequence from being masked by the more abundant wild-type DNA. Nucleic acids possess the ability to recognize complementary sequences through Watson-Crick base-pair interactions. These interactions are capitalized in sequence-specific extractions by hybridizing target nucleic acid to a complementary oligonucleotide probe modified with a functional group (i.e., biotin).[42] This functional group allows the probe to be captured by or bound to a support. Commercial methods for sequence-specific extractions utilize streptavidin-coated magnetic beads and biotin-modified oligonucleotides. The extraction of nucleic acids with streptavidin-coated beads is facilitated by the strong interaction between the probe and support phase as the streptavidin beads poorly extract DNA without the probe. The bond between streptavidin and biotin is one of the strongest non-covalent interactions known in nature ($K_d = 4 \times 10^{14}$ M) and is resistant to organic solvents, detergents, and elevated temperatures.[43] Although streptavidin-coated magnetic beads and biotinylated probes are effective at selectively extracting nucleic acids, the beads are prone to aggregation and sedimentation, which can clog microfluidic devices and reduce extraction efficiencies due to a lack of surface area.[44,45] Most commercial kits utilizing streptavidin-coated magnetic beads also recommend performing the sequence-specific extraction after a total nucleic acid extraction as biological fluids, which drastically decreases sample throughputs.

1.4 Overview of nucleic acid amplification methods

PCR is an enzymatic nucleic acid amplification method capable of rapidly generating millions of copies of DNA from as little as a single DNA strand. Since its discovery in 1986, PCR has become the cornerstone of forensics, clinical, and environmental applications.[46–48] PCR consists of three distinct steps that are illustrated in Figure 1-1. Initially, DNA is denatured at 90-98°C. Oligonucleotide primers hybridize to complementary regions on the single-stranded DNA (ssDNA) at temperatures ranging from 55-65°C. A thermally stable DNA polymerase subsequently extends the sequence to generate a new DNA strand. This process is generally repeated for 40 cycles to exponentially generate large quantities of the target DNA region.

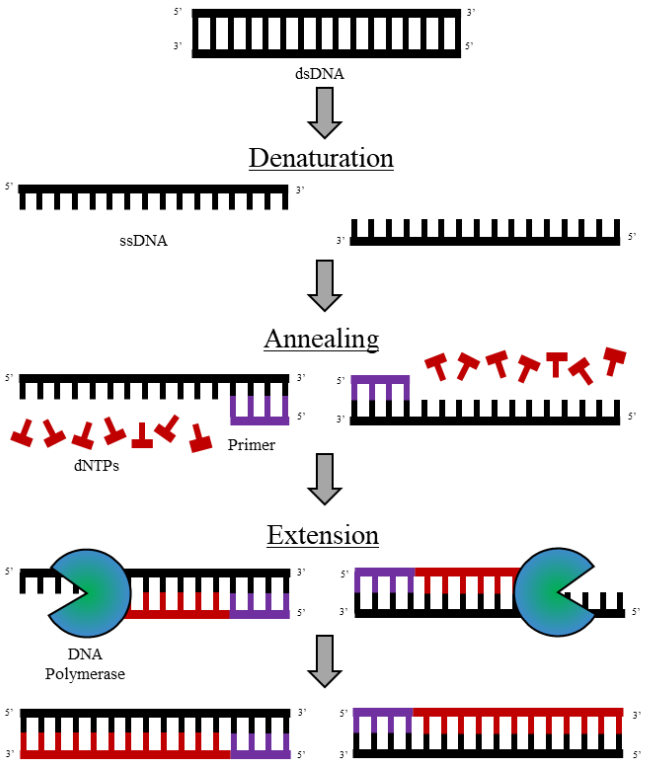

Figure 1-1 Schematic illustrating PCR amplification.

PCR products can be detected after amplification by separating amplicons using agarose gel electrophoresis. However, agarose gels with fluorescence detection are only semi-quantitative and require a substantial amount of time to acquire high-quality gels. To reduce the amount of time needed for DNA analysis, quantitative PCR (qPCR) was developed to track the accumulation of DNA amplicons in real-time using intercalating DNA binding dyes such as SYBR green or sequence-specific probes labeled with a fluorescent reporter dye and a quencher.[49,50] Non-specific DNA binding dyes strongly fluoresce when bound to double-stranded DNA (dsDNA) and poorly fluoresce with RNA or ssDNA.[51] Taqman or hydrolysis probes are comprised of a sequence-specific DNA oligonucleotide containing a fluorophore (i.e., fluorescein (FAM), hexachlorofluorescein (HEX), or cyanine 5 (CY5)) and a quencher. During the PCR annealing step, the Taqman probe anneals to the target at the same time as the primers. As the DNA polymerase extends the sequence, the 5'→3' exonuclease activity of the polymerase degrades the probe separating the fluorophore from the quencher allowing fluorescence detection. qPCR can permit quantitative analysis as samples corresponding to a low threshold cycle (Cq) indicate a higher initial quantity of DNA than samples with a high Cq. The Cq is the cycle number where the fluorescence signal from the PCR product is above the background

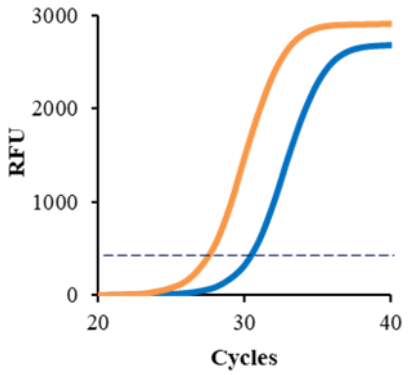

Figure 1-2 qPCR amplification curves generated from two samples that initially contained more (orange) and relatively less (blue) DNA.

signal. A calibration curve can be constructed by plotting the collected Cq against the logarithm of the initial amount of DNA in the reaction. The amount of DNA within a PCR cycle, in theory, should double with each cycle, and PCR efficiency can be calculated from the slope of the standard curve. The equation for PCR efficiency is shown in Equation 1. In general, the

$$\text{Amplification Efficiency} = \left(10^{\left(\frac{-1}{slope}\right)} - 1\right) \times 100\% \quad (1)$$

amplification efficiency should fall between 90-110%, and deviations from this range generally indicate that the primers were poorly designed, impurities, or pipetting errors.[52,53]

1.5 Organization of the dissertation

Chapter 2 describes the integration of four DNA-enriched MILs into custom-designed qPCR buffers to relieve inhibition caused by the MIL. The four hydrophobic MILs were either suspended from a rod magnet or dispersed in a sample to extract *KRAS* DNA. DNA was preconcentrated in the MIL and desorbed during the qPCR reaction. The addition of a Ni(II)-based MIL to the reaction buffer did not affect the amplification efficiency. In contrast, adding commercial magnetic beads to the qPCR assay slightly inhibited the reaction.

Chapter 3 describes the integration of three Ni(II)-based MILs into a multiplex-qPCR assay to simultaneously amplify three circulating tumor DNA fragments. Allelic discrimination between single nucleotide polymorphisms (SNPs) was obtained with a hydrophobic MIL integrated into the multiplex-qPCR assay, and the amplification efficiency of all three sequences fell between 90-110%, suggesting that all three sequences are simultaneously amplifying without inhibition. The MILs were then employed as DNA extraction solvents to successfully preconcentrate the three fragments from a plasma matrix.

Chapter 4 describes the development of a dispersive sequence-specific DNA extraction using hybridization probes called ion-tagged oligonucleotides (ITOs) and one of three Mn(II)-based

MILs. The dispersive method allowed for lower detection limits compared to the previously reported static ITO-MIL extraction method. Dispersing the MIL in the sample also shortened the extraction time required to 11 min while previously reported studies required 30 min. The MILs were designed to limit the co-extraction of proteins by integrating aromatic groups into the chemical structure of the MIL. The ITO-MIL extraction method was capable of selectively preconcentrating the *KRAS* DNA 4-fold from a diluted plasma matrix, while commercial streptavidin-coated magnetic beads and biotinylated probes fail to selectively extract DNA from a diluted plasma matrix.

Chapter 5 details the investigation into the sequence-specific extraction of the low abundant *BRAF* V600E from plasma, artificial urine, and artificial sputum matrices containing large amounts of wild-type *BRAF*. The introduction of the dispersive ITO-MIL extraction prior to qPCR detection allowed for samples consisting of 0.1% *BRAF* V600E (50 $fg \cdot \mu L^{-1}$ V600E *BRAF*, 50,000 $fg \cdot \mu L^{-1}$ wild-type *BRAF* to be distinguished from the 100% wild-type *BRAF* standard. In contrast, the 9% *BRAF* V600E standard (50 $fg \cdot \mu L^{-1}$ *BRAF* V600E, 500 $fg \cdot \mu L^{-1}$ wild-type *BRAF*) could not be distinguished from the 100% WT *BRAF* standard using qPCR alone.

Chapter 6 describes the development of a one-step cell lysis and DNA extraction method using nine hydrophobic MILs. The effect of the cation, ligand, and metal center on the lysis of blood cells investigated where the Ni(II)-based MILs with aromatic components in either the cation or anion structure captured the most human genomic DNA from a blood matrix. Picogram amounts of genomic DNA were recovered from the 1 min lysis and extraction step from 2-fold diluted blood, whole blood, and reconstituted dry bloodstains. Limited amounts of PCR inhibitors and DNases were coextracted by the MIL as evidenced by PCR efficiencies ranging from 90-110% and DNA being stable within the MIL for at least 24 h.

1.6 References

(1) Lei, Z.; Chen, B.; Koo, Y. M.; Macfarlane, D. R. Introduction: Ionic Liquids. *Chem. Rev.* **2017**, *117* (10), 6633–6635.

(2) Egorova, K. S.; Gordeev, E. G.; Ananikov, V. P. Biological Activity of Ionic Liquids and Their Application in Pharmaceutics and Medicine. *Chem. Rev.* **2017**, *117* (10), 7132–7189.

(3) Carmichael, A. J.; Seddon, K. R. Polarity Study of Some 1-Alkyl-3-Methylimidazolium Ambient-Temperature Ionic Liquids with the Solvatochromic Dye, Nile Red. *J. Phys. Org. Chem.* **2000**, *13* (10), 591–595.

(4) Clark, K. D.; Nacham, O.; Purslow, J. A.; Pierson, S. A.; Anderson, J. L. Magnetic Ionic Liquids in Analytical Chemistry: A Review. *Anal. Chim. Acta* **2016**, *934*, 9–21.

(5) Hayashi, S.; Hamaguchi, H. Discovery of a Magnetic Ionic Liquid [Bmim]FeCl4. *Chem. Lett.* **2004**, *33* (12), 1590–1591.

(6) Pierson, S. A.; Nacham, O.; Clark, K. D.; Nan, H.; Mudryk, Y.; Anderson, J. L. Synthesis and Characterization of Low Viscosity Hexafluoroacetylacetonate-Based Hydrophobic Magnetic Ionic Liquids. *New J. Chem.* **2017**, *41* (13), 5498–5505.

(7) Clark, K. D.; Yamsek, M. M.; Nacham, O.; Anderson, J. L. Magnetic Ionic Liquids as PCR-Compatible Solvents for DNA Extraction from Biological Samples. *Chem. Commun.* **2015**, *51* (94), 16771–16773.

(8) Wu, K.; Shen, X. Designing a New Type of Magnetic Ionic Liquid: A Strategy to Improve the Magnetic Susceptibility. *New J. Chem.* **2019**, *43* (40), 15857–15860.

(9) Chand, D.; Farooq, M. Q.; Pathak, A. K.; Li, J.; Smith, E. A.; Anderson, J. L. Magnetic Ionic Liquids Based on Transition Metal Complexes with N-Alkylimidazole Ligands. *New J. Chem.* **2019**, *43* (1), 20–23.

(10) Benelli, C.; Gatteschi, D. Magnetism of Lanthanides in Molecular Materials with Transition-Metal Ions and Organic Radicals. *Chem. Rev.* **2002**, *102* (6), 2369–2387.

(11) Trujillo-Rodríguez, M. J.; Nacham, O.; Clark, K. D.; Pino, V.; Anderson, J. L.; Ayala, J. H.; Afonso, A. M. Magnetic Ionic Liquids as Non-Conventional Extraction Solvents for the Determination of Polycyclic Aromatic Hydrocarbons. *Anal. Chim. Acta* **2016**, *934*, 106–113.

(12) Benedé, J. L.; Anderson, J. L.; Chisvert, A. Trace Determination of Volatile Polycyclic Aromatic Hydrocarbons in Natural Waters by Magnetic Ionic Liquid-Based Stir Bar Dispersive Liquid Microextraction. *Talanta* **2018**, *176* (June 2017), 253–261.

(13) Trujillo-Rodríguez, M. J.; Pino, V.; Anderson, J. L. Magnetic Ionic Liquids as Extraction Solvents in Vacuum Headspace Single-Drop Microextraction. *Talanta* **2017**, *172* (April), 86–94.

(14) Zgoła-Grześkowiak, A.; Grześkowiak, T. Dispersive Liquid-Liquid Microextraction. *TrAC - Trends Anal. Chem.* **2011**, *30* (9), 1382–1399.

(15) Trujillo-Rodriguez, M. J.; Nan, H.; Varona, M.; Emaus, M. N.; Souza, I. D.; Anderson, J. L. Advances of Ionic Liquids in Analytical Chemistry. *Anal. Chem.* **2019**, *91* (1), 505–531.

(16) Del Sesto, R. E.; McCleskey, T. M.; Burrell, A. K.; Baker, G. a; Thompson, J. D.; Scott, B. L.; Wilkes, J. S.; Williams, P. Structure and Magnetic Behavior of Transition Metal Based Ionic Liquids. *Chem. Commun.* **2008**, 447–449.

(17) Nacham, O.; Clark, K. D.; Yu, H.; Anderson, J. L. Synthetic Strategies for Tailoring the Physicochemical and Magnetic Properties of Hydrophobic Magnetic Ionic Liquids. *Chem. Mater.* **2015**, *27* (3), 923–931.

(18) Nacham, O.; Clark, K. D.; Anderson, J. L. Synthesis and Characterization of the Physicochemical and Magnetic Properties for Perfluoroalkyl Ester and Fe(Iii) Carboxylate-Based Hydrophobic Magnetic Ionic Liquids. *RSC Adv.* **2016**, *6* (14), 11109–11117.

(19) Farooq, M. Q.; Chand, D.; Odugbesi, G. A.; Varona, M.; Mudryk, Y.; Anderson, J. L. Investigating the Effect of Ligand and Cation on the Properties of Metal Fluorinated Acetylacetonate Based Magnetic Ionic Liquids. *New J. Chem.* **2019**, *43*, 11334–11341.

(20) So, H.; Lee, K.; Seo, Y. H.; Murthy, N.; Pisano, A. P. Hierarchical Silicon Nanospikes Membrane for Rapid and High-Throughput Mechanical Cell Lysis. *ACS Appl. Mater. Interfaces* **2014**, *6* (10), 6993–6997.

(21) Emaus, M. N.; Varona, M.; Eitzmann, D. R.; Hsieh, S. A.; Zeger, V. R.; Anderson, J. L. Nucleic Acid Extraction: Fundamentals of Sample Preparation Methodologies, Current Advancements, and Future Endeavors. *TrAC - Trends Anal. Chem.* **2020**, *130*, 115985.

(22) Nan, L.; Jiang, Z.; Wei, X. Emerging Microfluidic Devices for Cell Lysis: A Review. *Lab Chip* **2014**, *14* (6), 1060–1073.

(23) Taller, D.; Richards, K.; Slouka, Z.; Senapati, S.; Hill, R.; Go, D. B.; Chang, H. C. On-Chip Surface Acoustic Wave Lysis and Ion-Exchange Nanomembrane Detection of Exosomal RNA for Pancreatic Cancer Study and Diagnosis. *Lab Chip* **2015**, *15* (7), 1656–1666.

(24) Schrader, C.; Schielke, A.; Ellerbroek, L.; Johne, R. PCR Inhibitors - Occurrence, Properties and Removal. *J. Appl. Microbiol.* **2012**, *113*, 1014–1026.

(25) Berasaluce, A.; Matthys, L.; Mujika, J.; Antoñana-Díez, M.; Valero, A.; Agirregabiria, M. Bead Beating-Based Continuous Flow Cell Lysis in a Microfluidic Device. *RSC Adv.* **2015**, *5* (29), 22350–22355.

(26) Ressmann, A. K.; García, E. G.; Khlan, D.; Gaertner, P.; Mach, R. L.; Krska, R.; Brunner, K.; Bica, K. Fast and Efficient Extraction of DNA from Meat and Meat Derived Products Using Aqueous Ionic Liquid Buffer Systems. *New J. Chem.* **2015**, *39* (6), 4994–5002.

(27) Fister, S.; Fuchs, S.; Mester, P.; Kilpeläinen, I.; Wagner, M.; Rossmanith, P. The Use of Ionic Liquids for Cracking Viruses for Isolation of Nucleic Acids. *Sep. Purif. Technol.* **2015**, *155* (April 2004), 38–44.

(28) Martzy, R.; Bica-Schröder, K.; Pálvölgyi, Á. M.; Kolm, C.; Jakwerth, S.; Kirschner, A. K. T.; Sommer, R.; Krska, R.; Mach, R. L.; Farnleitner, A. H.; et al. Simple Lysis of Bacterial Cells for DNA-Based Diagnostics Using Hydrophilic Ionic Liquids. *Sci. Rep.* **2019**, *9* (1), 1–10.

(29) Fuchs-Telka, S.; Fister, S.; Mester, P. J.; Wagner, M.; Rossmanith, P. Hydrophobic Ionic Liquids for Quantitative Bacterial Cell Lysis with Subsequent DNA Quantification. *Anal. Bioanal. Chem.* **2017**, *409* (6), 1503–1511.

(30) Neuzil, P.; Zhang, C.; Pipper, J.; Oh, S.; Zhuo, L. Ultra Fast Miniaturized Real-Time PCR: 40 Cycles in Less than Six Minutes. *Nucleic Acids Res.* **2006**, *34* (11).

(31) Kramvis, A.; Bukofzer, S.; Kew, M. C. Comparison of Hepatitis B Virus DNA Extractions from Serum by the QIAamp Blood Kit, GeneReleaser, and the Phenol-Chloroform Method. *J. Clin. Microbiol.* **1996**, *34* (11), 2731–2733.

(32) Ahmed, I.; Islam, M.; Arshad, W.; Mannan, A.; Ahmad, W.; Mirza, B. High-Quality Plant DNA Extraction for PCR: An Easy Approach. *J. Appl. Genet.* **2009**, *50* (2), 105–107.

(33) Chomczynski, P.; Sacchi, N. Single-Step Method of RNA Isolation by Acid Guanidinium Thiocyanate-Phenol-Chloroform Extraction. *Anal. Biochem.* **1987**, *162* (1), 156–159.

(34) Renshaw, M. A.; Olds, B. P.; Jerde, C. L.; Mcveigh, M. M.; Lodge, D. M. The Room Temperature Preservation of Filtered Environmental DNA Samples and Assimilation into a Phenol-Chloroform-Isoamyl Alcohol DNA Extraction. *Mol. Ecol. Resour.* **2015**, *15* (1), 168–176.

(35) Nagy, M.; Otremba, P.; Krüger, C.; Bergner-Greiner, S.; Anders, P.; Henske, B.; Prinz, M.; Roewer, L. Optimization and Validation of a Fully Automated Silica-Coated Magnetic Beads Purification Technology in Forensics. *Forensic Sci. Int.* **2005**, *152* (1), 13–22.

(36) Alexander, P. J.; Rajanikanth, G.; Bacon, C. D.; Bailey, C. D. Recovery of Plant DNA Using a Reciprocating Saw and Silica-Based Columns. *Mol. Ecol. Notes* **2007**, *7* (1), 5–9.

(37) Rohland, N.; Hofreiter, M. Ancient Dna Extraction from Bones and Teeth. *Nat. Protoc.* **2007**, *2* (7), 1756–1762.

(38) Yates, S.; Penning, M.; Goudsmit, J.; Frantzen, I.; Van de Weijer, B.; Van Strijp, D.; Van Gemen, B. Quantitative Detection of Hepatitis B Virus DNA by Real-Time Nucleic Acid Sequence-Based Amplification with Molecular Beacon Detection. *J. Clin. Microbiol.* **2001**, *39* (10), 3656–3665.

(39) Wang, J. H.; Cheng, D. H.; Chen, X. W.; Du, Z.; Fang, Z. L. Direct Extraction of Double-Stranded DNA into Ionic Liquid 1-Butyl-3-Methylimidazolium Hexafluorophosphate and Its Quantification. *Anal. Chem.* **2007**, *79* (2), 620–625.

(40) Li, T.; Joshi, M. D.; Ronning, D. R.; Anderson, J. L. Ionic Liquids as Solvents for in Situ Dispersive Liquid-Liquid Microextraction of DNA. *J. Chromatogr. A* **2013**, *1272*, 8–14.

(41) Clark, K. D.; Nacham, O.; Yu, H.; Li, T.; Yamsek, M. M.; Ronning, D. R.; Anderson, J. L. Extraction of DNA by Magnetic Ionic Liquids: Tunable Solvents for Rapid and Selective DNA Analysis. *Anal. Chem.* **2015**, *87* (3), 1552–1559.

(42) Dundas, C. M.; Demonte, D.; Park, S. Streptavidin-Biotin Technology: Improvements and Innovations in Chemical and Biological Applications. *Appl. Microbiol. Biotechnol.* **2013**, *97* (21), 9343–9353.

(43) Green, N. M. Avidin and Streptavidin. *Methods Enzymol.* **1990**, *184*, 51–67.

(44) Fan, Z. H.; Mangru, S.; Granzow, R.; Heaney, P.; Ho, W.; Dong, Q.; Kumar, R. Dynamic DNA Hybridization on a Chip Using Paramagnetic Beads. *Anal. Chem.* **1999**, *71* (21), 4851–4859.

(45) Leslie, D. C.; Li, J.; Strachan, B. C.; Begley, M. R.; Finkler, D.; Bazydlo, L. A. L.; Barker, N. S.; Haverstick, D. M.; Utz, M.; Landers, J. P. New Detection Modality for Label-Free Quantification of DNA in Biological Samples via Superparamagnetic Bead Aggregation. *J. Am. Chem. Soc.* **2012**, *134*, 5689–5696.

(46) Jobling, M. A.; Gill, P. Encoded Evidence: DNA in Forensic Analysis. *Nat. Rev. Genet.* **2004**, *5*, 739.

(47) Schwarzenbach, H.; Hoon, D. S. B.; Pantel, K. Cell-Free Nucleic Acids as Biomarkers in Cancer Patients. *Nat. Rev. Cancer* **2011**, *11*, 426.

(48) Bremen, S. U.; Miller, D. N.; Bryant, J. E.; Madsen, E. L.; Ghiorse, W. C. Evaluation and Optimization of DNA Extraction and Purification Procedures for Soil and Sediment Samples Evaluation and Optimization of DNA Extraction and Purification Procedures for Soil and Sediment Samples. *Appl. Environ. Microbiol.* **1999**, *65* (11), 4715–4724.

(49) Higuchi, R.; Dollinger, G.; Walsh, P. S.; Griffith, R. Specific Dna Sequences. *Nat. Biotechnol.* **1992**, *10* (April), 413–417.

(50) Kubista, M.; Andrade, J. M.; Bengtsson, M.; Forootan, A.; Jonák, J.; Lind, K.; Sindelka, R.; Sjöback, R.; Sjögreen, B.; Strömbom, L.; et al. The Real-Time Polymerase Chain Reaction. *Mol. Aspects Med.* **2006**, *27* (2–3), 95–125.

(51) Dragan, A. I.; Pavlovic, R.; McGivney, J. B.; Casas-Finet, J. R.; Bishop, E. S.; Strouse, R. J.; Schenerman, M. A.; Geddes, C. D. SYBR Green I: Fluorescence Properties and Interaction with DNA. *J. Fluoresc.* **2012**, *22* (4), 1189–1199.

(52) Bustin, S. A.; Benes, V.; Garson, J. A.; Hellemans, J.; Huggett, J.; Kubista, M.; Mueller, R.; Nolan, T.; Pfaffl, M. W.; Shipley, G. L. The MIQE Guidelines : Minimum Information for Publication of Quantitative Real-Time PCR Experiments. *Clin. Chem.* **2009**, *622*, 611–622.

(53) Broeders, S.; Huber, I.; Grohmann, L.; Berben, G.; Taverniers, I.; Mazzara, M.; Roosens, N.; Morisset, D. Guidelines for Validation of Qualitative Real-Time PCR Methods. *Trends Food Sci. Technol.* **2014**, *37* (2), 115–126.

CHAPTER 2.

PRECONCENTRATION OF DNA USING MAGNETIC IONIC LIQUIDS THAT ARE COMPATIBLE WITH REAL-TIME PCR FOR RAPID NUCLEIC ACID QUANTIFICATION

Modified from a manuscript published in *Analytical and Bioanalytical Chemistry*

Miranda N. Emaus, Kevin D. Clark, Paige Hinners, and Jared L. Anderson

Department of Chemistry, Iowa State University, Ames, Iowa 50011, United States

Abstract

Nucleic acid extraction and purification represents a major bottleneck in DNA analysis. Traditional methods for DNA purification often require reagents that may inhibit quantitative polymerase chain reaction (qPCR) if not sufficiently removed from the sample. Approaches that employ magnetic beads may exhibit lower extraction efficiencies due to sedimentation and aggregation. In this study, four hydrophobic magnetic ionic liquids (MILs) were investigated as DNA extraction solvents with the goal of improving DNA enrichment factors and compatibility with downstream bioanalytical techniques. By designing custom qPCR buffers, DNA-enriched MILs including trihexyl(tetradecyl)phosphonium tris(hexafluoroacetylaceto)nickelate(II) ($[P_{6,6,6,14}^+][Ni(hfacac)_3^-]$), $[P_{6,6,6,14}^+]$ tris(hexafluoroacetylaceto)colbaltate(II) ($[Co(hfacac)_3^-]$), $[P_{6,6,6,14}^+]$ tris(hexafluoroacetylaceto)manganate(II) ($[Mn(hfacac)_3^-]$), or $[P_{6,6,6,14}^+]$ tetrakis(hexafluoroacetylaceto)dysprosate(III) ($[Dy(hfacac)_4^-]$) could be directly incorporated into reaction system thereby circumventing the need for time consuming DNA recovery steps. Incorporating MILs into the reaction buffer did not significantly impact the amplification efficiency of the reaction (91.1%). High enrichment factors were achieved using the $[P_{6,6,6,14}^+][Ni(hfacac)_3^-]$ MIL for the extraction of single-stranded and double-stranded DNA with extraction times as short as 2 min. When compared to a commercial magnetic bead-based

platform, the [$P_{6,6,6,14}^{+}$][$Ni(hfacac)_3^{-}$] MIL was capable of producing higher enrichment factors for single-stranded DNA and similar enrichment factors for double-stranded DNA. The MIL-based method was applied for the extraction and direct qPCR amplification of mutation prone-*KRAS* oncogene fragment in plasma samples.

2.1 Introduction

DNA amplification by polymerase chain reaction (PCR) has become the cornerstone of nucleic acid analysis for forensic[1], clinical[2], and environmental applications[3]. Although PCR is capable of selectively amplifying and detecting small quantities of nucleic acid, the technique has a low tolerance toward impurities. Therefore, target DNA needs to be purified from complex matrices such as blood, plasma, and urine.[4] Traditional phenol-chloroform based liquid-liquid extraction (LLE) may provide high quality nucleic acid, but is difficult to automate and requires organic solvents that are potentially harmful to users and the environment.[5] As an alternative, solid phase extraction (SPE) methods are capable of purifying DNA without the need of toxic organic solvents. However, SPE generally relies on multiple time consuming centrifugation steps and requires a centrifuge or vacuum apparatus that renders the method difficult to automate. Silica-based magnetic beads are commercially available magnetoactive extraction sorbents that can be dispersed in a sample to bind dehydrated DNA through a combination of electrostatic and hydrogen bonding interactions. Subsequent application of a magnetic field permits rapid collection of DNA-enriched beads thereby removing several centrifugation steps from a DNA extraction procedure.[6] However, magnetic bead-based DNA extraction methods are expensive and require high concentrations of guanidine HCl and organic solvents that can inhibit PCR if these reagents are insufficiently removed. These approaches are also limited by sedimentation of the magnetic substrate, which decreases the amount of DNA that can be extracted and may clog

microfluidic devices.[7] As a result, alternative DNA extraction methods need to be thoroughly explored to avoid use of toxic organic solvents necessary for LLE, circumvent the use of multiple centrifugation steps required in commercial SPE kits, and overcome sedimentation caused by magnetic beads.

An ideal extraction method should be capable of rapidly purifying and preconcentrating DNA from complex samples into a medium that is compatible with downstream analysis. Large forensic and clinical case backlogs have produced a demand for rapid and fully automated DNA extraction methods that facilitate high throughput analysis.[8] Magnetic ionic liquids (MILs) are a subclass of ionic liquids (ILs) containing a paramagnetic component in either the cation or anion that can be manipulated by the application of an external magnetic field. Similar to conventional ILs, MILs can be designed to exhibit high thermal stability, low vapor pressure, and tunable physiochemical properties.[9-11] Recently, MILs have been applied as extraction solvents for the isolation of DNA[12,13], viable bacterial cells[14], hormones[15], and pharmaceuticals.[16,17] Using carefully designed PCR buffers, MIL-based DNA extraction was successfully coupled to endpoint PCR allowing for direct amplification of target DNA from the MIL extraction solvent.[18] The transfer of DNA-enriched MIL into the PCR mixture immediately after the extraction step circumvented the need for tedious DNA recovery and purification procedures, decreasing overall analysis times.[18] However, endpoint PCR requires a time consuming post-amplification electrophoretic separation step prior to amplicon detection and is only capable of providing semi-quantitative information.

Quantitative PCR (qPCR) overcomes the aforementioned disadvantages of endpoint PCR by allowing nucleic acid amplification to be monitored in real-time. During SYBR Green I – based qPCR assays, the fluorescent dye binds to dsDNA as it accumulates due to enzymatic

amplification resulting in an increase in fluorescence as the amount of amplicon DNA increases. The concentration of template DNA initially present in the reaction can be related to the threshold cycle (Cq), which is defined as the cycle in which the fluorescent signal surpasses a defined fluorescence threshold. A lower Cq value indicates that the reaction initially contained more template DNA compared to a reaction generating a higher Cq value. The Cq value is linearly related to the log of the initial concentration of template DNA undergoing amplification, and by generating a standard curve the efficiency of the reaction can be determined. Coupling MIL-based DNA extraction to direct qPCR amplification has the potential to provide a streamlined method for DNA extraction, amplification, and quantification.

Herein, we report a MIL-based extraction method for short DNA sequences that can be directly coupled with qPCR analysis. A series of low viscosity, hydrophobic MILs consisting of trihexyl(tetradecyl)phosphonium tris(hexafluoroacetylaceto)nickelate(II) ($[P_{6,6,6,14}^+][Ni(hfacac)_3^-]$), $[P_{6,6,6,14}^+]$ tris(hexafluoroacetylaceto)colbaltate(II) ($[Co(hfacac)_3^-]$), $[P_{6,6,6,14}^+]$ tris(hexafluoroacetylaceto)manganate(II) ($[Mn(hfacac)_3^-]$), and $[P_{6,6,6,14}^+]$ tetrakis(hexafluoroacetylaceto)dysprosate(III) ($[Dy(hfacac)_4^-]$) were studied to examine their DNA extraction capabilities and compatibility with qPCR amplification. After MIL-based DNA extraction, the MIL is rapidly collected using a magnet thereby avoiding the multiple centrifugation steps required in traditional extraction procedures. The $[P_{6,6,6,14}^+][Ni(hfacac)_3^-]$ MIL was capable of preconcentrating a fragment of the *KRAS* gene, which is a mutation prone gene linked to pancreatic, colorectal, and lung cancer.[2] The MIL-based method extracted sufficient *KRAS* template from an aqueous solution in as short as 2 min without chaotropic salts or toxic organic solvents that are typically required for silica-based SPE methods or traditional LLE. By using custom designed qPCR buffers, DNA could be directly amplified from all four

MILs examined. Incorporating other DNA sorbent materials such as magnetic beads or chitosan microparticles can also result in successful DNA amplification, but the efficiency of the amplification reaction often suffer and limit the use of these materials[19]. However, the addition of the $[P_{6,6,6,14}^{+}][Ni(hfacac)_3^{-}]$ MIL to the qPCR buffer was successful without sacrificing the amplification efficiency. The MIL-based extraction method was also applied towards the extraction of *KRAS* gene from a plasma sample followed by direct qPCR analysis demonstrating the potential MIL-based extractions have towards the extraction of DNA from clinical samples.

2.2 Materials and Methods

2.2.1 Reagents and Materials

Manganese(II) chloride tetrahydrate was purchased from Alfa Aesar (Ward Hill, MA, USA). Nickel(II) chloride (98%), ammonium hydroxide (28-30% solution in water), and 1,1,1,5,5,5-hexafluoroacetylacetone (99%) were purchased from Acros Organics (Morris Plains, NJ, USA). Anhydrous diethyl ether (99.0%) was purchased from Avantor Performance Materials Inc. (Center Valley, PA, USA). Trihexyl(tetradecyl)phosphonium chloride (97.7%) was purchased from Strem Chemicals (Newburyport, MA, USA). Ethylenediaminetetraacetic acid (EDTA), bovine serum albumin (BSA), plasma from human, deoxyribonucleic acid sodium salt form salmon testes, cobalt(II) chloride hexahydrate (98.0%), dysprosium(III) chloride hexahydrate (99.9%), Pluronic F-108 (average molecular weight = 14600 g/mol), guanidine hydrochloride (99%), and magnesium chloride hexahydrate were purchased from Sigma-Aldrich (St. Louis, MO, USA). SYBR Green I (10,000x) was purchased from Life Technologies (Carlsbad, CA, USA). SsoAdvanced Universal SYBR Green Supermix and a *KRAS*, human PrimePCR™ SYBR green assay (120 base pair amplicon length) (additional information can be found on Bio-Rad's website) were purchased from Bio-Rad Laboratories (Hercules, CA, USA). PCR caps, tube

strips, and Dynabeads Myone Silane magnetic beads were purchased from Thermo Fisher Scientific (Waltham, MA, USA). Tris-HCl was purchased from RPI (Mount Prospect, IL, USA). Neodymium rod and cylinder magnets (0.20 T, 0.66 T, and 0.9 T) were purchased from K&J Magnetics (Pipersville, PA, USA). A nickel Atomax hollow cathode (1.5 in) lamp was purchased from PerkinElmer (Waltham, MA, USA). Deionized water (18.2 MΩ cm) obtained from a Milli-Q water purification system was used for the preparation of all solutions (Millipore, Bedford, MA, USA).

The four MILs investigated in this study were synthesized and characterized using previously reported procedures.[20] The chemical structures of the four MILs are shown in Figure 2-1. All MILs were purified using diethyl ether and water and subsequently dried in a vacuum oven overnight. When not in use, the MIL solvents were stored in a desiccator.

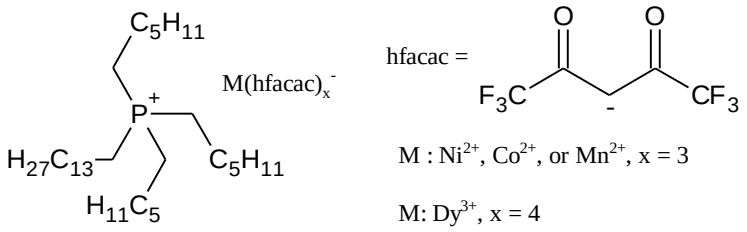

Figure 2-1 Chemical structures of the four hydrophobic MILs used in this study for the extraction of DNA.

2.2.2 MIL-based Extraction Methods

The general MIL single drop microextraction (SDME) procedure utilized in this study is depicted in Figure 2-2a. A 2 mL solution containing 2×10^4 copies/µL of single-stranded *KRAS* template was prepared in a 2.5 mL glass vial. A 10 µL volume of the ssDNA solution was removed and used as a standard. An optimized volume (e.g., 2 µL) of MIL was suspended from a magnetic rod (B = 0.20 T) and placed into the ssDNA solution. The solution was agitated using an Eppendorf I24R incubator shaker (Eppendorf, Hamburg, Germany) set at a rotation rate of

200 rpm. After 20 min, the recovered MIL was washed with deionized water to remove residual sample solution, and a 0.3 µL aliquot of DNA-enriched MIL was placed into a qPCR tube for downstream analysis.

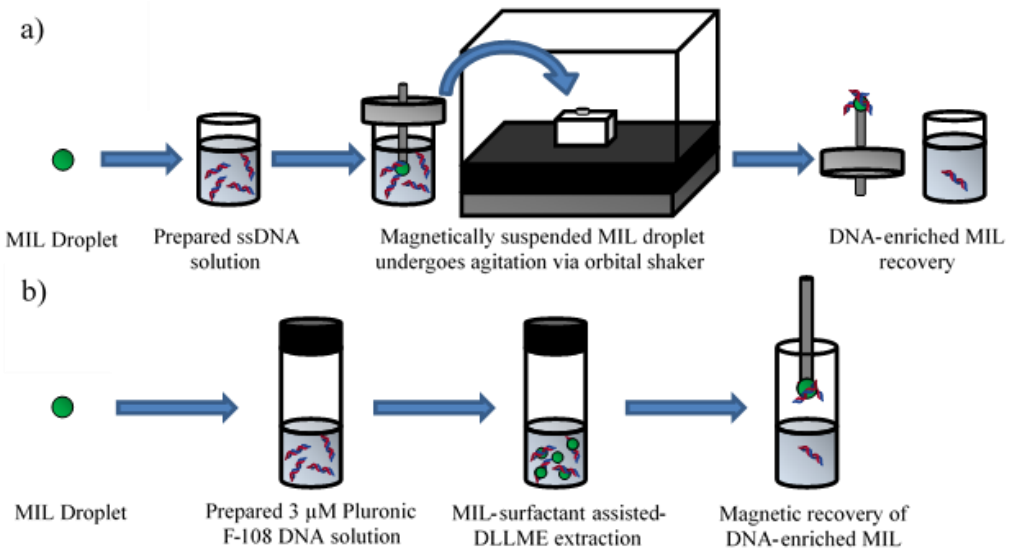

Figure 2-2 Schematic illustrating the general procedures for (a) MIL-SDME and (b) MIL-SA-DLLME.

The general procedure used for MIL surfactant-assisted (SA) dispersive liquid-liquid microextraction (DLLME) is shown in Figure 2-2b. A solution containing 3 µM of Pluronic F-108, 10 mM Tris-HCl (pH 8), and 2×10^4 copies/µL of single-stranded *KRAS* template was prepared in a 5 mL screw cap glass vial. An optimized volume of MIL (e.g., 6 µL) was added to the aqueous solution and agitated using a Barnstead/Thermolyne Type 16700 mixer (Dubuque, IA, USA). After 120 s, the MIL was separated from the aqueous solution using a rod magnet (B = 0.66 T) and washed with deionized water. A 0.3 µL aliquot of DNA enriched MIL was placed into a qPCR tube for downstream analysis.

DNA extractions using magnetic beads were performed as suggested by the manufacturer. A 2 mL solution containing 2×10^4 copies/µL of template was prepared in a 5 mL

screw cap glass vial, and a 10 µL aliquot was removed for use as a standard. To the sample solution, 2 mL of 6 M guanidine HCl and 0.5 mL of isopropanol were added. An excess amount of magnetic beads (720 µg) was added to the sample solution to ensure that sufficient beads were present to extract all the target DNA present in the sample solution (100-fold excess amount of beads). After a 1 min dispersion using a vortex, the beads were collected using an external magnet (B = 0.9 T) and washed twice with isopropanol. The beads were subsequently suspended in 10 µL of H_2O and 72 µg of DNA-enriched magnetic beads were added to the qPCR buffer.

2.2.3 PCR Amplification Conditions

Incorporating 0.3 µL of $[P_{6,6,6,14}^+][Ni(hfacac)_3^-]$ or $[P_{6,6,6,14}^+][Co(hfacac)_3^-]$ MIL to qPCR amplification systems required 10 µL of SsoAdvanced Supermix, 7.7 µL of H_2O, 1 µL of 20x PrimePCR assay mix, and 1 µL of 20x SYBR Green I for a final volume of 20 µL. The addition of 0.3 µL $[P_{6,6,6,14}^+][Mn(hfacac)_3^-]$ MIL to a 20 µL qPCR mixture required 10 µL SsoAdvanced Supermix, 6 µL H_2O, 1 µL of 20x PrimePCR assay mix, 1 µL 80 mM EDTA, and 1 µL 20x SYBR Green I. The inclusion of 0.3 µL $[P_{6,6,6,14}^+][Dy(hfacac)_4^-]$ MIL to the PCR mixture required 10 µL SsoAdvanced Supermix, 2.6 µL of 50 mM $MgCl_2$, 2.6 µL of H_2O, 1 µL of 20x PrimePCR assay mix, 1 µL 10 mg/mL BSA, 1 µL 100 mM EDTA, and 1 µL 20x SYBR Green I for a final volume of 20 µL. The addition of 72 µg of magnetic beads to the qPCR mixture required 10 µL of SsoAdvanced Supermix, 8 µL H_2O, and 1 µL of 20x PrimePCR assay mix for a total volume of 20 µL.

A Bio-Rad CFX96 Touch Real-time PCR was utilized for DNA amplification using the following temperature program: 2 min initial denaturation at 95 °C and 40 cycles comprised of a 5 s denaturation step at 95 °C and 30 s annealing step at 60 °C followed by an optical detection

step. Melt curves were developed after qPCR amplification starting at 65°C for 5 s and increasing to 95°C in 0.5°C increments.

The amount of DNA extracted by the hydrophobic MIL was determined from the Cq values associated with each reaction, which were determined using the fluorescence threshold provided by the Bio-Rad CFX Maestro software. Standard curves were constructed for both single and double-stranded *KRAS* template (see Figures 2-S1 and 2-S2) and used to determine the concentration of DNA extracted by the MIL. The enrichment factors (E_f) for each MIL-based extraction were calculated as shown in equation 1, where C_{MIL} is the concentration of DNA extracted using the MIL and C_{Std} represents the concentration of template in the aqueous sample solution prior to extraction.

$$E_f = \frac{C_{MIL}}{C_{Std}} \quad (1)$$

2.2.4 Determination of Soluble Metal Ions using Atomic Absorption (AA) Spectroscopy

A Shimadzu AA 7000 atomic absorption spectrometer (Kyoto, Japan) was used to determine the concentration of Ni^{2+} in the aqueous layer after MIL-based extraction using the method of standard addition. After a 2 min MIL-SA-DLLME procedure using 6 µL of the $[P_{6,6,6,14}^{+}][Ni(hfacac)_3^{-}]$ MIL, 400 µL of the aqueous solution were diluted to 5 mL and spiked with 0 to 60 µM of $NiCl_2$. To examine the effect that the nonionic surfactant had on the solubility of the MIL during DNA extraction, 6 µL of the $[P_{6,6,6,14}^{+}][Ni(hfacac)_3^{-}]$ MIL were dispersed in the aqueous solution containing various surfactant concentrations for a desired vortex time. An 1800 µL aliquot of the aqueous phase was then diluted to 5000 µL of water and analyzed by AA spectroscopy. The concentration of Ni^{2+} found in the aqueous solution was then determined from the standard curve shown in Figure 2-S3.

2.3 Results and Discussion

2.3.1 Mitigating the Inhibition of qPCR Amplification Derived from Hydrophobic MILs

The direct addition of DNA enriched MILs to the qPCR buffer allows for DNA desorption during the reaction and eliminates the need for tedious and time consuming DNA recovery steps. Previous studies have demonstrated positive qPCR amplification after directly transferring DNA extraction sorbents (e.g., chitosan microparticles or magnetic beads) to the PCR buffer.[19] However, the reported amplification efficiencies fell below 90%, which precludes reliable DNA quantification.[19] Although the elevated temperatures used during qPCR are capable of desorbing DNA from the MIL, it is also possible that thermal cycling may increase the solubility of certain MILs within the reaction buffer, as previously observed for the $[P_{6,6,6,14}^+]$ tetrachloroferrate(III) and trioctylbenzylammonium bromotrichloroferrate(III) MILs.[18] Despite the utility of the paramagnetic metal component for imparting magnetic susceptibility to the MIL, transition and rare-earth metals are known qPCR inhibitors when dissolved in reaction mixtures.[4,21]

In this study, DNA amplification in the presence of 0.3 µL of $[P_{6,6,6,14}^+][Ni(hfacac)_3^-]$ or 0.3 µL of $[P_{6,6,6,14}^+][Co(hfacac)_3^-]$ MILs was successful without the use of any additives. However, the fluorescence signals from reaction systems containing the $[P_{6,6,6,14}^+][Ni(hfacac)_3^-]$ or $[P_{6,6,6,14}^+][Co(hfacac)_3^-]$ MILs were depressed relative to a standard reaction that did not contain MIL. To investigate whether dissolved components of the MIL were inhibiting the fluorescence signal, 0.3 µL of $[P_{6,6,6,14}^+][Ni(hfacac)_3^-]$ MIL and 10 µL H_2O were incubated using the qPCR temperature program. After 40 cycles, 8 µL of the aqueous layer were removed from the sample tube (without disturbing the insoluble MIL phase) and were added to a qPCR mixture as a substitute for the pure water ordinarily used. As shown in Figure 2-S4, there was no

significant difference in the amplification curves generated with pure water and water that was subjected to incubation with MIL indicating that metal ions dissolved into the qPCR solution are not responsible for the diminished fluorescence signal. Another possibility is that the concentration of free SYBR Green I decreases due to partitioning to the MIL phase during qPCR. To mitigate the depletion of fluorophore from the aqueous phase, additional SYBR Green I was added to the reaction to recover amplification, as shown in Table 2-1.

Despite successful amplification with the Ni(II) and Co(II)-based MILs, DNA amplification with the $[P_{6,6,6,14}^+][Mn(hfacac)_3^-]$ or $[P_{6,6,6,14}^+][Dy(hfacac)_4^-]$ MIL in the qPCR mixture was inhibited even in the presence of additional SYBR Green I. To combat inhibition caused by the cationic and anionic components of MILs, several additives including EDTA, additional $MgCl_2$, and albumin have previously been examined.[18] Metal chelators such as EDTA are often added to qPCR buffers to sequester metal ions that would otherwise inhibit the reaction

Table 2-1 Summary of qPCR buffer optimization for the incorporation of 0.3 µL of $[P_{6,6,6,14}^+][Ni(hfacac)_3^-]$, $[P_{6,6,6,14}+][Co(hfacac)_3^-]$, $[P_{6,6,6,14}^+][Mn(hfacac)_3^-]$, or $[P_{6,6,6,14}^+][Dy(hfacac)_4^-]$ into the amplification of 200,000 copies/µL of *KRAS* template. N/A indicates that qPCR amplification was not successful.

	Additives	Cq	Standard Deviation (n = 3)
KRAS Standard	None	23.85	0.32
$[P_{6,6,6,14}^+][Ni(hfacac)_3^-]$	None	24.98	0.16
	1x SYBR Green I	23.94	0.08
$[P_{6,6,6,14}^+][Co(hfacac)_3^-]$	None	25.34	0.73
	1x SYBR Green I	24.56	0.69
$[P_{6,6,6,14}^+][Mn(hfacac)_3^-]$	None	N/A	N/A
	4 mM EDTA	25.71	0.17
	4 mM EDTA and 1x SYBR Green I	24.11	0.40
$[P_{6,6,6,14}^+][Dy(hfacac)_4^-]$	None	N/A	N/A
	5 mM EDTA	N/A	N/A
	5 mM EDTA and 0.5 mg/mL BSA	N/A	N/A
	5 mM EDTA, 0.5 mg/mL BSA, and 6.5 mM $MgCl_2$	25.65	0.41
	5 mM EDTA, 0.5 mg/mL BSA, 6.5 mM $MgCl_2$, and 1x SYBR Green I	24.11	0.31

due to competitive effects with essential Mg^{2+} cofactors. To determine whether EDTA could recover qPCR amplification reactions containing 0.3 µL of the $[P_{6,6,6,14}^+][Mn(hfacac)_3^-]$ MIL, different concentrations of EDTA (from 1 to 15 mM) were added to the master mix and tested. Of the range of concentrations investigated, 4 mM EDTA was the most effective at eliminating inhibition. Amplification using the $[P_{6,6,6,14}^+][Mn(hfacac)_3^-]$ MIL also required additional SYBR Green I dye to restore the fluorescence signal. However, the addition of EDTA to reaction mixtures containing the $[P_{6,6,6,14}^+][Dy(hfacac)_4^-]$ MIL did not result in DNA amplification. In a study by Kreader, BSA was shown to relieve qPCR inhibition caused by iron(III) ions.[21] Unfortunately, reactions containing a final BSA concentration of 0.5 to 1 µg/mL did not amplify DNA in the presence of the $[P_{6,6,6,14}^+][Dy(hfacac)_4^-]$ MIL, regardless of whether EDTA was present or not. Reactions containing $[P_{6,6,6,14}^+][Dy(hfacac)_4^-]$ may require additional Mg^{2+} ions for the DNA polymerase to function, but amplification was not successful with an additional 3.5 to 13 mM Mg^{2+} without BSA or EDTA. However, amplification with 0.3 µL of $[P_{6,6,6,14}^+][Dy(hfacac)_4^-]$ MIL in the qPCR mixture was successful when BSA, EDTA, and additional $MgCl_2$ were all present in the reaction buffer (see Table 1), similar to previous findings[18]. The final composition of the master mix for the $[P_{6,6,6,14}^+][Dy(hfacac)_4^-]$ MIL included 5 mM EDTA to chelate any liberated Dy^{3+}, 0.5 µg/mL BSA, and an additional 6.5 mM Mg^{2+}. With additional SYBR Green I, the amplification with 0.3 µL of $[P_{6,6,6,14}^+][Dy(hfacac)_4^-]$ was able to occur uninhibited.

The melting temperature of *KRAS* template after MIL-based extraction and qPCR amplification was examined to investigate whether the DNA sequence was altered due to the MIL. Figure 2-S5 shows that the melting temperature of the template DNA was not significantly

different compared to a *KRAS* standard (± 0.5 °C). This suggests that the sequence was not altered in agreement with previous MIL-based DNA extraction and amplification studies[12,18].

2.3.2 Optimization of MIL-based Extraction Method

Clinical and forensic samples types often contain DNA at very low concentration and require preconcentration prior to downstream analysis. In this study, a sample solution below clinically relevant concentrations was examined (2×10^4 copies/µL of single-stranded *KRAS*)[22]. Figure 2-3 shows that among the four studied MILs with different metal centers (e.g. nickel(II), cobalt(II), manganese(II), or dysprosium(III)), the $[P_{6,6,6,14}^+][Ni(hfacac)_3^-]$ MIL extracted ssDNA

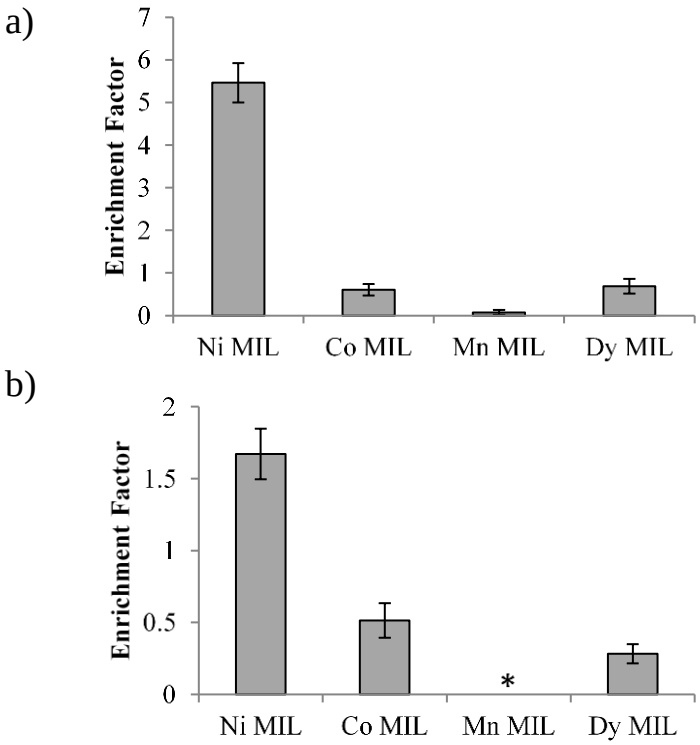

Figure 2-3 Extraction solvent optimization for MIL-SDME (a) and MIL-SA-DLLME (b) using $[P_{6,6,6,14}^+][Ni(hfacac)_3^-]$, $[P_{6,6,6,14}^+][Co(hfacac)_3^-]$, $[P_{6,6,6,14}^+][Mn(hfacac)_3^-]$, and $[P_{6,6,6,14}^+][Dy(hfacac)_4^-]$ MILs. MIL-SDME conditions: *KRAS* template concentration: 2×10^4 copies/µL; total solution volume: 2.0 mL; extraction time: 10 min; MIL volume: 2 µL; rotation rate: 200 rpm. MIL-SA-DLLME conditions: *KRAS* template concentration: 2×10^4 copies/µL; total solution volume: 2.0 mL; extraction time: 60 s; MIL volume: 10 µL; Pluronic F-108 concentration: 3 µM. *Enrichment factor of ssDNA extracted by $[P_{6,6,6,14}^+][Mn(hfacac)_3^-]$ was not determined as the Cq values obtained were outside the standard curve.

most efficiently using MIL-SDME and MIL-SA-DLLME. Therefore, the $[P_{6,6,6,14}^{+}][Ni(hfacac)_3^{-}]$ MIL was used for subsequent extractions.

The volume of the $[P_{6,6,6,14}^{+}][Ni(hfacac)_3^{-}]$ MIL used to extract template DNA was optimized for both SDME and SA-DLLME methods. Using MIL-SDME, 1.5 to 6 µL of the $[P_{6,6,6,14}^{+}][Ni(hfacac)_3^{-}]$ MIL was suspended from a rod magnet (B = 0.2 T) and directly immersed in an aqueous solution of DNA. Using an extraction time of 10 min, relatively smaller MIL volumes produced larger enrichment factors with 2 µL providing the highest E_f values, as shown in Figure 2-S6. In MIL-SA-DLLME, 5 to 10 µL of the $[P_{6,6,6,14}^{+}][Ni(hfacac)_3^{-}]$ MIL were dispersed in the DNA solution. Again, smaller volumes of MIL generally were optimum with 6 µL producing the largest enrichment factor, as shown in Figure 2-S7. Using MIL volumes of 1.5 µL for SDME or 5 µL for DLLME, the lower surface area of the MIL extraction phase appears to contribute to the diminished enrichment factor. However, extractions utilizing larger volumes of extraction solvent also resulted in lower enrichment factors. This is likely due to the final concentration of template in the MIL phase being lower due to the large volume of MIL.

Equilibrium can often be achieved more rapidly by agitating the sample during the extraction. However, in the case of MIL-SDME methods the extraction solvent is suspended from a magnet and is susceptible to falling into the sample during agitation. Therefore, droplet stability normally dictates the amount of agitation that can be applied in SDME. The rotation rate of the shaker used for MIL-SDME was optimized from 100-200 rpm, as shown in Figure 2-S8. The enrichment factor was found to increase when higher rotation rates were used. However, the maximum rotation rate was found to be at 200 rpm as higher rotation rates dislodged the magnetic rod from the glass vial.

The addition of a non-ionic surfactant was necessary for the MIL-SA-DLLME method to prevent the MIL from interacting with the glass vial instead of the magnet. By adding Pluronic F-108 surfactant to the sample solution, simple and rapid recovery of the MIL after dispersion was achieved. However, the concentration of surfactant can greatly alter the extraction with increasing surfactant concentrations improving the enrichment factor up to the critical micelle concentration.[23] The concentration of Pluronic F-108 was optimized from 2 to 5 µM using the MIL-SA-DLLME procedure, with a concentration of 3 µM producing the highest enrichment factor as shown in Figure 2-S9. When higher concentrations of surfactant were examined, the extraction phase tended to disperse into smaller droplets. However, the addition of Pluronic F-108 was also found to increase the miscibility of the hydrophobic MIL within the sample solution. Since dissolution of MIL would presumably increase the metal ion concentration, the concentration of Ni^{2+} in the sample solution was determined using AA. After performing extractions with 3 and 5 µM Pluronic F-108, AA experiments showed an increase in the concentration of Ni^{2+} from 65.23 ± 1.97 µM to 105.27 ± 7.58 µM indicating that an increased solubility of the MIL correlated to an increase in surfactant concentration. In addition, it is possible that DNA can interact with dissolved $[P_{6,6,6,14}^{+}][Ni(hfacac)_3^{-}]$ MIL resulting in lower enrichment factors.

Extraction time is an important parameter to optimize for both SDME and DLLME methods. An optimum extraction time for SDME and DLLME is the shortest time required for the analytes to reach equilibrium between the extraction phase and aqueous solution. In MIL-SDME, time points from 5 to 30 min were examined with equilibrium being achieved after 20 min, as indicated in Figure 2-S10. Time points from 30 to 300 s were studied for MIL-SA-DLLME. As shown in Figure 2-4, a 2 min vortex time produced the largest enrichment factor.

Since MIL may dissolve into the aqueous solution at longer time points allowing DNA to interact with dissolved $[P_{6,6,6,14}^+][Ni(hfacac)_3^-]$ MIL instead of the immiscible MIL phase, AA was used to determine the concentration of Ni^{2+} found after DNA extractions were performed from 30 to 300 s using MIL-SA-DLLME. Figure 2-4 shows that the concentration of Ni^{2+} ions in the aqueous solution increased at longer time intervals. The higher concentration of Ni^{2+} in the aqueous layer indicates that more of the $[P_{6,6,6,14}^+][Ni(hfacac)_3^-]$ MIL dissolved over time suggesting that DNA may prefer to interact with miscible MIL components resulting in lower enrichment factors.

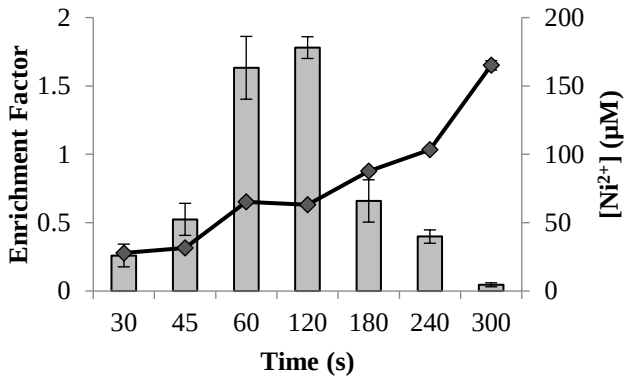

Figure 2-4 Extraction time optimization for MIL-SA-DLLME method using the $[P_{6,6,6,14}^+][Ni(hfacac)_3^-]$ MIL (gray bar) as an extraction solvent. The concentration of Ni^{2+} detected in the aqueous solution post extraction is also plotted as a function of time (◊). *KRAS* template concentration: 2×10^4 copies/µL; total solution volume: 2.0 mL; MIL volume: 6 µL; Pluronic F-108 surfactant concentration: 3 µM.

In DNA extraction procedures, the pH of biological samples is often modified during pretreatment in order to lyse cells, prevent coextraction of impurities, and/or prevent damage to target DNA.[24] The pKa of the DNA phosphate backbone is below the pH range tested in this study indicating that DNA molecules should maintain an overall negative charge.[25] To obtain the desired pH, the sample solution contained 10 mM Tris-HCl and the pH was adjusted from 4 to 10 using HCl or NaOH. The extraction of ssDNA using the $[P_{6,6,6,14}^+][Ni(hfacac)_3^-]$ MIL

exhibited a pH dependence for both MIL-SDME and MIL-SA-DLLME methods, as shown in Figure 2-S11 and S2-12, respectively. Extreme pH values (i.e., 4 and 10) were observed to produce lower enrichment factors. For both techniques, pH 8 provided the highest enrichment factors for ssDNA and was used for the remaining MIL-SA-DLLME experiments.

DNA in natural systems exists primarily in double-stranded form[26] making it necessary to examine the enrichment factor of dsDNA as well as ssDNA. As shown in Figure 2-5, lower enrichment factors were noted for dsDNA compared to ssDNA for both MIL-SDME and MIL-SA-DLLME indicating that there may be dependence on molecular weight. When comparing the two optimized MIL-based DNA extraction methods, the MIL-SDME method produced higher enrichment factors compared to the MIL-SA-DLLME method (see Figure 2-5). Therefore, this method was used for the remainder of the study.

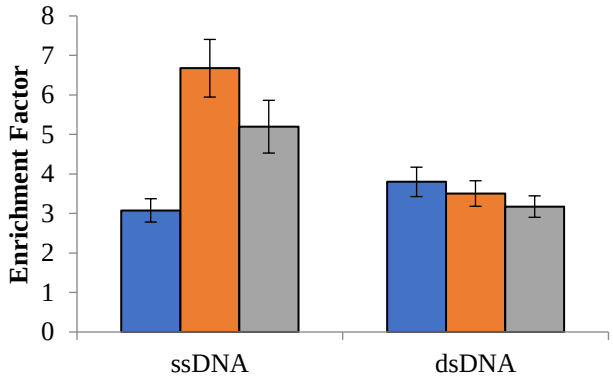

Figure 2-5 Comparison of ssDNA and dsDNA enrichment factors using magnetic-bead based extraction (blue), MIL-SDME (red), and MIL-SA-DLLME (green). MIL-SA-DLLME conditions: *KRAS* template concentration: 2×10^4 copies/µL; Tris-HCl concentration: 10 mM; pH 8; total solution volume: 2.0 mL; time: 120 s; MIL volume: 6 µL. MIL-SDME conditions: *KRAS* template concentration: 2×10^4 copies/µL; total solution volume: 2.0 mL; time: 20 min; MIL volume: 2 µL; rotation rate: 200 rpm. Magnetic bead extraction conditions: *KRAS* template concentration: 2×10^4 copies/µL; solution volume: 2.0 mL; concentration of Guanidine HCl: 3 M; extraction time: 1 min; mass of magnetic beads: 720 µg.

2.3.3 Comparison to Magnetic Bead-Based DNA Extractions

Cell-free DNA (cfDNA) is comprised of short DNA fragments and can be found in plasma making it intensely studied in clinical chemistry for diagnostic applications.[2,22,27-29] The concentration of specific cfDNA sequences such as *KRAS* has been shown to correlate to different stages of cancer suggesting that less invasive liquid biopsies could be used for cancer diagnosis, prognosis, and treatment monitoring.[2] Magnetic bead-based DNA extractions have been applied for the extraction of cfDNA from plasma samples, thereby removing time consuming centrifugation steps required in traditional SPE methods.[30] DNA-enriched magnetic beads can also be directly added into the qPCR buffer to avoid a time consuming DNA recovery step. Therefore, the MIL-SDME method was compared to a commercially available magnetic bead-based method recommended for nucleic acid extraction and purification. dsDNA and ssDNA were extracted with silica-based magnetic beads according to the manufacturer's instructions. By adding the beads directly to a PCR mixture, DNA can be desorbed from the magnetic beads by rehydrating the extracted DNA. The main disadvantage of magnetic beads is the high concentration of chaotropic salts used during the extraction procedure that can inhibit qPCR amplification, if not sufficiently removed. Therefore, the MIL-SDME method was compared as an alternative DNA extraction method to a commercially-available magnetic bead-based method. As shown in Figure 2-5, the enrichment factor of dsDNA using the magnetic bead and MIL-SDME methods were similar, but both MIL-based methods were capable producing higher enrichment factors for ssDNA compared to the magnetic bead-based method tested.

In qPCR, amplification efficiency relates to the ability of the DNA polymerase to double the amount of DNA in the reaction mixture with each cycle. Amplification efficiencies lower than 90% or higher than 110% indicate the presence of inhibitors or adsorption of qPCR

components and result in difficulties with quantification.[19] Therefore, it is important to investigate the influence of adding MILs and magnetic beads to the qPCR buffer on amplification efficiency. As shown in Figure 2-6, the amplification efficiency associated with incorporating magnetic beads into the PCR mixture was found to be just 81.9%. In comparison, direct qPCR using the $[P_{6,6,6,14}^+][Ni(hfacac)_3^-]$ MIL did not significantly alter the amplification efficiency and was determined to be 91.1%. The lower efficiency associated with the magnetic beads makes DNA quantification difficult and represents a significant advantage of incorporating DNA-enriched MILs into the qPCR master mix.

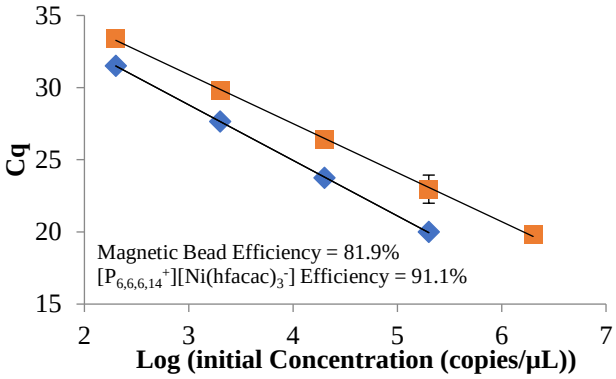

Figure 2-6 Standard curve generated using the optimized MIL-SDME (□) method with $[P_{6,6,6,14}^+][Ni(hfacac)_3^-]$ and magnetic bead-based extraction method (◊). MIL-SDME conditions: total solution volume: 2.0 mL; extraction time: 20 min; MIL volume: 2 µL; rotation rate: 200 rpm. Magnetic bead extraction conditions: solution volume: 2.0 mL; concentration of guanidine HCl: 3 M; extraction time: 1 min; mass of magnetic beads: 720 µg.

Determining the loading capacity of the $[P_{6,6,6,14}^+][Ni(hfacac)_3^-]$ MIL and the magnetic beads is important as some biological samples may contain large amounts of non-target DNA that could saturate the MIL. Therefore, the loading capacity of the $[P_{6,6,6,14}^+][Ni(hfacac)_3^-]$ MIL was determined by extracting target DNA in a sample solution containing increasing amounts of non-target DNA. Short non-target DNA was prepared by shearing DNA from salmon testes to fragments less than 250 base pairs through sonication as confirmed by gel electrophoresis (see Figure 2-S13). Sheared salmon DNA was spiked into a sample solution (0 to 2 µg/mL)

containing 2×10^4 copies/µL of double-stranded *KRAS* and subjected to MIL-SDME and direct PCR amplification. As shown in Figure 2-S14, 2 µL of $[P_{6,6,6,14}^+][Ni(hfacac)_3^-]$ MIL successfully extracted double-stranded *KRAS* in the presence of up to 0.2 µg/mL of sheared salmon DNA without impacting the Cq value for the target template. To extract target DNA from larger concentrations of total nucleic acid, larger volumes of MIL can be utilized for MIL-SDME (see Figure 2-S15). In comparison, when the same experiment was performed using 720 µg of magnetic beads (enough beads to extract 100-fold excess of the amount of target DNA in the solution), the magnetic beads could not maintain the same amount of extracted *KRAS* when in the presence of 0.2 ng/mL of sheared salmon DNA, as shown in Figure 2-S16.

In clinical applications, cfDNA fragments can be extracted from plasma samples, but the proteins, hormones and electrolytes comprising the plasma can reduce the efficiency of the reaction or potentially inhibit qPCR.[4] In order to test the clinical applicability of the MIL-SDME method, target DNA was extracted from human plasma. Human plasma was diluted ten-fold and spiked with 2×10^4 copies/µL of double-stranded *KRAS* template to determine the effect of the sample matrix on MIL-SDME and magnetic bead-based extraction. Both the MILs and the magnetic beads exhibited an approximate twenty-fold decrease in enrichment factors compared to extractions from pure water at the same DNA concentration. As shown in Figure 2-S17, magnetic beads were observed to produce slightly higher enrichment factors (1.2-fold) compared to the MIL.

2.4 Conclusions

There is a constant desire to further improve DNA extraction methods by increasing sample throughput and compatibility with techniques used for downstream analysis. In this study, four hydrophobic MILs were investigated as DNA extraction solvents. By utilizing a

magnetic field, MIL droplets can be rapidly collected on a magnet thereby forgoing several lengthy centrifugation steps. Custom-designed qPCR buffers were designed to enable the direct incorporation of DNA-enriched MIL the reaction system and facilitate successful DNA amplification and real-time amplicon detection. High enrichment factors were observed using both the MIL-SDME and MIL-SA-DLLME methods for both ssDNA and dsDNA using the $[P_{6,6,6,14}^{+}][Ni(hfacac)_3^{-}]$ MIL as the extraction solvent with the qPCR buffer requiring only excess SYBR Green I. When comparing the MIL-based extraction to a commercial magnetic bead-based platform, the $[P_{6,6,6,14}^{+}][Ni(hfacac)_3^{-}]$ MIL was capable of extracting greater quantities of ssDNA compared to the magnetic beads. The addition of magnetic beads to the qPCR buffer was also shown to significantly decrease the efficiency of the reaction whereas the $[P_{6,6,6,14}^{+}][Ni(hfacac)_3^{-}]$ MIL did not lower the amplification efficiency below 90%. When examining the extraction of *KRAS* gene fragment from a plasma sample, the $[P_{6,6,6,14}^{+}][Ni(hfacac)_3^{-}]$ MIL was capable of extracting a sufficient amount of target template for qPCR detection, indicating that MILs are promising solvents for the extraction of cfDNA fragments from a plasma matrix.

Acknowledgements J.L.A. acknowledges funding from the Chemical Measurement and Imaging Program at the National Science Foundation (CHE-1413199).

References

(1) Jobling, M. A.; Gill, P. Encoded Evidence: DNA in Forensic Analysis. Nat. Rev. Genet. 2004, 5, 739.

(2) Schwarzenbach, H.; Hoon, D. S. B.; Pantel, K. Cell-Free Nucleic Acids as Biomarkers in Cancer Patients. Nat. Rev. Cancer 2011, 11, 426.

(3) Bremen, S. U.; Miller, D. N.; Bryant, J. E.; Madsen, E. L.; Ghiorse, W. C. Evaluation and Optimization of DNA Extraction and Purification Procedures for Soil and Sediment Samples Evaluation and Optimization of DNA Extraction and Purification Procedures for Soil and Sediment Samples. Appl. Environ. Microbiol. 1999, 65 (11), 4715–4724.

(4) Schrader, C.; Schielke, A.; Ellerbroek, L.; Johne, R. PCR Inhibitors - Occurrence, Properties and Removal. J. Appl. Microbiol. 2012, 113, 1014–1026.

(5) Patel, R.; Kvach, J. T.; Mounts, P. Isolation and Restriction Endonuclease Analysis of Mycobacterial DNA. J. Gen. Microbiol. 1986, 132 (2), 541–551.

(6) Wen, J.; Legendre, L. A.; Bienvenue, J. M.; Landers, J. P. Purification of Nucleic Acids in Microfluidic Devices. Anal. Chem. 2008, 80 (17), 6472–6479.

(7) Fan, Z. H.; Mangru, S.; Granzow, R.; Heaney, P.; Ho, W.; Dong, Q.; Kumar, R. Dynamic DNA Hybridization on a Chip Using Paramagnetic Beads. Anal. Chem. 1999, 71 (21), 4851–4859.

(8) An, J.; Trujillo-Rodríguez, M. J.; Pino, V.; Anderson, J. L. Non-Conventional Solvents in Liquid Phase Microextraction and Aqueous Biphasic Systems. J. Chromatogr. A 2017, 1500, 1–23.

(9) Butler, J. M. U.S. Initiatives to Strengthen Forensic Science & International Standards in Forensic DNA. Forensic Sci. Int. Genet. 2015, 18, 4–20.

(10) Hayashi, S.; Hamaguchi, H. Discovery of a Magnetic Ionic Liquid [Bmim]FeCl4. Chem. Lett. 2004, 33 (12), 1590–1591.

(11) Del Sesto, R. E.; McCleskey, T. M.; Burrell, A. K.; Baker, G. a; Thompson, J. D.; Scott, B. L.; Wilkes, J. S.; Williams, P. Structure and Magnetic Behavior of Transition Metal Based Ionic Liquids. Chem. Commun. 2008, 447–449.

(12) Krieger, B. M.; Lee, H. Y.; Emge, T. J.; Wishart, J. F.; Castner Edward W., J. Ionic Liquids and Solids with Paramagnetic Anions. Phys. Chem. Chem. Phys. 2010, 12 (31), 8919–8925.

(13) Clark, K. D.; Nacham, O.; Yu, H.; Li, T.; Yamsek, M. M.; Ronning, D. R.; Anderson, J. L. Extraction of DNA by Magnetic Ionic Liquids: Tunable Solvents for Rapid and Selective DNA Analysis. Anal. Chem. 2015, 87 (3), 1552–1559.

(14) Clark, K. D.; Varona, M.; Anderson, J. L. Ion-Tagged Oligonucleotides Coupled with a Magnetic Liquid Support for the Sequence-Specific Capture of DNA. Angew. Chemie - Int. Ed. 2017, 56 (26), 7630–7633.

(15) Clark, K. D.; Purslow, J. A.; Pierson, S. A.; Nacham, O.; Anderson, J. L. Rapid Preconcentration of Viable Bacteria Using Magnetic Ionic Liquids for PCR Amplification and Culture-Based Diagnostics. Anal. Bioanal. Chem. 2017, 409 (21), 4983–4991.

(16) Merib, J.; Spudeit, D. A.; Corazza, G.; Carasek, E.; Anderson, J. L. Magnetic Ionic Liquids as Versatile Extraction Phases for the Rapid Determination of Estrogens in Human Urine by Dispersive Liquid-Liquid Microextraction Coupled with High-Performance Liquid Chromatography-Diode Array Detection. Anal. Bioanal. Chem. 2018, 410 (19), 4689–4699.

(17) Yu, H.; Merib, J.; Anderson, J. L. Faster Dispersive Liquid-Liquid Microextraction Methods Using Magnetic Ionic Liquids as Solvents. J. Chromatogr. A 2016, 1463, 11–19.

(18) Chatzimitakos, T.; Binellas, C.; Maidatsi, K.; Stalikas, C. Magnetic Ionic Liquid in Stirring-Assisted Drop-Breakup Microextraction: Proof-of-Concept Extraction of Phenolic Endocrine Disrupters and Acidic Pharmaceuticals. Anal. Chim. Acta 2016, 910, 53–59.

(19) Clark, K. D.; Yamsek, M. M.; Nacham, O.; Anderson, J. L. Magnetic Ionic Liquids as PCR-Compatible Solvents for DNA Extraction from Biological Samples. Chem. Commun. 2015, 51 (94), 16771–16773.

(20) Pandit, K. R.; Nanayakkara, I. A.; Cao, W.; Raghavan, S. R.; White, I. M. Capture and Direct Amplification of DNA on Chitosan Microparticles in a Single PCR-Optimal Solution. Anal. Chem. 2015, 87 (21), 11022–11029.

(21) Pierson, S. A.; Nacham, O.; Clark, K. D.; Nan, H.; Mudryk, Y.; Anderson, J. L. Synthesis and Characterization of Low Viscosity Hexafluoroacetylacetonate-Based Hydrophobic Magnetic Ionic Liquids. New J. Chem. 2017, 41 (13), 5498–5505.

(22) Kreader, C. A. Relief of Amplification Inhibition in PCR with Bovine Serum Albumin or T4 Gene 32 Protein. Appl. Environ. Microbiol. 1996, 62 (3), 1102–1106.

(23) Taly, V.; Pekin, D.; Benhaim, L.; Kotsopoulos, S. K.; Le Corre, D.; Li, X.; Atochin, I.; Link, D. R.; Griffiths, A. D.; Pallier, K.; et al. Multiplex Picodroplet Digital PCR to Detect KRAS Mutations in Circulating DNA from the Plasma of Colorectal Cancer Patients. Clin. Chem. 2013, 59 (12), 1722–1731.

(24) Behbahani, M.; Najafi, F.; Bagheri, S.; Bojdi, M. K.; Salarian, M.; Bagheri, A. Application of Surfactant Assisted Dispersive Liquid-Liquid Microextraction as an Efficient Sample Treatment Technique for Preconcentration and Trace Detection of Zonisamide and Carbamazepine in Urine and Plasma Samples. J. Chromatogr. A 2013, 1308 (20), 25–31.

(25) Purohit, H. J.; Kapley, A.; Moharikar, A. A.; Narde, G. A Novel Approach for Extraction of PCR-Compatible DNA from Activated Sludge Samples Collected from Different Biological Effluent Treatment Plants. J. Microbiol. Methods 2003, 52 (3), 315–323.

(26) Wang, H.; Wang, J.; Zhang, S. Binding Gibbs Energy of Ionic Liquids to Calf Thymus DNA: A Fluorescence Spectroscopy Study. Phys. Chem. Chem. Phys. 2011, 13 (9), 3906–3910.

(27) Stroun, M.; Anker, P.; Lyautey, J.; Lederrey, C.; Maurice, P. A. Isolation and Characterization of DNA from the Plasma of Cancer Patients. Eur. J. Cancer Clin. Oncol. 1987, 23 (6), 707–712.

(28) Thierry, A. R.; Mouliere, F.; El Messaoudi, S.; Mollevi, C.; Lopez-Crapez, E.; Rolet, F.; Gillet, B.; Gongora, C.; Dechelotte, P.; Robert, B.; et al. Clinical Validation of the Detection of KRAS and BRAF Mutations from Circulating Tumor DNA. Nat. Med. 2014, 20 (4), 430–435.

(29) Devonshire, A. S.; Whale, A. S.; Gutteridge, A.; Jones, G.; Cowen, S.; Foy, C. A.; Huggett, J. F. Towards Standardisation of Cell-Free DNA Measurement in Plasma: Controls for Extraction Efficiency, Fragment Size Bias and Quantification. Anal. Bioanal. Chem. 2014, 406 (26), 6499–6512.

(30) Sparks, A. B.; Struble, C. A.; Wang, E. T.; Song, K.; Oliphant, A. Noninvasive Prenatal Detection and Selective Analysis of Cell-Free DNA Obtained from Maternal Blood: Evaluation for Trisomy 21 and Trisomy 18. Am. J. Obstet. Gynecol. 2012, 206 (4), 319.e1-319.e9.

(31) Stemmer, C.; Beau-Faller, M.; Pencreac'h, E.; Guerin, E.; Schneider, A.; Jaqmin, D.; Quoix, E.; Gaub, M.-P.; Oudet, P. Use of Magnetic Beads for Plasma Cell-Free DNA Extraction: Toward Automation of Plasma DNA Analysis for Molecular Diagnostics. Clin. Chem. 2003, 49 (11), 1953 LP – 1955.

CHAPTER 3.

DEVELOPMENT OF A MULTIPLEX-QPCR ASSAY CONTAINING DNA-ENRICHED MAGNETIC IONIC LIQUIDS FOR ALLELIC DISCRIMINATION BETWEEN CIRCULATING TUMOR DNA FRAGMENTS

Modified from a manuscript published in *Analytica Chimica Acta*

Miranda N. Emaus and Jared L. Anderson

Department of Chemistry, Iowa State University, Ames, Iowa 50011, United States

Abstract

Multiplex amplification of DNA can be highly valuable in circulating tumor DNA (ctDNA) analysis due to the sheer number of potential mutations. However, commercial ctDNA extraction methods struggle to preconcentrate low concentrations of DNA and require multiple sample handling steps. Recently, magnetic ionic liquids (MILs) have been used to extract DNA and integrated into a quantitative polymerase chain reaction (qPCR). However, in previous studies, DNA could not be preconcentrated from plasma in previous studies and only one fragment could be amplified per reaction. In this study, MILs were utilized as DNA extraction solvents and directly integrated into a multiplex-qPCR buffer to simultaneously amplify wild-type *KRAS*, G12S *KRAS*, and wild-type *BRAF*, three clinically-relevant genes whose mutation status can affect the success of anti-EGFR therapy. DNA was desorbed from the MIL solvent during a multiplex-PCR without having a significant effect on the amplification efficiency, and allelic discrimination of single nucleotide polymorphisms could still be achieved. Enrichment factors over 35 for all three sequences were achieved from Tris buffer using the $[N_{8,8,8,Bz}^{+}][Ni(hfacac)_3^{-}]$ and $[P_{6,6,6,14}^{+}][Ni(Phtfacac)_3^{-}]$ MILs. DNA could still be preconcentrated from 2-fold diluted human plasma using the $[N_{8,8,8,Bz}^{+}][Ni(hfacac)_3^{-}]$ MIL.

Extractions from undiluted plasma were reproducible with the $[P_{6,6,6,14}^{+}][Ni(Phtfacac)_3^{-}]$ MIL although DNA was not preconcentrated with enrichment factors around 0.6 for all three fragments. Compared to commercial DNA extraction methods (i.e., silica-based spin columns and magnetic beads), the MIL-based extraction could achieve higher enrichment factors in Tris buffer and plasma. The ability of the MIL-based dispersive liquid-liquid microextraction (DLLME) direct-multiplex-qPCR method to simultaneously achieve high enrichment factors of multiple DNA fragments from human plasma is highly promising in the field of ctDNA detection.

3.1 Introduction

Tumor assessment using circulating tumor DNA (ctDNA) can provide a non-invasive option for cancer diagnosis, assessment of residual disease, and treatment response.[1,2] ctDNA originates from primary or metastatic tumor cells that have undergone apoptosis or necrosis.[3,4] The mutational status of certain genes can have significant impact on the success rate of cancer treatment.[2,5] For example, it has been found that mutated *KRAS* and *BRAF* genes correlate to a low success rate of anti-EGFR therapy with Cetuximab and Panitumumab.[6,7] The ability to detect and discern ctDNA mutations from wild-type DNA has ultimately led the way for molecular guided therapies. However, detection of ctDNA is challenging especially during the early stages of cancer due to a low abundance of ctDNA.[2,8] In addition, multiple mutations can be associated with a single gene, and mutations associated with *KRAS*, *BRAF*, and *PIK3CA* are often single nucleotide polymorphisms (SNPs), which can cause false positive results due to mishybridization.[1,3,4,9] Therefore, ctDNA detection methods need to be capable of rapidly decerning low concentrations of SNPs from wild-type DNA.

There are significant advantages of detecting multiple ctDNA sequences simultaneously, such as achieving higher sample throughput and reduced analysis costs.[10] Multiplex quantitative polymerase chain reaction (qPCR) methods have been developed to detect DNA fragments simultaneously using fluorescently-tagged probes. Taqman probes consist of a short oligonucleotide complementary to the target sequence with a fluorophore and quencher. When the probe anneals to the target sequence, the DNA polymerase separates the probe from the quencher producing a detectable signal that allows the amplification of DNA to be monitored in real-time.[11,12] However, the development of a multiplex-qPCR method is challenging. Often times, great care is needed to ensure that amplification bias does not occur, competition for PCR reagents does not prevent amplification of low abundance targets, and that a proper annealing temperature is used so the Taqman probe anneals to the proper target.[13,14]

DNA extraction is generally the quintessential first step in DNA analysis and is often an overlooked bottle neck.[15,16] Without a competent DNA extraction, bioassays such as PCR and DNA sequencing would not be possible due to the high concentration of inhibitors present in biological and environmental matrices. Traditionally, phenol-chloroform-based methods are used to extract DNA. However, this method requires toxic chemicals and requires multiple sample handling steps that limit the practicality of the technique.[17] Commercial DNA extraction kits typically involve either silica-based spin columns or magnetic beads. These kits are simple to use, but often poorly extract low concentrations of small ctDNA fragments.[4,18] In addition, both spin columns and magnetic beads require several sample handling steps and reagents to isolate DNA. In general, the more steps introduced in the extraction procedure can also increase the probability of contamination from PCR inhibitors or DNA. Several non-commercial DNA extraction methods have been designed to overcome the limitations of commercial DNA

extractions. Recently, centrifugation assisted-immiscible fluid filtration (CIFF) was developed by Juang et al. to extract DNA using glass microparticles.[16] Transfer of the glass microparticles from the aqueous sample to a fluorinated oil eliminated the need for numerous wash steps that are commonplace in commercial methods. However, CIFF still requires a manual DNA recovery step as well as multiple reagents such as chaotropic salts and fluorinated oil that can inhibit PCR if not otherwise removed. Chitosan microparticles can efficiently extract DNA using electrostatic interactions.[19] Chitosan-based extractions do not require chaotropic salts or organic solvents like silica-based methods, and DNA can be desorbed from chitosan microparticles during PCR.[20] Using the PCR system to desorb DNA removes a sample handling step from the procedure. However, chitosan microparticles were shown to significantly decrease PCR efficiency likely due to the adsorption of PCR components to the particles.

Ionic liquids (ILs) have been widely used to extract DNA through hydrophobic and electrostatic interactions.[21-23] ILs are molten salts with melting temperatures under 100 °C that possess unique physical properties such as negligible vapor pressures, high thermal stability, and tunable physiochemical properties.[24-26] Magnetic ionic liquids (MILs) possess similar properties to ILs.[24,27-29] However, MILs contain a paramagnetic component in either the anion or cation structure, which allows MIL droplets to be collected on a magnet.[15,30] Hydrophobic MILs have been applied in dispersive liquid-liquid microextractions (DLLME) to rapidly extract DNA from complex matrices by dispersing fine droplets of the MIL.[15,31-33] Originally, DNA was recovered from the MIL phase using a short silica column followed by an alcohol precipitation step.[15] However, this procedure is highly extensive and time consuming. Therefore, work was done to shorten the desorption process by integrating the DNA-enriched MIL into a PCR buffer.[34-36] Thermal desorption of DNA during PCR allows for high enrichment factors while not having a

deleterious impact on the efficiency of the reaction.[35,37] The MIL-DLLME method coupled to direct-qPCR detection is efficient for extracting and quantifying short DNA sequences, such as ctDNA fragments. However, current approaches involving direct-qPCR with MIL solvents have only been applied to singleplex reactions. Although singleplex reactions are important, the development of a MIL-multiplex-PCR system to simultaneously detect multiple fragments would greatly improve sample throughput and allow for the detection and discrimination of SNPs.

In this study, three hydrophobic Ni(II)-based MILs were used as DNA extraction solvents. The DNA-enriched MILs were integrated into a custom designed multiplex-qPCR assay to successfully amplify three DNA sequences simultaneously. The efficiency of the reaction was not affected by the hydrophobic MIL, and allelic discrimination between the three sequences could be achieved even among the SNPs when the MIL was integrated into the multiplex-qPCR buffer. The volume of MIL dispersed and total extraction time was optimized for each MIL. Enrichment factors over 35 were achieved for all three DNA fragments with the $[N_{8,8,8,Bz}^{+}][Ni(hfacac)_3^{-}]$ and $[P_{6,6,6,14}^{+}][Ni(Phtfacac)_3^{-}]$ MILs. Compared to commercial DNA extraction methods (employing spin columns and magnetic bead), the MILs exhibited superior preconcentration of DNA in part due to the low desorption volume required for analysis. In addition, the $[P_{6,6,6,14}^{+}][Ni(Phtfacac)_3^{-}]$ MIL was capable of producing higher enrichment factors from undiluted plasma compared to commercial kits suggesting that the MIL-based extraction method could be beneficial in extracting ctDNA from clinical samples.

3.2 Materials and Methods

3.2.1 Reagents and Materials

Ammonium hydroxide (28-30% solution in water), 1,1,1,5,5,5-hexafluoroacetylacetone (99%), 1-phenyl-4,4,4-trifluoro-1,3-butanedione (99%), nickel(II) chloride (98%), and

trioctylamine (97%) were purchased from Acros Organics (Morris Plains, NJ, USA). Anhydrous diethyl ether (99.0%) was purchased from Avantor Performance Materials Inc. (Center Valley, PA, USA). Trihexyl(tetradecyl)phosphonium chloride (97.7%) was purchased from Strem Chemicals (Newburyport, MA, USA). Agarose was purchased from Lab Express (Ann Arbor, MI, USA). Cyanine5 (Cy5) carboxylic acid was purchased from Lumiprobe (Hunt Valley, MD, USA). Ethylenediaminetetraacetic acid (EDTA) (99.4-100.06%), benzyl bromide (98%), chloroform (>99.8%), lyophilized plasma from human (4% trisodium citrate), lithium bis[(trifluoromethyl)sulfonyl]imide ($[Li^+][NTf_2^-]$), guanidine hydrochloride (>98.0), and magnesium chloride hexahydrate (99.0-102.0%) were purchased from Sigma-Aldrich (St. Louis, MO, USA). Proteinase K was purchased from New England Biolabs (Ipswich, MA, USA). Apheresis derived pooled human plasma (Na_2EDTA anticoagulant) was obtained from Innovative Research (Novi, MI, USA). SYBR Green I (10,000x) was purchased from Life Technologies (Carlsbad, CA, USA). Primers, probes, and oligonucleotides (sequences shown in Table S1) were acquired from Integrated DNA Technologies (Coralville, IA, USA). Modified plasmids (3.9 Kbp) were obtained from Eurofin Genomics (Louisville, KY, USA) and contained an insert consisting of 166 bp wild type *KRAS*, 166 bp G12S *KRAS* mutation, or 210 bp wild type *BRAF*. Optically clear PCR caps, tube strips, Taqman universal PCR master mix, isopropanol (99.9%), and Dynabeads myone silane magnetic beads were acquired from Thermo Fisher Scientific (Waltham, MA, USA). Tris-HCl was obtained from RPI (Mount Prospect, IL, USA). Neodymium rod (0.66 T) and cylinder magnets (0.9 T) were purchased from K&J Magnetics (Pipersville, PA, USA). Microwell plates (364) were purchased from Corning (Corning, NY, USA). Deionized water (18.2 MΩ cm), obtained from a Milli-Q water purification system, was used to prepare all aqueous solutions (Millipore, Bedford, MA, USA).

3.2.2 MIL Synthesis

Chemical structures of the three MILs are shown in Figure 3-S1. The $[NH_4^+][Ni(hfacac)_3^-]$ salt, $[P_{6,6,6,14}^+][Ni(hfacac)_3^-]$ MIL, and $[P_{6,6,6,14}^+][Ni(Phtfacac)_3^-]$ MIL were synthesized and characterized using previously reported procedures.[38,39] The $[N_{8,8,8,Bz}^+][Br^-]$ salt was synthesized as previously reported and characterized using ^{1}H NMR (Varion MR-400, Palo Alto, CA, USA) as shown in Figure 3-S2.[40] The $[N_{8,8,8,Bz}^+][Ni(hfacac)_3^-]$ MIL was synthesized by stirring equimolar amounts of $[N_{8,8,8,Bz}^+][Br^-]$ and $[NH_4^+][Ni(hfacac)_3^-]$ in 50 mL of methanol overnight. The product was subsequently dried in a vacuum oven and purified using diethyl ether and water. The $[P_{6,6,6,14}^+][NTf_2^-]$ IL was synthesized by mixing equimolar amounts of the $[P_{6,6,6,14}^+][Cl^-]$ IL and $[Li^+][NTf_2^-]$ overnight in 30 mL of methanol. The $[N_{8,8,8,Bz}^+][NTf_2^-]$ IL was synthesized by mixing equimolar amounts of the $[N_{8,8,8,Bz}^+][Br^-]$ IL and $[Li^+][NTf_2^-]$ overnight in 30 mL of methanol. The $[P_{6,6,6,14}^+][NTf_2^-]$ and $[N_{8,8,8,Bz}^+][NTf_2^-]$ ILs was subsequently purified with diethyl ether and characterized by ^{1}H NMR as shown in Figure 3-S3 and 3-S4, respectively. Elemental analysis results were acquired using a Thermo FlashSmart 2000 CHNS/O Combustion Elemental Analyzer (Thermo Scientific, Waltham, MA, USA). Carbon/hydrogen/nitrogen (CHN) calculated for $[P_{6,6,6,14}^+][Ni(Phtfacac)_3^-]$: %C = 62.68, %H = 7.30, %N = 0.00; Found: %C = 62.27, %H = 7.34, %N = 0.11. Calculated for $[N_{8,8,8,Bz}^+][Ni(hfacac)_3^-]$: %C = 49.12, %H = 5.47, and %N = 1.25; Found: %C = 49.54, %H = 5.39, %N = 1.37.

3.2.3 qPCR Assays and Conditions

A 3.9 Kbp plasmid from Eurofin Genomics containing either a 166 bp wild-type *KRAS*, 166 bp G12S *KRAS*, or 210 wild-type *BRAF* insert was individually amplified by PCR. The PCR products were subsequently separated on a 1% agarose gel. Amplified DNA was recovered from the gel using the QIAquick Gel Extraction kit (Qiagen, Hilden, Germany) according to the

manufacturer's instructions. The purified DNA was quantified using a NanoDrop 2000c spectrophotometer (Thermo Scientific, Waltham, MA, USA).

A Bio-Rad CFX96 Touch Real-time PCR (Hercules, CA, USA) was utilized for qPCR amplification of the *KRAS* and *BRAF* targets using the following program: 10 min initial denaturation at 95 °C followed by 40 cycles comprised of a 15 s denaturation step at 95 °C and a 1 min annealing step. After each cycle, an optical detection step was used to track the reaction in real-time. The qPCR products were heated from 65°C to 95°C in 0.5°C increments. Melt curve analysis of 30 ppm of a 15-mer oligonucleotide to either a complementary sequence and a sequence containing a 1 nucleotide (nt) mismatch was achieved using the following program: initial 5 min denaturation step at 90°C, 10 min annealing step at 20°C, and a ramp from 20°C to 95°C in 0.5°C increments.

The amount of *KRAS* primers, *BRAF* primers, wild-type *KRAS* probe, G12S *KRAS* probe, *BRAF* probe, EDTA, and $MgCl_2$ was optimized to ensure efficient amplification. Annealing temperatures were optimized (54-65 °C) to ensure allelic discrimination between all three DNA sequences, as determined using the Bio-Rad CFX Maestro software. Amplification of target DNA standards was achieved using the following assay conditions: 1x Taqman universal PCR mastermix, 1.25 mM $MgCl_2$, 1 µM forward *KRAS* primers, 1 µM reverse *KRAS* primers, 1 µM forward *BRAF* primers, 1 µM reverse *BRAF* primers, 150 nM wild-type *KRAS* probe, 150 nM G12S *KRAS* probe, and 150 nM *BRAF* probe. The addition of 0.3 µL $[P_{6,6,6,14}^{+}][Ni(hfacac)_3^{-}]$ MIL to a 20 µL multiplex-qPCR mixture required 1x Taqman universal PCR mastermix, 1.25 mM $MgCl_2$, 1 µM forward *KRAS* primers, 1 µM reverse *KRAS* primers, 1 µM forward *BRAF* primers, 1 µM reverse *BRAF* primers, 150 nM wild-type *KRAS* probe, 150 nM G12S *KRAS* probe, and 150 nM *BRAF* probe. The addition of 0.3 µL $[P_{6,6,6,14}^{+}][Ni(Phtfacac)_3^{-}]$ MIL to a 20

µL multiplex-qPCR mixture required 1x Taqman universal PCR mastermix, 1.25 mM $MgCl_2$, 1 µM forward *KRAS* primers, 1 µM reverse *KRAS* primers, 1 µM forward *BRAF* primers, 1 µM reverse *BRAF* primers, 75 nM wild-type *KRAS* probe, 250 nM G12S *KRAS* probe, and 150 nM *BRAF* probe. qPCR amplification with 0.3 µL of the $[N_{8,8,8,Bz}^+][Ni(hfacac)_3^-]$ MIL was achieved using the 1x Taqman universal PCR mastermix, 2 mM EDTA, 1.25 mM $MgCl_2$, 1 µM forward *KRAS* primers, 1 µM reverse *KRAS* primers, 1 µM forward *BRAF* primers, 1 µM reverse *BRAF* primers, 150 nM wild-type *KRAS* probe, 150 nM G12S *KRAS* probe, and 150 nM *BRAF* probe for a final volume of 20 µL. Melt curves of qPCR products were achieved by adding 2x SYBR Green I to the reaction tube containing MIL and 1x SYBR Green I for standard reactions.

The quantitation cycle (Cq) was determined using the fluorescence threshold provided by the Bio-Rad CFX Maestro software and used to determine the amount of wild-type *KRAS*, G12S *KRAS*, and wild-type *BRAF* extracted by the hydrophobic MIL. Standard curves were constructed for wild-type *KRAS*, G12S *KRAS*, and wild-type *BRAF* template with and without MIL present in the multiplex-qPCR buffer. The standard curves were used to determine the concentration of DNA initially present in the reaction. The enrichment factor obtained for each extraction was calculated using equation 1, where C_{MIL} is the concentration of a one of the DNA fragments extracted by the MIL and C_{Std} represents the concentration of template in the aqueous sample solution prior to extraction. Preconcentration is achieved when the enrichment factor was above 1.

$$Enrichment\ Factor = \frac{C_{MIL}}{C_{Std}} \qquad \text{Equation 1}$$

3.2.4 Examining the Capture of Fluorophore during MIL-qPCR

In order to investigate the drop in fluorescence signal upon adding the hydrophobic MIL to the multiplex-qPCR system, 150 nM Cy5 probe was incubated with 0.3 µL of MIL. The static

extraction proceeded for 10 min before determining the amount of fluorophore remaining in the aqueous phase using a Biotek Synergy H1 Multi-mode microplate reader (Winooski, VT, USA) using an excitation and emission wavelength of 646 nm and 665 nm respectively. A 150 nM solution of Cy5 and 0.3 µL of MIL was subjected to qPCR cycling to track the decrease in fluorescence signal throughout the reaction. Prior to thermal cycling, all samples were heated at 50 °C for 2 min and 95 °C for 10 min in order to mimic the multiplex-qPCR procedure.

3.2.5 Capture of Target DNA

The general procedure used to extract target DNA fragments using DLLME is shown in Fig 3-1. A 1.0 mL solution of 0.5 fg μL^{-1} wild-type *KRAS*, 0.5 fg μL^{-1} G12S *KRAS*, and 0.5 fg μL^{-1} wild-type *BRAF* targets was prepared in 2 mM Tris buffer (pH 8). An optimized volume of MIL was dispersed using a Barnstead/Thermolyne Type 16700 mixer (Dubuque, IA, USA) for a specific length of time. After dispersing the hydrophobic MIL, DNA-enriched MIL droplets were collected using a rod magnet (B = 0.66 T). The recovered MIL was washed with deionized water, and a 0.3 µL aliquot of DNA-enriched MIL was placed in a qPCR tube for downstream analysis. For all extractions using human plasma, 0.5 fg μL^{-1} wild-type *KRAS*, 0.5 fg μL^{-1} G12S *KRAS*, and 0.5 fg μL^{-1} wild-type *BRAF* was spiked into the plasma.

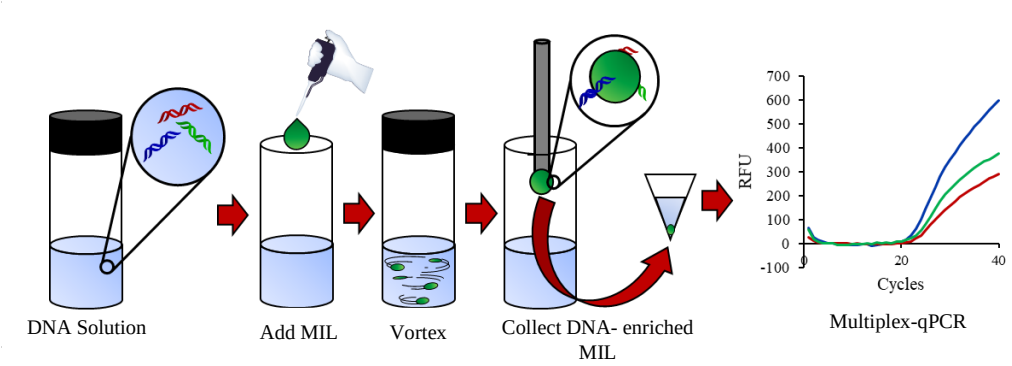

Figure 3-1 General procedure used to extract and detect wild-type *KRAS*, G12S *KRAS*, and *BRAF* DNA. DNA-enriched MIL was added to the reaction buffer for multiplex-qPCR detection using three different Taqman probes

DNA extractions using the QiaAMP DNA mini kit were performed as specified by the manufacturer. Briefly, 16 units of proteinase K were added to 1 mL 0.5 fg μL^{-1} wild-type *KRAS*, 0.5 fg μL^{-1} G12S *KRAS*, and 0.5 fg μL^{-1} wild-type *BRAF* target. A 1 mL volume of lysis buffer (AL buffer) was added to the sample and allowed to incubate for 10 min at 56 °C. Next, 1 mL of ethanol was added to the sample before placing the solution into a spin column. The column was centrifuged for 1 min at 1.3×10^4 rpm. The flow through was discarded and 0.5 mL of wash buffer 1 (AW1 buffer) was added to the column. The sample was centrifuged again for 1 min. The flow through was discarded and 0.5 mL of wash buffer 2 (AW2 buffer) was placed in the column. The column was then centrifuged for 3 min at 1.3×10^4 rpm and the flow through discarded. The column was again centrifuged for an additional minute to ensure that the wash buffers were thoroughly removed from the column. Lastly, 20 µL or 200 µL of elution buffer (AE buffer) were added to the column to elute the DNA.

Extractions using the Dynabeads myone silane magnetic beads were performed as recommended by the manufacturer. Briefly, 16 units of proteinase K were added to 0.5 fg μL^{-1} wild-type *KRAS*, 0.5 fg μL^{-1} G12S *KRAS*, and 0.5 fg μL^{-1} wild-type *BRAF* target and allowed to incubate for 2 min. Afterwards, 350 µL of 6 M guanidine hydrochloride was added to the sample and allowed to incubate for 10 min at 55 °C. Isopropanol (400 µL) and 2 mg of magnetic beads were then added to the sample. The beads were dispersed for 30 s using a vortex and then agitated on an Eppendorf I24R incubator shaker (Eppendorf, Hamburg, Germany) at 100 rpm. The sample was subsequently vortexed again for 30 s and the beads collected on a 0.9 T magnet. The aqueous phase was removed, and the beads were washed three times using 950 µL isopropanol. After the final wash step, the beads were dried using air to ensure that isopropanol

did not contaminate the reaction. The beads were suspended in 50 µL 2 mM Tris buffer and vortexed for 2 min to desorb captured DNA.

3.3 Results and Discussion

3.3.1 Optimization of Multiplex-qPCR Assay

A multiplex-qPCR system containing no MIL was first optimized to ensure good efficiency and allelic discrimination among the three DNA fragments. The concentration of primers (500-1250 nM), probes (75-350 nM), and $MgCl_2$ (0-5 mM) was optimized for the standard reaction. The annealing temperature was optimized (54-64°C) in order to discriminate between SNPs. An optimum annealing temperature of 63 °C was chosen as it exhibited good allelic discrimination for the standard reactions, as shown in Figure 3-S5. A standard curve was then generated for each DNA sequence, as shown in Figure 3-S6.

In order to successfully integrate a hydrophobic MIL into the multiplex-qPCR system, the concentration of EDTA was optimized between a range of 0-6 mM for each MIL-multiplex-qPCR. EDTA is capable of chelating solubilized metal ions thereby preventing PCR inhibition caused by the anion component of the MIL.[34,35] The $[P_{6,6,6,14}^+][Ni(hfacac)_3^-]$ and

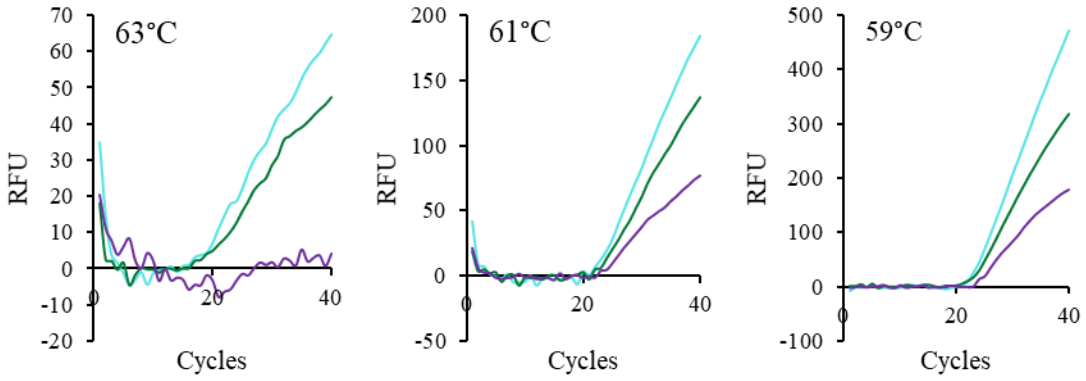

Figure 3-2 qPCR curves of (green) wild-type *KRAS*, (blue) G12S *KRAS*, (violet) wild-type *BRAF* generated by spiking 0.3 µL of the $[P_{6,6,6,14}^+][Ni(hfacac)_3^-]$ MIL into the reaction and annealing at 59, 61, and 63 °C.

$[P_{6,6,6,14}^+][Ni(Phtfacac)_3^-]$ MILs did not require additional EDTA in order to achieve amplification, and the $[N_{8,8,8,Bz}^+][Ni(hfacac)_3^-]$ MIL only required 2 mM EDTA. However, the high annealing temperature (63 °C) used for the standard reactions significantly inhibited the reaction, as shown in Figure 3-2. Therefore, the annealing temperature was optimized at 59 °C for the $[P_{6,6,6,14}^+][Ni(hfacac)_3^-]$ and $[P_{6,6,6,14}^+][Ni(Phtfacac)_3^-]$ MILs and 62 °C for the $[N_{8,8,8,Bz}^+][Ni(hfacac)_3^-]$ MIL in order to relieve inhibition but still permit the SNPs to be distinguished from each other. Afterwards, the concentration of $MgCl_2$ was optimized between 0-5 mM to ensure optimum qPCR efficiency during simultaneous amplification of all three DNA sequences; 2.5 mM $MgCl_2$ was selected as the optimum concentration of all three MILs examined.

After optimizing the multiplex reaction buffer, allelic discrimination plots and standard curves were developed for the three MILs. As shown in Figure 3-3, integration of the $[P_{6,6,6,14}^+][Ni(hfacac)_3^-]$, $[N_{8,8,8,Bz}^+][Ni(hfacac)_3^-]$, $[P_{6,6,6,14}^+][Ni(Phtfacac)_3^-]$ MILs into the multiplex-qPCR buffer still allowed for distinct clusters when plotting the endpoint fluorescence signal associated with each probe. The plots show that discrimination between different DNA sequences could be achieved when the MIL was added to the reaction buffer. In addition, the amplification efficiencies fell to between 90-110%, as shown in Figure S7, suggesting that DNA is successfully being duplicated with each cycle.

3.3.2 Investigation into Primer Annealing

Previous studies have suggested that ILs and MILs can decrease the melting temperature (Tm) of DNA fragments.[36,41] In this study, the same phenomenon was observed when optimizing the annealing temperature and performing melt curves of a 15-mer DNA fragment (see Figure 3-4). This is interesting as slight increases in ionic strength can significantly increase the melting

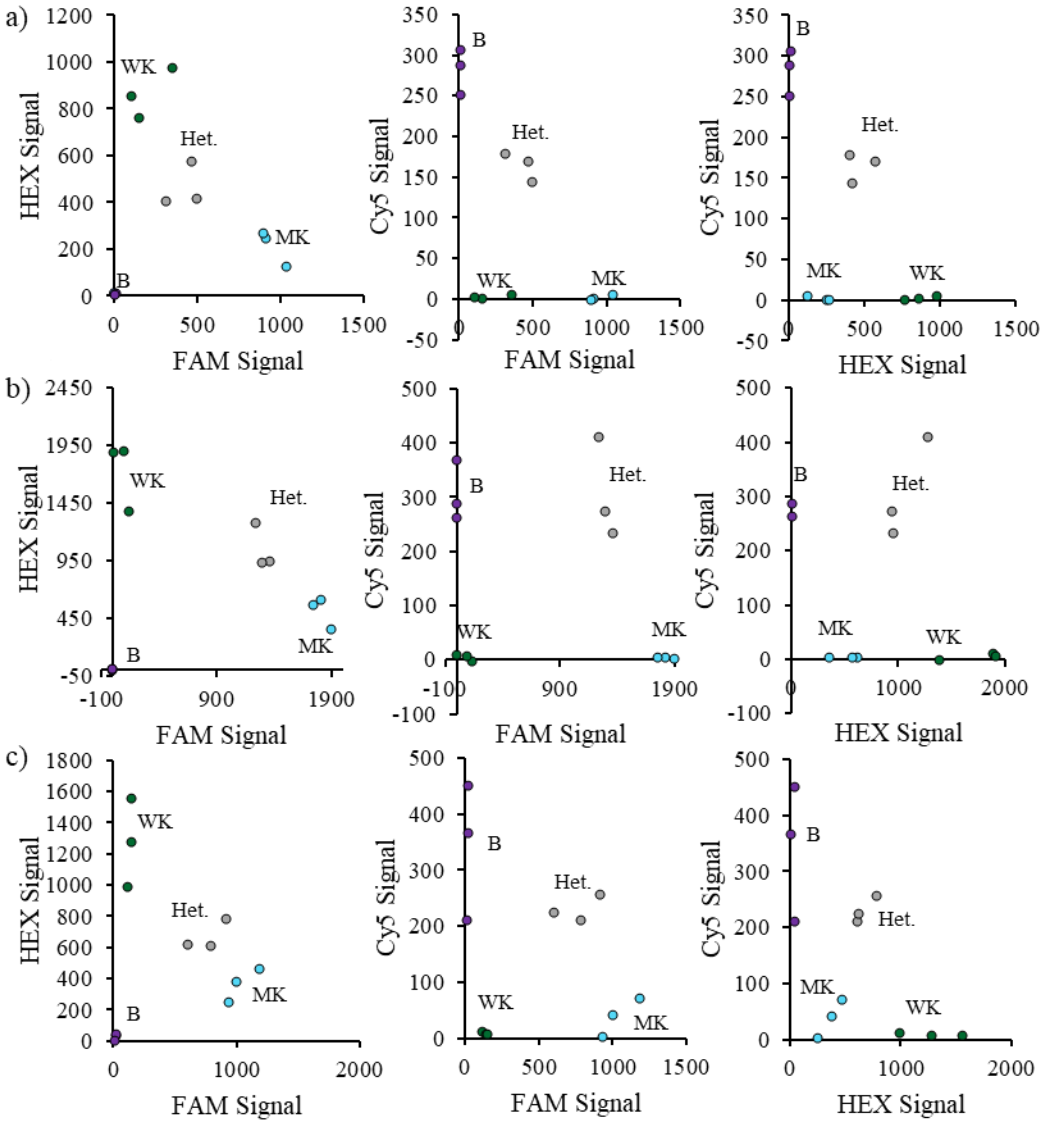

Figure 3-3 Allelic discrimination associated with spiking DNA into the multiplex-qPCR system containing the (a) $[P_{6,6,6,14}^+][Ni(hfacac)_3^-]$, (b) $[N_{8,8,8,Bz}^+][Ni(hfacac)_3^-]$, and (c) $[P_{6,6,6,14}^+][Ni(Phtfacac)_3^-]$ MILs. Het., heterozygous; B, wild-type *BRAF*; WK, wild-type *KRAS*; MK, G12S *KRAS*. Triplicate reactions were performed for each cluster.

temperature of DNA.[42] The melting temperature also decreased when adding an equimolar amount of $[P_{6,6,6,14}^+][NTf_2^-]$ and $[N_{8,8,8,Bz}^+]NTf_2^-]$ ILs to the buffer, as shown in Figure 3-4. This finding suggests that the cation is responsible for the decrease in annealing temperature. It is likely that the cation is undergoing hydrophobic interactions with DNA fragments allowing for a

decrease in annealing temperature similar to the behavior of cationic surfactants when present at concentrations below the critical micelle concentration.[42]

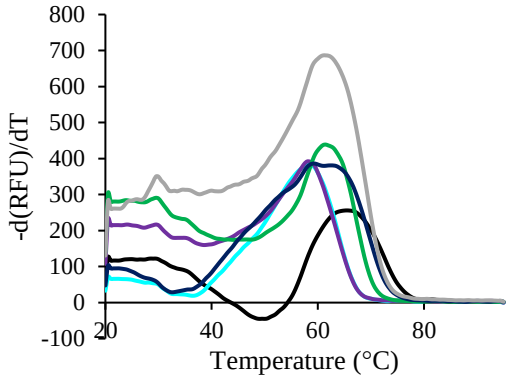

Figure 3-4 Melt curves of a 15-mer DNA oligonucleotide in the presence of (green) $[P_{6,6,6,14}^+][Ni(hfacac)_3^-]$, (blue) $[N_{8,8,8,Bz}^+][Ni(hfacac)_3^-]$, (violet) $[P_{6,6,6,14}^+][Ni(Phtfacac)_3^-]$, (grey) $[N_{8,8,8,Bz}^+][NTf_2^-]$, and (navy) $[P_{6,6,6,14}^+][NTf_2^-]$ ILs compared to a (black) standard without IL.

The melting temperatures of a 1 nt mismatch fragment and 15-mer oligonucleotide were also examined. As shown in Table S2, the $[P_{6,6,6,14}^+][Ni(hfacac)_3^-]$ MIL did not stabilize the mismatch whereas the mismatch was slightly destabilized when the $[P_{6,6,6,14}^+][Ni(Phtfacac)_3^-]$ MIL was added to the buffer. However, in the case of the $[N_{8,8,8,Bz}^+][Ni(hfacac)_3^-]$ MIL, the mismatch was stabilized by adding the MIL into the buffer, which explains the observation that a higher annealing temperature is required in order to differentiate between the wild-type and mutant *KRAS* fragments.

The melting temperatures of the 89 bp G12S *KRAS* DNA were examined in order to determine the extent to which the three hydrophobic MILs affect longer DNA sequences. As shown in Figure 3-S8, there was no significant difference between the melting temperatures of DNA when the MIL is present compared to the standard, suggesting that the MIL interacts stronger with shorter DNA fragments. Therefore, melt curves should be able to identify DNA fragments when the MIL is present in the qPCR buffer.[43] As shown in Figure 3-S9, the melt

curves after MIL-DLLME and direct qPCR amplification were within 0.5 °C from the standard. This suggests that the MIL does not alter the DNA sequence during either the extraction or PCR amplification, as has been reported in previous studies.[15,34,35]

3.3.3 Partitioning of the Hydrophobic Probe to the MIL Phase

When the hydrophobic MILs were added to the reaction buffer, the fluorescence signal drastically decreased compared to the standard. In previous studies, inhibition caused by SYBR Green I partitioning to the MIL phase during qPCR was relieved by adding additional SYBR Green I to the buffer.[35,37] However, increasing the concentration of the Taqman probe generally did not enhance the fluorescence signal. To investigate whether inhibition originates from the fluorophore partitioning to the MIL phase or MIL quenching the signal, a 150 nM solution of Cy5 was incubated with 0.3 µL of each of the three hydrophobic MILs. A six-point standard curve of Cy5 (see Figure 3-S10a) was generated to quantify the amount of Cy5 extracted by the MIL. As shown in Figure 3-S10b, extraction efficiencies of 50.27 ± 0.28%, 26.11 ± 1.68%, and 37.18 ± 1.27% for Cy5 were obtained with the $[P_{6,6,6,14}^+][Ni(hfacac)_3^-]$, $[P_{6,6,6,14}^+][Ni(Phtfacac)_3^-]$, and $[N_{8,8,8,Bz}^+][Ni(hfacac)_3^-]$ MILs, respectively, after sitting at room temperature for 10 min. The effect of PCR cycling on the partitioning of Cy5 to the MIL was also investigated, as shown in Figure 3-S11. Extraction efficiencies plateaued with increasing cycles for the $[P_{6,6,6,14}^+][Ni(hfacac)_3^-]$ and $[N_{8,8,8,Bz}^+][Ni(hfacac)_3^-]$ MILs, suggesting quenching of the fluorophore by MIL that dissolves into the aqueous phase at elevated temperatures used in PCR.[36,44]

3.3.4 Optimization of MIL-DLLME Method

Cell-free DNA (cfDNA) is generally present at the ng mL^{-1} level in plasma.[8,45,46] However, ctDNA can comprise less than 0.01% of the total amount of cfDNA depending on the

type and stage of cancer.[2,46] Therefore, a clinically relevant concentration of 0.5 fg μL^{-1} wild-type *KRAS*, 0.5 fg μL^{-1} G12S *KRAS*, and 0.5 fg μL^{-1} wild-type *BRAF* fragments was used during optimization in this study.

The volume of MIL dispersed was first optimized to achieve the highest enrichment factors. As shown in Figure 3-S12, optimal volumes for the $[P_{6,6,6,14}^+][Ni(hfacac)_3^-]$, $[N_{8,8,8,Bz}^+][Ni(hfacac)_3^-]$, and $[P_{6,6,6,14}^+][Ni(Phtfacac)_3^-]$ MILs were found to be 6, 8, and 6 µL, respectively. Similar to previously reported studies, lower volumes of MIL were capable of achieving higher enrichment factors compared to larger volumes of MIL, suggesting that extracted DNA is being diluted within the MIL.[32,35,37] Subsequently, the extraction time was optimized. The optimum extraction times for the $[P_{6,6,6,14}^+][Ni(hfacac)_3^-]$, $[N_{8,8,8,Bz}^+][Ni(hfacac)_3^-]$, and $[P_{6,6,6,14}^+][Ni(Phtfacac)_3^-]$ MILs were found to be 2, 2, and 3 min, respectively, as shown in Figure 3-S13.

In order to ensure that the three sequences can still be distinguished from each other after desorbing DNA from the MIL, allelic discrimination plots were generated for all three MILs by extracting only one DNA fragment using the optimized procedure. Distinct clusters were still observed when plotting the fluorescence signals (see Figure 3-S14) suggesting that the desorption of DNA from the MIL does not affect the ability of the reaction to discriminate between the different DNA sequences, even if the sequences are SNPs. As shown in Figure 3-S15, similar enrichment factors were achieved when extracting either one or all three DNA fragments. The mutation load of *KRAS* was found to be on average 8.4% during stage II/III colorectal cancer and 21.8% during stage IV.[47] Therefore, the MIL-multiplex-qPCR system was evaluated by performing extractions of 0.5 and 5% G12S *KRAS*. As shown in Fig. S16, when G12S *KRAS* is present at 0.5 fg μL^{-1} (10-fold less compared to wild-type *KRAS* and *BRAF*) the

reaction was not significantly affected in the case of all three MILs. However, when the concentration of G12S *KRAS* was 100-fold less than wild-type *KRAS* and *BRAF*, the efficiency was significantly impacted (see Fig. S17) due to the consumption of PCR reagents.[14,48,49] In order to improve the sensitivity, future studies should investigate using a sequence-specific DNA extraction or PCR clamp to limit the amount of wild-type DNA amplified.

3.3.5 Extractions from a Plasma Matrix

Plasma matrices are highly complex and contain a number of PCR inhibitors such as albumin, immunoglobulin G, and lactoferrin.[50,51] In addition, common anticoagulants such as EDTA or heparin can also inhibit PCR. Therefore, it is necessary to evaluate the performance of a ctDNA extraction procedure in plasma. The extraction of DNA from 10-fold diluted citrate plasma and 10-fold diluted Na_2EDTA plasma was evaluated to examine the effect of the anticoagulant on MIL-DLLME. As shown in Figure 3-S18, no significant difference was observed between the citrate and Na_2EDTA plasma when using the $[P_{6,6,6,14}^+][Ni(hfacac)_3^-]$ MIL. However, this was not the case when comparing the Na_2EDTA and citrate plasma with the $[N_{8,8,8,Bz}^+][Ni(hfacac)_3^-]$ and $[P_{6,6,6,14}^+][Ni(Phtfacac)_3^-]$ MILs, as determined using the Student's t-test (probability value < 0.05). In particular, there was a sharp decrease in enrichment factor when performing extractions from the 10-fold diluted citrate plasma with the $[N_{8,8,8,Bz}^+][Ni(hfacac)_3^-]$ MIL, as shown in Figure 3-S18b. There was also a slight decrease in enrichment factors when performing extractions from a 10-fold diluted citrate matrix with the $[P_{6,6,6,14}^+][Ni(Phtfacac)_3^-]$ MIL.

Although performing extractions from a diluted plasma matrix can be beneficial to reduce the matrix effect, a lower concentration of DNA is present. Therefore, different dilutions of Na_2EDTA plasma were examined with the $[N_{8,8,8,Bz}^+][Ni(hfacac)_3^-]$ and $[P_{6,6,6,14}^+][Ni(Phtfacac)_3^-]$

MILs as they exhibited the best performance in 10-fold diluted plasma. Preconcentration was still achieved in 2 and 4-fold diluted plasma with the $[N_{8,8,8,Bz}^+][Ni(hfacac)_3^-]$ MIL and 4-fold diluted plasma with the $[P_{6,6,6,14}^+][Ni(Phtfacac)_3^-]$ MIL, as shown in Figure 3-5. Enrichment factors of 0.64 ± 0.11, 0.69 ± 0.14, and 0.64 ± 0.09 were achieved for wild-type *KRAS*, G12S *KRAS*, and wild-type *BRAF* from undiluted plasma with the $[P_{6,6,6,14}^+][Ni(Phtfacac)_3^-]$ MIL, as shown in Figure 3-5b. The results were not reproducible when attempting to use the $[N_{8,8,8,Bz}^+][Ni(hfacac)_3^-]$ MIL as an extraction solvent in undiluted plasma. In order to determine whether qPCR inhibitors are co-extracted by the MIL, a standard curve was generated by carrying out extractions from 10-fold diluted plasma for the $[P_{6,6,6,14}^+][Ni(hfacac)_3^-]$ MIL and 4-fold diluted plasma for the $[N_{8,8,8,Bz}^+][Ni(hfacac)_3^-]$ and $[P_{6,6,6,14}^+][Ni(Phtfacac)_3^-]$ MILs. Reaction efficiencies between 90-110% were achieved with the $[P_{6,6,6,14}^+][Ni(hfacac)_3^-]$ and $[P_{6,6,6,14}^+][Ni(Phtfacac)_3^-]$ MILs, suggesting that PCR inhibitors are not being co-extracted by this MIL (see Figure 3-S19). However, the $[N_{8,8,8,Bz}^+][Ni(hfacac)_3^-]$ MIL produced an efficiency of 119.4%, 113.2%, and 149.4% for wild-type *KRAS*, G12S *KRAS*, and wild-type *BRAF*, respectively, when extracting from 4-fold diluted plasma. These high efficiencies suggest that the DNA polymerase activity is being inhibited by a plasma component that was co-extracted by the MIL.[52]

3.3.6 Comparison to Commercial DNA Extraction Procedures

Commercial means of extracting ctDNA utilize silica-based magnetic beads and silica-based spin columns.[18,45] However, these methods require several lengthy sample handling steps (i.e, centrifugation or collection of magnetic beads) that can increase the probability of contamination. There have also been reports suggesting that commercial-based methods suffer at extracting low concentrations of DNA.[18] Therefore, the enrichment factors achieved using the

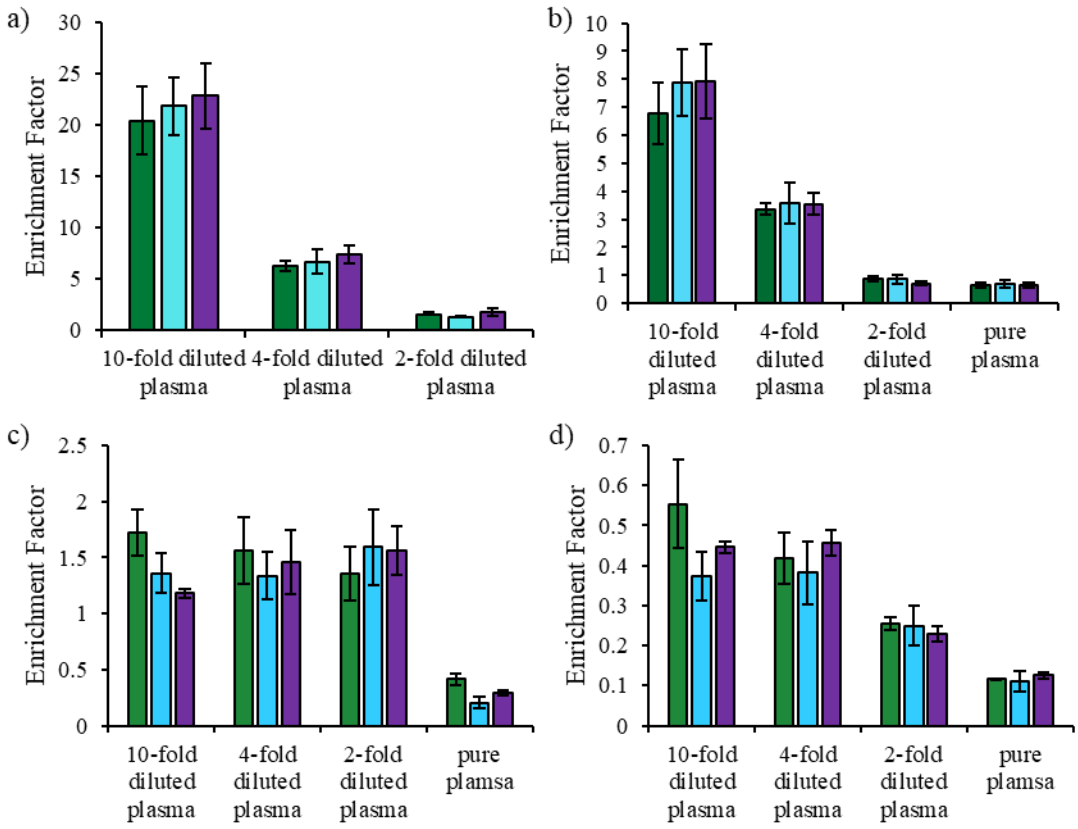

Figure 3-5 Extractions of (green) wild-type *KRAS*, (blue) G12S *KRAS*, and (violet) wild-type *BRAF* from diluted plasma containing Na_2EDTA as an anticoagulant with the (a) $[N_{8,8,8,Bz}^+][Ni(hfacac)_3^-]$ MIL, (b) $[P_{6,6,6,14}^+][Ni(Phtfacac)_3^-]$ MIL, (c) QiAMP spin columns, and (d) Dynabeads myone silane magnetic beads. Wild-type *KRAS*, G12S *KRAS*, and wild-type *BRAF* template concentration: 0.5 fg μL^{-1}, sample volume: 1.0 mL; $[P_{6,6,6,14}^+][Ni(hfacac)_3^-]$ volume: 6 µL; $[N_{8,8,8,Bz}^+][Ni(hfacac)_3^-]$ volume: 8 µL; $[P_{6,6,6,14}^+][Ni(Phtfacac)_3^-]$ volume: 6 µL; magnetic bead mass: 2 mg. Triplicate extractions were performed under each condition.

optimized MIL-DLLME method were compared to commercial magnetic bead and silica columns. As shown in Figure 3-6, the MIL-DLLME method produced higher enrichment factors when extracting target DNA fragments from 2 mM Tris buffer. Although the columns extracted most of the DNA present in solution, enrichment factors were poor compared to the MIL-DLLME method likely due to the high desorption volume (200 µL) recommended by the manufacturer. However, changing the desorption volume to 20 µL only slightly improved the E_f (see Figure 3-6). The similar enrichment factors between the two desorption volumes suggests

that at lower elution volumes there is not enough buffer to sufficiently elute the DNA.[45] The $[N_{8,8,8,Bz}^{+}][Ni(hfacac)_3^{-}]$ and $[P_{6,6,6,14}^{+}][Ni(Phtfacac)_3^{-}]$ MILs outperformed commercial methods when performing extractions from 4- and 10-fold diluted plasma. The $[N_{8,8,8,Bz}^{+}][Ni(hfacac)_3^{-}]$ MIL produced similar enrichment factors to the QiaAMP spin columns with 2-fold diluted plasma. However, extractions using the QiaAMP spin columns and Dynabeads myone silane magnetic beads were not affected by higher concentrations of plasma compared to the MILs, as shown in Figure 3-5. In addition, extractions from pure plasma were reproducible using the QiaAMP spin columns and Dynabeads myone silane magnetic beads. However, enrichment factors associated with the $[P_{6,6,6,14}^{+}][Ni(Phtfacac)_3^{-}]$ MIL were significantly higher than both of the silica-based DNA extraction methods as determined using the Student's t-test (probability value < 0.05).

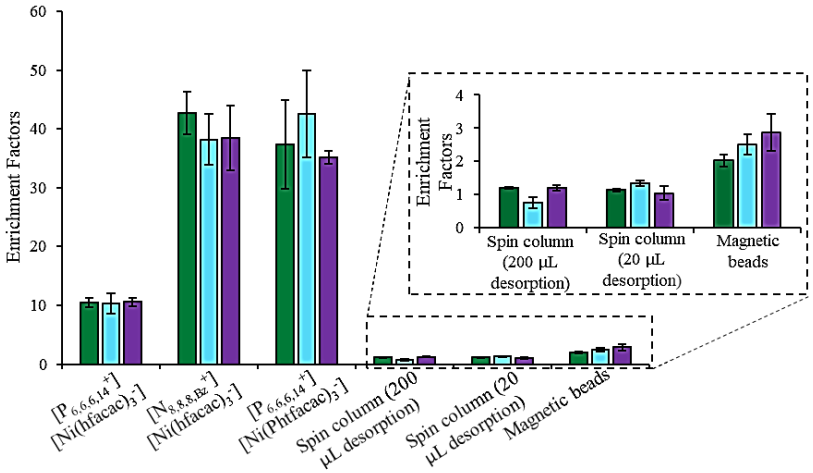

Figure 3-6 Enrichment factors of (green) wild-type *KRAS*, (blue) G12S *KRAS*, and (violet) wild-type *BRAF* obtained for the optimized MIL-DLLME and commercial methods using the $[P_{6,6,6,14}^{+}][Ni(hfacac)_3^{-}]$ MIL, $[N_{8,8,8,Bz}^{+}][Ni(hfacac)_3^{-}]$ MIL, $[P_{6,6,6,14}^{+}][Ni(Phtfacac)_3^{-}]$ MIL, QiaAMP spin column (desorption volume 200 µL), QiaAMP spin column (desorption volume 20 µL), and Dynabeads myone silane magnetic beads. Wild-type *KRAS*, G12S *KRAS*, and wild-type *BRAF* template concentration: fg μL^{-1}, sample volume: 1.0 mL; $[P_{6,6,6,14}^{+}][Ni(hfacac)_3^{-}]$ volume: 6 µL; $[N_{8,8,8,Bz}^{+}][Ni(hfacac)_3^{-}]$ volume: 8 µL; $[P_{6,6,6,14}^{+}][Ni(Phtfacac)_3^{-}]$ volume: 6 µL; magnetic bead mass: 2 mg. Triplicate extractions were performed using each extraction method.

3.4 Conclusions

Therefore, three MILs were utilized to rapidly preconcentrate clinically-relevant concentrations of ctDNA within 2-3 min. Integrating the MIL into a custom designed multiplex-qPCR assay allows for a simple method to desorb DNA from the hydrophobic MIL. The addition the MIL into the multiplex-qPCR buffer did not have a deleterious effect on the amplification efficiency when simultaneously amplifying three DNA fragments, and the fragments could easily be discerned from each other using allelic discrimination plots. However, in order to achieve amplification as well as allelic discrimination, the annealing temperature was lower compared to the standard reaction due to hydrophobic interactions between the MIL and probe. Enrichment factors as high as 42.68 ± 3.63, 38.16 ± 4.30, and 38.78 ± 5.52 were obtained from Tris buffer for the wild-type *KRAS*, G12S *KRAS*, and wild-type *BRAF*, respectively, using the $[N_{8,8,8,Bz}^{+}][Ni(hfacac)_3^{-}]$ MIL, and preconcentration was still obtainable while dispersing the MIL in 2, 4, and 10-fold diluted plasma. Compared to commercial kits, the MIL-based extraction was better at preconcentrating DNA fragments from a plasma matrix with the $[P_{6,6,6,14}^{+}][Ni(Phtfacac)_3^{-}]$ MIL capable of achieving enrichment factors over 0.6 for all three DNA fragments from undiluted plasma whereas enrichment factors above of 0.3 and 0.1 were achieved with the QiaAMP spin columns and dynabeads myone silane magnetic beads, respectively. The low enrichment factors from the kits are in part due to the high desorption volumes required to sufficiently desorb DNA compared to the MILs. The ability of MILs to rapidly preconcentrate DNA from plasma is essential in ctDNA analysis especially during the early stages of cancer where there are low abundances of mutant DNA. Therefore, the MIL-DLLME method has potential to be highly beneficial towards ctDNA analysis in clinically-relevant samples.

Acknowledgments

Nabeel Abbasi and Muhammad Qamar Farooq are thanked for their assistance in this study. J. L. A acknowledges funding from the Chemical Measurement and Imaging Program at the National Science Foundation (CHE-1709372).

References

(1) Bettegowda, C.; Sausen, M.; Leary, R. J.; Kinde, I.; Wang, Y.; Agrawal, N.; Bartlett, B. R.; Wang, H.; Luber, B.; Alani, R. M.; et al. Detection of Circulating Tumor DNA in Early- and Late-Stage Human Malignancies. Sci. Transl. Med. 2014, 6 (224), 224ra24-224ra24.

(2) Diehl, F.; Li, M.; Dressman, D.; He, Y.; Shen, D.; Szabo, S.; Diaz, L. A.; Goodman, S. N.; David, K. A.; Juhl, H.; et al. Detection and Quantification of Mutations in the Plasma of Patients with Colorectal Tumors. Proc. Natl. Acad. Sci. U. S. A. 2005, 102 (45), 16368–16373.

(3) Xu, S.; Lou, F.; Wu, Y.; Sun, D.; Zhang, J.; Chen, W.; Ye, H.; Liu, J.; Wei, S.; Zhao, M.; et al. Circulating Tumor DNA Identified by Targeted Sequencing in Advanced-Stage Non-Small Cell Lung Cancer Patients. Cancer Lett. 2016, 370, 324–331.

(4) Rodda, A. E.; Parker, B. J.; Spencer, A.; Corrie, S. R. Extending Circulating Tumor DNA Analysis to Ultralow Abundance Mutations: Techniques and Challenges. ACS Sensors 2018, 3, 540–560.

(5) Kidess, E.; Heirich, K.; Wiggin, M.; Vysotskaia, V.; Visser, C.; Marziali, A.; Wiedenmann, B.; Norton, J. A.; Lee, M.; Jeffrey, S. S.; et al. Mutation Profiling of Tumor DNA from Plasma and Tumor Tissue of Colorectal Cancer Patients with a Novel , High-Sensitivity Multiplexed Mutation Detection Platform. Oncotarget 2014, 6 (4), 2549–2561.

(6) Spindler, K.-L. G.; Pallisgaard, N.; Vogelius, I.; Jakobsen, A. Quantitative Cell-Free DNA, KRAS, and BRAF Mutations in Plasma from Patients with Metastatic Colorectal Cancer during Treatment with Cetuximab and Irinotecan. Clin. Cancer Res. 2012, 18 (4), 1177–1185.

(7) De Roock, W.; Claes, B.; Bernasconi, D.; De Schutter, J.; Biesmans, B.; Fountzilas, G.; Kalogeras, K. T.; Kotoula, V.; Papamichael, D.; Laurent-Puig, P.; et al. Effects of KRAS, BRAF, NRAS, and PIK3CA Mutations on the Efficacy of Cetuximab plus Chemotherapy in Chemotherapy-Refractory Metastatic Colorectal Cancer: A Retrospective Consortium Analysis. Lancet Oncol. 2010, 11 (8), 753–762.

(8) Kelley, S. O. What Are Clinically Relevant Levels of Cellular and Biomolecular Analytes? ACS Sensors 2017, 2, 193–197.

(9) Garrido, P., Olmedo, M. E., Gómez, A., Ares, L. P., López-Ríos, F.; Rosa-Rosa, J. M., Palacios, J. Treating KRAS-Mutant NSCLC: Latest Evidence and Clinical Consequences. Mult. Scler. J. 2017, 9 (9), 589–597.

(10) Edwards, M. C.; Gibbs, R. A. Multiplex PCR : Advantages , Development , and Applications. PCR Methods Appl. 1994, 3 (4), S65–S75.

(11) Navarro, E.; Serrano-Heras, G.; Castaño, M. J.; Solera, J. Real-Time PCR Detection Chemistry. Clin. Chim. Acta 2015, 439, 231–250.

(12) Holland, P. M.; Abramson, R. D.; Watson, R.; Gelfand, D. H. Detection of Specific Polymerase Chain-Reaction Product By Utilizing the 5'->3' Exonuclease Activity of Thermus Aquaticus DNA Polymerase. Proc. Natl. Acad. Sci. U. S. A. 1991, 88 (16), 7276–7280.

(13) Bustin, S. A.; Benes, V.; Garson, J. A.; Hellemans, J.; Huggett, J.; Kubista, M.; Mueller, R.; Nolan, T.; Pfaffl, M. W.; Shipley, G. L. The MIQE Guidelines : Minimum Information for Publication of Quantitative Real-Time PCR Experiments. Clin. Chem. 2009, 622, 611–622.

(14) Elnifro, E. M.; Ashshi, A. M.; Cooper, R. J.; Klapper, P. E. Multiplex PCR: Optimization and Application in Diagnostic Virology. Clin. Microbiol. Rev. 2000, 13 (4), 559–570.

(15) Clark, K. D.; Nacham, O.; Yu, H.; Li, T.; Yamsek, M. M.; Ronning, D. R.; Anderson, J. L. Extraction of DNA by Magnetic Ionic Liquids: Tunable Solvents for Rapid and Selective DNA Analysis. Anal. Chem. 2015, 87 (3), 1552–1559.

(16) Juang, D. S.; Berry, S. M.; Li, C.; Lang, J. M.; Beebe, D. J. Centrifugation-Assisted Immiscible Fluid Filtration for Dual-Bioanalyte Extraction. Anal. Chem. 2019, 91 (18), 11848–11855.

(17) Kramvis, A.; Bukofzer, S.; Kew, M. C. Comparison of Hepatitis B Virus DNA Extractions from Serum by the QIAamp Blood Kit, GeneReleaser, and the Phenol-Chloroform Method. J. Clin. Microbiol. 1996, 34 (11), 2731–2733.

(18) Sorber, L.; Zwaenepoel, K.; Deschoolmeester, V.; Roeyen, G.; Lardon, F.; Rolfo, C.; Pauwels, P. A Comparison of Cell-Free DNA Isolation Kits: Isolation and Quantification of Cell-Free DNA in Plasma. J. Mol. Diagnostics 2017, 19 (1), 162–168.

(19) Cao, W.; Easley, C. J.; Ferrance, J. P.; Landers, J. P. Chitosan as a Polymer for PH-Induced DNA Capture in a Totally Aqueous System. Anal. Chem. 2006, 78 (20), 7222–7228.

(20) Pandit, K. R.; Nanayakkara, I. A.; Cao, W.; Raghavan, S. R.; White, I. M. Capture and Direct Amplification of DNA on Chitosan Microparticles in a Single PCR-Optimal Solution. Anal. Chem. 2015, 87 (21), 11022–11029.

(21) Li, T.; Joshi, M. D.; Ronning, D. R.; Anderson, J. L. Ionic Liquids as Solvents for in Situ Dispersive Liquid-Liquid Microextraction of DNA. J. Chromatogr. A 2013, 1272, 8–14.

(22) Wang, J. H.; Cheng, D. H.; Chen, X. W.; Du, Z.; Fang, Z. L. Direct Extraction of Double-Stranded DNA into Ionic Liquid 1-Butyl-3-Methylimidazolium Hexafluorophosphate and Its Quantification. Anal. Chem. 2007, 79 (2), 620–625.

(23) Gonzalez García, E.; Ressmann, A. K.; Gaertner, P.; Zirbs, R.; Mach, R. L.; Krska, R.; Bica, K.; Brunner, K. Direct Extraction of Genomic DNA from Maize with Aqueous Ionic Liquid Buffer Systems for Applications in Genetically Modified Organisms Analysis. Anal. Bioanal. Chem. 2014, 406 (30), 7773–7784.

(24) Trujillo-Rodriguez, M. J.; Nan, H.; Varona, M.; Emaus, M. N.; Souza, I. D.; Anderson, J. L. Advances of Ionic Liquids in Analytical Chemistry. Anal. Chem. 2019, 91 (1), 505–531.

(25) An, J.; Trujillo-Rodríguez, M. J.; Pino, V.; Anderson, J. L. Non-Conventional Solvents in Liquid Phase Microextraction and Aqueous Biphasic Systems. J. Chromatogr. A 2017, 1500, 1–23.

(26) Lei, Z.; Chen, B.; Koo, Y. M.; Macfarlane, D. R. Introduction: Ionic Liquids. Chem. Rev. 2017, 117 (10), 6633–6635.

(27) Clark, K. D.; Nacham, O.; Purslow, J. A.; Pierson, S. A.; Anderson, J. L. Magnetic Ionic Liquids in Analytical Chemistry: A Review. Anal. Chim. Acta 2016, 934, 9–21.

(28) Del Sesto, R. E.; McCleskey, T. M.; Burrell, A. K.; Baker, G. a; Thompson, J. D.; Scott, B. L.; Wilkes, J. S.; Williams, P. Structure and Magnetic Behavior of Transition Metal Based Ionic Liquids. Chem. Commun. 2008, 447–449.

(29) Joseph, A.; Zyła, G.; Thomas, V. I.; Nair, P. R.; Padmanabhan, A. S.; Mathew, S. Paramagnetic Ionic Liquids for Advanced Applications: A Review. J. Mol. Liq. 2016, 218, 319–331.

(30) Lee, S. H.; Ha, S. H.; Ha, S. S.; Jin, H. B.; You, C. Y.; Koo, Y. M. Magnetic Behavior of Mixture of Magnetic Ionic Liquid [Bmim] Fe Cl4 and Water. J. Appl. Phys. 2007, 101 (9), 1–4.

(31) Emaus, M. N.; Zhu, C.; Anderson, J. L. Selective Hybridization and Capture of KRAS DNA from Plasma and Blood Using Ion-Tagged Oligonucleotide Probes Coupled to Magnetic Ionic Liquids. Anal. Chim. Acta 2020, 1094, 1–10.

(32) Marengo, A.; Cagliero, C.; Sgorbini, B.; Anderson, J. L.; Emaus, M. N.; Bicchi, C.; Bertea, C. M.; Rubiolo, P. Development of an Innovative and Sustainable One - Step Method for Rapid Plant DNA Isolation for Targeted PCR Using Magnetic Ionic Liquids. Plant Methods 2019, 1–11.

(33) Bowers, A. N.; Trujillo-Rodríguez, M. J.; Farooq, M. Q.; Anderson, J. L. Extraction of DNA with Magnetic Ionic Liquids Using in Situ Dispersive Liquid–Liquid Microextraction. Anal. Bioanal. Chem. 2019, 411 (28), 7375–7385.

(34) Clark, K. D.; Yamsek, M. M.; Nacham, O.; Anderson, J. L. Magnetic Ionic Liquids as PCR-Compatible Solvents for DNA Extraction from Biological Samples. Chem. Commun. 2015, 51 (94), 16771–16773.

(35) Emaus, M. N.; Clark, K. D.; Hinners, P.; Anderson, J. L. Preconcentration of DNA Using Magnetic Ionic Liquids That Are Compatible with Real-Time PCR for Rapid Nucleic Acid Quantification. Anal. Bioanal. Chem. 2018, 410 (17), 4135–4144.

(36) Ding, X.; Clark, K. D.; Varona, M.; Emaus, M. N.; Anderson, J. L. Magnetic Ionic Liquid-Enhanced Isothermal Nucleic Acid Amplification and Its Application to Rapid Visual DNA Analysis. Anal. Chim. Acta 2018, 1045, 132–140.

(37) Emaus, M. N.; Varona, M.; Anderson, J. L. Sequence-Specific Preconcentration of a Mutation Prone KRAS Fragment from Plasma Using Ion-Tagged Oligonucleotides Coupled to QPCR Compatible Magnetic Ionic Liquid Solvents. Anal. Chim. Acta 2019, 1068, 1–10.

(38) Farooq, M. Q.; Chand, D.; Odugbesi, G. A.; Varona, M.; Mudryk, Y.; Anderson, J. L. Investigating the Effect of Ligand and Cation on the Properties of Metal Fluorinated Acetylacetonate Based Magnetic Ionic Liquids. New J. Chem. 2019, 43, 11334–11341.

(39) Pierson, S. A.; Nacham, O.; Clark, K. D.; Nan, H.; Mudryk, Y.; Anderson, J. L. Synthesis and Characterization of Low Viscosity Hexafluoroacetylacetonate-Based Hydrophobic Magnetic Ionic Liquids. New J. Chem. 2017, 41 (13), 5498–5505.

(40) Nacham, O.; Clark, K. D.; Yu, H.; Anderson, J. L. Synthetic Strategies for Tailoring the Physicochemical and Magnetic Properties of Hydrophobic Magnetic Ionic Liquids. Chem. Mater. 2015, 27 (3), 923–931.

(41) Shi, Y.; Liu, Y.-L.; Lai, P.-Y.; Tseng, M.-C.; Tseng, M.-J.; Li, Y.; Chu, Y.-H. Ionic Liquids Promote PCR Amplification of DNA. Chem. Commun. 2012, 48 (43), 5325–5327.

(42) Rosa, M.; Dias, R.; Miguel, M. da G.; Lindman, B. DNA - Cationic Surfactant Interactions Are Different for Double- and Single-Stranded DNA. Biomacromolecules 2005, 6, 2164–2171.

(43) Han, Y.; Khu, D.-M.; Monteros, M. J. High-Resolution Melting Analysis for SNP Genotyping and Mapping in Tetraploid Alfalfa (Medicago Sativa L.). Mol. Breed. 2012, 29, 489–501.

(44) Santra, K.; Clark, K. D.; Maity, N.; Petrich, J. W.; Anderson, J. L. Exploiting Fluorescence Spectroscopy to Identify Magnetic Ionic Liquids Suitable for the Isolation of Oligonucleotides. J. Phys. Chem. B 2018, 122 (31), 7747–7756.

(45) Xue, X.; Teare, M. D.; Holen, I.; Zhu, Y. M.; Woll, P. J. Optimizing the Yield and Utility of Circulating Cell-Free DNA from Plasma and Serum. Clin. Chim. Acta 2009, 404 (2), 100–104.

(46) Bronkhorst, A. J.; Aucamp, J.; Pretorius, P. J. Cell-Free DNA: Preanalytical Variables. Clin. Chim. Acta 2015, 450, 243–253.

(47) Mouliere, F.; Messaoudi, S. El; Gongora, C.; Guedj, A. S.; Robert, B.; del Rio, M.; Molina, F.; Lamy, P. J.; Lopez-Crapez, E.; Mathonnet, M.; et al. Circulating Cell-Free DNA from Colorectal Cancer Patients May Reveal High KRAS or BRAF Mutation Load. Transl. Oncol. 2013, 6 (3), 319–328.

(48) Multer, G. L.; Boynton, K. A. PCR Bias in Amplification of Androgen Receptor Alleles, a Trinucleotide Repeat Marker Used in Clonality Studies. Nucleic Acids Res. 1995, 23 (8), 1411–1418.

(49) Milbury, C. A.; Chen, C. C.; Mamon, H.; Liu, P.; Santagata, S.; Makrigiorgos, G. M. Multiplex Amplification Coupled with COLD-PCR and High Resolution Melting Enables Identification of Low-Abundance Mutations in Cancer Samples with Low DNA Content. J. Mol. Diagnostics 2011, 13 (2), 220–232.

(50) Schrader, C.; Schielke, A.; Ellerbroek, L.; Johne, R. PCR Inhibitors - Occurrence, Properties and Removal. J. Appl. Microbiol. 2012, 113, 1014–1026.

(51) Ra, P.; Al-soud, W. A.; Jo, L. J.; Rådstro, P. Purification and Characterization of PCR-Inhibitory Components in Blood Cells. 2001, 39 (2), 485–493.

(52) Svec, D.; Tichopad, A.; Novosadova, V.; Pfaffl, M. W.; Kubista, M. How Good Is a PCR Efficiency Estimate: Recommendations for Precise and Robust QPCR Efficiency Assessments. Biomol. Detect. Quantif. 2015, 3, 9–16.

CHAPTER 4.

SEQUENCE-SPECIFIC PRECONCENTRATION OF A MUTATION PRONE *KRAS* FRAGMENT FROM PLASMA USING ION-TAGGED OLIGONUCLEOTIDES COUPLED TO QPCR COMPATIBLE MAGNETIC IONIC LIQUID SOLVENTS

Modified from a manuscript published in *Analytica Chimica Acta*

Miranda N. Emaus, Marcelino Varona, and Jared L. Anderson

Department of Chemistry, Iowa State University, Ames, Iowa 50011, United States

Abstract

Circulating tumor DNA (ctDNA) is a source of mutant DNA found in plasma and holds great promise in guiding cancer diagnostics, prognostics, and treatment. However, ctDNA fragments are challenging to detect in plasma due to their low abundance compared to wild-type DNA. In this study, a series of ion-tagged oligonucleotides (ITO) were synthesized using thiol-ene click chemistry and designed to selectively anneal target DNA. The ITO-DNA duplex was subsequently captured using a hydrophobic magnetic ionic liquid (MIL) as a liquid support. Extracted target DNA was quantified by adding the DNA-enriched MIL to the quantitative polymerase chain reaction (qPCR) buffer to streamline the extraction procedure. Clinically relevant concentrations of the mutation prone *KRAS* fragment, which has been linked to colorectal, lung, and bladder cancer, were preconcentrated using the ITO-MIL strategy allowing for enrichment factors as high as 19.49 ± 1.44 from pure water and 4.02 ± 0.50 from 10-fold diluted plasma after a 1 min extraction. Preconcentration could only be achieved when adding the ITO probe to the sample validating the selectivity of the ITO in the capture process. In addition, the amplification efficiency of qPCR was not affected when performing extractions from a diluted-plasma matrix demonstrating that the ITO-MIL approach coupled to direct-qPCR

can be used to quantitate DNA from complex matrices. In comparison, commercially available steptavidin-coated magnetic beads were observed to lose selectivity when performing extractions from a 10-fold diluted plasma matrix. The selectivity of the ITO-MIL method, coupled with the ability to rapidly preconcentrate clinically relevant concentrations of target DNA from 10-fold diluted plasma, suggests that this method has the potential to be applied towards the extraction of ctDNA fragments from clinical samples.

4.1. Introduction

Detection of low levels of circulating tumor DNA (ctDNA) holds great promise in guiding cancer diagnostics, prognosis, and treatment.[1,2] ctDNA is believed to originate from tumor cells that have undergone apoptosis or necrosis resulting in the release of tumor DNA into the bloodstream.[3] However, there is a low abundance of ctDNA in plasma especially in the early stages of cancer (i.e., less than 0.01%), and the presence of high levels of wild-type DNA can increase the probability of false-positive results due to primer mishybridization or mask present ctDNA.[4] In addition, ctDNA sequences such as *KRAS* and *EGFR* are prone to single nucleotide polymorphisms (SNPs) and differentiation of mutant ctDNA fragments from wild-type DNA is imperative to guiding cancer treatment.[2,5,6] Therefore, to distinguish SNPs from wild-type DNA, a sequence-specific DNA extraction method is often required to preconcentrate target ctDNA fragments.

There are several approaches to achieve sequence-specific ctDNA extraction and preconcentration. Synchronous coefficient of drag alteration (SCODA) is a novel microfluidic method for ctDNA preconcentration and analysis.[7] SCODA uses an oligonucleotide-functionalized electrophoresis gel to preconcentrate DNA sequences when exposed to a rotating electric field. Although SCODA is successful at preconcentrating low concentrations of ctDNA

mutations with limits of detection of 0.001% mutation abundance without PCR amplification, the technique is expensive and has limited sample throughput.[8] Commercially-available streptavidin magnetic beads have been widely used in the extraction of ctDNA.[3,9] In this approach, target DNA anneals to a biotinylated DNA probe followed by the probe-target complex binding to streptavidin coated magnetic beads, which are collected using an external magnet. Differential strand separation at critical temperature (DISSECT) is another magnetic bead-based extraction procedure that utilizes a dual-biotinylated probe conjugated to streptavidin-coated magnetic beads to extract both wild-type and mutant ctDNA fragments.[10] With DISSECT, the desorption temperature is controlled so that only the mutant DNA desorbs from the magnetic beads while wild-type DNA remains hybridized to the probe. DISSECT is highly sensitive and can detect 1 mutant allele in the presence of 10,000 wild-type fragments. However, magnetic beads are prone to aggregation and sedimentation, which decreases the amount of DNA extracted.[11,12] The ideal sequence-specific DNA extraction method should rapidly and selectively isolating SNPs from complex media. However, current methods such as SCODA and DISSECT suffer from high economic costs, sedimentation, and time-consuming purifications steps, and alternative extraction procedures should be investigated to improve sample throughput, selectivity, and detection limits.

An attractive alternative to traditional bead-based approaches is the use of paramagnetic liquid extraction solvents such as magnetic ionic liquids (MILs). MILs are a subclass of ionic liquids (ILs) that contain a paramagnetic component in either the cation or anion. MILs exhibit a number of interesting properties including negligible vapor pressure at room temperature, high thermal stability, magnetic susceptibility, and tunable physiochemical properties.[13-15] These properties enable the use of MILs as extraction solvents in a wide range of applications,

including the sequence-specific extraction of DNA.[16,17] In particular, strategies that couple ion-tagged oligonucleotide (ITO) probes and MILs represent an economical, particle-free alternative towards sequence-specific DNA extraction with low background DNA co-extraction and high extraction efficiencies. ITOs are designed to form a duplex with a single-stranded DNA target and can be captured by the MIL solvent through various interactions, such as hydrophobic interactions. ITOs are typically synthesized via the thiol-ene click reaction between a 3' thiol-modified oligonucleotide and an allylimidazolium IL.

Quantitative polymerase chain reaction (qPCR) is an important tool in DNA analysis capable of rapidly amplifying and quantifying small amounts of DNA. The reaction can be monitored in real-time using fluorescent probes such as SYBR Green or FAM, eliminating the lengthy electrophoretic separation step required in end-point PCR. However, qPCR is highly susceptible to inhibition and requires an initial DNA purification step in order to obtain accurate quantification.[18] Current sequence-specific DNA extraction procedures often require a time-consuming extraction step (i.e., up to 60 min).[19] Extraction times can often be dramatically reduced by employing dispersive liquid-liquid microextraction (DLLME) as opposed to static extraction methods. DLLME involves dispersing the extraction solvent into small droplets which significantly increases the surface area of the extraction phase. DLLME methods can take as little time as 1 min, and the high agitation rate prevents sedimentation of the extraction solvent.[20-22] MILs have recently been employed as DLLME solvents in order to circumvent the numerous centrifugation steps required to sediment traditionally employed organic solvents.[23] The paramagnetic properties of MILs can be exploited to rapidly collect droplets using a magnet resulting in more efficient extraction procedures.

One major bottleneck in DNA extraction procedures is the recovery step. Commercial magnetic beads recommend a 10 min thermal desorption step which ultimately reduces sample throughput. One approach to overcoming this bottleneck is introducing the extraction phase to the qPCR buffer and using elevated temperatures of qPCR to desorb target DNA to the reaction. However, introducing magnetic beads or chitosan microparticles to the reaction buffer decreases the amplification efficiency making quantification unreliable.[24] It has been shown that MILs can be directly added to PCR by designing a buffer capable of relieving any inhibition caused by the MIL with minimal effect on the amplification efficiency.[25] The use of direct-MIL-qPCR streamlines the extraction procedure by removing time-consuming DNA recovery steps.

Although previously reported ITO-MIL approaches have provided a selective DNA extraction method capable of extracting large amounts of DNA from cell lysate compared to commercially available magnetic bead-based methods, the ITO-MIL strategy has only been applied to high concentrations of target DNA (282 pM) and required lengthy extraction and desorption steps.[16,26] To overcome the aforementioned disadvantages of previously reported ITO-MIL methods a dispersive extraction method was developed to rapidly preconcentrate low concentrations of (3.3 fM) of the mutation prone *KRAS* oncogene fragment from plasma. DNA-enriched MIL was subsequently incorporated into the qPCR buffer to further increase sample throughputs. The extraction of albumin and DNA by three hydrophobic, manganese(II)-based MILs consisting of trihexyl(tetradecyl)phosphonium ($[P_{6,6,6,14}^+]$) tris(hexafluoroacetylaceto)manganate(II) ($[Mn(hfacac)_3^-]$), trioctylbenzylammonium ($[N_{8,8,8,Bz}^+]$) $[Mn(hfacac)_3^-]$, and $[N_{8,8,8,Bz}^+]$ bis(hexafluoroacetylaceto)phenyltrifluoroacetylacetomanganate(II) ($[Mn(hfacac)_2(Phtfacac)^-]$) were evaluated. MILs were specifically designed to provide minimal background DNA and

protein extraction while maintaining qPCR compatibility. ITOs were designed to contain a 20 nt oligonucleotide complimentary to the *KRAS* amplicon. In addition, four ITOs containing either alkyl or aromatic moieties and different anions were investigated as DNA extraction probes. Once the ITO annealed to the target sequence, the ITO-DNA duplex was preconcentrated in as little as 1 min followed by collection of MIL droplets using an external magnet. Furthermore, DNA was desorbed from the MIL during qPCR thereby avoiding lengthy desorption steps. Incorporation of the DNA-enriched MIL into the qPCR buffer did not significantly affect the amplification efficiency when extracting *KRAS* target from pure water or 10-fold diluted plasma. The ITO-MIL-DLLME method obtained enrichment factors as high as 19.49 ± 1.44 from pure water, and selectively preconcentrated DNA from a diluted plasma matrix indicating its potential for the analysis of ctDNA from clinical samples.

4.2 Materials and Methods

4.2.1 Reagents and Materials

Manganese(II) chloride tetrahydrate (98.0-101.0%) was purchased from Alfa Aesar (Ward Hill, MA, USA). Ammonium hydroxide (28-30% solution in water), 1,1,1,5,5,5-hexafluoroacetylacetone (99%), 1-phenyl-4,4,4-trifluoro-1,3-butanedione (99%), and trioctylamine (97%) were purchased from Acros Organics (Morris Plains, NJ, USA). Anhydrous diethyl ether (99.0%) was purchased from Avantor Performance Materials Inc. (Center Valley, PA, USA). Trihexyl(tetradecyl)phosphonium chloride (97.7%) was purchased from Strem Chemicals (Newburyport, MA, USA). Ethylenediaminetetraacetic acid (EDTA) (99.4-100.06%), bovine serum albumin (BSA) (≥96%), allyl bromide, 1-bromooctane (99%), benzylimidazole (99%), triethylamine (≥99.5%), LC-MS grade acetonitrile (≥99.9%), lyophilized plasma from human (4% trisodium citrate), deoxyribonucleic acid sodium salt from salmon testes (stDNA),

and magnesium chloride hexahydrate (99.0-102.0%) were purchased from Sigma-Aldrich (St. Louis, MO, USA). SYBR Green I (10,000x) was purchased from Life Technologies (Carlsbad, CA, USA). Urea (>99%) and tris(2-carboxyethyl)phosphine (TCEP) (>98%) were purchased from P212121 (Ypsilanti, MI, USA). Ammonium persulfate (APS) (≥98.0%), 40% acrylamide, bis-acrylamide solution 29:1, SsoAdvanced Universal SYBR Green Supermix, and a *KRAS*, human PrimePCR^{TM} SYBR green assay (120 base pair amplicon; additional information can be found on Bio-Rad's website) were purchased from Bio-Rad Laboratories (Hercules, CA, USA). Thiolated, biotinylated, and unmodified oligonucleotides (sequences shown in Table S1) were purchased from Integrated DNA Technologies (Coralville, IA, USA). PCR caps, tube strips, sodium chloride, and Dynabeads Myone Steptavidin C1 magnetic beads were purchased from Thermo Fisher Scientific (Waltham, MA, USA). Tris-HCl was purchased from RPI (Mount Prospect, IL, USA). Neodymium rod (0.66 T) and cylinder magnets (0.9 T) were purchased from K&J Magnetics (Pipersville, PA, USA) and used to collect dispersed MIL droplets or magnetic beads. Deionized water (18.2 MΩ cm), obtained from a Milli-Q water purification system, was used to prepare all aqueous solutions (Millipore, Bedford, MA, USA).

4.2.2 Instrumentation

ITO characterization was performed using an Agilent 1260 Infinity high performance liquid chromatograph (HPLC) with a diode array detector coupled to an Agilent 6230B accurate mass time of flight (TOF) mass spectrometer with an electrospray source. A Zorbax Extend C_{18} column (50 mm × 2.1 mm i.d. × 1.8 µm particle size) purchased from Agilent Technologies was used for the separation and characterization of ITOs. The column was equilibrated for 20 min at 0.2 mL min^{-1} with a mobile phase composition of 95:5 A:B where mobile phase A was 5 mM triethylammonium acetate (pH 7.4) and B was LC-MS grade acetonitrile. In order to prevent

non-volatile imidazolium salts and urea from entering the mass spectrometer, LC eluent was diverted to the waste for the first 8 min. Gradient elution was performed using the following program: 5% B for 5 min, gradient increase 5% to 19.4% B from 5 to 17 min, increased 19.4% to 35% B from 17 to 18 min, held at 35% B from 18 to 20 min, increased 35% B to 100% B from 20 to 30 min, and held at 100% B from 30 to 33 min. The nebulizing gas was set to 35 psi. The drying (N_2) gas flow rate was 9 L min^{-1} with a temperature of 350 °C and a capillary voltage of 4000 V. Spectra were acquired from 100-3000 m/z with a scan rate of 1 spectrum sec^{-1}.

HPLC separations were performed on an Agilent Technologies 1260 system with variable wavelength detection (Santa Clara, CA, USA) to investigate the capability of the investigated MILs to extract DNA and protein as well as to examine loading of the DNA-ITO duplex to the MIL phase. A TSKgel DEAE-NPR anion exchange column (35 mm × 4.6 mm i.d. × 2.5 µm particle size) with a TSKgel DEAE-NPR guard column (5 mm × 4.6 mm i.d. × 5 µm particle size) was obtained from Tosoh Bioscience (King of Prussia, PA, USA) and used to examine the DNA and protein extraction ability of the three MILs. When separating and detecting stDNA, the column was equilibrated with a mobile phase composition of 50:50 A:B (i.e, mobile phase A: 20 mM Tris-HCl (pH 8) and mobile phase B: 1 M NaCl and 20 mM Tris-HCl (pH 8)). Gradient elution was achieved from 50% mobile phase B and ramping to 100% B from 0 to 10 min. In the separation of 20 bp DNA, the column was first equilibrated with mobile phase A for 20 min followed by gradient elution from 0% to 50% mobile phase B from 0 to 10 min and increase to 100% B from 10 to 15 min. In order to separate BSA, the column was first equilibrated with mobile phase A for 20 min followed by gradient elution from 0% to 50% B from 0 to 15 and increase to 100% B from 15 to 20 min. A flow rate of 0.5 mL min^{-1} was used for all HPLC separations. DNA and albumin were detected at 260 and 280 nm, respectively.

Denaturing polyacrylamide gel electrophoresis (PAGE) was performed using a Mini Protean 3 electrophoresis system from Bio-Rad Laboratories with an ECPS 3000/150 power supply from Pharmacia (Stockholm, Sweden). An 18% polyacrylamide gel was prepared using 7 M urea to separate the ITOs from unreacted oligonucleotides. A 30 min pre-run was performed at 200 V and 150 W to equilibrate the gel and improve band resolution. Once the sample was loaded, the gel was run at 200 V and 150 W for approximately 1 h with an ice bath to cool the electrophoresis tank.

qPCR amplification was achieved using a Bio-Rad CFX96 Touch Real-time PCR, and the following amplification program was used: 2 min denaturation step at 95 °C for 2 min, followed by 40 cycles of 5 s at 95°C and 30 x at 60 °C. Melt curves of qPCR products were achieved by heating from 65°C to 95°C in 0.5°C 5 s^{-1} increments. Melt curves of qPCR products were achieved by starting at 65°C for 5 s and increasing to 95°C in 0.5°C increments. Melt curves analysis of the ITO to a complementary sequence and sequences containing a 1 or 2 nucleotide (nt) mismatch was achieved using the following program: initial 5 min denaturation step at 90°C, 10 min annealing step at 20°C, and heating ramp from 20°C to 95°C in 0.5°C increments every 5 s.

4.2.3 MIL and ITO synthesis

Chemical structures of the three MILs are shown in Figure 4-1(**1-3**). The $[NH_4^+][Mn(hfacac)_3^-]$ salt and $[P_{6,6,6,14}^+][Mn(hfacac)_3^-]$ MIL were synthesized and characterized using a previously reported procedure.[27] The $[N_{8,8,8,Bz}^+]$ cation was synthesized as previously reported and characterized using NMR, as shown in Figure 4-S1.[28] The $[N_{8,8,8,Bz}^+][Mn(hfacac)_3^-]$ MIL was synthesized by stirring equimolar amounts of $[N_{8,8,8,Bz}^+][Br^-]$ and $[NH_4^+][Mn(hfacac)_3^-]$ in 30 mL of methanol overnight. The $[NH_4^+]$ hexafluoroacetylacetonate ($[hfacac^-]$) and $[NH_4^+]$

phenyltrifluoroacetylacetonate ([Phtfacac$^-$]) salts were prepared by dissolving either hexafluoroacetylacetone (hfacac) or phenyltrifluoroacetylacetone (Phtfacac) in 30 mL of ethanol with equimolar amounts of [NH_4^+][OH^-]. The product was subsequently dried for 5 hr in a vacuum oven. The [NH_4^+][$Mn(hfacac)_2(Phtfacac)^-$] salt was synthesized by reacting 2 molar equivalents of [NH_4^+][hfacac$^-$], 1 molar equivalent of [NH_4^+][Phtfacac$^-$], and 1 molar equivalent of $MnCl_2$ overnight in ethanol. The [$N_{8,8,8,Bz}^+$][$Mn(hfacac)_2(Phtfacac)^-$] MIL was synthesized by stirring equimolar amounts of [$N_{8,8,8,Bz}^+$][Br^-] and [NH_4^+][$Mn(hfacac)_2(Phtfacac)^-$] salts in 30 mL of methanol overnight. All three MILs were purified using diethyl ether and water and subsequently dried overnight in a vacuum oven. The MIL solvents were stored in a desiccator when not in use. Elemental analysis results were acquired using a PE 2100 Series II combustion analyzer (Perkin Elmer Inc., Waltham, M.A.). Carbon/hydrogen/nitrogen (CHN) calculated for [N_{888Bz}^+][$Mn(hfacac)_2(Phtfacac)^-$]: %C = 54.26, %H = 5.89, %N = 1.24; Found: %C = 53.47, %H= 5.75, %N = 1.56. Calculated for [P_{66614}^+][$Mn(hfacac)_3^-$]: %C = 48.67, %H = 6.17; Found: %C = 50.15, %H = 6.16. Calculated for [N_{888Bz}^+][$Mn(hfacac)_3^-$]: %C = 49.29, %H = 5.49, and %N = 1.25; Found: %C = 50.22, %H = 5.45, %N = 1.80.

Chemical structures of the four ITOs used in this study are shown in Figure 4-1(**4-7**). ITOs were prepared according to previously reported methods.[16] By reacting the [$AOIM^+$]-*KRAS* [Br^-] and [$ABzIM^+$]-*KRAS* [Br^-] ITOs with an equimolar amount of KPF_6, the [$AOIM^+$]-*KRAS* [PF_6^-] and [$ABzIM^+$]-*KRAS* [PF_6^-] ITOs were prepared. All ITOs were characterized using HPLC-TOF MS, as shown in Table S2 and Figure 4-S2.

4.2.4 Background DNA and Protein Co-extraction by MILs

To investigate the protein extraction capabilities of the three MILs, a 20 µL volume of MIL was added to a 1 mL solution of 1 mg mL^{-1} BSA and manually agitated for 30 s. After

dispersing the MIL, 20 µL of the aqueous solution was subjected to anion exchange chromatography for quantitative analysis. To ensure low background DNA co-extraction by the MIL, two different DNA sequences were examined involving the addition of a 20 µL volume of MIL to 50 ng/µL stDNA, or 18.3 ng/µL 20 bp DNA. The solution was manually agitated for 30 s. Subsequently, 20 µL of the aqueous solution was subjected to anion exchange separation for analysis.

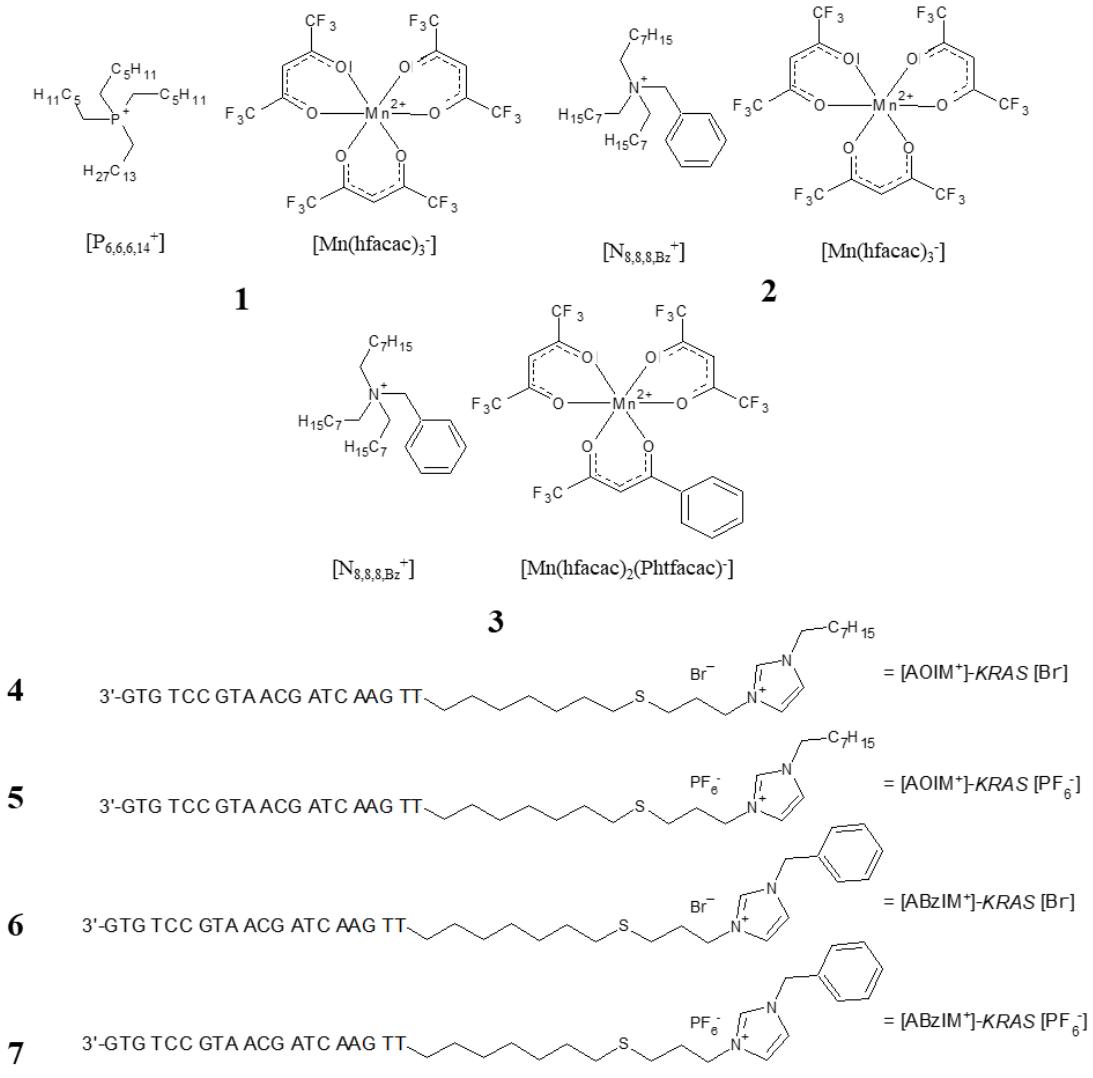

Figure 4-1 Chemical structures of the manganese(II)-based hydrophobic MILs (**1-3**) and octyl- and benzyl-imidazolium-based ITO (**4-7**) structures used for all experiments.

4.2.5 Examining DNA-ITO Duplex Loading to MIL

To determine the optimum ITO and MIL pair, a 1 µL aliquot of MIL was added to a 60 µL solution containing 25 mM NaCl and 1 ng μL^{-1} ITO-DNA duplex solution. The solution was then incubated for 10 min at room temperature. Subsequently, 20 µL of the aqueous phase was subjected to anion exchange chromatographic analysis.

4.2.6 Annealing and Capture of Target DNA

The general procedure used to anneal target *KRAS* template to the ITO and subsequent extraction using DLLME is shown in Figure 4-2. A 1 mL solution of 25 mM NaCl, 2×10^4 copies μL^{-1} of *KRAS* template, and an optimized amount of ITO was prepared in a 5 mL screw cap glass vial. A 10 µL aliquot was then removed and used as a standard. The DNA solution was heated to 90°C using a Fisher Isotemp 2322 water bath (Rochester, MN, USA) for 2 min to melt the DNA duplex and then cooled to 30°C for 8 min to anneal the target DNA to the ITO. Subsequently, an optimized volume of MIL was dispersed using a Barnstead/Thermolyne Type 16700 mixer (Dubuque, IA, USA) for an optimal amount of time. MIL droplets were collected using a rod magnet (B = 0.66 T) and subsequently washed with deionized water (18.2 MΩ cm). A 0.3 µL aliquot of DNA-enriched MIL was then placed into a qPCR tube for downstream analysis.

Sequence-specific DNA extractions using Dynabeads Myone Steptavidin C1 beads were performed according to the manufacturer's instructions. A 1 mL solution of 25 mM NaCl, 2×10^4 copies μL^{-1} of template, and 332 fM biotinylated probe was prepared in a 5 mL screw cap glass vial. A 10 µL aliquot of this solution was used as a standard. The sample solution was heated for 5 min at 90°C and then cooled on ice for 5 min. The magnetic beads (i.e., 10 µg) were washed three times with 5 mM Tris-HCl (pH 7.5), 0.5 mM EDTA, and 1 M NaCl prior to adding magnetic beads to the sample solution. The sample was agitated using a New Brunswick

Scientific incubator shaker (Edison, NJ, USA) for 10 min at 250 rpm. Subsequently, the beads were collected using an external magnet (B = 0.9 T) and washed three times with 5 mM Tris-HCl (pH 7.5), 0.5 mM EDTA, and 1 M NaCl. The beads were then suspended in 20 µL of H_2O and heated at 90°C for 10 min to desorb captured DNA.

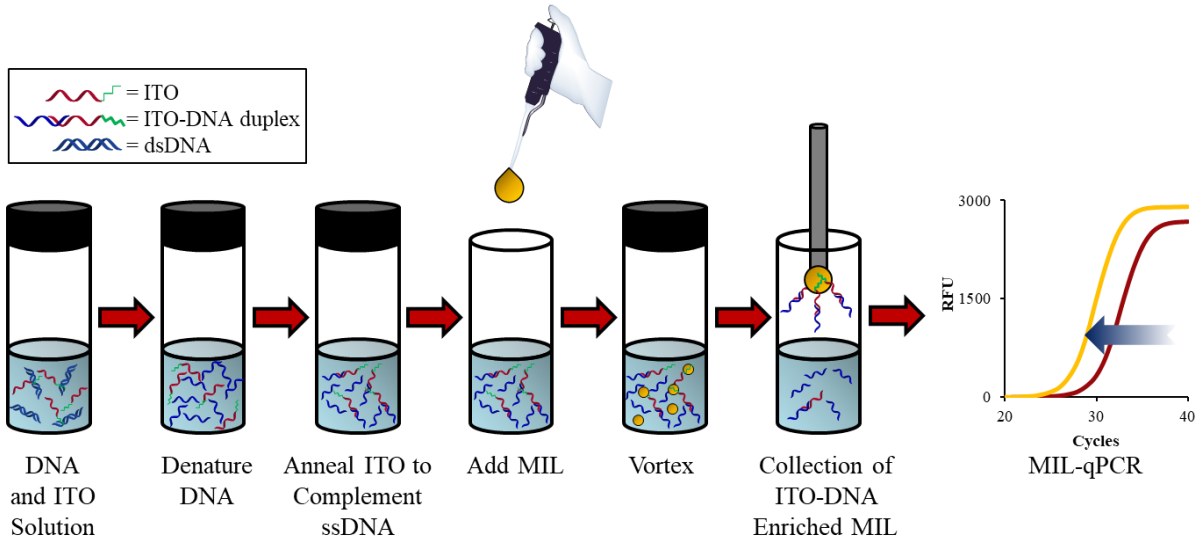

Figure 4-2 General extraction procedure used to capture target *KRAS* DNA. DNA-enriched MIL was added to the reaction buffer for qPCR detection.

4.2.7 qPCR Amplification

The addition of 0.3 µL $[P_{6,6,6,14}^+][Mn(hfacac)_3^-]$ MIL to a 20 µL qPCR mixture required 1x SsoAdvanced Supermix, 1x PrimePCR assay mix, 4 mM EDTA, and additional 1x SYBR Green I. qPCR amplification with 0.3 µL of the $[N_{8,8,8,Bz}^+][Mn(hfacac)_3^-]$ MIL was achieved using the 1x SsoAdvanced Supermix, 1x PrimePCR assay mix, 6.25 mM $MgCl_2$, 4 mM EDTA, and an additional 0.4x SYBR Green I for a final volume of 20 µL. The addition of 0.3 µL $[N_{8,8,8,Bz}^+][Mn(hfacac)_2(Phtfacac)^-]$ MIL to a 20 µL qPCR mixture required 1x SsoAdvanced Supermix, 1x PrimePCR assay mix, 2.5 mM $MgCl_2$, 2 mM EDTA, and additional 1x SYBR Green I.

The threshold cycle (Cq) was determined using the fluorescence threshold provided by the Bio-Rad CFX Maestro software and used to determine the amount of the *KRAS*-ITO duplex extracted by the hydrophobic MIL. A standard curve was constructed for *KRAS* template (see Figure 4-S3) and to determine the concentration of DNA extracted using the ITO-MIL-DLLME procedure. The enrichment factors (E_f) obtained for each extraction were calculated using equation 1, where C_{MIL} is the concentration of DNA extracted using the MIL and C_{Std} represents the concentration of target DNA initially present in the sample.

$$E_f = \frac{C_{MIL}}{C_{Std}} \qquad \text{Equation 4-1}$$

4.3 Results and Discussion

4.3.1 qPCR Conditions to Mitigate the Inhibitory Effects of MILs

In order to remove tedious sample handing steps and increase sample throughputs, DNA-enriched MIL was incorporated into the qPCR buffer where DNA is capable of desorbing from the MIL due to the elevated temperatures required for the reaction. However, it has been previously shown that hydrophobic MILs can dissolve under the elevated temperatures required for PCR.[29] Solubilized MIL components can inhibit PCR amplification; nevertheless, qPCR inhibition can be relieved through the addition of EDTA, BSA, additional $MgCl_2$, additional Tris-HCl, and additional SYBR Green I.

The inhibition of qPCR due to the addition of $[P_{6,6,6,14}^+][Mn(hfacac)_3^-]$, $[N_{8,8,8,Bz}^+][Mn(hfacac)_3^-]$, and $[N_{8,8,8,Bz}^+][Mn(hfacac)_2(Phtfacac)^-]$ MILs was mitigated by titrating 0-8 mM $MgCl_2$, 0-8 mM EDTA, and 0-1x SYBR Green I into the buffer. Incorporation of 0.3 µL of $[P_{6,6,6,14}^+][Mn(hfacac)_3^-]$ MIL to the qPCR buffer required 4 mM EDTA and 1x SYBR Green I, as previously reported.[25] The addition of 0.3 µL of the $[N_{8,8,8,Bz}^+][Mn(hfacac)_3^-]$ MIL to the qPCR buffer was optimized to require 4 mM EDTA, 6.25 mM $MgCl_2$, and 0.4x SYBR Green I. Inhibition caused by 0.3 µL of the $[N_{8,8,8,Bz}^+][Mn(hfacac)_2(Phtfacac)^-]$ MIL

required 4 mM EDTA, 2.5 mM $MgCl_2$, and 1x SYBR Green I in order to achieve amplification. Addition of EDTA to the MIL-qPCR buffer chelates solubilized anion providing relief to qPCR inhibition. Without additional SYBR green in solution, the fluorescence signal remains low likely due to the partitioning of SYBR Green I to the hydrophobic MIL phase.[30]

The addition of excess oligonucleotides to a PCR reaction can either accelerate the reaction or lead to the formation of primer-dimers.[31-34] Therefore, to investigate the effect of the ITO on the reaction, 4×10^6 copies of ITO were spiked into the qPCR buffer. However, as shown in Figure 4-S4, spiking ITOs into the qPCR did not affect the Cq nor did the melt curve indicate the presence of primer-dimers. In this case, it appears that the addition of ITO did not affect the reaction likely due to the low concentration of the probe.

Examination of the melting temperature (T_m) can be used to differentiate SNPs.[35] Therefore, the T_m of qPCR product was examined to investigate whether the MIL-based DNA extraction or direct qPCR amplification altered the DNA sequence. Figure 4-S5 shows that the T_m of extracted target DNA was comparable to the *KRAS* standard (± 0.5 °C) suggesting that the sequence was not altered due to the MIL This result is in agreement with previous MIL-based DNA amplification studies.[29]

4.3.2 MIL and ITO Screening

An ideal MIL solvent should be capable of capturing the ITO-DNA duplex while not extracting background DNA and plasma components. However, plasma contains 35-80 mg mL^{-1} of protein making it an extremely challenging and complex matrix due to the fact that plasma proteins can inhibit qPCR amplification.[18,36-38] Furthermore, plasma contains high levels of background DNA presenting a challenge for targeted analysis. Therefore, to prevent co-extraction of background DNA, manganese(II)-based MILs were investigated as they have been

previously shown to poorly extract DNA.[16,25] In addition, manganese(II) binds poorly to albumin, which makes up over 50% of the total protein content of plasma.[39-41] As shown in Figure 4-3, the addition of aromatic moieties to either the cation or anion component of the MIL was shown to reduce the amount of BSA extracted. The three MILs were also tested to examine the extraction efficiency of short (20 bp) and long (20 Kbp) DNA fragments. All three MILs extracted less than 2% of either DNA sequence, as shown in Figure 4-3.

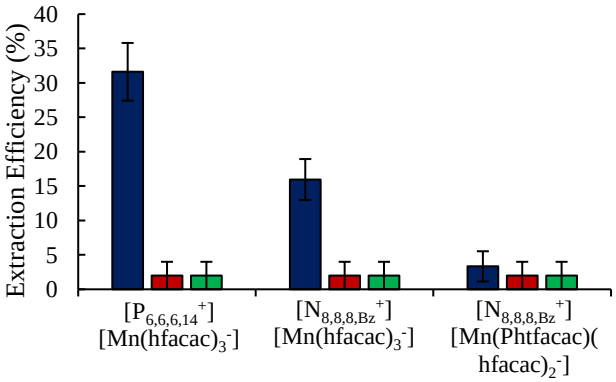

Figure 4-3 Extraction efficiency of BSA (blue), stDNA (red), and 20 bp DNA (green) using the $[P_{6,6,6,14}^+]$ $[Mn(hfacac)_3^-]$, $[N_{8,8,8,Bz}^+]$ $[Mn(hfacac)_3^-]$, and $[N_{8,8,8,Bz}^+][Mn(hfacac)_2(Phtfacac)^-]$ MILs. BSA concentration: 1 mg mL^{-1}, stDNA concentration: 50 ng μL^{-1}, 20 bp DNA concentration: 18.3 ng μL^{-1}; sample volume: 1 mL; agitation time: 30 s; MIL volume: 20 µL.

Previously, it was reported that DNA-ITO duplexes interact with the MIL solvent primarily through hydrophobic interactions.[16] Exchanging the $[Br^-]$ anion of the ITO with a more hydrophobic anion, such as $[PF_6^-]$, has the potential to facilitate stronger interactions with the MIL solvent and possibly improve loading efficiency. As shown in Figure 4-4, 56.94 ± 1.61% of the target was extracted by the $[P_{6,6,6,14}^+][Mn(hfacac)_3^-]$ MIL using the $[AOIM^+]$-*KRAS* $[PF_6^-]$ ITO while only 48.18 ± 3.89%, 45.98 ± 3.32%, and 38.59 ± 4.90% was loaded using the $[AOIM^+]$-*KRAS* $[Br^-]$, $[ABzIM^+]$-*KRAS* $[Br^-]$, and $[ABzIM^+]$-*KRAS* $[PF_6^-]$ ITOs, respectively. In addition, incorporation of aromatic moieties into the ITO and MIL structures facilitated π-π stacking interactions and provided a modest increase in the amount of ITO loaded to the MIL. As

shown in Figure 4-4, 65.94 ± 9.55% of the [ABzIM$^+$]-*KRAS* [Br$^-$] ITO-DNA duplex was loaded onto the [$N_{8,8,8,Bz}^+$][Mn(hfacac)$_3^-$] MIL whereas only 26.13 ± 3.44%, 37.83 ± 1.28%, and 20.17 ± 2.04% was loaded using the [AOIM$^+$]-*KRAS* [Br$^-$], [AOIM$^+$]-*KRAS* [PF_6^-], and [ABzIM$^+$]-*KRAS* [PF_6^-] ITOs, respectively. Using the [$N_{8,8,8,Bz}^+$][Mn(hfacac)$_2$(Phtfacac)$^-$] MIL as an extraction solvent, 16.56 ± 3.36% [AOIM$^+$]-*KRAS* [Br$^-$], 42.05 ± 0.72% [AOIM$^+$]-*KRAS* [PF_6^-], 53.69 ± 2.27% [ABzIM$^+$]-*KRAS* [Br$^-$] ITO, and 25.10 ± 4.91% [ABzIM$^+$]-*KRAS* [PF_6^-] ITO was loaded onto the MIL solvent, as shown in Figure 4-4.

4.3.3 Optimization of the ITO-MIL-DLLME Method

Cell-free DNA (cfDNA) is present in relatively high concentrations (1-100 pM) in blood, plasma, and serum.[42] However, certain tumor mutations can comprise less than 0.01% of the

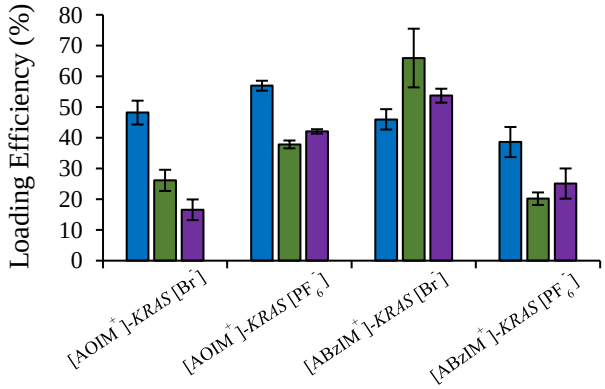

Figure 4-4 Loading efficiencies of the ITO-DNA duplex to the MIL phase using the [AOIM$^+$]-*KRAS* [Br$^-$], [AOIM$^+$]-*KRAS* [PF_6^-], [ABzIM$^+$]-*KRAS* [Br$^-$], and [ABzIM$^+$]-*KRAS* [PF_6^-] ITOs and [$P_{6,6,6,14}^+$][Mn(hfacac)$_3^-$] (blue), [$N_{8,8,8,Bz}^+$][Mn(hfacac)$_3^-$] (green), and [$N_{8,8,8,Bz}^+$][Mn(Phtfacac)(hfacac)$_2^-$] (purple) MILs. ITO concentration: 1 ng μL^{-1}; *KRAS* complement: 1 ng μL^{-1}; NaCl concentration: 25 mM; sample volume: 60 μL; MIL volume: 1 μL; extraction time: 10 min.

total amount of cfDNA.[43] Therefore, a clinically relevant concentration of 2×10^4 copies μL^{-1} (33 fM) of target *KRAS* fragments was used during optimization. A 1 mL sample volume was selected in order to maintain the minimum sample volume capable of being dispersed.

The amount of ITO versus the amount of DNA present in the solution was first optimized. The sample was initially heated to 90°C to denature the DNA duplex followed by a cooling step to 30°C. After annealing the ITO to the target DNA, 6 μL of MIL was added to the solution. The solution was vortexed for 1 min, and the DNA-enriched MIL was recovered from the aqueous solution using a rod magnet (B = 0.66 T) and subjected to qPCR analysis. As shown in Figure 4-S6, a 10-fold excess of either [$AOIM^+$]-*KRAS* [PF_6^-] and [$ABzIM^+$]-*KRAS* [Br^-] ITO was found to be optimum for the [$P_{6,6,6,14}^+$][$Mn(hfacac)_3^-$], [$N_{8,8,8,Bz}^+$][$Mn(hfacac)_3^-$], and [$N_{8,8,8,Bz}^+$][$Mn(hfacac)_2(Phtfacac)^-$] MILs. Target DNA can either reanneal to the complimentary sequence or anneal to the ITO. Therefore, to increase the probability that target DNA anneals to the ITO, an excess amount of ITO was needed. However, high concentrations of ITO may result in the MIL extracting unhybridized ITO instead of the desired ITO-DNA complex.

The volume of MIL dispersed in the solution was also optimized for all three MILs. A volume of 8 μL of [$P_{6,6,6,14}^+$][$Mn(hfacac)_3^-$] MIL was found to be optimum while dispersing 6 μL and 4 μL of [$N_{8,8,8,Bz}^+$][$Mn(hfacac)_3^-$] and [$N_{8,8,8,Bz}^+$][$Mn(hfacac)_2(Phtfacac)^-$] MILs, respectively, produced the highest extraction efficiencies, as shown in Figure 4-S7. Larger volumes of MIL generally resulted in lower E_f as DNA can be diluted within the MIL.[44]

Additionally, the extraction time was optimized to achieve the highest E_f in the shortest amount of time. As shown in Figure 4-S8, an extraction time of 3 min was optimum for the [$P_{6,6,6,14}^+$][$Mn(hfacac)_3^-$] MIL while 1 min was optimum for the [$N_{8,8,8,Bz}^+$][$Mn(hfacac)_3^-$] and [$N_{8,8,8,Bz}^+$][$Mn(hfacac)_2(Phtfacac)^-$] MILs. After the optimum times for the [$P_{6,6,6,14}^+$][$Mn(hfacac)_3^-$] and [$N_{8,8,8,Bz}^+$][$Mn(hfacac)_3^-$] MILs, a sharp decrease in the amount of DNA extracted was observed.

4.3.4 Comparison to Commercial Sequence-Specific Magnetic Beads

Streptavidin magnetic beads have been used to capture specific ctDNA mutations from clinical plasma samples.[3,9,10] A significant drawback to using magnetic beads is their propensity to aggregate and sediment, which is especially problematic when extraction of low concentrations of target DNA requires the beads to be suspended for long periods of time. MILs are uniquely capable of overcoming these issues as they can be easily dispersed into fine droplets that remain suspended in solution for extended periods of time.[45] Due to these properties, MILs have the potential to provide unique advantages over commercial magnetic beads in sequence-specific DNA extractions. The ITO-MIL-DLLME procedure was compared to the commercial Dynabeads Myone streptavidin C1 magnetic beads. As shown in Figure 4-5a, extractions performed using the $[P_{6,6,6,14}^+][Mn(hfacac)_3^-]$ and $[N_{8,8,8,Bz}^+][Mn(hfacac)_3^-]$ MILs produced E_f values of 19.49 ± 1.44 and 16.44 ± 2.21 outperforming the commercial streptavidin Dynabeads, which provided a respectable E_f of 9.73 ± 0.42 from pure water. When examining the amount of DNA co-extracted by the MIL and magnetic beads, the optimized extraction was performed without either the ITO or biotinylated probe. As shown in Figure 4-5a, a low E_f from pure water was obtained without ITO and biotinated probe present in solution. The limited co-extraction of DNA by the MIL solvent indicates that DNA extracted can be attributed to the ITO or the biotinylated probe.

When comparing the extraction of *KRAS* target from 10-fold diluted plasma using the three MILs and the commercial magnetic beads, the $[ABzIM^+]$-*KRAS* $[Br^-]$ ITO and $[N_{8,8,8,Bz}^+][Mn(hfacac)_3^-]$ MIL produced the highest E_f, as shown in Figure 4-5b. The $[N_{8,8,8,Bz}^+][Mn(hfacac)_2(Phtfacac)^-]$ MIL experienced only a two-fold decrease in E_f, which may be linked to the low BSA extraction efficiency associated with this MIL. However, extractions

using the magnetic beads from 10-fold diluted plasma produced an E_f of only 1.30 ± 0.07, possibly due to the biotinylated probe interacting with plasma proteins.[46] This is supported by the fact that the E_f obtained using streptavidin-coated magnetic beads, with or without the biotinylated probe, were within error (i.e., 1.25 ± 0.18). As shown in Figure 4-5b, low E_f values were achieved when the ITO was not present in solution suggesting that the ITO plays a dominant role in preconcentrating DNA from the plasma solution. However, selectivity was lost when performing extractions with the steptavidin-coated magnetic beads from 10-fold diluted plasma.

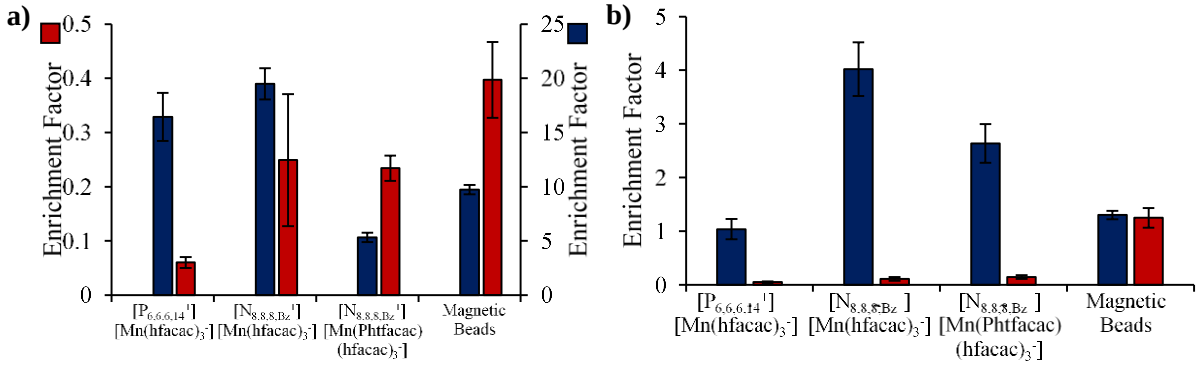

Figure 4-5 Enrichment factor obtained for the sequence-specific extraction of KRAS target using the $[P_{6,6,6,14}^+]$ $[Mn(hfacac)_3^-]$ MIL, $[N_{8,8,8,Bz}^+][Mn(hfacac)_3^-]$ MIL , $[N_{8,8,8,Bz}^+]$ $[Mn(hfacac)_2(Phtfacac)^-]$ MIL, and Dynabeads Myone Steptavidin C1 magnetic beads from pure water (a) and 10-fold diluted plasma (b) with (blue) and without (red) ITO or biotinylated probe. $[P_{6,6,6,14}^+]$ $[Mn(hfacac)_3^-]$ MIL conditions: KRAS template concentration: 2×10^4 copies μL^{-1}, amount of $[AOIM^+]$-*KRAS* $[PF_6^-]$ ITO relative to DNA: 10x, NaCl concentration: 25 mM, sample volume: 1.0 mL, MIL volume: 8 µL; extraction time: 3 min. $[N_{8,8,8,Bz}^+][Mn(hfacac)_3^-]$ MIL conditions: KRAS template concentration: 2×10^4 copies μL^{-1}, amount of $[ABzIM^+]$-*KRAS* $[Br^-]$ relative to DNA: 10x, NaCl concentration: 25 mM, sample volume: 1.0 mL, MIL volume: 6 µL: extraction time: 1 min. $[N_{8,8,8,Bz}^+]$ $[Mn(hfacac)_2(Phtfacac)^-]$ MIL conditions: KRAS template concentration: 2×10^4 copies μL^{-1}, amount of $[ABzIM^+]$-*KRAS* $[Br^-]$ relative to DNA: 10x, NaCl concentration: 25 mM, sample volume: 1.0 mL, MIL volume: 4 µL; extraction time: 1 min. Dynabeads Myone Steptavidin C1 magnetic beads conditions: KRAS template concentration: 2×10^4 copies μL^{-1}, concentration of biotinylated probe: 332 fM, NaCl concentration: 25 mM, mass of magnetic beads: 10 µg; sample volume: 1.0 mL; extraction time: 10 min; agitation rate: 250 rpm; desorption time: 10 min; desorption volume: 20 µL.

In order to determine whether the ITO-MIL-DLLME-qPCR method could be used for accurate quantification, calibration curves for each MIL were constructed by performing a series of five extractions at different concentration levels followed by the determination of amplification efficiency using equation 2. Ideally, the amplification efficiency should range between 90-110% indicating that DNA is successfully duplicated with each cycle and that

$$Efficency = \left(10^{\left(-\frac{1}{slope}\right)} - 1\right) * 100\% \qquad \text{Equation 2}$$

quantification can be achieved.[47] It was observed that all three MILs did not significantly alter the amplification efficiency when incorporated into the qPCR buffer. The $[P_{6,6,6,14}^+]$ $[Mn(hfacac)_3^-]$ MIL produced an efficiency of 100.1%, while the $[N_{8,8,8,Bz}^+][Mn(hfacac)_3^-]$ MILs exhibited an efficiency of 107.9%, and the $[N_{8,8,8,Bz}^+][Mn(hfacac)_2(Phtfacac)^-]$ MIL enabled an efficiency of 107.9%, as shown in Figure 4-6. Calibration curves from 10-fold diluted plasma were also constructed for all three MILs to determine if quantification could be achieved from a more complex medium. As shown in Figure 4-7, the amplification efficiencies associated with the extraction of *KRAS* from 10-fold diluted plasma fell between 90-110% with the addition of the $[P_{6,6,6,14}^+][Mn(hfacac)_3^-]$, $[N_{8,8,8,Bz}^+][Mn(hfacac)_3^-]$, and $[N_{8,8,8,Bz}^+][Mn(hfacac)_2(Phtfacac)^-]$ MIL to the qPCR buffer resulting in efficiencies of 106.3%, 109.3%, and 103.5% respectively. Amplification efficiencies obtained from the ITO-MIL-DLLME procedure in pure water and diluted plasma indicate that there is little inhibition attributed to adding manganese(II)-based MILs to the qPCR buffer and that this method can be used for quantification purposes

4.3.5 Selectivity of the ITO-MIL-DLLME Method

The detection of low abundance ctDNA is of particular importance for early cancer detection, prognosis, and treatment monitoring.[48] However, several common ctDNA fragments are SNPs that complicate ctDNA detection.[2] In order to investigate the selectivity of the ITO

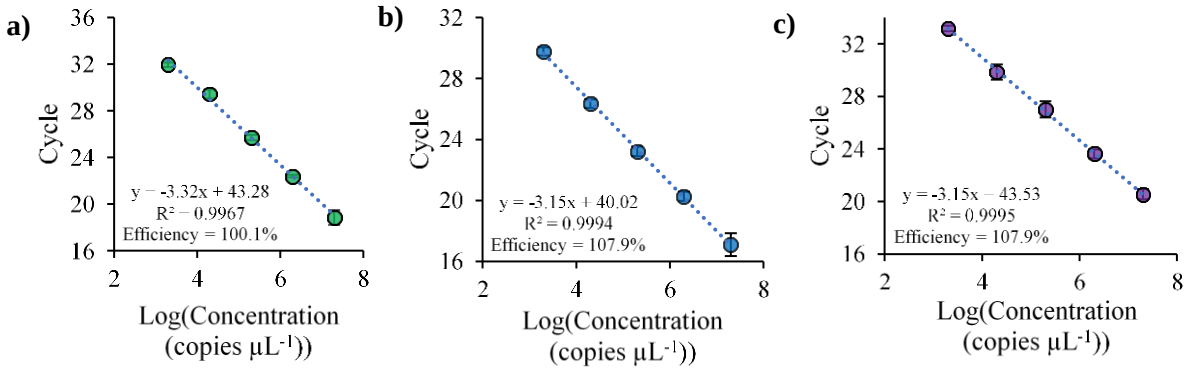

Figure 4-6 Standard curves generated using the optimized MIL-DLLME method for the (a) $[P_{6,6,6,14}^+]$ $[Mn(hfacac)_3^-]$, (b) $[N_{8,8,8,Bz}^+][Mn(hfacac)_3^-]$, (c) $[N_{8,8,8,Bz}^+]$ $[Mn(hfacac)_2(Phtfacac)^-]$ MILs as extraction solvents. $[P_{6,6,6,14}^+]$ $[Mn(hfacac)_3^-]$ MIL conditions: *KRAS* template concentration: 2×10^4 copies μL^{-1}, amount of $[AOIM^+]$-*KRAS* $[PF_6^-]$ relative to DNA: 10x, NaCl concentration: 25 mM, sample volume: 1.0 mL, MIL volume: 8 µL; extraction time: 3 min. $[N_{8,8,8,Bz}^+][Mn(hfacac)_3^-]$ MIL conditions: *KRAS* template concentration: 2×10^4 copies μL^{-1}, amount of $[ABzIM^+]$-*KRAS* $[Br^-]$ relative to DNA: 10x, NaCl concentration: 25 mM, sample volume: 1.0 mL, MIL volume: 6 µL: extraction time: 1 min. $[N_{8,8,8,Bz}^+]$ $[Mn(hfacac)_2(Phtfacac)^-]$ MIL conditions: *KRAS* template concentration: 2×10^4 copies μL^{-1}, amount of $[ABzIM^+]$-*KRAS* $[Br^-]$ ITO relative to DNA: 10x, NaCl concentration: 25 mM, sample volume: 1.0 mL, MIL volume: 4 µL; extraction time: 1 min.

probes for the complementary sequence and 1-2 nt mismatch, melt curve analysis was performed. If the oligonucleotides are not complimentary, the T_m will decrease indicating instability of the hybridization.[49] Therefore, to examine the selectivity of the ITOs towards target DNA, the T_m of the ITO to a complementary oligonucleotide (20 nt), 1 nt mismatch (20 nt), and 2 nt mismatch (20 nt) was examined. Figure 4-S9 shows that the T_m significantly decreased when examining the hybridization of the ITO to the 1 nt mismatch, and a T_m could not be determined when hybridizing the $[AOIM^+]$-*KRAS* $[PF_6^-]$, $[ABzIM^+]$-*KRAS* $[Br^-]$, and $[ABzIM^+]$-*KRAS* $[PF_6^-]$ ITOs to the 2 nt mismatch.

Background cfDNA in cancer patients is approximately the same length as ctDNA (i.e, about 166 bp) and is present in high concentrations, typically 0-1000 ng mL^{-1} for cancer patients

with mutation abundances less than 0.01%.[4,8,50] To examine the effect of background DNA on the ITO-MIL-DLLME method, stDNA was sheared to around 150 bp and spiked into the aqueous sample. stDNA was sheared using a sonication method involving 30 s cycles (30s of

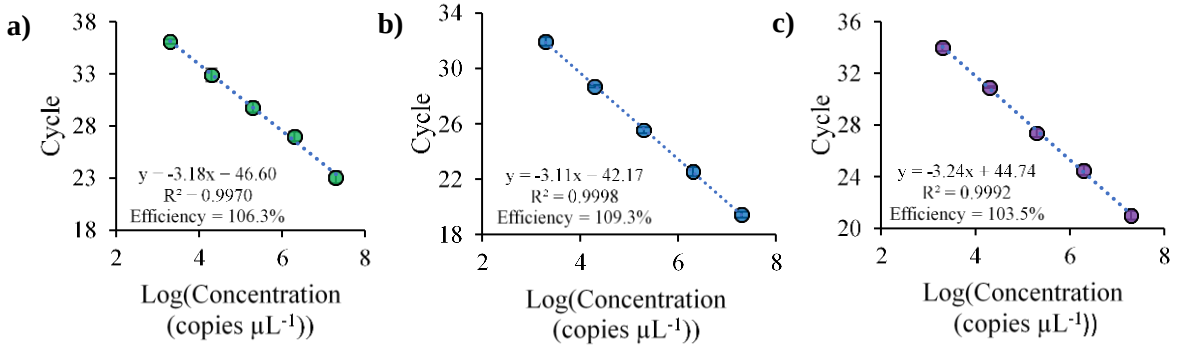

Figure 4-7 Standard curves generated using the optimized MIL-DLLME method from 10-fold diluted plasma for the (a) $[P_{6,6,6,14}^+]$ $[Mn(hfacac)_3^-]$, (b) $[N_{8,8,8,Bz}^+][Mn(hfacac)_3^-]$, (c) $[N_{8,8,8,Bz}^+]$ $[Mn(hfacac)_2(Phtfacac)^-]$ MILs as extraction solvents. $[P_{6,6,6,14}^+]$ $[Mn(hfacac)_3^-]$ MIL conditions: *KRAS* template concentration: 2×10^4 copies μL^{-1}, amount of $[AOIM^+]$-*KRAS* $[PF_6^-]$ ITO relative to DNA: 10x, NaCl concentration: 25 mM, sample volume: 1.0 mL, MIL volume: 8 µL; extraction time: 3 min. $[N_{8,8,8,Bz}^+][Mn(hfacac)_3^-]$ MIL conditions: *KRAS* template concentration: 2×10^4 copies μL^{-1}, amount of $[ABzIM^+]$-*KRAS* $[Br^-]$ ITO relative to DNA: 10x, NaCl concentration: 25 mM, sample volume: 1.0 mL, MIL volume: 6 µL: extraction time: 1 min. $[N_{8,8,8,Bz}^+]$ $[Mn(hfacac)_2(Phtfacac)^-]$ MIL conditions: *KRAS* template concentration: 2×10^4 copies μL^{-1}, amount of $[ABzIM^+]$-*KRAS* $[Br^-]$ ITO relative to DNA: 10x, NaCl concentration: 25 mM, sample volume: 1.0 mL, MIL volume: 4 µL; extraction time: 1 min.

of sonication followed by a 30 s rest period) for 1 h and verified by gel electrophoresis, as shown in Figure 4-S10a. Figure 4-S10b shows that the E_f did not significantly decrease when performing extractions from a sample solution containing 2×10^4 copies μL^{-1} of target *KRAS* and 1000 ng mL^{-1} of sheared stDNA (mutation abundance of 0.009%) indicating that clinically-relevant concentrations of background cfDNA do not have a significant effect on the extraction of low-abundance target sequences.

4.4 Conclusions

Circulating tumor DNA is difficult to isolate due to the presence of SNPs and large amounts of background DNA and proteins in human plasma. In this study, three hydrophobic MILs were designed and synthesized to function as liquid supports in the capture of the target ITO duplex without co-extraction of background DNA or protein. The fine dispersion of MIL solvent facilitated the formation of droplets with high surface area to capture the target ITO duplex without sedimentation. After collecting the MIL droplets on a magnetic rod, the MILs were directly added to qPCR using specially designed buffers that mitigated inhibition from MILs during the thermal cycling process. Incorporation of the manganese(II)-based MILs to the qPCR buffer did not significantly affect the amplification efficiency even when extractions were performed from diluted human plasma, indicating no significant inhibition. Target *KRAS* DNA was preconcentrated from pure water and 10-fold diluted plasma in as little as 1 min using the $[P_{6,6,6,14}^{+}][Mn(hfacac)_3^{-}]$, $[N_{8,8,8,Bz}^{+}][Mn(hfacac)_3^{-}]$, and $[N_{8,8,8,Bz}^{+}][Mn(hfacac)_2(Phtfacac)^{-}]$ MILs. Compared to commercially-available streptavidin magnetic beads, the ITO-MIL-DLLME approach using the $[N_{8,8,8,Bz}^{+}][Mn(hfacac)_3^{-}]$ and $[N_{8,8,8,Bz}^{+}][Mn(hfacac)_2(Phtfacac)^{-}]$ MILs produced a higher E_f when extracting target DNA from diluted plasma. The magnetic beads were unable to selectively preconcentrate target DNA from 10-fold diluted plasma while the ITO-MIL~~-ITO~~ procedure maintained selectivity towards the ITO-DNA duplex. The ability of the ITO-MIL system to selectively preconcentrate low concentrations of target DNA from diluted plasma indicates the promise that the ITO-MIL-DLLME method has in the detection of ctDNA fragments from clinical samples.

Acknowledgments

Chenghui Zhu, Muhammad Qamar Farooq, Idaira Pacheco-Fernández, and María J. Trujillo-Rodríguez are thanked for their assistance in this study. J. L. A acknowledges funding from the Chemical Measurement and Imaging Program at the National Science Foundation (CHE-1709372).

References

(1) Bettegowda, C.; Sausen, M.; Leary, R. J.; Kinde, I.; Wang, Y.; Agrawal, N.; Bartlett, B. R.; Wang, H.; Luber, B.; Alani, R. M.; et al. Detection of Circulating Tumor DNA in Early- and Late-Stage Human Malignancies. Sci. Transl. Med. 2014, 6 (224), 224ra24-224ra24.

(2) Xu, S.; Lou, F.; Wu, Y.; Sun, D.; Zhang, J.; Chen, W.; Ye, H.; Liu, J.; Wei, S.; Zhao, M.; et al. Circulating Tumor DNA Identified by Targeted Sequencing in Advanced-Stage Non-Small Cell Lung Cancer Patients. Cancer Lett. 2016, 370, 324–331.

(3) Diehl, F.; Li, M.; Dressman, D.; He, Y.; Shen, D.; Szabo, S.; Diaz, L. A.; Goodman, S. N.; David, K. A.; Juhl, H.; et al. Detection and Quantification of Mutations in the Plasma of Patients with Colorectal Tumors. Proc. Natl. Acad. Sci. U. S. A. 2005, 102 (45), 16368–16373.

(4) Ossandon, M. R.; Agrawal, L.; Bernhard, E. J.; Conley, B. A.; Dey, S. M.; Divi, R. L.; Guan, P.; Lively, T. G.; McKee, T. C.; Sorg, B. S.; et al. Circulating Tumor DNA Assays in Clinical Cancer Research. JNCI J. Natl. Cancer Inst. 2018, 110 (9), 929–934.

(5) Garrido, P., Olmedo, M. E., Gómez, A., Ares, L. P., López-Ríos, F.; Rosa-Rosa, J. M., Palacios, J. Treating KRAS-Mutant NSCLC: Latest Evidence and Clinical Consequences. Mult. Scler. J. 2017, 9 (9), 589–597.

(6) Zinsky, R.; Servet, B.; Bartsch, H.; Schirren, J.; Fisseler-eckhoff, A. Analysis of KRAS Mutations of Exon 2 Codons 12 and 13 by SNaPshot Analysis in Comparison to Common DNA Sequencing. Gastroenterol. Res. Pract. 2010, 2010 (17).

(7) Kidess, E.; Heirich, K.; Wiggin, M.; Vysotskaia, V.; Visser, C.; Marziali, A.; Wiedenmann, B.; Norton, J. A.; Lee, M.; Jeffrey, S. S.; et al. Mutation Profiling of Tumor DNA from Plasma and Tumor Tissue of Colorectal Cancer Patients with a Novel , High-Sensitivity Multiplexed Mutation Detection Platform. Oncotarget 2014, 6 (4), 2549–2561.

(8) Rodda, A. E.; Parker, B. J.; Spencer, A.; Corrie, S. R. Extending Circulating Tumor DNA Analysis to Ultralow Abundance Mutations: Techniques and Challenges. ACS Sensors 2018, 3, 540–560.

(9) Taniguchi, K.; Uchida, J.; Nishino, K.; Kumagai, T.; Okuyama, T.; Okami, J. Quantitative Detection of EGFR Mutations in Circulating Tumor DNA Derived from Lung Adenocarcinomas. Clin. Cancer Res. 2011, 17 (24), 7808–7815.

(10) Guha, M.; Castellanos-rizaldos, E.; Makrigiorgos, G. M. DISSECT Method Using PNA-LNA Clamp Improves Detection of EGFR T790m Mutation. PLoS One 2013, 8 (6), e67782.

(11) Leslie, D. C.; Li, J.; Strachan, B. C.; Begley, M. R.; Finkler, D.; Bazydlo, L. A. L.; Barker, N. S.; Haverstick, D. M.; Utz, M.; Landers, J. P. New Detection Modality for Label-Free Quantification of DNA in Biological Samples via Superparamagnetic Bead Aggregation. J. Am. Chem. Soc. 2012, 134, 5689–5696.

(12) Fan, Z. H.; Mangru, S.; Granzow, R.; Heaney, P.; Ho, W.; Dong, Q.; Kumar, R. Dynamic DNA Hybridization on a Chip Using Paramagnetic Beads. Anal. Chem. 1999, 71 (21), 4851–4859.

(13) Hayashi, S.; Hamaguchi, H. Discovery of a Magnetic Ionic Liquid [Bmim]FeCl4. Chem. Lett. 2004, 33 (12), 1590–1591.

(14) Del Sesto, R. E.; McCleskey, T. M.; Burrell, A. K.; Baker, G. a; Thompson, J. D.; Scott, B. L.; Wilkes, J. S.; Williams, P. Structure and Magnetic Behavior of Transition Metal Based Ionic Liquids. Chem. Commun. 2008, 447–449.

(15) Krieger, B. M.; Lee, H. Y.; Emge, T. J.; Wishart, J. F.; Castner Edward W., J. Ionic Liquids and Solids with Paramagnetic Anions. Phys. Chem. Chem. Phys. 2010, 12 (31), 8919–8925.

(16) Clark, K. D.; Varona, M.; Anderson, J. L. Ion-Tagged Oligonucleotides Coupled with a Magnetic Liquid Support for the Sequence-Specific Capture of DNA. Angew. Chemie - Int. Ed. 2017, 56 (26), 7630–7633.

(17) Peng, X.; Clark, K. D.; Ding, X.; Zhu, C.; Varona, M.; Emaus, M. N.; An, J.; Anderson, J. L. Coupling Oligonucleotides Possessing a Poly-Cytosine Tag with Magnetic Ionic Liquids for Sequence-Specific DNA Analysis. Chem. Commun. 2018, 54, 10284–10287.

(18) Schrader, C.; Schielke, A.; Ellerbroek, L.; Johne, R. PCR Inhibitors - Occurrence, Properties and Removal. J. Appl. Microbiol. 2012, 113, 1014–1026.

(19) DeVos, T.; Tetzner, R.; Model, F.; Weiss, G.; Schuster, M.; Distler, J.; Steiger, K. V.; Grützmann, R.; Pilarsky, C.; Habermann, J. K.; et al. Circulating Methylated SEPT9 DNA in Plasma Is a Biomarker for Colorectal Cancer. Clin. Chem. 2009, 55 (7), 1337–1346.

(20) Jamali, M. R.; Tavakoli, M.; Rahnama, R. Development of Ionic Liquid-Based in Situ Solvent Formation Microextraction for Iron Speciation and Determination in Water and Food Samples. J. Mol. Liq. 2016, 216, 666–670.

(21) Jha, R. R.; Singh, C.; Pant, A. B.; Patel, D. K. Ionic Liquid Based Ultrasound Assisted Dispersive Liquid-Liquid Micro-Extraction for Simultaneous Determination of 15 Neurotransmitters in Rat Brain, Plasma and Cell Samples. Anal. Chim. Acta 2018, 1005, 43–53.

(22) Trujillo-Rodriguez, M. J.; Nan, H.; Varona, M.; Emaus, M. N.; Souza, I. D.; Anderson, J. L. Advances of Ionic Liquids in Analytical Chemistry. Anal. Chem. 2019, 91 (1), 505–531.

(23) Clark, K. D.; Nacham, O.; Purslow, J. A.; Pierson, S. A.; Anderson, J. L. Magnetic Ionic Liquids in Analytical Chemistry: A Review. Anal. Chim. Acta 2016, 934, 9–21.

(24) Pandit, K. R.; Nanayakkara, I. A.; Cao, W.; Raghavan, S. R.; White, I. M. Capture and Direct Amplification of DNA on Chitosan Microparticles in a Single PCR-Optimal Solution. Anal. Chem. 2015, 87 (21), 11022–11029.

(25) Emaus, M. N.; Clark, K. D.; Hinners, P.; Anderson, J. L. Preconcentration of DNA Using Magnetic Ionic Liquids That Are Compatible with Real-Time PCR for Rapid Nucleic Acid Quantification. Anal. Bioanal. Chem. 2018, 410 (17), 4135–4144.

(26) Clark, K. D.; Zhu, C.; Anderson, J. L. Maximizing Ion-Tagged Oligonucleotide Loading on Magnetic Ionic Liquid Supports for the Sequence-Specific Extraction of Nucleic Acids. Anal. Chem. 2019, 91, 5945–5952.

(27) Pierson, S. A.; Nacham, O.; Clark, K. D.; Nan, H.; Mudryk, Y.; Anderson, J. L. Synthesis and Characterization of Low Viscosity Hexafluoroacetylacetonate-Based Hydrophobic Magnetic Ionic Liquids. New J. Chem. 2017, 41 (13), 5498–5505.

(28) Nacham, O.; Clark, K. D.; Yu, H.; Anderson, J. L. Synthetic Strategies for Tailoring the Physicochemical and Magnetic Properties of Hydrophobic Magnetic Ionic Liquids. Chem. Mater. 2015, 27 (3), 923–931.

(29) Clark, K. D.; Yamsek, M. M.; Nacham, O.; Anderson, J. L. Magnetic Ionic Liquids as PCR-Compatible Solvents for DNA Extraction from Biological Samples. Chem. Commun. 2015, 51 (94), 16771–16773.

(30) Khimji, I.; Doan, K.; Bruggeman, K.; Huang, P. J.; Vajha, P.; Liu, J. Extraction of DNA Staining Dyes from DNA Using Hydrophobic Ionic Liquids. Chem. Commun. 2013, 49, 4537–4539.

(31) Lebedev, A. V; Paul, N.; Yee, J.; Timoshchuk, V. A.; Shum, J.; Miyagi, K.; Kellum, J.; Hogrefe, R. I.; Zon, G. Hot Start PCR with Heat-Activatable Primers : A Novel Approach for Improved PCR Performance. Nucleic Acids Res. 2008, 36 (20), 1–18.

(32) Han, J.; Lee, H.; Nguyen, N. Y.; Beaucage, S. L.; Puri, R. K. Novel Multiple 5′-Amino-Modified Primer for DNA Microarrays. Genomics 2005, 86 (2), 252–258.

(33) Brownie, J.; Shawcross, S.; Theaker, J.; Whitcombe, D.; Ferrie, R.; Newton, C.; Little, S. The Elimination of Primer-Dimer Accumulation in PCR. Nucleic Acids Res. 1997, 25 (16), 3235–3241.

(34) Czerny, T. High Primer Concentration Improves PCR Amplification from Random Pools. Nucleic Acids Res. 1996, 24 (5), 985–986.

(35) Lipsky, R. H.; Mazzanti, C. M.; Rudolph, J. G.; Xu, K.; Vyas, G.; Bozak, D.; Radel, M. Q.; Goldman, D. DNA Melting Analysis for Detection of Single Nucleotide Polymorphisms. Clin. Chem. 2001, 644 (4), 635–644.

(36) Al-soud, W. A. B. U.; Jo, L. J.; Rådstro, P. Identification and Characterization of Immunoglobulin G in Blood as a Major Inhibitor of Diagnostic PCR. J. Clin. Microbiol. 2000, 38 (1), 345–350.

(37) Wadsworth, G.R.; Oliveiro, C. J. Plasma Protein Concentration of Normal Adults Living in Singapore. Br. Med. J. 1953, 2 (4846), 1138–1139.

(38) Shen, Y.; Jacobs, J. M.; Camp, D. G.; Fang, R.; Moore, R. J.; Smith, R. D.; Xiao, W.; Davis, R. W.; Tompkins, R. G. Ultra-High-Efficiency Strong Cation Exchange LC/RPLC/MS/MS for High Dynamic Range Characterization of the Human Plasma Proteome. Anal. Chem. 2004, 76 (4), 1134–1144.

(39) Quinlan, G. J.; Martin, G. S.; Evans, T. W. Albumin : Biochemical Properties and Therapeutic Potential. Hepatology 2005, 41 (6), 1211–1219.

(40) Topala, T., Bodoki, A., Oprean, L., Oprean, R. Bovine Serum Albumin Interactions with Metal Complexes. Clujul Med. 2014, 87 (4), 215–219.

(41) Scheuhammer, A.M., Cherian, M. G. Binding of Manganese in Human and Rat Plasma. Biochem. Biophys. Acta 1985, 840, 163–169.

(42) Kelley, S. O. What Are Clinically Relevant Levels of Cellular and Biomolecular Analytes? ACS Sensors 2017, 2, 193–197.

(43) Diehl, F.; Schmidt, K.; Choti, M. A.; Romans, K.; Goodman, S.; Li, M.; Thornton, K.; Agrawal, N.; Sokoll, L.; Szabo, S. A.; et al. Circulating Mutant DNA to Assess Tumor Dynamics. Nat. Med. 2008, 14 (9), 985–990.

(44) Rezaee, M.; Yamini, Y.; Faraji, M. Evolution of Dispersive Liquid – Liquid Microextraction Method. J. Chromatogr. A 2010, 1217 (16), 2342–2357.

(45) Rezaee, M.; Assadi, Y.; Milani Hosseini, M. R.; Aghaee, E.; Ahmadi, F.; Berijani, S. Determination of Organic Compounds in Water Using Dispersive Liquid-Liquid Microextraction. J. Chromatogr. A 2006, 1116, 1–9.

(46) Sanghvi, R. S.; Lemons, R. M.; Baker, H.; Thoene, J. G. A Simple Method for Determination of Plasma and Urinary Biotin. Clin. Chim. Acta 1982, 124, 85–90.

(47) Yuan, J. S.; Reed, A.; Chen, F.; Jr, C. N. S. Statistical Analysis of Real-Time PCR Data. BMC Bioinformatics 2006, 7 (85), 1–12.

(48) Milbury, C. A.; Li, J.; Makrigiorgos, G. M. PCR-Based Methods for the Enrichment of Minority Alleles and Mutations. Clin. Chem. 2009, 55 (4), 632–640.

(49) Schutz, E.; von Ahsen, N. Spreadsheet Software for Thermodynamic Melting Point Prediction of Oligonucleotide Hybridization with and without Mismatches. Biotechniques 1999, 27 (6), 1218–1224.

(50) Heitzer, E.; Ulz, P.; Geigl, J. B. Reviews Circulating Tumor DNA as a Liquid Biopsy for Cancer. Clin. Chem. 2015, 61 (1), 112–123.

CHAPTER 5.

SELECTIVE EXTRACTION OF LOW ABUNDANCE *BRAF* V600E MUTATION FROM PLASMA, URINE, AND SPUTUM USING ION-TAGGED OLIGONUCLEOTIDES AND MAGNETIC IONIC LIQUIDS

Modified from a manuscript published in *Analytical and Bioanalytical Chemistry*

Miranda N. Emaus and Jared L. Anderson

Department of Chemistry, Iowa State University, Ames, Iowa 50011, United States

Abstract

Sequence-specific DNA extractions have the potential to improve the detection of low abundance mutations from complex matrices, making them ideal for circulating tumor DNA analysis during the early stages of cancer. Ion-tagged oligonucleotides (ITOs) are oligonucleotides modified with an allylimidazolium salt via thiolene click chemistry. The allylimidazolium-based tag allows the ITO-DNA duplex to be selectively captured by a hydrophobic magnetic ionic liquid (MIL). In this study, the selectivity of the ITO-MIL method was examined by extracting low abundance of the *BRAF* V600E mutation – a common single-nucleotide polymorphism associated with several different cancers – from diluted human plasma, artificial urine, and diluted artificial sputum. Quantitative polymerase chain reaction (qPCR) was not able to distinguish a 9% *BRAF* V600E standard (50 fg·μL^{-1} *BRAF* V600E, 500 fg·μL^{-1} wild-type *BRAF*) from the 100% wild-type *BRAF* (50 fg·μL^{-1}) standard. However, introducing the ITO-MIL extraction prior to qPCR allowed for samples consisting of 0.1% *BRAF* V600E (50 fg·μL^{-1} V600E *BRAF*, 50,000 fg·μL^{-1} wild-type *BRAF* to be distinguished from the 100% wild-type *BRAF* standard.

5.1 Introduction

Cancer biomarkers can play several vital roles in patient care. Detection of tumor DNA can aid in diagnosis and provide information on patient prognosis.[1] Additionally, these biomarkers can help predict the success of specific cancer treatments and lead to personalized therapies.[2,3] Mutations in the *BRAF* gene are prominent in several cancers, including colorectal cancer, breast cancer, melanoma, lung cancer, and papillary thyroid cancer.[4,5] The *BRAF* V600E mutation, in particular, has been linked to poor survival and recurrence rates.[6] Tissue biopsies are the gold standard for cancer diagnosis but are highly invasive. The invasive nature of tissue biopsies makes it challenging to continuously monitor disease progression. Liquid biopsies are a potential alternative to tissue biopsies that involve non-invasively sampling circulating tumor DNA (ctDNA) from blood, urine, or sputum.[7,8] However, during the early stages of cancer, there is a low abundance of somatic mutations relative to wild-type (WT) DNA, making them challenging to detect.[9] Current ctDNA detection methods often rely on polymerase chain reaction (PCR). However, amplification of low abundance mutations poses a problem as the target sequence can be masked, resulting in preferential amplification of high abundance single-nucleotide polymorphisms (SNPs). Selective amplification of target sequences can be done using clamping probes to prevent elongation of the WT fragment[10] or careful optimization of the annealing temperature to ensure that allele-specific primers anneal to the target sequence.[11] However, these methods can be challenging to optimize, expensive, and may not work for all mutations.[12-14]

Sequence-specific DNA extractions are a potential supplement to selective amplification methods. In this approach, modified oligonucleotides anneal to the target via Watson-Crick base pairing and are captured by a solid sorbent, such as streptavidin-coated magnetic beads.[15,16]

However, solid particles can aggregate, resulting in reduced surface area to extract nucleic acids. A novel extraction method utilizes ion-tagged oligonucleotides (ITOs) and magnetic ionic liquids (MILs) to selectively preconcentrate target DNA.[17] Similar to ionic liquids (ILs), MILs exhibit advantageous properties, such as high thermal stabilities, negligible vapor pressures, and tunable solvation properties.[18-22] A prominent feature of MILs is the paramagnetic component within the chemical structure, allowing the insoluble solvent to respond to an external magnet. The paramagnetic component of the MIL also appears to play a role in the amount of DNA the MIL can extract, with manganese(II)-based MILs often exhibiting inferior DNA extraction capabilities compared to nickel(II)-based MILs.[23-24] ITOs are synthesized via a thiolene click reaction between a thiolated oligonucleotide and an allylimidazolium salt. The imidazolium-modified oligonucleotides are designed to anneal to target DNA and interact with MILs through hydrophobic, π-π stacking, and fluorophillic interactions.[25] Previous studies have reported that the ITO-MIL method can selectively extract DNA from a plant cell lysate, bacteria cell lysate, diluted plasma, diluted whole blood, and saline.[17,26-28] Another advantage of MILs compared to solid sorbents is their ability to be PCR compatible.[23,29,30] DNA-enriched MILs can be integrated into custom-designed PCR buffers where DNA is thermally desorbed during the reaction to significantly improve sample throughput.

In this study, the selectivity of the ITO-MIL method was investigated by extracting low abundance of the *BRAF* V600E mutation from several complex matrices. The annealing temperature of the ITO to the target DNA was carefully optimized to minimize co-extraction of WT *BRAF* in 25 mM NaCl, artificial urine, 2-fold diluted artificial sputum, and 4-fold diluted human plasma. Hydrolysis probes were employed to simultaneously monitor the amplification of WT *BRAF* and *BRAF* V600E. K-means clustering was used to determine whether extractions

using the ITOs could be statistically distinguished from the standards. Using the ITO-MIL method, 0.1-0.5% *BRAF* V600E could be distinguished from the 100% WT *BRAF* standard depending on the complex matrix with limited co-extraction of PCR inhibitors. Without employing the ITO-MIL extraction method, the 9% *BRAF* V600E standards could not be statistically distinguished from the 100% WT *BRAF* DNA. The ITO-MIL extraction method was also capable of selectively isolating fragmented *BRAF* V600E DNA from 25 mM NaCl, artificial urine, 2-fold diluted artificial sputum, and 4-fold diluted human plasma. The ability of the ITO-MIL method to selectively extract fragmented DNA from complex matrices suggests that this method has potential in clinical applications to improve the sensitivity of detecting low abundance mutations.

5.2 Materials and Methods

5.2.1 Reagents and Materials

Creatinine (99+%), manganese(II) chloride tetrahydrate (99+%), trioctylamine (97%) and 1,1,1,5,5,5-hexafluoroacetylacetone (99%) were purchased from Acros Organics (Morris Plains, NJ, USA). Anhydrous diethyl ether (99.0%) was purchased from Avantor Performance Materials Inc. (Center Valley, PA, USA). Difco vitamin assay casamino acids were purchased from BD (Franklin Lakes, NJ, USA). Trihexyl(tetradecyl)phosphonium chloride (97.7%) was purchased from Strem Chemicals (Newburyport, MA, USA). Ethylenediaminetetraacetic acid (EDTA) (99.4-100.06%), allyl bromide, 1-bromooctane (99%), benzylimidazole (99%), triethylamine (≥99.5%), LC-MS grade acetonitrile (≥99.9%), mucin from porcine stomach type (II), magnesium chloride hexahydrate (99.0-102.0%), and salmon testes DNA (~20 Kbp) were purchased from Sigma-Aldrich (St. Louis, MO, USA). SYBR Green I (10,000x) was purchased from Life Technologies (Carlsbad, CA, USA). Urea (>99%) and tris(2-carboxyethyl)phosphine

(TCEP) (>98%) were purchased from P212121 (Ypsilanti, MI, USA). Ammonium persulfate (APS) (≥98.0%), SSO Advanced Universal Supermix, and 40% acrylamide, bis-acrylamide solution 29:1 were purchased from Bio-Rad Laboratories (Hercules, CA, USA). Ammonium hydroxide (28-30% solution in water), PCR caps, tube strips, potassium chloride (99.70%), potassium phosphate monobasic (100%), sodium chloride (100.3%), sodium phosphate dibasic (99.8%), Taqman Universal master mix were purchased from Thermo Fisher Scientific (Waltham, MA, USA). Diethylene triamine pentaacetic acid (>98.0%) was purchased from TCI (Tokyo, Japan). Tris base and tris-HCl was purchased from RPI (Mount Prospect, IL, USA). Apheresis derived pooled human plasma (Na_2EDTA anticoagulant) was obtained from Innovative Research (Novi, MI, USA). All oligonucleotides (sequences shown in Table S1) were purchased from Integrated DNA Technologies (Coralville, IA, USA). A neodymium rod magnet (0.66 T) was purchased from K&J Magnetics (Pipersville, PA, USA) and used to collect dispersed MIL droplets or magnetic beads. Deionized water (18.2 MΩ cm), obtained from a Milli-Q water purification system, was used to prepare all aqueous solutions (Millipore, Bedford, MA, USA).

A 3.9 Kbp plasmid from Eurofin Genomics containing either a 210 WT *BRAF* or 210 *BRAF* V600E insert (sequences listed in Table 5-S1) was individually amplified using PCR. The PCR products were subsequently separated on a 1% agarose gel. Amplified DNA was recovered from the gel using the QIAquick Gel Extraction kit (Qiagen, Hilden, Germany) according to the manufacturer's instructions. Purified DNA was quantified using a NanoDrop 2000c spectrophotometer (Thermo Scientific, Waltham, MA, USA).

5.2.2 MIL and ITO synthesis

Chemical structures of the two MILs used in this study are shown in Fig. 5-1 (1-2). The MILs were synthesized and purified as previously reported.[28,31] The MIL solvents were stored in a desiccator at room temperature when not in use. Chemical structures of the two ITOs used in this study are shown in Fig. 5-1 (3-4). ITOs were prepared according to previously reported

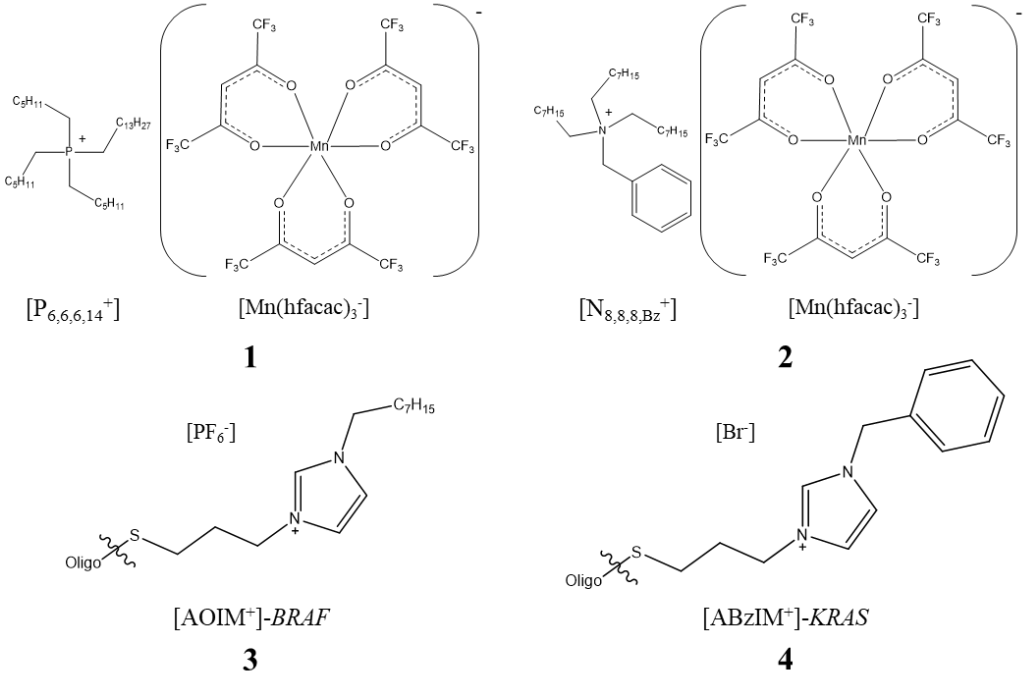

Figure 5-1 Chemical structures of the manganese(II)-based hydrophobic MILs (**1-2**) and octyl- and benzyl-imidazolium-based ITO (**3-4**) structures used within this study.

methods.[17,25] All ITOs were characterized using HPLC-TOF-MS; the theoretical and observed mass to charge ratios of the ITOs are shown in Table S2.

5.2.3 Preparation of Artificial Matrices

The artificial plasma solution was prepared as described by Przondziono et al.[32] Briefly, 0.68 g NaCl, 0.02 g $CaCl_2$, 0.04 g KCl, 0.01 g $MgSO_4$, 0.22 g $NaHCO_3$, 0.0126 g Na_2HPO_4, and 0.0026 g NaH_2PO_4 was dissolved in a 100 mL volumetric flask. The artificial urine was prepared

by dissolving 1.9820 g urea, 0.7013 g NaCl, 0.2218 g M KH_2PO_4, 0.0568 g Na_2HPO_4, and 0.1697 g creatinine in a 100 mL volumetric flask.[33]

Artificial sputum was prepared as described by Varona et al.[34] Briefly, 0.5 g of mucin, 0.4 g salmon testes DNA, 0.59 mg of diethyl triamine pentaacetic acid, 0.5 g NaCl, 0.22 g of KCl, and 0.181 g of Tris-base was dissolved in 80 mL of water in a volumetric flask. Once dissolved, 0.5 g of casamino acids were added. The pH was adjusted to 7.0, and the solution volume was brought to 100 mL. The solution was autoclaved prior to the addition of 0.5 mL of egg yolk emulsion to the mixture.

5.2.4 Annealing and Capture of Target DNA

The general procedure used to anneal the ITO to *BRAF* V600E DNA and its subsequent extraction is shown in Fig. 5-2. Extraction conditions were modified from Emaus et al.[28] A 1 mL

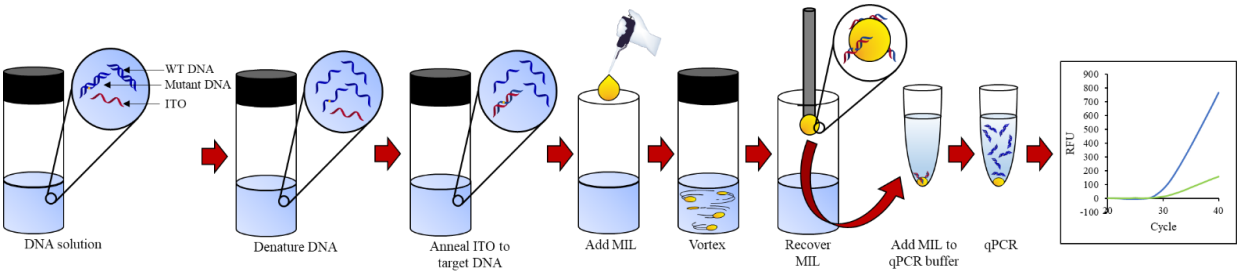

Figure 5-2 Schematic describing the sequence-specific extraction of *BRAF* V600E DNA using MILs and ITOs.

sample containing 50 fg·µL^{-1} of *BRAF* V600E DNA, 50-50,000 fg·µL^{-1} WT *BRAF* DNA, and 178 pg·µL^{-1} of either the [AOIM$^+$]-*BRAF* [PF_6^-] or [ABzIM$^+$]-*BRAF* [Br^-] ITO was prepared in a 5 mL screw cap glass vial. The sample was heated to 90°C using a Fisher Isotemp 2322 water bath (Rochester, MN, USA) for 2 min to denature the DNA duplex and then cooled at an optimized annealing temperature for 8 min. Immediately following the annealing step, 6 µL of the [$P_{6,6,6,14}^+$][$Mn(hfacac)_3^-$] or 8 µL of the [$N_{8,8,8,Bz}^+$][$Mn(hfacac)_3^-$] MIL was dispersed for 2 min or 1 min, respectively, using a Barnstead/Thermolyne Type 16700 mixer (Dubuque, IA, USA).

Extractions using the [$P_{6,6,6,14}^+$][Mn(hfacac)$_3^-$] MIL utilized the [AOIM$^+$]-*BRAF* [PF_6^-] ITO, and extractions with the [$N_{8,8,8,Bz}^+$][Mn(hfacac)$_3^-$] MIL used the [ABzIM$^+$]-*BRAF* [Br^-] ITO. The 25 mM NaCl, artificial urine, and 4-fold diluted human plasma sample matrices contained 5% DMSO to lower the annealing temperature. Extractions from 2-fold diluted artificial sputum only required a 30 s dispersion step due to the high solubility of the MILs in the artificial sputum matrix. DNA-enriched MIL droplets were collected using a rod magnet (B = 0.66 T) and subsequently washed with deionized water (18.2 MΩ cm). A 0.3 µL aliquot of DNA-enriched MIL was placed in a quantitative PCR (qPCR) tube for downstream analysis. All extractions were performed in triplicate.

5.2.5 qPCR Amplification

Standard reactions were performed using the following buffer: 1x Taqman Universal Master Mix, 1 µM forward *BRAF* primer, 1 µM reverse *BRAF* primer, 150 nM V600E *BRAF* probe, 75 nM WT *BRAF* probe. The addition of 0.3 µL [$P_{6,6,6,14}^+$][Mn(hfacac)$_3^-$] MIL to a 20 µL qPCR mixture required 1x Taqman Universal Master Mix, 1 µM forward *BRAF* primer, 1 µM reverse *BRAF* primer, 150 nM V600E *BRAF* probe, 75 nM WT *BRAF* probe, 6 mM EDTA, and 2.5 mM $MgCl_2$. Amplification with 0.3 µL of the [$N_{8,8,8,Bz}^+$][Mn(hfacac)$_3^-$] MIL was achieved using the 1x Taqman Universal Master Mix, 1 µM forward *BRAF* primer, 1 µM reverse *BRAF* primer, 150 nM V600E *BRAF* probe, 75 nM WT *BRAF* probe, 4 mM EDTA, and 2.5 mM $MgCl_2$ for a final volume of 20 µL.

A Bio-Rad CFX96 Touch Real-time PCR (Hercules, CA, USA) was utilized for qPCR amplification. Amplification of standards and reactions containing the [$P_{6,6,6,14}^+$][Mn(hfacac)$_3^-$] MIL used the following program: 10 min initial denaturation at 95°C followed by 40 cycles comprised of a 15 s denaturing step at 95°C, a 60 s annealing step at 61°C, and an optical

detection step. Reactions containing 0.3 µL of the $[N_{8,8,8,Bz}^{+}][Mn(hfacac)_3^{-}]$ MIL required an annealing temperature of 60°C to discriminate between the WT and *BRAF* V600E sequences.

Single-stranded *BRAF* V600E DNA was generated using asymmetric PCR.[35] A PCR buffer consisting of 1x SSO Universal Supermix, 1 µM reverse *BRAF* primer, 10 nM forward *BRAF* primer was used to preferentially amplify the sense strand. A 1:100 forward to reverse primer ratio was used to preferentially amplify one of the DNA strands, as described in Podar et al.[35] PCR product was separated on a 1% agarose gel and isolated using the QIAquick Gel Extraction kit. The annealing temperature of the ITO to ssDNA was determined using an initial 5 min denaturation step at 90°C, followed by a 10 min annealing step at 20°C, and a ramp from 20°C for 5 s and increasing to 95°C in 0.5°C increments.

The threshold cycle (Cq) and endpoint fluorescence signal were determined using the fluorescence threshold provided by the Bio-Rad CFX Maestro software and used to determine the amount of the *BRAF* V600E-ITO duplex extracted by the hydrophobic MIL. Standard curves were constructed for the V600E and WT *BRAF* template (see Fig. 5-S1). Discrimination between the WT and *BRAF* V600E DNA was determined using the Bio-Rad CFX Maestro software, and allelic discrimination plots were developed using the endpoint fluorescence signals (see Fig. 5-S2).

5.2.6 HPLC Conditions

HPLC separations of sheared DNA were performed on an LC-20A liquid chromatograph (Shimadzu, Japan) consisting of two LC-20AT pumps, a SPD-20 UV-vis detector, and a DGU-20A3 degasser. A 35 mm × 4.6 mm i.d. × 2.5 µm TSKgel DEAE-NPR anion exchange column with a 5 mm × 4.6 mm i.d. × 5 µm TSKgel DEAE-NPR guard column was obtained from Tosoh Bioscience (King of Prussia, PA, USA). The column was initially equilibrated with mobile phase

A (20 mM Tris-HCl, pH 8) for 20 min followed by gradient elution from 0% to 60% mobile phase B (20 mM Tris-HCl, 1 M NaCl, pH 8) over 10 min. A flow rate of 0.5 $mL \cdot min^{-1}$ was used for all HPLC separations, and DNA was detected at 260 nm.

5.2.7 Statistical Analysis

K-means clustering was used to determine if the extractions could be distinguished from the 100% WT *BRAF* standards using the HEX and FAM endpoint signals. These calculations were done by determining the centroid for each triplicate. The sum of square differences was calculated to determine the distance of a data point to the centroid of the standard and extraction triplicates. Data points were then assigned clusters based on the shortest distance to the centroid. The Student *t*-test was performed to determine if there was a statistical difference between the Cq values associated with extractions of different concentrations of *BRAF* V600E DNA. Probability values (p-values) were determined from the *t*-test results, and a significance level of 0.05 was chosen. Therefore, if the p-value is less than 0.05, the two data sets were considered statistically different.

5.3 Results and Discussion

5.3.1 Annealing temperature of the ITO to the target DNA

Selective extraction of DNA is dependent on the ability of the ITO to anneal to complementary DNA. However, the sample matrix can significantly influence the annealing temperature.[36,37] Therefore, the annealing temperature must be carefully optimized for the desired sequence and sample matrix. Melt curves of the ITO to single-stranded *BRAF* V600E DNA were developed in 25 mM NaCl, 4-fold diluted artificial plasma salts, artificial urine, and 2-fold diluted artificial sputum salts, as shown in Fig. 5-3. Melt curves generated in the artificial sputum

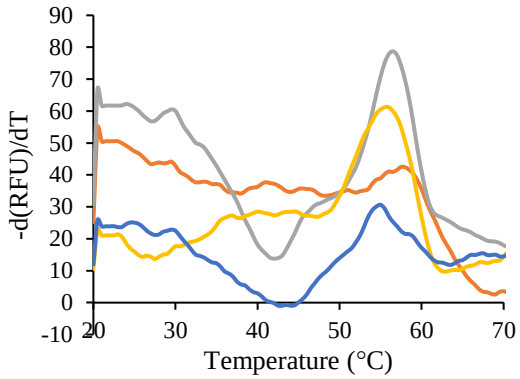

Figure 5-3 Melt curves of single-stranded *BRAF* V600E DNA to the complementary ITO in (yellow) 25 mM NaCl, (blue) 4-fold diluted plasma salt solution, (gray) artifical urine, and (orange) 2-fold diluted artifical sputum salt solution.

were generated without salmon testes DNA, mucins, and egg yolk emulsion in solution. The peak of the melt curve indicates the temperature at which 50% of the DNA is not annealed to the ITO. At temperatures higher than the peak, the ITO will poorly anneal to the target DNA, and DNA will be poorly extracted.

The most critical step to selectively extract a mutant SNP is the optimization of the annealing step. When the annealing temperature was too high, a low amount of both DNA sequences was detected, suggesting that the ITO was not annealing to the target (see Fig. 5-S3a). Conversely, when the annealing temperature was too low, a large amount of WT *BRAF* was detected compared to the mutant target, as shown in Fig. 5-S3b. The optimized annealing temperature was determined to be the temperature at which the lowest signal of WT *BRAF* was detected, as shown in Fig. 5-S3c. Using melt curves as a guide, the annealing temperature for each matrix was optimized by performing extractions with annealing temperatures from 35-60°C. The annealing temperature was optimized to 45°C for 25 mM NaCl, 40°C for 4-fold diluted plasma, 57°C for artificial urine, and 57°C for 2-fold diluted artificial sputum when performing extractions with either the [AOIM$^+$]-*BRAF* or [ABzIM$^+$]-*BRAF* ITOs.

5.3.2 Selectivity of the ITO-MIL-DLLME Method

Extractions of 0.1, 0.2, 0.5, 0.9, 9, 20, 33.3, and 50% *BRAF* V600E DNA (50 fg·µL^{-1} *BRAF* V600E, 50-50,000 fg·µL^{-1} WT *BRAF*) were performed to evaluate the ability of the ITO-MIL procedure to extract a low abundance mutation from a complex matrix. Cluster plots were developed by plotting the endpoint fluorescence signals from the HEX and FAM probes from each reaction, as shown in Fig. 5-4. Standard reactions containing less than 9% of *BRAF* V600E mutant could not be distinguished from the 100% WT *BRAF* standard by K-means clustering. However, the ITO-MIL extraction could distinguish as little as 0.1% *BRAF* V600E mutant with the $[N_{8,8,8,Bz}^{+}][Mn(hfacac)_3^{-}]$ MIL in 2-fold diluted artificial sputum. As little as 0.2% and 0.5% *BRAF* V600E mutant could be distinguished from the 100% WT BRAF standard when performing extractions from artificial urine and 25 mM NaCl, respectively, using the $[N_{8,8,8,Bz}^{+}][Mn(hfacac)_3^{-}]$ MIL. In comparison, the $[P_{6,6,6,14}^{+}][Mn(hfacac)_3^{-}]$ MIL was able to selectively preconcentrate sufficient mutant DNA to distinguish the ITO-MIL extraction from a 100% WT standard in solution comprised of 0.2%, 0.5%, 0.9% *BRAF* V600E in 2-fold diluted artificial sputum, 25 mM NaCl, artificial urine, respectively. Results from K-means clustering also correlate with threshold cycles achieved after performing the ITO-MIL extraction (see Fig. 5-S4). Once the 100% WT *BRAF* standard could no longer be distinguished from the extraction by K-means clustering, the Cq values associated with the low abundance *BRAF* V600E mutant extraction were significantly higher ($p < 0.05$) compared to the 50% *BRAF* V600E extraction from the same matrix.

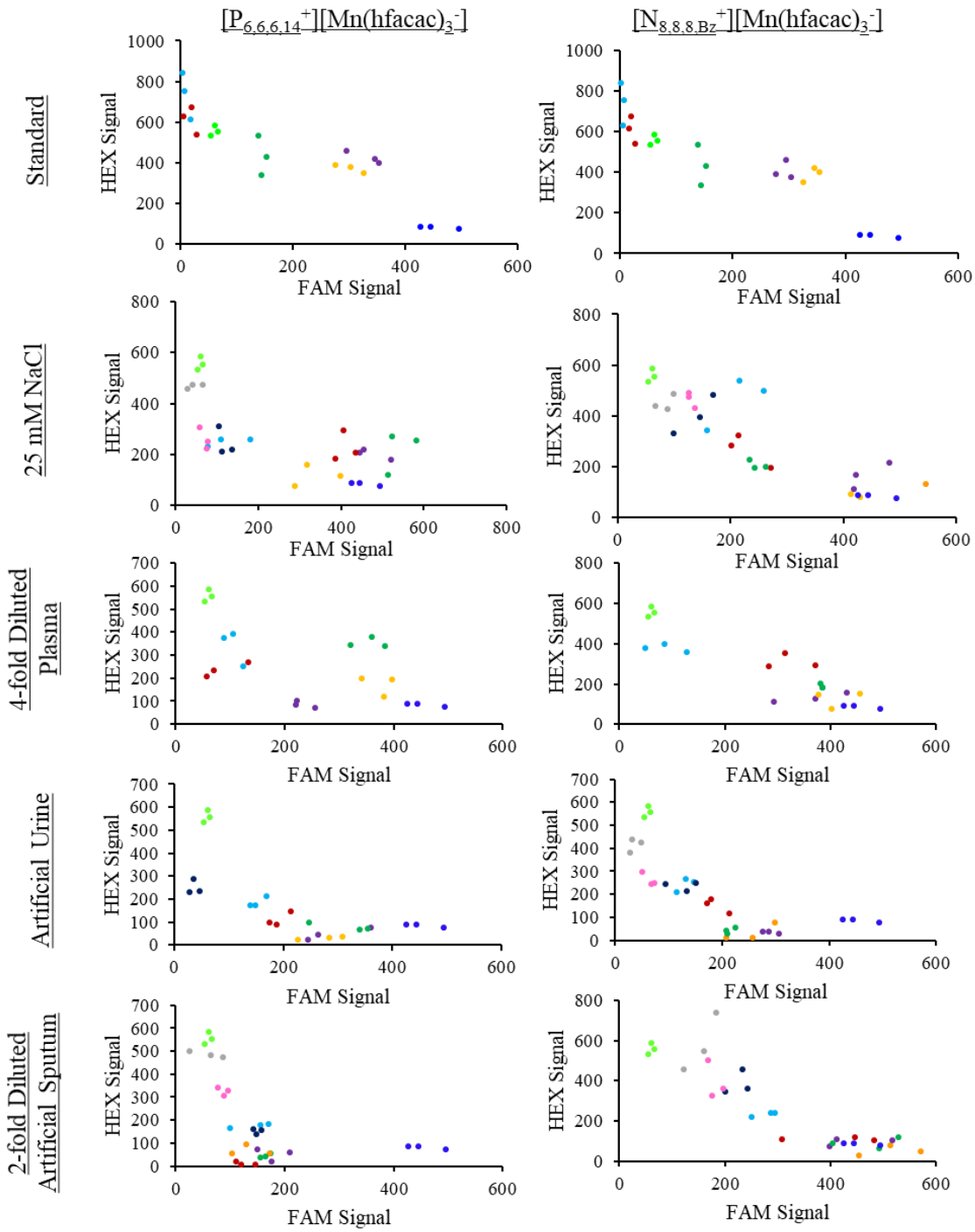

Figure 5-4 Cluster plots of endpoint fluorescence signals from the FAM and HEX probes from the extraction of 50% (orange), 33.3% (violet), 20% (green), 9.9% (red), 0.9% (light blue), 0.5% (dark blue), 0.2% (pink), and 0.1% (grey) *BRAF* V600E mutant DNA along with (bright green) 100% WT BRAF and (royal blue) 100% V600E BRAF standards.

It was observed that the ITO-MIL extraction with 178 pg·µL^{-1} ITO struggled to selectively preconcentrate the mutant BRAF fragment from 4-fold diluted human plasma compared to the other sample matrices. It was hypothesized that the ITO might adsorb to protein components of the plasma matrix.[38] To test this, the concentration of ITO was optimized, as shown in Fig. 5-S4. It was found that 356 pg·µL^{-1} [AOIM^{+}]-*BRAF* or [ABzIM^{+}]-*BRAF* ITO was ideal for performing extractions in 4-fold diluted plasma. Ultimately, using both MILs extractions of 0.2% V600E *BRAF* could be distinguished from the 100% WT *BRAF* standard by K-means clustering when 356 pg·µL^{-1} of ITO was used, as shown in Fig. 5-5. Similar to previous results with other matrices, the Cq values associated with the extraction of 0.1% *BRAF* V600E mutant DNA from diluted plasma were significantly higher based on the Student *t*-test compared to extractions above 0.2% *BRAF* V600E mutant (see Fig. 5-S5).

Degradation of ctDNA is rapid with a half-life ranging from 16 min to 2.5 h in blood and 2.6 h to 5.1 h in urine.[39,40] Recent studies have reported cell-free DNA in cancer patients to be

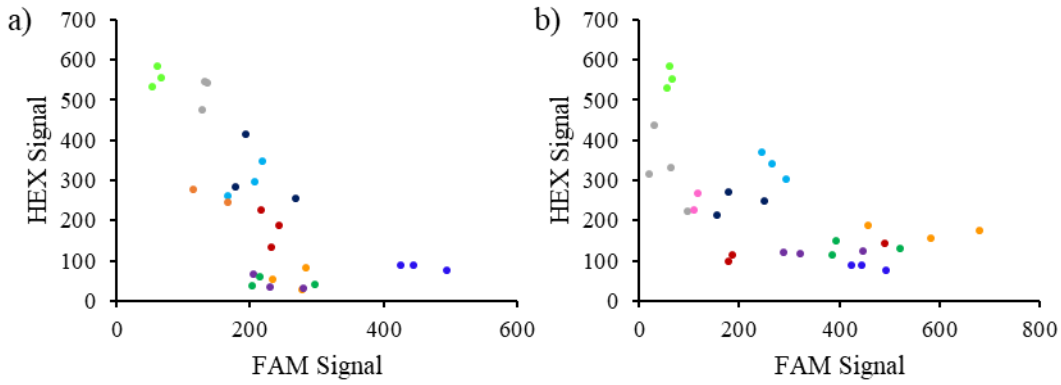

Figure 5-5 Cluster plots developed from the endpoint FAM and HEX signals after extracting target DNA from 4-fold diluted human plasma samples after optimization of the ITO amount consisting of 50% (orange), 33.3% (violet), 20% (green), 9.9% (red), 0.9% (light blue), 0.5% (dark blue), 0.2% (pink), and 0.1% (grey) *BRAF* V600E mutant DNA along with (bright green) 100% WT BRAF and (royal blue) 100% V600E BRAF standards.

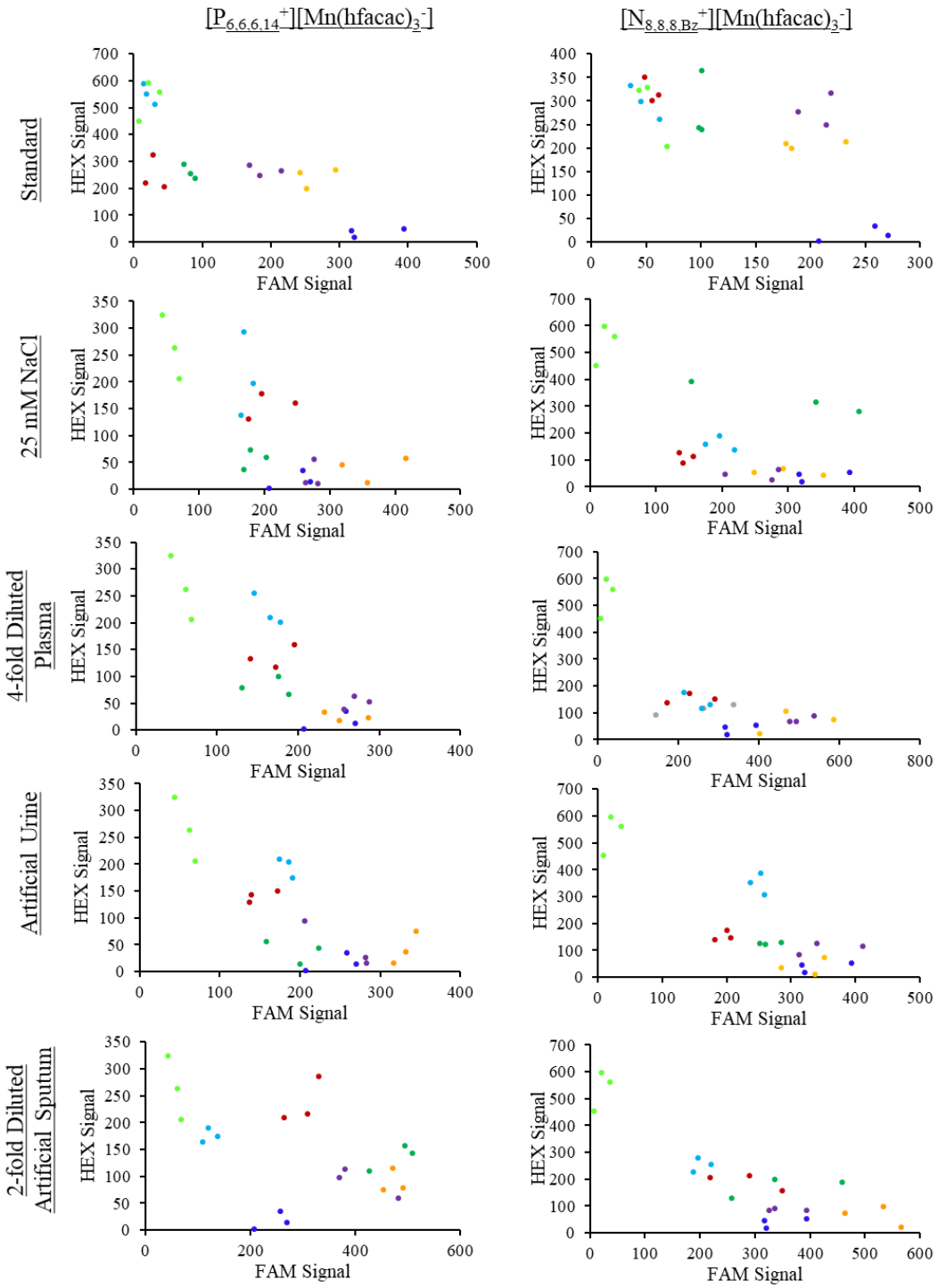

Figure 5-6 Cluster plots of the endpoint fluorescence signals corresponding to the FAM and HEX probes after the amplification and extraction of samples containing 50% (orange), 33.3% (violet), 20% (green), 9.9% (red), 0.9% (light blue) *BRAF* V600E mutant along with (bright green) 100% WT BRAF and (royal blue) 100% V600E BRAF standards after 30 min of shearing via sonication.

shorter than 145 bp.[41,42] Therefore, ITO-MIL extraction was applied to sheared DNA to evaluate the efficiency of the extraction with highly fragmented DNA. Plasmids containing the *BRAF* V600E and WT *BRAF* sequences were sheared for 30 min via sonication, and fragmentation was confirmed via anion exchange chromatography, as shown in Fig. 5-S6. Extractions from 0.9, 9, 20, 33, and 50% sheared *BRAF* V600E DNA were performed, and the *BRAF* V600E mutant was still preferentially extracted, as shown in Fig. 5-6. This preferential extraction suggests that the ITO-MIL method can be applied to fragmented DNA to selectively preconcentrate target DNA.

The selectivity of the optimized ITO-MIL method was compared to reported sequence-specific PCR methods for the detection of *BRAF* V600E mutant (Table 5-1). The selectivity of the ITO-MIL method outperformed sequence-specific amplification methods such as co-amplification at lower denaturation temperature (COLD) and was comparable to amplification refractory mutation system (ARMS) PCR. Clamping methods significantly outperformed the ITO-MIL extraction. However, the advantage of the ITO-MIL method originates from the rapid and selective extraction directly from complex matrices like artificial sputum and human plasma. For example, Mancini et al. utilized a QiaAMP spin column kit (Qiagen, Hilden Germany) that takes approximately 40-60 min to extract DNA.[43] In contrast, the ITO-MIL method required as little as 11 min. However, during early stages of cancer, the mutation abundance can be less than 0.01% suggesting that even lower detection limits are required.[9] Coupling the ITO-MIL method with a PCR clamp (i.e., locked nucleic acid or peptide nucleic acid) specific to WT *BRAF* could further lower detection limits of low abundance target, allowing for better detection of ctDNA biomarkers during the early stages of cancer.

Table 5-1 Comparison of the ITO-MIL method for *BRAF* V600E mutation to other sequence-specific DNA amplification techniques reported in literature.

Extraction Method	Sample Matrix	Type of PCR amplification	Sensitivity	Reference
ITO-MIL	Plasma, artificial urine, artificial sputum	qPCR	0.1-0.5%	This method
QiaAMP DNA Blood Mini Kit	FFPE[a] blocks from metastatic colorectal carcinoma patients	LNA[b]/DNA-Clamp PCR	0.01%	[2]
QiaAMP DNA Blood Mini Kit	Sporadic colorectal cancer tissue samples	COLD[c]-PCR	0.8%	[43]
ZR genomic DNA I kit	Thyroid tumor samples	ARMS[d]-PCR	0.5%	[44]
QiaAMP DNA FFPE Tissue Kit	Paraffin-embedded melanoma samples	RFLP[e]-ARMS-qPCR	0.1%	[45]

[a] Formalin-fixed, paraffin-embedded tissue (FFPE)
[b] Locked nucleic acid (LNA)
[c] Co-amplification at lower denaturation temperature (COLD)
[d] Amplification refractory mutation system (ARMS)
[e] Restriction fragment length polymorphism (RFLP)

5.3.3 Evaluation of PCR inhibitor Co-extraction

Matrices such as urine, plasma, and sputum contain several PCR inhibitors, including urea and IgG.[46] Therefore, the amplification efficiency of the reaction was calculated from standard curves developed by extracting different concentrations of *BRAF* V600E and WT *BRAF* (50% *BRAF* V600E) DNA. Standard curves for *BRAF* V600E were generated, as shown in Fig. 5-S7, as the mutant fragment was selectively extracted. The amplification efficiency ranged between 90-110% in all six standard curves. This suggests that DNA was successfully duplicated with each cycle, and limited amounts of PCR inhibitors were co-extracted by the manganese(II)-based MILs during the dispersive extraction despite the complex and diverse nature of the plasma, artificial urine, and artificial sputum sample matrices.

5.4 Conclusions

By carefully optimizing the annealing temperature, the co-extraction of WT *BRAF* could be minimized while permitting the ITO-DNA duplex to be captured by the MIL. Introducing the ITO-MIL extraction improved the sensitivity over 10-fold and allowed for the detection of 0.1% *BRAF* V600E mutant DNA in 2-fold diluted artificial sputum. Sensitivities as low as 0.2%, 0.2%, and 0.5% were reported while extracting the *BRAF* V600E mutant in human plasma, artificial urine, and 25 mM NaCl, respectively. Selectivity was maintained when performing extractions from sheared plasmids containing WT and *BRAF* V600E inserts. The ability of the ITO-MIL extraction method to selectively preconcentrate low abundance, fragmented DNA from complex matrices has potential in the field of ctDNA analysis where non-invasive sampling is highly desired.

Acknowledgments

J.L.A acknowledges funding from the Chemical Measurement and Imaging Program at the National Science Foundation (CHE-1709372).

Compliance with ethical standards

Conflicts of interest

The authors declare that they have no conflict of interest.

Research involving human participants and/or animals informed consent

This article does not contain any studies with human participants or animals performed by any of the authors.

References

(1) Sawyers, C. L. The Cancer Biomarker Problem. Nature 2008, 452 (7187), 548–552.

(2) Chen, D.; Huang, J. F.; Xia, H.; Duan, G. J.; Chuai, Z. R.; Yang, Z.; Fu, W. L.; Huang, Q. High-Sensitivity PCR Method for Detecting BRAF V600Emutations in Metastatic Colorectal Cancer Using LNA/DNA Chimeras to Block Wild-Type Alleles. Anal. Bioanal. Chem. 2014, 406 (9–10), 2477–2487.

(3) Thierry, A. R.; Mouliere, F.; El Messaoudi, S.; Mollevi, C.; Lopez-Crapez, E.; Rolet, F.; Gillet, B.; Gongora, C.; Dechelotte, P.; Robert, B.; et al. Clinical Validation of the Detection of KRAS and BRAF Mutations from Circulating Tumor DNA. Nat. Med. 2014, 20 (4), 430–435.

(4) Davies, H.; Bignell, G. R.; Cox, C.; Stephens, P.; Edkins, S.; Clegg, S.; Teague, J.; Woffendin, H.; Garnett, M. J.; Bottomley, W.; et al. Mutations of the BRAF Gene in Human Cancer. Nature 2002, 417 (6892), 949–954.

(5) Yokota, T.; Ura, T.; Shibata, N.; Takahari, D.; Shitara, K.; Nomura, M.; Kondo, C.; Mizota, A.; Utsunomiya, S.; Muro, K.; et al. BRAF Mutation Is a Powerful Prognostic Factor in Advanced and Recurrent Colorectal Cancer. Br. J. Cancer 2011, 104 (5), 856–862.

(6) Bhatia, P.; Friedlander, P.; Zakaria, E. A.; Kandil, E. Impact of BRAF Mutation Status in the Prognosis of Cutaneous Melanoma: An Area of Ongoing Research. Ann. Transl. Med. 2015, 3 (2), 1–7.

(7) Wu, Z.; Yang, Z.; Li, C. S.; Zhao, W.; Liang, Z. X.; Dai, Y.; Zhu, Q.; Miao, K. L.; Cui, D. H.; Chen, L. A. Differences in the Genomic Profiles of Cell-Free DNA between Plasma, Sputum, Urine, and Tumor Tissue in Advanced NSCLC. Cancer Med. 2019, 8 (3), 910–919.

(8) Peng, M.; Chen, C.; Hulbert, A.; Brock, M. V.; Yu, F. Non-Blood Circulating Tumor DNA Detection in Cancer. Oncotarget 2017, 8 (40), 69162–69173.

(9) Diehl, F.; Li, M.; Dressman, D.; He, Y.; Shen, D.; Szabo, S.; Diaz, L. A.; Goodman, S. N.; David, K. A.; Juhl, H.; et al. Detection and Quantification of Mutations in the Plasma of Patients with Colorectal Tumors. Proc. Natl. Acad. Sci. U. S. A. 2005, 102 (45), 16368–16373.

(10) Dominguez, P. L.; Kolodney, M. S. Wild-Type Blocking Polymerase Chain Reaction for Detection of Single Nucleotide Minority Mutations from Clinical Specimens. Oncogene 2005, 24 (45), 6830–6834

(11) Li, J.; Wang, L.; Mamon, H.; Kulke, M. H.; Berbeco, R.; Makrigiorgos, G. M. Replacing PCR with COLD-PCR Enriches Variant DNA Sequences and Redefines the Sensitivity of Genetic Testing. Nat. Med. 2008, 14 (5), 579–584.

(12) Milbury, C. A.; Li, J.; Makrigiorgos, G. M. PCR-Based Methods for the Enrichment of Minority Alleles and Mutations. Clin. Chem. 2009, 55 (4), 632–640.

(13) You, Y.; Moreira, B. G.; Behlke, M. A.; Owczarzy, R. Design of LNA Probes That Improve Mismatch Discrimination. Nucleic Acids Res. 2006, 34 (8), 1–11.

(14) Di Giusto, D. A. Strong Positional Preference in the Interaction of LNA Oligonucleotides with DNA Polymerase and Proofreading Exonuclease Activities: Implications for Genotyping Assays. Nucleic Acids Res. 2004, 32 (3), 1–8.

(15) Taniguchi, K.; Uchida, J.; Nishino, K.; Kumagai, T.; Okuyama, T.; Okami, J. Quantitative Detection of EGFR Mutations in Circulating Tumor DNA Derived from Lung Adenocarcinomas. Clin. Cancer Res. 2011, 17 (24), 7808–7815.

(16) Milbury, C. A.; Chen, C. C.; Mamon, H.; Liu, P.; Santagata, S.; Makrigiorgos, G. M. Multiplex Amplification Coupled with COLD-PCR and High Resolution Melting Enables Identification of Low-Abundance Mutations in Cancer Samples with Low DNA Content. J. Mol. Diagnostics 2011, 13 (2), 220–232.

(17) Clark, K. D.; Varona, M.; Anderson, J. L. Ion-Tagged Oligonucleotides Coupled with a Magnetic Liquid Support for the Sequence-Specific Capture of DNA. Angew. Chemie - Int. Ed. 2017, 56 (26), 7630–7633.

(18) Clark, K. D.; Nacham, O.; Purslow, J. A.; Pierson, S. A.; Anderson, J. L. Magnetic Ionic Liquids in Analytical Chemistry: A Review. Anal. Chim. Acta 2016, 934, 9–21.

(19) Lei, Z.; Chen, B.; Koo, Y. M.; Macfarlane, D. R. Introduction: Ionic Liquids. Chem. Rev. 2017, 117 (10), 6633–6635.

(20) Hallett, J. P.; Welton, T. Room-Temperature Ionic Liquids: Solvents for Synthesis and Catalysis. 2. Chem. Rev. 2011, 111 (5), 3508–3576.

(21) Del Sesto, R. E.; McCleskey, T. M.; Burrell, A. K.; Baker, G. a; Thompson, J. D.; Scott, B. L.; Wilkes, J. S.; Williams, P. Structure and Magnetic Behavior of Transition Metal Based Ionic Liquids. Chem. Commun. 2008, 447–449.

(22) Lee, S. H.; Ha, S. H.; Ha, S. S.; Jin, H. B.; You, C. Y.; Koo, Y. M. Magnetic Behavior of Mixture of Magnetic Ionic Liquid [Bmim] Fe Cl4 and Water. J. Appl. Phys. 2007, 101 (9), 1–4.

(23) Emaus, M. N.; Clark, K. D.; Hinners, P.; Anderson, J. L. Preconcentration of DNA Using Magnetic Ionic Liquids That Are Compatible with Real-Time PCR for Rapid Nucleic Acid Quantification. Anal. Bioanal. Chem. 2018, 410 (17), 4135–4144.

(24) Bowers, A. N.; Trujillo-Rodríguez, M. J.; Farooq, M. Q.; Anderson, J. L. Extraction of DNA with Magnetic Ionic Liquids Using in Situ Dispersive Liquid–Liquid Microextraction. Anal. Bioanal. Chem. 2019, 411 (28), 7375–7385.

(25) Clark, K. D.; Zhu, C.; Anderson, J. L. Maximizing Ion-Tagged Oligonucleotide Loading on Magnetic Ionic Liquid Supports for the Sequence-Specific Extraction of Nucleic Acids. Anal. Chem. 2019, 91, 5945–5952.

(26) Emaus, M. N.; Zhu, C.; Anderson, J. L. Selective Hybridization and Capture of KRAS DNA from Plasma and Blood Using Ion-Tagged Oligonucleotide Probes Coupled to Magnetic Ionic Liquids. Anal. Chim. Acta 2020, 1094, 1–10.

(27) Marengo, A.; Emaus, M. N.; Bertea, C. M.; Bicchi, C.; Rubiolo, P.; Cagliero, C.; Anderson, J. L. Arabidopsis Thaliana ITS Sequence-Specific DNA Extraction by Ion-Tagged Oligonucleotides Coupled with a Magnetic Ionic Liquid. Anal. Bioanal. Chem. 2019, 411 (25), 6583–6590.

(28) Emaus, M. N.; Varona, M.; Anderson, J. L. Sequence-Specific Preconcentration of a Mutation Prone KRAS Fragment from Plasma Using Ion-Tagged Oligonucleotides Coupled to qPCR Compatible Magnetic Ionic Liquid Solvents. Anal. Chim. Acta 2019, 1068, 1–10.

(29) Clark, K. D.; Yamsek, M. M.; Nacham, O.; Anderson, J. L. Magnetic Ionic Liquids as PCR-Compatible Solvents for DNA Extraction from Biological Samples. Chem. Commun. 2015, 51 (94), 16771–16773.

(30) Emaus, M. N.; Anderson, J. L. Simultaneous Cell Lysis and DNA Extraction from Whole Blood Using Magnetic Ionic Liquids. Anal. Bioanal. Chem. 2020, 412 (29), 8039–8049.

(31) Pierson, S. A.; Nacham, O.; Clark, K. D.; Nan, H.; Mudryk, Y.; Anderson, J. L. Synthesis and Characterization of Low Viscosity Hexafluoroacetylacetonate-Based Hydrophobic Magnetic Ionic Liquids. New J. Chem. 2017, 41 (13), 5498–5505.

(32) Przondziono, J.; Walke, W.; Hadasik, E.; Młynarski, R. Forecasting of Corrosion Properties of Steel Wires for Production of Guide Wires for Cardiological Treatment. Adv. Mater. Sci. Eng. 2013, 2013.

(33) Mayrovitz, H.; Sims, N. Biophysical Effects of Water and Synthetic Urine. Adv. Ski. Wound Care 2001, 14 (6), 302–308.

(34) Varona, M.; Ding, X.; Clark, K. D.; Anderson, J. L. Solid-Phase Microextraction of DNA from Mycobacteria in Artificial Sputum Samples to Enable Visual Detection Using Isothermal Amplification. Anal. Chem. 2018, 90 (11), 6922–6928.

(35) Poddar, S. K. Symmetric vs Asymmetric PCR and Molecular Beacon Probe in the Detection of a Target Gene of Adenovirus. Mol. Cell. Probes 2000, 14 (1), 25–32.

(36) Sintra, T. E.; Nasirpour, M.; Siopa, F.; Rosatella, A. A.; Gonçalves, F.; Coutinho, J. A. P.; Afonso, C. A. M.; Ventura, S. P. M. Ecotoxicological Evaluation of Magnetic Ionic Liquids. Ecotoxicol. Environ. Saf. 2017, 143 (May), 315–321.

(37) Owczarzy, R.; You, Y.; Moreira, B. G.; Manthey, J. A.; Huang, L.; Behlke, M. A.; Walder, J. A. Effects of Sodium Ions on DNA Duplex Oligomers: Improved Predictions of Melting Temperatures. Biochemistry 2004, 43 (12), 3537–3554.

(38) Kreader, C. A. Relief of Amplification Inhibition in PCR with Bovine Serum Albumin or T4 Gene 32 Protein. Appl. Environ. Microbiol. 1996, 62 (3), 1102–1106.

(39) Cheng, T. H. T.; Jiang, P.; Tam, J. C. W.; Sun, X.; Lee, W. S.; Yu, S. C. Y.; Teoh, J. Y. C.; Chiu, P. K. F.; Ng, C. F.; Chow, K. M.; et al. Genomewide Bisulfite Sequencing Reveals the Origin and Time-Dependent Fragmentation of Urinary CfDNA. Clin. Biochem. 2017, 50 (9), 496–501.

(40) Kim, C. J.; Park, J.; Sunkara, V.; Kim, T. H.; Lee, Y.; Lee, K.; Kim, M. H.; Cho, Y. K. Fully Automated, on-Site Isolation of CfDNA from Whole Blood for Cancer Therapy Monitoring. Lab Chip 2018, 18 (9), 1320–1329.

(41) Keller, L.; Belloum, Y.; Wikman, H.; Pantel, K. Clinical Relevance of Blood-Based ctDNA Analysis: Mutation Detection and Beyond. Br. J. Cancer 2020, 1–14.

(42) Mouliere, F.; Rosenfeld, N. Circulating Tumor-Derived DNA Is Shorter than Somatic DNA in Plasma. Proc. Natl. Acad. Sci. U. S. A. 2015, 112 (11), 3178–3179.

(43) Mancini, I.; Santucci, C.; Sestini, R.; Simi, L.; Pratesi, N.; Cianchi, F.; Valanzano, R.; Pinzani, P.; Orlando, C. The Use of COLD-PCR and High-Resolution Melting Analysis Improves the Limit of Detection of KRAS and BRAF Mutations in Colorectal Cancer. J. Mol. Diagnostics 2010, 12 (5), 705–711.

(44) Schrader, C.; Schielke, A.; Ellerbroek, L.; Johne, R. PCR Inhibitors - Occurrence, Properties and Removal. J. Appl. Microbiol. 2012, 113, 1014–1026.

(45) Huang, T.; Zhuge, J.; Zhang, W. W. Sensitive Detection of BRAF V600E Mutation by Amplification Refractory Mutation System (ARMS)-PCR. Biomark. Res. 2013, 1 (1), 1–6.

(46) Zhang, Y.; Qu, S.; Zhao, J.; Yu, T.; Guo, L.; Yin, S.; Hu, X.; Chen, W.; Lai, W.; Huang, J. A Novel Rflp-Arms Taqman Pcr-Based Method for Detecting the Braf V600e Mutation in Melanoma. Oncol. Lett. 2018, 16 (2), 1615–1621.

CHAPTER 6.

SIMULTANEOUS CELL LYSIS AND DNA EXTRACTION FROM WHOLE BLOOD USING MAGNETIC IONIC LIQUIDS

Modified from a manuscript published in *Analytical and Bioanalytical Chemistry*

Miranda N. Emaus and Jared Anderson

Department of Chemistry, Iowa State University, Ames, Iowa 50011, United States

Abstract

Conventional DNA sample preparation methods involve tedious sample handling steps that require numerous inhibitors of the polymerase chain reaction (PCR) and instrumentation to implement. These disadvantages limit the applicability of conventional cell lysis and DNA extraction methods in high throughput applications, particularly in forensics and clinical laboratories. To overcome these drawbacks, a series of nine hydrophobic magnetic ionic liquids (MILs) previously shown to preconcentrate DNA were explored as cell lysis reagents. The MILs were found to lyse white blood cells from whole blood, 2-fold diluted blood, and dry blood samples while simultaneously extracting human genomic DNA. The identity of metal ion incorporated within the MIL appears to cause hemolysis while the cationic component further reduces the cell's integrity. Over 500 pg of human genomic DNA was isolated from 50 µL of whole blood using the trioctylbenzylammonium tris(hexafluoroacetylaceto)nickelate(II) ($[N_{8,8,8,Bz}^{+}][Ni(hfacac)_3^{-}]$) MIL and 800 pg DNA was isolated from a dry blood samples using the trihexyl(tetradecyl)phosphonium tris(phenyltrifluoroacetylaceto)nickelate(II) ($[P_{6,6,6,14}^{+}][Ni(Phfacac)_3^{-}]$) MIL following a 1 min vortex step. A rapid, one-step cell lysis and DNA extraction from blood is ideal for settings that seek high-throughput analysis while minimizing the potential for contamination.

6.1 Introduction

Genomic DNA analysis from blood samples is highly important in forensic and clinical applications. Nucleic acid (NA) testing protocols for human immunodeficiency virus (HIV) and hepatitis B virus (HBV) target human genomic DNA, as the virus integrates genomic information into the host's white blood cells (WBCs).[1-3] These NA tests are capable of detecting the virus prior to antibody formation and are necessary to rapidly screen blood and organ donations. However, according to the American Red Cross, conventional NA tests for viruses require greater technical skill and expensive equipment compared to antibody testing. In addition, the isolation of human genomic DNA is commonly during investigations to determine the source of a bloodstain. In both forensic and clinical applications, there is a great need to rapidly analyze DNA from blood. Sample preparation is often considered an overlooked bottleneck in NA analysis as poor cell lysis and DNA extraction often limits the sensitivity of bioassays. Therefore, the development of highly efficient yet simple lysis and DNA extraction procedures are needed.

The separation of WBCs from red blood cells (RBCs) through mechanical or chemical means (i.e., centrifugation or selective red blood cell lysis) is often the first step in sampling NAs from whole blood due to the low abundance of WBCs.[4,5] Despite improved sensitivity, the isolation of WBCs is challenging and time-consuming. Therefore, interest exists in extracting NAs from whole blood to enhance sample throughput. Conventional methods for chemical cell lysis involve detergents, such as Triton X-100, to solubilize the cell membrane and release intracellular components.[6] Despite being cheap and simple to implement, chemical lysis methods typically require additional purification steps as the lysis reagent often inhibit downstream detection.[7,8] A recent advancement in the chemical lysis of cells involves the use of ionic liquids

(ILs) to lyse gram-positive and gram-negative cells, as well as viruses.[9-11] ILs are molten salts with melting points below 100 °C that exhibit a number of unique physiochemical properties.[12,13] Although ILs are effective at lysing cells, ILs often inhibit downstream detection. This often necessitates the dilution of their lysate and the amount of purified DNA prior to analysis by quantitative polymerase chain reaction (qPCR).

Human genomic DNA extractions from blood generally involve alkaline extraction, phenol-chloroform extraction, or spin column-based extraction.[6,14] These methods utilize large volumes of toxic organic solvents and require numerous time-consuming sample handling steps which limit their applicability. In particular, phenol and chloroform are known carcinogens and harmful towards the environment and their use, therefore, should be minimized. Methods involving simultaneous cell lysis and DNA extraction have reported a reduction in the number of sample handling steps. Nanayakkara et al. investigated chitosan microparticles in the lysis of WBCs via bead beating.[15] Bead beating is a common mechanical cell lysis method that imparts mechanical shear to the cells.[6,16] The chitosan-modified microparticles were simultaneously used to extract genomic DNA through electrostatic interactions. To improve sample throughput, the modified magnetic beads were added directly into the reaction buffer. However, the chitosan-microparticles were observed to significantly inhibit qPCR, limiting the sensitivity of the extraction method.[17]

Magnetic ionic liquids (MILs) have been shown to efficiently extract DNA from a number of complex matrices.[18-20] MILs are a subclass of ILs that contain a paramagnetic component in either the cation or anion allowing the solvent to respond to an external magnet, while still possessing similar physiochemical properties to ILs.[21-23] In addition, MILs can be designed to be qPCR compatible, permitting DNA-enriched MILs to be integrated into custom-

designed qPCR buffers to efficiently desorb DNA during amplification.[24-26] Thermal desorption during PCR has been shown to reduce the overall sample preparation time without impacting the efficiency of the reaction. However, the performance of DNA extraction is often secondary to the lysis efficiency, as poor lysis efficiencies limit the availability of DNA to extract.

In this study, a series of nine MILs were investigated as cell lysis agents. The hydrophobic MIL was dispersed in whole blood facilitating the lysis of WBCs, while simultaneously extracting human genomic DNA. The type of ligand, metal, and cation was found to play an important role in the amount of DNA extracted as well as the lysis efficiency. MILs containing a Ni(II) metal center and aromatic moieties in either the cationic component or ligand were found to exhibit superior extraction of human genomic DNA. However, MILs containing the Dy(III) or Gd(III) metal centers extracted significantly more DNA when the MIL is dispersed in blood compared to Tris buffer, suggesting that they are efficient at lysing cells but not extracting DNA. It was found that over 500 pg and 800 pg of genomic DNA was extracted from 50 µL whole blood and dried bloodstains, respectively, using MILs after only a 1 min vortex step. In comparison, commercial spin-column kits required a much longer extraction procedure of over 60 min. Integrating MILs into the qPCR buffer for thermal desorption did not have a deleterious effect on the amplification efficiency but greatly improved sample throughput. These results suggest that MILs are highly effective at rapidly lysing white blood cells and simultaneously extracting DNA for downstream analysis.

6.2 Methods and Materials

Ammonium hydroxide (28-30% solution in water), 1,1,1,5,5,5-hexafluoroacetylacetone (99%), and 1-phenyl-4,4,4-trifluoro-1,3-butanedione (99%) was purchased from Alfa Aesar (Ward Hill, MA, USA). Anhydrous diethyl ether (99.0%) was purchased from Avantor

Performance Materials Inc. (Center Valley, PA, USA). The 1-methyl-3-octylimidazolium bromide (99%) ([$OMIM^+$][Br^-]) IL was purchased from IoLITec (Tuscaloosa, AL, USA). Gadolinium(III) chloride hexahydrate (99.9%) and 1-tetradecanol (97%) was purchased from Beantown Chemicals (Hudson, NH, USA). Trihexyl(tetradecyl)phosphonium ([$P_{6,6,6,14}^+$]) chloride (97.7%) and dysprosium(III) chloride hexahydrate (99.9%) were purchased from Strem Chemicals (Newburyport, MA, USA). Ethylenediaminetetraacetic acid (EDTA) (99.4-100.06%), magnesium chloride hexahydrate (99.0-102.0%), lithium bis[(trifluoromethyl)sulfonyl]imide ([Li^+][NTf_2^-]), cobalt chloride (97%), benzenesulfonyl chloride (99%), bovine serum albumin (BSA) (≥96%), deoxyribonucleic acid sodium salt from salmon testes (20, 000 bp), Wright stain solution, LC-MS grade acetonitrile (ACN) (≥99.9%), 1-methylimidzaole (99%), and LC-MS grade methanol (≥99.8%) were purchased from MilliporeSigma (St. Louis, MO, USA). SYBR Green I (10,000x) was purchased from Life Technologies (Carlsbad, CA, USA). Proteinase K was purchased from New England Biolabs (Ipswich, MA, USA). Agarose and Tris(hydroxymethyl)aminomethane (Tris) hydrochloride (HCl) were purchased from P212121 (Ypsilanti, MI, USA). SsoAdvanced Universal SYBR Green Supermix (2x) was purchased from Bio-Rad Laboratories (Hercules, CA, USA). Primers (see Table S1) were purchased from Integrated DNA Technologies (Coralville, IA, USA). Modified plasmids (3.9 Kbp) containing a 210 bp insert (see Table 6-S1) were obtained from Eurofin Genomics (Louisville, KY, USA). PCR caps, tube strips, potassium chloride (99.7%), sodium phosphate dibasic anhydrous (99.8%), potassium phosphate monobasic (100.0%), dimethylsulfoxide (DMSO) (>99.7%), nickel chloride (98%), pyridine (99.9%), 1,1,1-trifluoro-2,4-pentadione (98%), sodium chloride, fresh human whole blood, frosted glass slides, and P5 grade filter paper were purchased from Fisher Scientific (Waltham, MA, USA). Neodymium magnets (0.2 T) were purchased from K&J

Magnetics (Pipersville, PA, USA). Deionized water (18.2 MΩ cm), obtained from a Milli-Q water purification system, was used to prepare all aqueous solutions (Millipore, Bedford, MA, USA).

6.2.1 Magnetic Ionic Liquid and Ionic Liquid Synthesis

The structures of the MILs used in this study are shown in Figure 6-1. The [$P_{6,6,6,14}^+$] tris(hexafluoroacetylaceto)nickelate(II) ([$Ni(hfacac)_3^-$]), [$P_{6,6,6,14}^+$] tris(hexafluoroacetylaceto)colbaltate(II) ([$Co(hfacac)_3^-$]), [$P_{6,6,6,14}^+$] tetrakis(hexafluoroacetylaceto)dysprosate(III) ([$Dy(hfacac)_4^-$]), [$P_{6,6,6,14}^+$] tetrakis(hexafluoroacetylaceto)gadolinate(III) ([$Gd(hfacac)_4^-$]), [$P_{6,6,6,14}^+$] tris(phenyltrifluoroacetylaceto)nickelate(II) ([$Ni(Phtfacac)_3^-$]), [$P_{6,6,6,14}^+$] tris(1,1,1-trifluoroacetylacetylaceto)nickelate(II) ([$Ni(tfacac)_3^-$]), and trioctylbenzylammonium ([$N_{8,8,8,Bz}^+$]) [$Ni(hfacac)_3^-$] MILs were synthesized and characterized as previously reported. [25,27,28] The [$P_{6,6,6,14}^+$][NTf_2^-], [$N_{8,8,8,Bz}^+$][NTf_2^-], 1-tetradecyl-3-methylimidazolium ([$C_{14}MIM^+$]) benzylsulfonate ([BS^-]), and ammonium ([NH_4^+]) [$Ni(hfacac)_3^-$] salts were synthesized according to previously published procedures.[25,27,28] The [$OMIM^+$][$Ni(hfacac)_3^-$] MIL was synthesized by mixing equimolar amounts of [NH_4^+][$Ni(hfacac)_3^-$] and [$OMIM^+$][Br^-] overnight in 50 mL of methanol. The [$C_{14}MIM^+$][$Ni(hfacac)_3^-$] MIL was synthesized by mixing equimolar amounts of [NH_4^+][$Ni(hfacac)_3^-$] and [$C_{14}MIM^+$][BS^-] overnight in 50 mL of methanol. The products were subsequently dried in a vacuum oven and purified using diethyl ether and water.

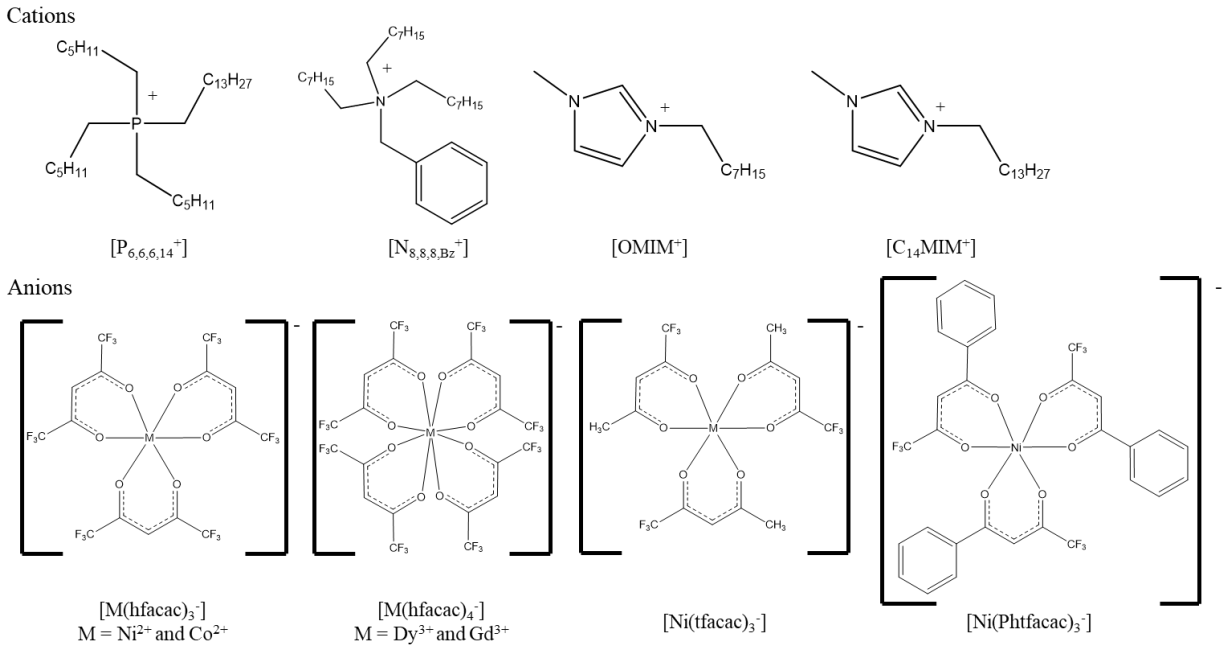

Figure 6-1 Structure of the cationic and anionic components for the nine MILs evaluated in this study.

6.2.2 PCR assays and Conditions

A Bio-Rad CFX96 Touch Real-time PCR (Hercules, CA, USA) was utilized for qPCR amplification of the human genomic DNA and 98 base-pair (bp) sequence (see Table S1) using the following program: 2 min initial denaturation at 95 °C followed by 40 cycles comprised of a 5 s denaturation step at 95 °C and a 30 s annealing step. An optical detection step was performed after the annealing step to track the progress of the reaction in real-time.

The β-actin gene in human genomic DNA was amplified in the absence of MIL in reaction buffer using 1x SsoAdvanced Supermix, 5% DMSO, and 1 µM primers. The addition of 0.3 µL of $[P_{6,6,6,14}^+][Ni(hfacac)_3^-]$, $[P_{6,6,6,14}^+][Ni(Phtfacac)_3^-]$, $[N_{8,8,8,Bz}^+][Ni(hfacac)_3^-]$, or $[OMIM^+][Ni(hfacac)_3^-]$ MILs to the reaction buffer required 1x SsoAdvanced Supermix, 5% DMSO, 1 µM primers, and an additional 1x SYBR Green I to achieve uninhibited qPCR amplification. Quantitative PCR with 0.3 µL of $[C_{14}MIM^+][Ni(hfacac)_3^-]$ MIL in the reaction

buffer required 1x SsoAdvanced Supermix, 5% DMSO, 1 µM primers, additional 1.25 mM $MgCl_2$, and an additional 1x SYBR Green I. The addition of 0.3 µL of $[P_{6,6,6,14}^+][Ni(tfacac)_3^-]$ MIL required to the qPCR buffer 1x SsoAdvanced Supermix, 5% DMSO, and 1 µM primers for amplification. The addition of 0.3 µL of $[P_{6,6,6,14}^+][Co(hfacac)_3^-]$ MIL in the reaction buffer required 1x SsoAdvanced Supermix, 5% DMSO, 1 µM primers, and an additional 2x SYBR Green I. The addition of 0.3 µL of $[P_{6,6,6,14}^+][Dy(hfacac)_4^-]$ MIL to the reaction buffer required 1x SsoAdvanced Supermix, 5% DMSO, 1 µM primers, 6 mM EDTA, 7.5 mM $MgCl_2$, 0.5 $mg \cdot mL^{-1}$ BSA, and an additional 1x SYBR Green I. The addition of 0.3 µL of $[P_{6,6,6,14}^+][Gd(hfacac)_4^-]$ MIL to the qPCR buffer required 1x SsoAdvanced Supermix, 5% DMSO, 1 µM primers, 6 mM EDTA, 6.5 mM $MgCl_2$, 1.5 $mg \cdot mL^{-1}$ BSA, and an additional 1x SYBR Green I.

Amplification of a 98 bp DNA sequence was achieved using 1x SsoAdvanced Supermix and 1 µM primers. The addition of 0.3 µL of $[P_{6,6,6,14}^+][Ni(hfacac)_3^-]$, $[P_{6,6,6,14}^+][Ni(Phtfacac)_3^-]$, $[N_{8,8,8,Bz}^+][Ni(hfacac)_3^-]$, $[P_{6,6,6,14}^+][Co(hfacac)_3^-]$, and $[OMIM^+][Ni(hfacac)_3^-]$ MILs to the reaction buffer required 1x SsoAdvanced Supermix, 1 µM primers, and an additional 1x SYBR Green I to achieve uninhibited qPCR amplification. Amplification with 0.3 µL of $[C_{14}MIM^+][Ni(hfacac)_3^-]$ MIL in the qPCR buffer required 1x SsoAdvanced Supermix, 1 µM primers, additional 1.25 mM $MgCl_2$, and an additional 1x SYBR Green I. Amplification with 0.3 µL of $[P_{6,6,6,14}^+][Ni(tfacac)_3^-]$ MIL in the reaction buffer required 1x SsoAdvanced Supermix and 1 µM primers for amplification. The addition of 0.3 µL of $[P_{6,6,6,14}^+][Dy(hfacac)_4^-]$ MIL in the reaction buffer required 1x SsoAdvanced Supermix, 1 µM primers, 2 mM EDTA, 7.5 mM $MgCl_2$, 1.5 $mg \cdot mL^{-1}$ BSA, and additional 1x SYBR Green I. The addition of 0.3 µL of $[P_{6,6,6,14}^+][Gd(hfacac)_4^-]$ MIL to the reaction buffer required 1x SsoAdvanced Supermix, 5%

DMSO, 1 µM primers, 2 mM EDTA, 6.5 mM $MgCl_2$, 1.5 mg·mL^{-1} BSA, and additional 1x SYBR Green I.

6.2.3 Lysis and Extraction Conditions

DNA extractions were performed from a 50 µL sample of either 50 pg·µL^{-1} human genomic DNA or 5 fg·µL^{-1} 98 bp DNA. A 2 µL volume of MIL was dispersed for 1 min and collected on a rod magnet (B = 0.2 T). Recovered MIL was washed with deionized water and a 0.3 µL aliquot of DNA-enriched MIL was added to the qPCR buffer. All extractions were performed in triplicate.

The general procedure used to simultaneously lyse and capture DNA from WBCs is shown in Figure 6-2. An optimized volume of MIL was added to a 50 µL blood sample and dispersed using a Barnstead/Thermolyne Type 16700 mixer (Dubuque, IA, USA) for an optimized length of time. The MIL was collected using a rod magnet (B = 0.2 T) and washed three times with deionized water. A 0.3 µL aliquot of DNA-enriched MIL was added to a qPCR tube for downstream amplification and detection. All dispersions were performed in triplicate.

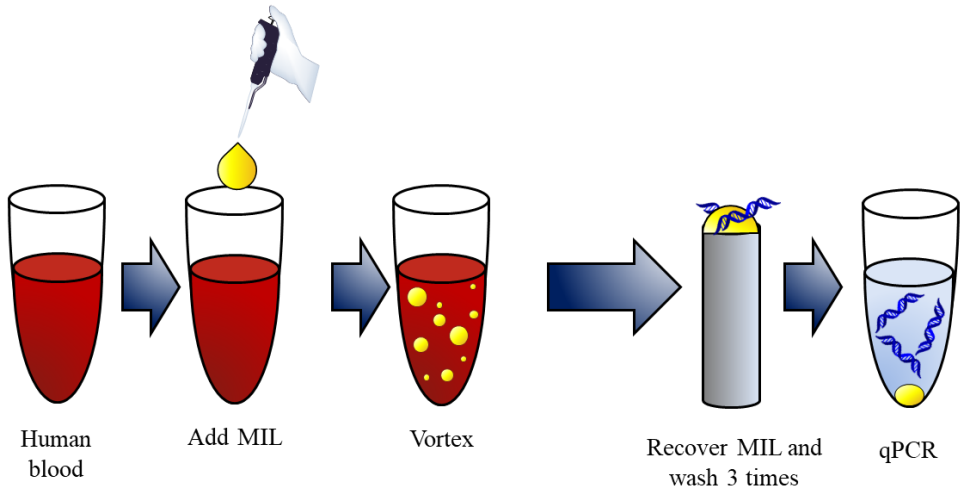

Figure 6-2 Schematic demonstrating the lysis of WBCs and extraction of DNA using MILs.

Dry bloodstains were prepared by aliquoting 50 µL of the whole blood on P5 filter paper (Fisher Scientific, Waltham, MA, USA). The blood was dried in a desiccator for 24 h. The filter paper was subsequently placed in 100 µL of phosphate buffer saline (137 mM NaCl, 2.7 mM KCl, 10 mM Na_2HPO_4, and KH_2PO_4, pH = 7.4) (PBS) for 5 min to desorb cells. The optimized volume of MIL was then dispersed for a specific amount of time to lyse WBCs and extract DNA. All extractions from dried blood samples were performed in triplicate.

WBC lysis and DNA extractions using the QiaAMP DNA mini kit were performed as specified by the manufacturer. Briefly, 50 µL of blood was diluted in PBS to 200 µL, and 16 units of proteinase K were added to the diluted blood. A 1 mL volume of lysis buffer (AL buffer) was added to the sample to lyse the cells for 10 min at 56 °C. After this, 1 mL of ethanol was added to the sample and mixed. The lysate was added to a silica column and centrifuged for 1 min at 1.3×10^4 rpm. The flow-through was discarded. Next, 0.5 mL of wash buffer 1 (AW1 buffer) was added to the column and centrifuged again for 1 min. The flow-through was discarded, and 0.5 mL of wash buffer 2 (AW2 buffer) was placed in the column. The column was then centrifuged for 3 min and the flow-through discarded. An additional 1 min centrifugation step was performed to ensure that the wash buffers were thoroughly removed. Lastly, 200 µL of elution buffer (AE buffer) was added to elute the purified DNA from the column.

6.2.4 Wright Staining Procedure

Wrights stains were developed based on the procedure described in Strober et al.[29] Briefly, 3 µL of blood was placed on a clean microscope slide. The blood was spread across the slide using a second slide. Once dry, 1 mL of methanol was placed on the dry blood to increase the cell's affinity for the stain. The slide was allowed to dry before 1 mL of Wright's stain was

placed on the slide for 2 min. Then, 2 mL of PBS was placed on the slide for 4 min. Slides were then rinsed with water to remove excess solution and allowed to air dry. Cells were visualized under a Micromaster microscope (Fisher Scientific, Waltham, MA, USA).

6.3 Results and Discussion

Integrating DNA-enriched MILs into a qPCR assay allows DNA to desorb from the solvent using the elevated temperatures required for PCR without impacting the amplification efficiency.[25,26] However, the elevated temperatures required for PCR may increase the solubility of the MIL, potentially inhibiting the reaction. PCR inhibition caused by MILs can be overcome by optimizing the amount of EDTA, SYBR Green I, BSA, and $MgCl_2$. The custom-designed qPCR buffers for each MIL are summarized in Table 6-S2. As shown in Figure 6-S1, standard curves were constructed by spiking human genomic DNA into the custom-designed qPCR buffers and used to quantify the amount of DNA extracted by the MIL. Quantification of human genomic DNA in the absence of MIL was carried out using the standard curve in Figure 6-S2a. The standard curve in Figure 6-S2b was used to quantify the 98 bp DNA fragment extracted by the MILs.

6.3.1 Extraction of Human Genomic DNA

To evaluate the ability of hydrophobic MILs to extract human genomic DNA, extractions were initially performed from 2 mM Tris buffer. As shown in Figure 6-3, the nine MILs examined all extracted human genomic DNA with the Ni(II)-based MILs containing an aromatic moiety within either the cation or ligand structure generally extracted the most DNA.

The ability of the MIL to extract DNA from blood was studied by spiking a non-targeted DNA sequence into the blood. As shown in Figure 6-S3a, the spiked DNA could be recovered from blood using all nine MILs, although several exhibited very low extraction efficiencies.

However, the blood matrix imparted a significant decrease in the amount of DNA extracted compared to extractions from Tris buffer (Figure 6-S3b). The $[N_{8,8,8,Bz}^+][Ni(hfacac)_3^-]$ and $[P_{6,6,6,14}^+][Ni(Phtfacac)_3^-]$ MILs were found to extract the most DNA from the blood matrix.

6.3.2 Optimizing the Lysis and Extraction of Human Genomic DNA from WBCs

The volume of MIL and extraction time were optimized from 2-9 µL and 15-120 s, respectively, to ensure the highest amount of DNA was extracted from 2-fold diluted blood. As shown in Figure 6-S4, 2 µL of MIL was optimum for the $[P_{6,6,6,14}^+][Co(hfacac)_3^-]$, $[OMIM^+][Ni(hfacac)_3^-]$, $[P_{6,6,6,14}^+][Dy(hfacac)_4^-]$, and $[P_{6,6,6,14}^+][Gd(hfacac)_4^-]$ MILs. It was found that a 3 µL volume of the $[C_{14}MIM^+][Ni(hfacac)_3^-]$ MIL and 5 µL of the $[N_{8,8,8,Bz}^+][Ni(hfacac)_3^-]$ MIL was optimum. For the $[P_{6,6,6,14}^+][Ni(Phtfacac)_3^-]$ MIL, 6 µL was optimum while 7 µL of the $[P_{6,6,6,14}^+][Ni(hfacac)_3^-]$ and $[P_{6,6,6,14}^+][Ni(tfacac)_3^-]$ MILs was optimum. Extractions with higher volumes of the $[P_{6,6,6,14}^+][Dy(hfacac)_4^-]$ and $[P_{6,6,6,14}^+][Gd(hfacac)_4^-]$ MILs were unsuccessful, and the MIL could not be recovered. An

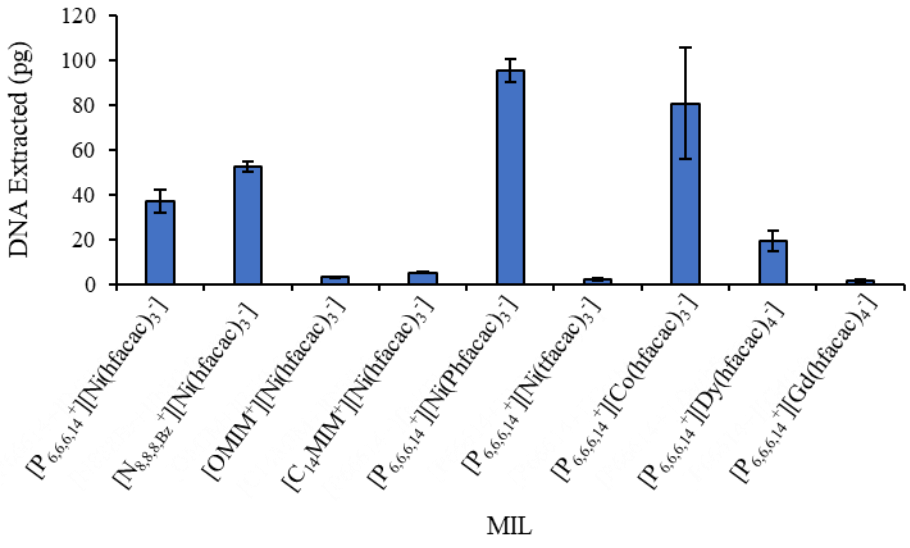

Figure 6-3 Extraction of 50 pg·µL^{-1} human genomic DNA from 2 mM Tris buffer using nine different MILs. Sample volume: 50 µL; MIL volume: 2 µL; extraction time: 1 min.

optimized vortex time of only 30 s was required for the $[P_{6,6,6,14}^+][Gd(hfacac)_4^-]$ MIL. The highest amount of DNA detected was achieved after a 1 min vortex with the $[P_{6,6,6,14}^+][Ni(hfacac)_3^-]$, $[P_{6,6,6,14}^+][Ni(Phtfacac)_3^-]$, $[N_{8,8,8,Bz}^+][Ni(hfacac)_3^-]$, $[P_{6,6,6,14}^+][Co(hfacac)_3^-]$, $[OMIM^+][Ni(hfacac)_3^-]$, $[C_{14}MIM^+][Ni(hfacac)_3^-]$, and $[P_{6,6,6,14}^+][Ni(tfacac)_3^-]$ MILs, as shown in Figure 6-S5. A vortex time of 90 s was optimum for the $[P_{6,6,6,14}^+][Dy(hfacac)_4^-]$ MIL.

The simultaneous lysis of WBCs and extraction of human genomic DNA was evaluated using the optimized extraction procedures for each MIL from 2-fold diluted blood, whole blood, and dry bloodstains. As shown in Figure 6-4, the $[N_{8,8,8,Bz}^+][Ni(hfacac)_3^-]$ MIL was most successful at lysing and extracting DNA from 2-fold diluted and whole blood. However, the $[P_{6,6,6,14}^+][Ni(Phtfacac)_3^-]$ MIL extracted more DNA from dry blood samples. It was found that commercial spin columns extracted more DNA from 2-fold diluted blood, whole blood, and dry bloodstains compared to the MILs. Interestingly, the Gd(III) and Dy(III) MILs recovered significantly more DNA from blood compared to Tris buffer. It is possible that the Gd(III) and Dy(III) MILs were more successful at lysing WBCs compared to the Ni(II) MIL, but their poor DNA extraction efficiencies hindered their overall performance. Although the spin columns were able to extract more DNA, the MIL-based method required only 1 min whereas the kits require over 60 min as well as additional instrumentation (centrifuge and water bath) and multiple reagents, making the extraction more cumbersome.[30]

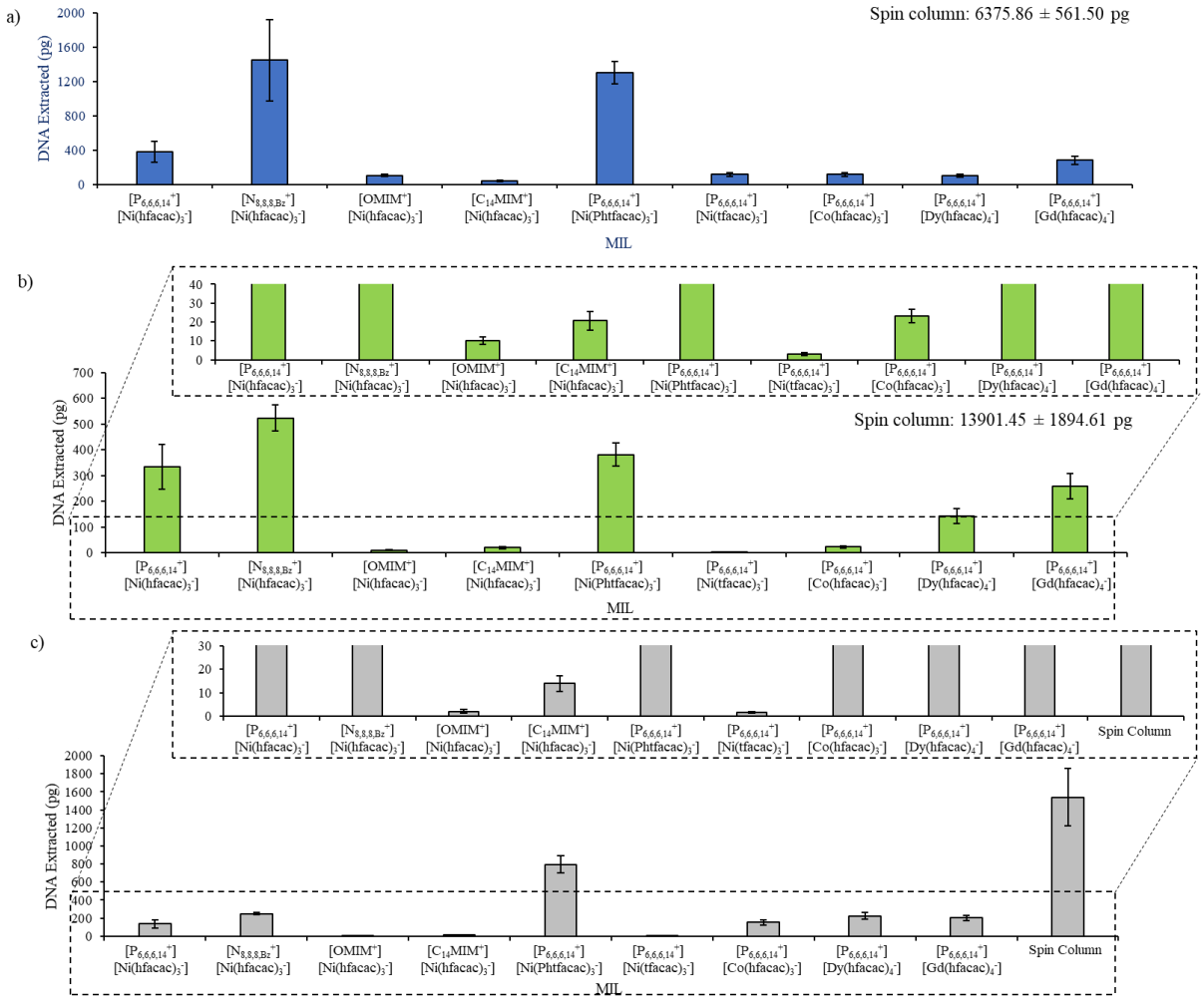

Figure 6-4 Amount of DNA detected following the use of MILs to lyse WBCs and extract DNA from (a) 2-fold diluted blood, (b) whole blood, and (c) dry bloodstains. The QiaAMP spin columns were able to extract (a) 6375.86 ± 561.50 pg, (b) 13901.45 ± 1894.61 pg, (c) and 1537.99 ± 319.04.

6.3.3 Evaluating of the Co-extraction of PCR Inhibitors

To evaluate the co-extraction of PCR inhibitors by the MIL from undiluted blood, serial dilutions of a 98 bp DNA sequence not found in blood were spiked into the qPCR buffer to

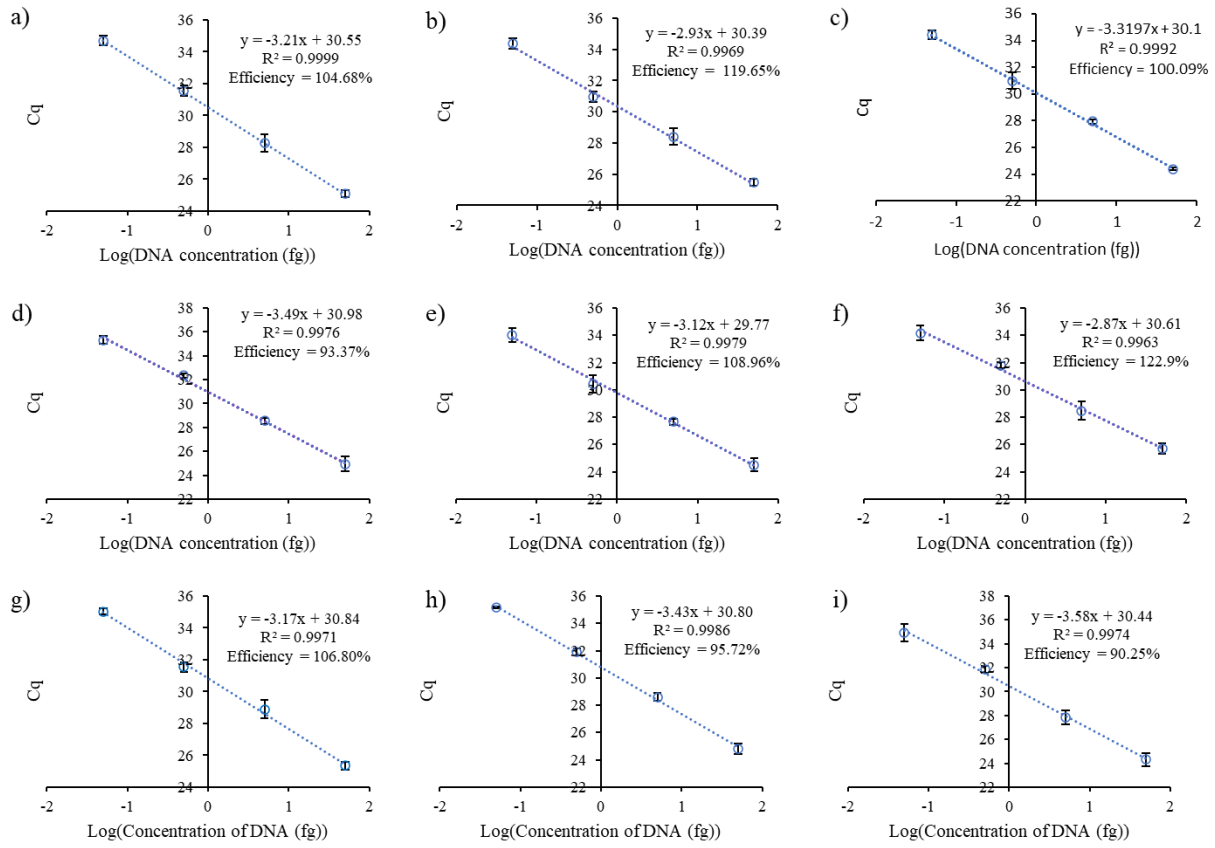

Figure 6-5 the amplification efficiencies associated with the $[P_{6,6,6,14}^{+}][Ni(hfacac)_3^{-}]$, $[P_{6,6,6,14}^{+}][Ni(Phtfacac)_3^{-}]$, $[P_{6,6,6,14}^{+}][Co(hfacac)_3^{-}]$, $[OMIM^{+}][Ni(hfacac)_3^{-}]$, $[C_{14}MIM^{+}][Ni(hfacac)_3^{-}]$, $[P_{6,6,6,14}^{+}][Dy(hfacac)_4^{-}]$, and $[P_{6,6,6,14}^{+}][Gd(hfacac)_4^{-}]$ MILs were between 90-110%. This suggests that DNA is being Figure 6-6 Standard curves generated by spiking a 98 bp DNA sequence into the qPCR reaction after dispersing the (a) $[P_{6,6,6,14}^{+}][Ni(hfacac)_3^{-}]$, (b) $[N_{8,8,8,Bz}^{+}][Ni(hfacac)_3^{-}]$, (c) $[OMIM^{+}][Ni(hfacac)_3^{-}]$, (d) $[C_{14}MIM^{+}][Ni(hfacac)_3^{-}]$, (e) $[P_{6,6,6,14}^{+}][Ni(Phtfacac)_3^{-}]$, (f) $[P_{6,6,6,14}^{+}][Ni(tfacac)_3^{-}]$, (g) $[P_{6,6,6,14}^{+}][Co(hfacac)_3^{-}]$, (h) $[P_{6,6,6,14}^{+}][Dy(hfacac)_4^{-}]$, and (i) $[P_{6,6,6,14}^{+}][Gd(hfacac)_4^{-}]$ MILs in whole blood.

generate standard curves. As shown in duplicated with each cycle and that limited amounts of qPCR inhibitors are being duplicated with each cycle and that limited amounts of qPCR inhibitors are being extracted by the MILs. However, amplification efficiencies associated with dispersing the $[N_{8,8,8,Bz}^{+}][Ni(hfacac)_3^{-}]$ and $[P_{6,6,6,14}^{+}][Ni(tfacac)_3^{-}]$ MILs in whole blood were above 110%, suggesting the co-extraction of PCR inhibitors by these MILs. Interestingly, decreasing the MIL volume dispersed in blood from the optimized volume (5 and 7 µL for the

$[N_{8,8,8,Bz}^+][Ni(hfacac)_3^-]$ and $[P_{6,6,6,14}^+][Ni(tfacac)_3^-]$ MILs, respectively) to 2 µL caused the amplification efficiencies to drop to 96.48% and 103.66% with the $[N_{8,8,8,Bz}^+][Ni(hfacac)_3^-]$ and $[P_{6,6,6,14}^+][Ni(tfacac)_3^-]$ MILs, respectively while developing standard curves with the 98 bp sequence (see Figure 6-S6). This suggests that PCR inhibitors are co-extracted more readily with larger volumes of MIL, likely due to the increased surface area facilitating mass transfer with PCR inhibitors.[13]

The amount of DNases co-extracted by the MIL from whole blood was evaluated by allowing the DNA-enriched MILs to incubate for up to 48 h at 25 °C prior to qPCR amplification. All nine MILs were found to preserve DNA extracted from Tris buffer for 48 h (see Figure 6-S7a). This suggests that the hexafluoroacetylacetonate-based MILs do not degrade DNA over time. As shown in Figure 6-S7b, there was no significant change in the amount of DNA detected using the $[P_{6,6,6,14}^+][Ni(Phtfacac)_3^-]$ and $[N_{8,8,8,Bz}^+][Ni(hfacac)_3^-]$ MILs after 48 h. However, a significant drop in the amount of DNA was observed using the Student t-test ($p < 0.05$) after 48 h with the $[P_{6,6,6,14}^+][Gd(hfacac)_4^-]$ MIL and 24 h with the $[P_{6,6,6,14}^+][Ni(hfacac)_3^-]$, $[P_{6,6,6,14}^+][Ni(hfacac)_3^-]$, $[C_{14}MIM^+][Ni(hfacac)_3^-]$, and $[P_{6,6,6,14}^+][Dy(hfacac)_4^-]$ MILs. The $[OMIM^+][Ni(hfacac)_3^-]$ and $[P_{6,6,6,14}^+][Ni(tfacac)_3^-]$ MILs were found to preserve DNA for only 6 h. The drop in the amount of DNA detected suggests nucleases are being extracted by the $[P_{6,6,6,14}^+][Ni(hfacac)_3^-]$, $[P_{6,6,6,14}^+][Co(hfacac)_3^-]$, $[C_{14}MIM^+][Ni(hfacac)_3^-]$, $[P_{6,6,6,14}^+][Gd(hfacac)_4^-]$, $[P_{6,6,6,14}^+][Dy(hfacac)_4^-]$, $[OMIM^+][Ni(hfacac)_3^-]$, and $[P_{6,6,6,14}^+][Ni(tfacac)_3^-]$ MILs. However, DNA was stable within the MIL for several hours after the extraction, possibly due to the hydrophobic microenvironment of the MIL limiting the activity of DNase.[31]

6.3.4 Insight into the Mechanism of Blood Cell Lysis by MILs

To investigate cell integrity after dispersing MILs in blood, blood smears were developed using Wright's stain. Wright's stain is comprised of two colorimetric stains: (1) eosin, which stains proteins in the cytosol red, and (2) methylene blue, which stains NAs in WBCs blue.[29] As shown in Figure 6-6, exposing blood cells to MILs (Figures 6-6c-k) caused a significant reduction in the central pallor of the RBCs compared to whole blood (Figure 6-6a). This suggests that proteins, such as hemoglobin, are not present in the cytoplasm due to the lysis of cells. Small spikes were also noted on RBCs exposed to the $[N_{8,8,8,Bz}^+][Ni(hfacac)_3^-]$, $[OMIM^+][Ni(hfacac)_3^-]$, and $[C_{14}MIM^+][Ni(hfacac)_3^-]$ MILs. Spurs cells are a morphological abnormality of RBCs associated with several diseases such as carcinoma and liver disease.[32-33] They form due to disturbances in the lipid composition of the cell membrane.[32,34,35] RBCs exposed to the $[P_{6,6,6,14}^+][Gd(hfacac)_4^-]$ MILs no longer exhibited a circular shape and appeared deformed. Few intact WBCs and free DNA was observed in the slides.

The effect that the MIL cation, ligand, and metal ion has on the lysis of WBCs was evaluated by spiking each component into 50 µL of blood. As shown in Figure 6-S8, the eosin stain was not retained in RBCs exposed to nickel(II) chloride, cobalt(II) chloride, dysprosium(III) chloride, or gadolinium(III) chloride. This may be linked to hemolysis generated through oxidative stress by the metal ion.[36] As shown in Figure 6-S9, the ligand may also play a role in cell lysis. No cells were observed after exposing the blood to hexafluoroacetylacetone, the chemical precursor used to form the metal hexafluoroacetylateonate-based MILs. However, non-viable RBCs were noted with phenyltrifluoroacetone and 1,1,1-trifluoroacetylacetone; no intact WBCs were noted. As shown in Figure 6-S10, the cation appears to also affect cell viability. The

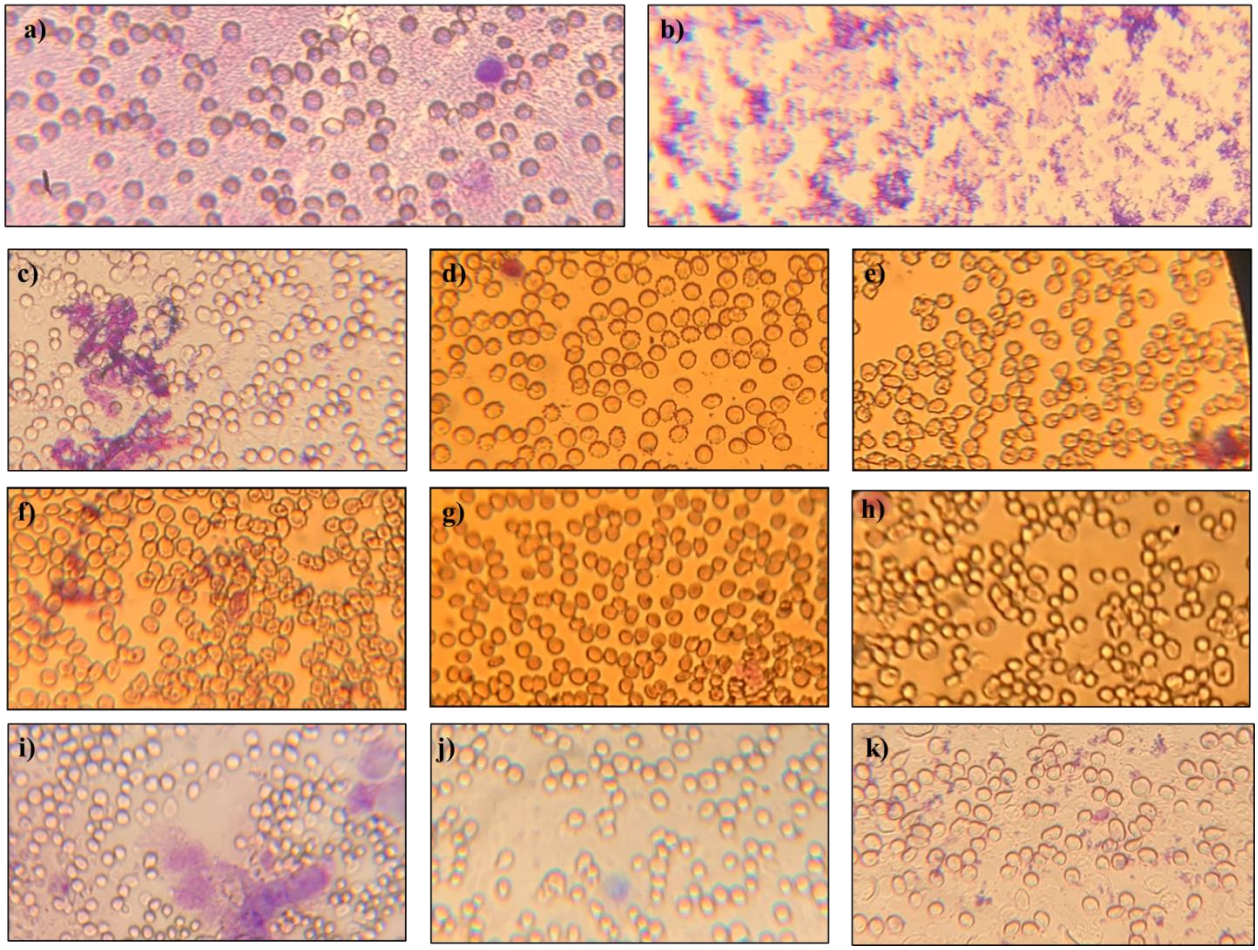

Figure 6-7 Images showing the Wright staining of (a) whole blood and (b) 4 µg of salmon testes DNA compared to whole blood exposed to (c) $[P_{6,6,6,14}^{+}][Ni(hfacac)_3^{-}]$, (d) $[N_{8,8,8,Bz}^{+}][Ni(hfacac)_3^{-}]$, (e) $[OMIM^{+}][Ni(hfacac)_3^{-}]$, (f) $[C_{14}MIM^{+}][Ni(hfacac)_3^{-}]$, (g) $[P_{6,6,6,14}^{+}][Ni(Phtfacac)_3^{-}]$, (h) $[P_{6,6,6,14}^{+}][Ni(tfacac)_3^{-}]$, (i) $[P_{6,6,6,14}^{+}][Co(hfacac)_3^{-}]$, (j) $[P_{6,6,6,14}^{+}][Dy(hfacac)_4^{-}]$, and (k) $[P_{6,6,6,14}^{+}][Gd(hfacac)_4^{-}]$ MILs in whole blood.

$[P_{6,6,6,14}^{+}][NTf_2^{-}]$ IL appears to completely lyse WBC and RBCs. RBCs exposed to the $[N_{8,8,8,Bz}^{+}][NTf_2^{-}]$ IL were noted to have spurs.

Previously, it was reported that a lipophilic cationic component imparts surfactant-like properties to the MIL.[25] RBCs form spurs in the presence of surfactants due to the intercalation of the surfactant molecules into the cell membrane.[37,38] The interaction of the surfactant then leads to solubilization of the cell membrane and consequently cell lysis.

6.4 Conclusions

The simultaneously lysing of WBCs and extraction of DNA shows great potential for consolidating sample preparation and achieving high throughput analysis. A short vortex step of 1 min was required to extract over 500 pg and 800 pg of human genomic DNA from 50 μL whole blood and dry blood, respectively, whereas commercial methods require an hour to lyse, extract, and recover NAs. From lysis to detection the MIL-based WBC lysis and genomic DNA extraction were substantially faster than the spin column method. All nine MILs could be integrated into the qPCR buffer without inhibiting the reaction, allowing for a chemical lysis method that did not inhibit downstream detection. Thermal desorption during qPCR greatly reduced the sample preparation time needed for isolating human genomic DNA. The qPCR efficiency was not affected by dispersing the small volumes of MIL in whole blood suggesting that the MILs co-extracted minimal amounts of qPCR inhibitors. Wright staining revealed a noticeable lack of WBCs, with the remaining RBCs appearing to have been lysed. The MIL cation, chelated metal ion, and ligand play a significant role in the ability of the MIL to lyse cells and extract NAs. MILs containing an aromatic component within the chemical structure were found to extract more DNA. The Gd(III) and Dy(III) MILs appeared to be more efficient at lysing cells. The utilization of MILs to chemically lyse cells and extract DNA is highly advantageous for nucleic acid analysis since the method could be fully automated. Finally, the simple 1 min sample preparation step is ideal for high throughput analysis.

Acknowledgements

M. N. E. would like to thank Paul M. Emaus for his support. J. L. A acknowledges funding from the Chemical Measurement and Imaging Program at the National Science Foundation (CHE-1709372).

Compliance with ethical standards

Conflicts of interest The authors declare no conflicts of interest.

References

(1) Stramer, S. L.; Wend, U.; Candotti, D.; Foster, G. A.; Hollinger, F. B.; Dodd, R. Y.; Allain, J.-P.; Gerlich, W. Nucleic Acid Testing to Detect HBV Infection in Blood Donors. N. Engl. J. Med. 2011, 364 (3), 236–247.

(2) Gonçalves, J.; Moreira, E.; Sequeira, I. J.; Rodrigues, A. S.; Rueff, J.; Brás, A. Integration of HIV in the Human Genome: Which Sites Are Preferential? A Genetic and Statistical Assessment. Int. J. Genomics 2016, 2016, 8–13.

(3) Choi, J.; Hyun, J. C.; Yang, S. On-Chip Extraction of Intracellular Molecules in White Blood Cells from Whole Blood. Sci. Rep. 2015, 5, 1–12.

(4) Albariño, C. G.; Romanowski, V. Phenol Extraction Revisited: A Rapid Method for the Isolation and Preservation of Human Genomic DNA from Whole Blood. Molecular and Cellular Probes. 1994, pp 423–427.

(5) Chen, X.; Cui, D.; Liu, C.; Li, H.; Chen, J. Continuous Flow Microfluidic Device for Cell Separation, Cell Lysis and DNA Purification. Anal. Chim. Acta 2007, 584 (2), 237–243.

(6) Ali, N.; Rampazzo, R. D. C. P.; Costa, A. Di. T.; Krieger, M. A. Current Nucleic Acid Extraction Methods and Their Implications to Point-of-Care Diagnostics. Biomed Res. Int. 2017, 2017.

(7) Nan, L.; Jiang, Z.; Wei, X. Emerging Microfluidic Devices for Cell Lysis: A Review. Lab Chip 2014, 14 (6), 1060–1073.

(8) Schrader, C.; Schielke, A.; Ellerbroek, L.; Johne, R. PCR Inhibitors - Occurrence, Properties and Removal. J. Appl. Microbiol. 2012, 113, 1014–1026.

(9) Fuchs-Telka, S.; Fister, S.; Mester, P. J.; Wagner, M.; Rossmanith, P. Hydrophobic Ionic Liquids for Quantitative Bacterial Cell Lysis with Subsequent DNA Quantification. Anal. Bioanal. Chem. 2017, 409 (6), 1503–1511.

(10) Fister, S.; Fuchs, S.; Mester, P.; Kilpeläinen, I.; Wagner, M.; Rossmanith, P. The Use of Ionic Liquids for Cracking Viruses for Isolation of Nucleic Acids. Sep. Purif. Technol. 2015, 155 (April 2004), 38–44.

(11) Martzy, R.; Bica-Schröder, K.; Pálvölgyi, Á. M.; Kolm, C.; Jakwerth, S.; Kirschner, A. K. T.; Sommer, R.; Krska, R.; Mach, R. L.; Farnleitner, A. H.; et al. Simple Lysis of Bacterial Cells for DNA-Based Diagnostics Using Hydrophilic Ionic Liquids. Sci. Rep. 2019, 9 (1), 1–10.

(12) Trujillo-Rodriguez, M. J.; Nan, H.; Varona, M.; Emaus, M. N.; Souza, I. D.; Anderson, J. L. Advances of Ionic Liquids in Analytical Chemistry. Anal. Chem. 2019, 91 (1), 505–531.

(13) Trujillo-Rodríguez, M. J.; Rocío-Bautista, P.; Pino, V.; Afonso, A. M. Ionic Liquids in Dispersive Liquid-Liquid Microextraction. TrAC - Trends Anal. Chem. 2013, 51, 87–106.

(14) Koshy, L.; Anju, A. L.; Harikrishnan, S.; Kutty, V. R.; Jissa, V. T.; Kurikesu, I.; Jayachandran, P.; Jayakumaran Nair, A.; Gangaprasad, A.; Nair, G. M.; et al. Evaluating Genomic DNA Extraction Methods from Human Whole Blood Using Endpoint and Real-Time PCR Assays. Mol. Biol. Rep. 2017, 44 (1), 97–108.

(15) Nanayakkara, I. A.; Cao, W.; White, I. M. Simplifying Nucleic Acid Amplification from Whole Blood with Direct Polymerase Chain Reaction on Chitosan Microparticles. Anal. Chem. 2017, 89 (6), 3773–3779.

(16) Berasaluce, A.; Matthys, L.; Mujika, J.; Antoñana-Díez, M.; Valero, A.; Agirregabiria, M. Bead Beating-Based Continuous Flow Cell Lysis in a Microfluidic Device. RSC Adv. 2015, 5 (29), 22350–22355.

(17) Pandit, K. R.; Nanayakkara, I. A.; Cao, W.; Raghavan, S. R.; White, I. M. Capture and Direct Amplification of DNA on Chitosan Microparticles in a Single PCR-Optimal Solution. Anal. Chem. 2015, 87 (21), 11022–11029.

(18) Clark, K. D.; Nacham, O.; Yu, H.; Li, T.; Yamsek, M. M.; Ronning, D. R.; Anderson, J. L. Extraction of DNA by Magnetic Ionic Liquids: Tunable Solvents for Rapid and Selective DNA Analysis. Anal. Chem. 2015, 87 (3), 1552–1559.

(19) Marengo, A.; Cagliero, C.; Sgorbini, B.; Anderson, J. L.; Emaus, M. N.; Bicchi, C.; Bertea, C. M.; Rubiolo, P. Development of an Innovative and Sustainable One - Step Method for Rapid Plant DNA Isolation for Targeted PCR Using Magnetic Ionic Liquids. Plant Methods 2019, 1–11.

(20) Bowers, A. N.; Trujillo-Rodríguez, M. J.; Farooq, M. Q.; Anderson, J. L. Extraction of DNA with Magnetic Ionic Liquids Using in Situ Dispersive Liquid–Liquid Microextraction. Anal. Bioanal. Chem. 2019, 411 (28), 7375–7385.

(21) Clark, K. D.; Nacham, O.; Purslow, J. A.; Pierson, S. A.; Anderson, J. L. Magnetic Ionic Liquids in Analytical Chemistry: A Review. Anal. Chim. Acta 2016, 934, 9–21.

(22) Del Sesto, R. E.; McCleskey, T. M.; Burrell, A. K.; Baker, G. a; Thompson, J. D.; Scott, B. L.; Wilkes, J. S.; Williams, P. Structure and Magnetic Behavior of Transition Metal Based Ionic Liquids. Chem. Commun. 2008, 447–449.

(23) Hayashi, S.; Hamaguchi, H. Discovery of a Magnetic Ionic Liquid [Bmim]FeCl4. Chem. Lett. 2004, 33 (12), 1590–1591.

(24) Clark, K. D.; Yamsek, M. M.; Nacham, O.; Anderson, J. L. Magnetic Ionic Liquids as PCR-Compatible Solvents for DNA Extraction from Biological Samples. Chem. Commun. 2015, 51 (94), 16771–16773.

(25) Emaus, M. N.; Anderson, J. L. Allelic Discrimination between Circulating Tumor DNA Fragments Enabled by a Multiplex-QPCR Assay Containing DNA-Enriched Magnetic Ionic Liquids. Anal. Chim. Acta 2020.

(26) Emaus, M. N.; Clark, K. D.; Hinners, P.; Anderson, J. L. Preconcentration of DNA Using Magnetic Ionic Liquids That Are Compatible with Real-Time PCR for Rapid Nucleic Acid Quantification. Anal. Bioanal. Chem. 2018, 410 (17), 4135–4144.

(27) Pierson, S. A.; Nacham, O.; Clark, K. D.; Nan, H.; Mudryk, Y.; Anderson, J. L. Synthesis and Characterization of Low Viscosity Hexafluoroacetylacetonate-Based Hydrophobic Magnetic Ionic Liquids. New J. Chem. 2017, 41 (13), 5498–5505.

(28) Farooq, M. Q.; Chand, D.; Odugbesi, G. A.; Varona, M.; Mudryk, Y.; Anderson, J. L. Investigating the Effect of Ligand and Cation on the Properties of Metal Fluorinated Acetylacetonate Based Magnetic Ionic Liquids. New J. Chem. 2019, 43, 11334–11341.

(29) Strober, W. Wright-Giemsa and Nonspecific Esterase Staining of Cells. Curr. Protoc. Cytom. 2000, 11 (1).

(30) Whitehouse, C. A.; Hottel, H. E. Comparison of Five Commercial DNA Extraction Kits for the Recovery of Francisella Tularensis DNA from Spiked Soil Samples. Mol. Cell. Probes 2007, 21 (2), 92–96.

(31) Clark, K. D.; Sorensen, M.; Nacham, O.; Anderson, J. L. Preservation of DNA in Nuclease-Rich Samples Using Magnetic Ionic Liquids. RSC Adv. 2016, 6 (46), 39846–39851.

(32) Silber, R. Of Acanthocytes, Spurs, Burrs, and Membranes. Blood 1969, 34 (1), 111–114.

(33) Owen, J. S.; Brown, D. J. C.; Harry, D. S.; McIntyre, N.; Beaven, G. H.; Isenberg, H.; Gratzer, W. B. Erythrocyte Echinocytosis in Liver Disease. Role of Abnormal Plasma High Density Lipoproteins. J. Clin. Invest. 1985, 76 (6), 2275–2285.

(34) Salvioli, G.; Rioli, G.; Lugli, R.; Salati, R. Membrane Lipid Composition of Red Blood Cells in Liver Disease: Regression of Spur Cell Anaemia after Infusion of Polyunsaturated Phosphatidylcholine. Gut 1978, 19 (9), 844–850.

(35) Beck, J. S. Echinocyte Formation: A Test Case for Mechanisms of Cell Shape Changes. J. Theor. Biol. 1978, 71 (4), 515–524.

(36) Ribarov, S. R.; Benov, L. C. Relationship between the Hemolytic Action of Heavy Metals and Lipid Peroxidation. BBA - Biomembr. 1981, 640 (3), 721–726.

(37) Shalel, S.; Streichman, S.; Marmur, A. The Mechanism of Hemolysis by Surfactants: Effect of Solution Composition. J. Colloid Interface Sci. 2002, 252 (1), 66–76.

(38) Manaargadoo-Catin, M.; Ali-Cherif, A.; Pougnas, J. L.; Perrin, C. Hemolysis by Surfactants - A Review. Adv. Colloid Interface Sci. 2016, 228, 1–16.

CHAPTER 7.

General Conclusions

The first chapter of this dissertation describes the characteristics of MILs and conventional methods for nucleic acid analysis. MILs are attractive in sample preparation due to the paramagnetic component within the chemical structure, allowing analyte-enriched droplets to respond to an external magnetic field. In contrast, traditional LLE methods require bulky equipment (i.e., centrifuge) to recover the extraction solvent. Traditional nucleic acid extraction methods (i.e., phenol-chloroform-based LLEs and silica-based SPEs) are tedious and time consuming, creating a significant bottleneck in DNA analysis. Although rapid and simple to perform, chemical lysis procedures require significant sample purification to remove the lysis reagent. Furthermore, mechanical lysis methods must be carefully optimized to ensure cells are lysed without shearing nucleic acids. Innovative nucleic acid sample preparation methods should be explored to overcome the limitations of conventional approaches to DNA analysis.

Chapter 2 of this dissertation details the integration of four hexafluoroacetylacetonate-based MILs that contain either a Ni(II), Co(II), Mn(II), or Dy(III) metal center into a qPCR assay. The concentration of EDTA, SYBR green I, magnesium chloride, and BSA within the qPCR assay was carefully optimized to relieve inhibition caused by the MILs. DNA was preconcentrated in the MIL using an optimized SDME or SA-DLLME method where the MIL was suspended on a rod magnet and agitated with an orbital shaker or dispersed using a vortex, respectively. The amount of DNA isolated by the MIL was compared to extractions performed with commercial silica-based magnetic beads. The MIL-SDME method outperformed the magnetic bead approach at preconcentrating ssDNA and extracted similar amounts of dsDNA. The addition of DNA-enriched MIL to the reaction buffer did not affect the amplification

efficiency suggesting that MILs are qPCR compatible. In contrast, the addition of magnetic beads to the reaction buffer decreased the amplification efficiency to 81.6%, suggesting that the beads inhibited the qPCR assay.

The third chapter of this dissertation chronicles the integration of a DNA-enriched MIL into a multiplex-qPCR assay to simultaneously amplify three ctDNA fragments. The MIL-multiplex-qPCR buffer composition (i.e., Taqman probe, EDTA, magnesium chloride, and primer concentrations) and annealing temperature were optimized to ensure simultaneous amplification of three ctDNA fragments. Allelic discrimination was achieved between all three DNA fragments, including two single nucleotide polymorphisms. Enrichment factors as high as 35 were achieved for all three DNA fragments. In comparison, commercial spin column and silica-based magnetic beads poorly preconcentrated DNA; this is partially due to the large desorption volume required to sufficiently desorb DNA from the silica sorbent. The MILs were also able to extract the three DNA fragments spiked into undiluted plasma.

In Chapter 4, the development of a dispersive, sequence-specific ITO-MIL extraction was described. Once the ITO probe was annealed to denatured DNA, the MIL was dispersed in a sample to preconcentrate ctDNA. The DNA-enriched MIL was then added to the custom-designed qPCR assay to desorb DNA during qPCR amplification. The sequence-specific extraction required only 11 min to preconcentrate femtomolar concentrations of DNA. The ITO-MIL extraction was able to selectively isolate DNA from complex matrices such as diluted plasma. In contrast, commercial sequence-specific extraction methods using streptavidin-coated magnetic beads with biotin-modified oligonucleotides could not selectively isolate DNA from diluted plasma.

In the fifth chapter of this dissertation, *BRAF* V600E was preconcentrated from diluted human plasma, artificial urine, and artificial sputum spiked with large amounts of wild-type *BRAF*. The amplification of wild-type *BRAF* and *BRAF* V600E was simultaneously monitored using sequence-specific Taqman probes. K-means clustering was used to statistically discriminated the endpoint fluorescent signals associated with ITO-MIL extractions compared to a wild-type *BRAF* standard (50 fg·μL wild-type *BRAF*). It was found that 0.1-0.5% *BRAF* V600E extracted from diluted plasma, artificial urine, and diluted artificial sputum could be distinguished from the 100% wild-type *BRAF* standards. In contrast, a 9% *BRAF* V600E standard could not be distinguished from the 100% wild-type *BRAF* standard.

The sixth chapter of this review describes the development of a one-step cell lysis and DNA extraction method using MILs. An aliquot of MIL was dispersed in a sample consisting of 2-fold diluted blood, whole blood, or reconstituted bloodstains and subsequently collected using a rod magnet. Picogram levels of human genomic DNA was recovered from the MIL using qPCR. The ligand, metal ion, and hydrophobic cation of the MIL contributed to the cell lysis, with the metal ion causing hemolysis and the hydrophobic cation interacting with the cell membrane. Sample preparation required as little as 30 s with the MILs, whereas conventional spin column extraction kits required 40-60 min suggesting that the MILs would be ideal for high throughput DNA analysis. Also, the addition of MIL dispersed in blood to the qPCR did not significantly impact the amplification efficiency, suggesting that MILs are chemical lysis reagents that do not inhibit downstream bioanalytical detection.

APPENDIX A

SUPPORTING INFORMATION ACCOMPANYING CHAPTER 2

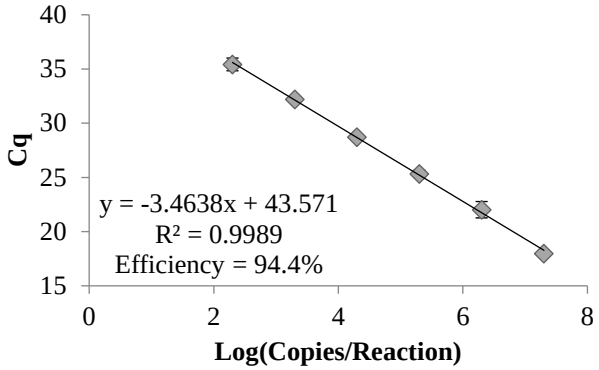

Figure 2-S1 Six point standard curve ranging from 200 to 2×10^7 copies per reaction to determine the amplification efficiency of single-stranded *KRAS* template and subsequent quantification.

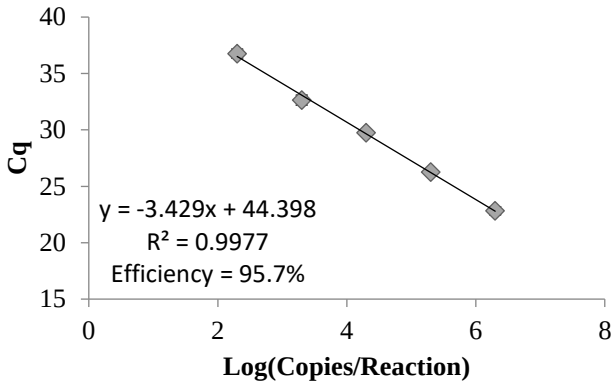

Figure 2-S2 Five point standard curve with 10-fold dilution to determine the amplification efficiency of double-stranded *KRAS* template and subsequent quantification.

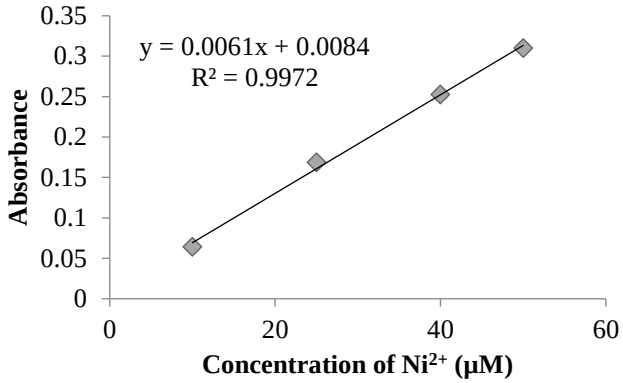

Figure 2-S3 Four point standard curve for $NiCl_2$ generated using atomic absorption spectroscopy developed for Ni^{2+} quantification.

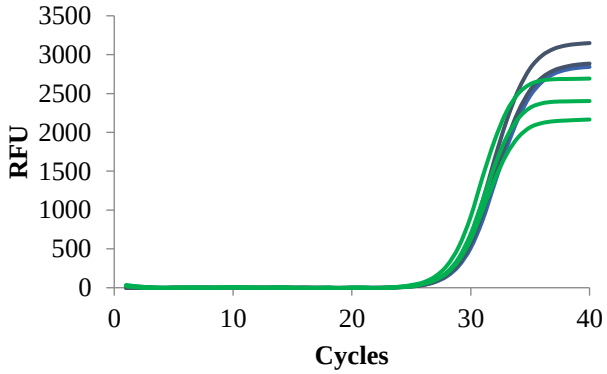

Figure 2-S4 Amplification curves generated by incubating 10 µL of water with and without $[P_{6,6,6,14}^{+}][Ni(hfacac)_3^{-}]$ using the PCR temperature program. Incubated water was used for subsequent qPCR (green) and compared to a standard reaction (blue).

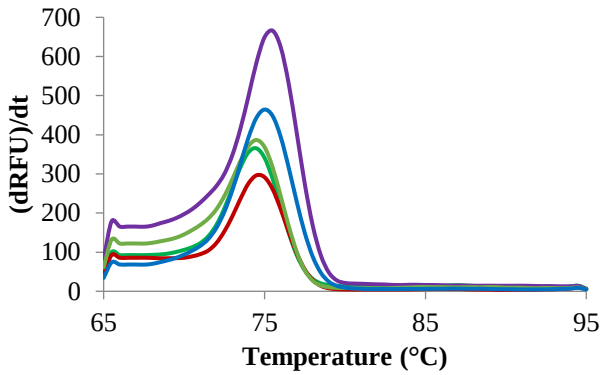

Figure 2-S5 Melt curves associated with *KRAS* template extracted using $[P_{6,6,6,14}^{+}][Ni(hfacac)_3^{-}]$ (green), $[P_{6,6,6,14}^{+}][Co(hfacac)_3^{-}]$ (red), $[P_{6,6,6,14}^{+}][Mn(hfacac)_3^{-}]$ (orange), and $[P_{6,6,6,14}^{+}][Dy(hfacac)_4^{-}]$ (violet) compared against a *KRAS* standard (blue).

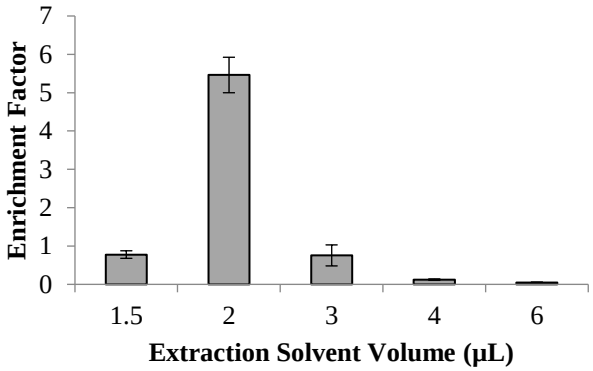

Figure 2-S6 Effect of extraction solvent volume for MIL-SDME using $[P_{6,6,6,14}^{+}][Ni(hfacac)_3^{-}]$ MIL as an extraction solvent. *KRAS* template concentration: 2×10^4 copies/µL; total solution volume: 2.0 mL; extraction time: 10 min; MIL volume: 2 µL; rotation rate: 200 rpm.

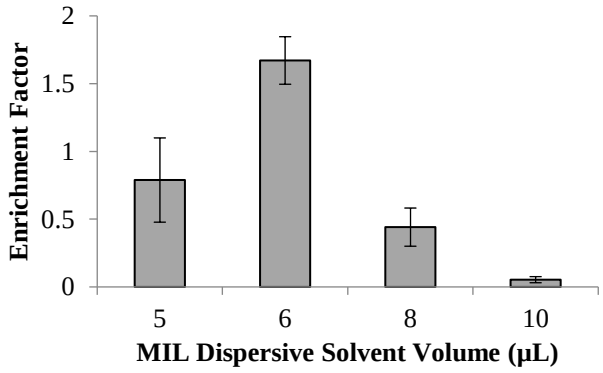

Figure 2-S7 Effect of MIL dispersive solvent volume optimization for MIL-DLLME method using $[P_{6,6,6,14}^{+}][Ni(hfacac)_3^{-}]$ as an extraction solvent. *KRAS* template concentration: 2×10^4 copies/µL; total solution volume: 2.0 mL; extraction time: 60 s; Pluronic F-108 concentration: 3 µM.

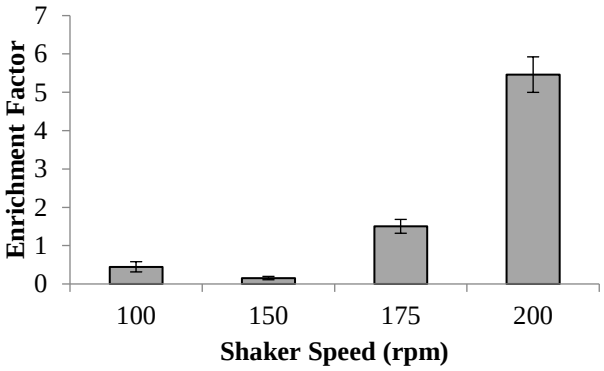

Figure 2-S8 Shaker speed optimization for SDME method using $[P_{6,6,6,14}^{+}][Ni(hfacac)_3^{-}]$ as an extraction solvent. *KRAS* template concentration: 2×10^4 copies/µL; total solution volume: 2.0 mL; extraction time: 10 min; MIL volume: 2 µL.

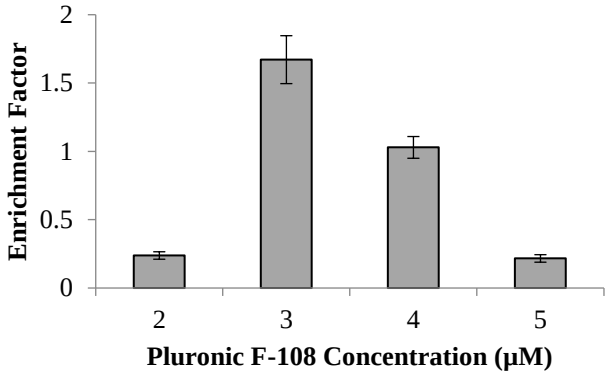

Figure 2-S9 Surfactant concentration optimization for MIL-SA-DLLME method using $[P_{6,6,6,14}^{+}][Ni(hfacac)_3^{-}]$. *KRAS* template concentration: 2×10^4 copies/µL; total solution volume: 2.0 mL; extraction time: 120 s; MIL volume: 6 µL.

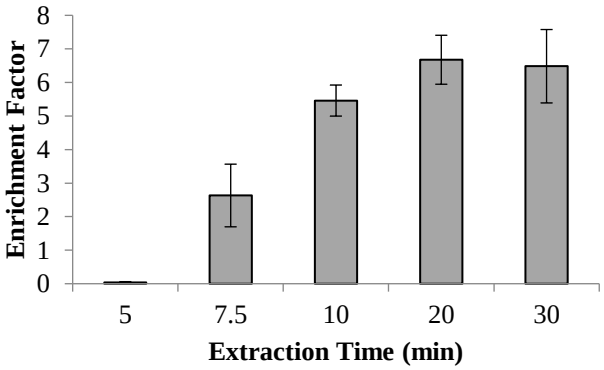

Figure 2-S10 Extraction time optimization of SDME using $[P_{6,6,6,14}^{+}][Ni(hfacac)_3^{-}]$ as an extraction solvent. *KRAS* template concentration: 2×10^4 copies/µL; total solution volume: 2.0 mL; MIL volume: 2 µL; rotation rate: 200 rpm.

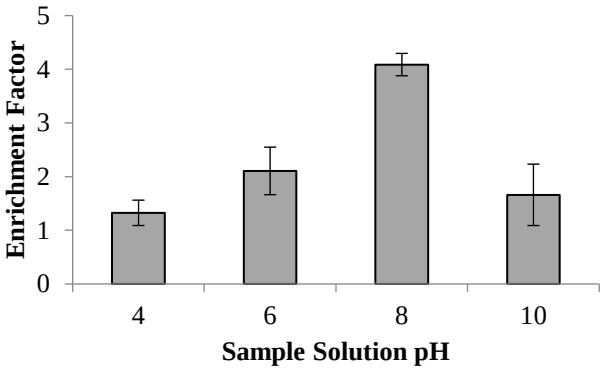

Figure 2-S11 Sample solution pH optimization for SDME method using $[P_{6,6,6,14}^{+}][Ni(hfacac)_3^{-}]$ as an extraction solvent. *KRAS* template concentration: 2×10^4 copies/µL; total solution volume: 2.0 mL; extraction time: 10 min; MIL volume: 2 µL; rotation rate: 200 rpm.

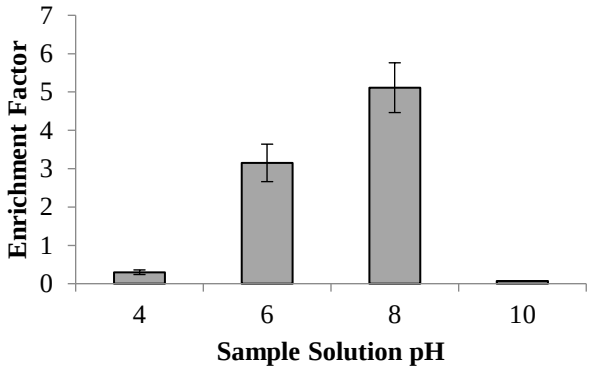

Figure 2-S12 Sample solution pH optimization for MIL-SA-DLLME method using $[P_{6,6,6,14}^{+}][Ni(hfacac)_3^{-}]$ as an extraction solvent. *KRAS* template concentration: 2×10^4 copies/µL; total solution volume: 2.0 mL; Tris-HCl concentration: 10 mM; extraction time: 120 s; MIL volume: 6 µL; Pluronic F-108 concentration: 3 µM.

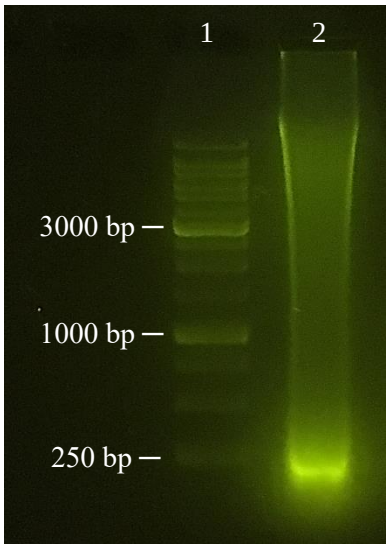

Figure 2-S13 Agarose gel (1%) electrophoresis separation confirming the length of the sheared DNA fragments from salmon testes DNA after being sonicated for 60 cycles of 30 s bursts and 30 s rest (lane 2) against a 1 Kbp DNA ladder (lane 1).

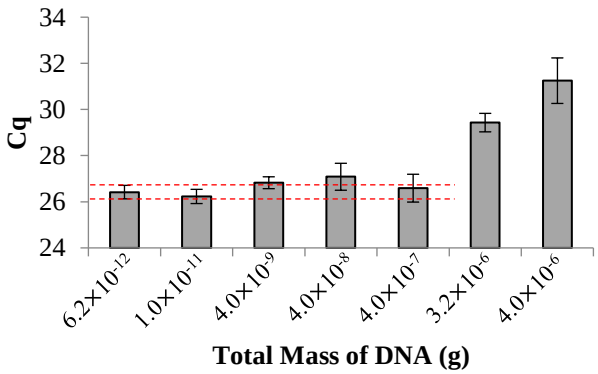

Figure 2-S14 MIL-SDME extractions of double-stranded *KRAS* template in the presence of non-target DNA using the $[P_{6,6,6,14}^{+}][Ni(hfacac)_3^{-}]$ MIL as an extraction solvent. *KRAS* template concentration: 2×10^4 copies/µL; total solution volume: 2.0 mL; extraction time: 20 min; MIL volume: 2 µL; rotation rate: 200 rpm

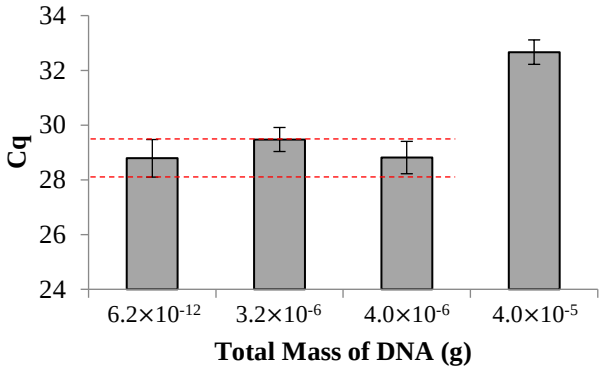

Figure 2-S15 MIL-SDME extractions of double-stranded *KRAS* template in the presence of non-target DNA using the $[P_{6,6,6,14}^{+}][Ni(hfacac)_3^{-}]$ MIL as an extraction solvent. *KRAS* template concentration: 2×10^4 copies/µL; total solution volume: 2.0 mL; extraction time: 20 min; MIL volume: 3 µL; rotation rate: 200 rpm.

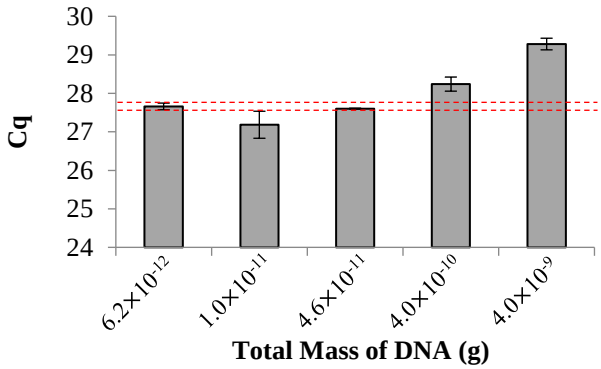

Figure 2-S16 Magnetic bead-based extraction of double-stranded *KRAS* template in the presence of non-target DNA. *KRAS* template concentration: 2×10^4 copies/µL; solution volume: 2.0 mL; concentration of guanidine HCl: 3 M; extraction time: 1 min; mass of magnetic beads: 720 µg.

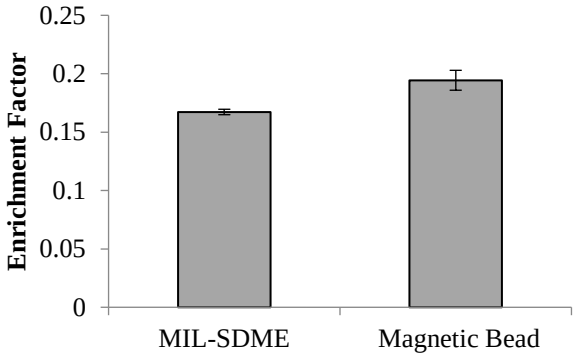

Figure 2-S17 Comparison of the MIL-SDME and magnetic bead-based DNA extraction from ten-fold diluted plasma matrix. MIL-SDME conditions: *KRAS* template concentration: $2x10^4$ copies/µL; total solution volume: 2.0 mL; time: 20 min; MIL volume: 2 µL. Magnetic bead extraction conditions: *KRAS* template concentration: 2×10^4 copies/µL; solution volume: 2.0 mL; concentration of Guanidine HCl: 3 M; time: 1 min; mass of magnetic beads: 720 µg

APPENDIX B

SUPPORTING INFORMATION ACCOMPANYING CHAPTER 3

Table 3-S1 All oligo sequences examined in this study.

Name	Sequence
Forward *KRAS* Primer	5'-AAGGCCTGCTGAAAATGACT-3'
Reverse *KRAS* Primer	5'-TCTGAATTAGCTGTATCGTCAAGG-3'
Wild-type *KRAS* Probe	5' ACTTGTGGTAGTTGGAGCTGGTGG -3'
G12S mutant *KRAS* Probe	5'- TTGTGGTAGTTGGAGCTAGTGGCG -3'
Forward *BRAF* Primer	5'-GGTCTAGCTACAGTGAAATCTCG-3'
Reverse *BRAF* Primer	5'-TAGCCTCAATTCTTACCATCCAC-3'
Wild-type *BRAF* Probe	5'-TGTTCAAACTGATGGGACCCACTCC-3'
15-mer Oligonucleotide	5'-TCA ACA TCA GTC TGA-3'
15-mer Oligonucleotide Compliment	5'-TCA GAC TGA TGT TGA-3'
1 nt Mismatch 15-mer Oligonucleotide	5'-TCA GAC TAA TGT TG-3'

Table 3-S2 Melting temperatures associated with the 15-mer oligonucleotide and its perfect complement and 1 nt mismatch.

	Tm of complement (°C) (n = 3)	Tm of 1 nt mismatch (°C) (n =3)	Difference (°C)
Standard	65.33 ± 0.29	56.33 ± 0.29	9.00 ± 0.00
$[P_{6,6,6,14}^{+}][Ni(hfacac)_3^{-}]$	61.67 ± 0.29	52.67 ± 0.58	9.00 ± 0.50
$[P_{6,6,6,14}^{+}][Ni(Phtfacac)_3^{-}]$	58.00 ± 0.00	47.67 ± 0.29	10.33 ± 0.29
$[N_{8,8,8,Bz}^{+}][Ni(hfacac)_3^{-}]$	57.83 ± 0.29	54.17 ± 0.29	3.67 ± 0.29

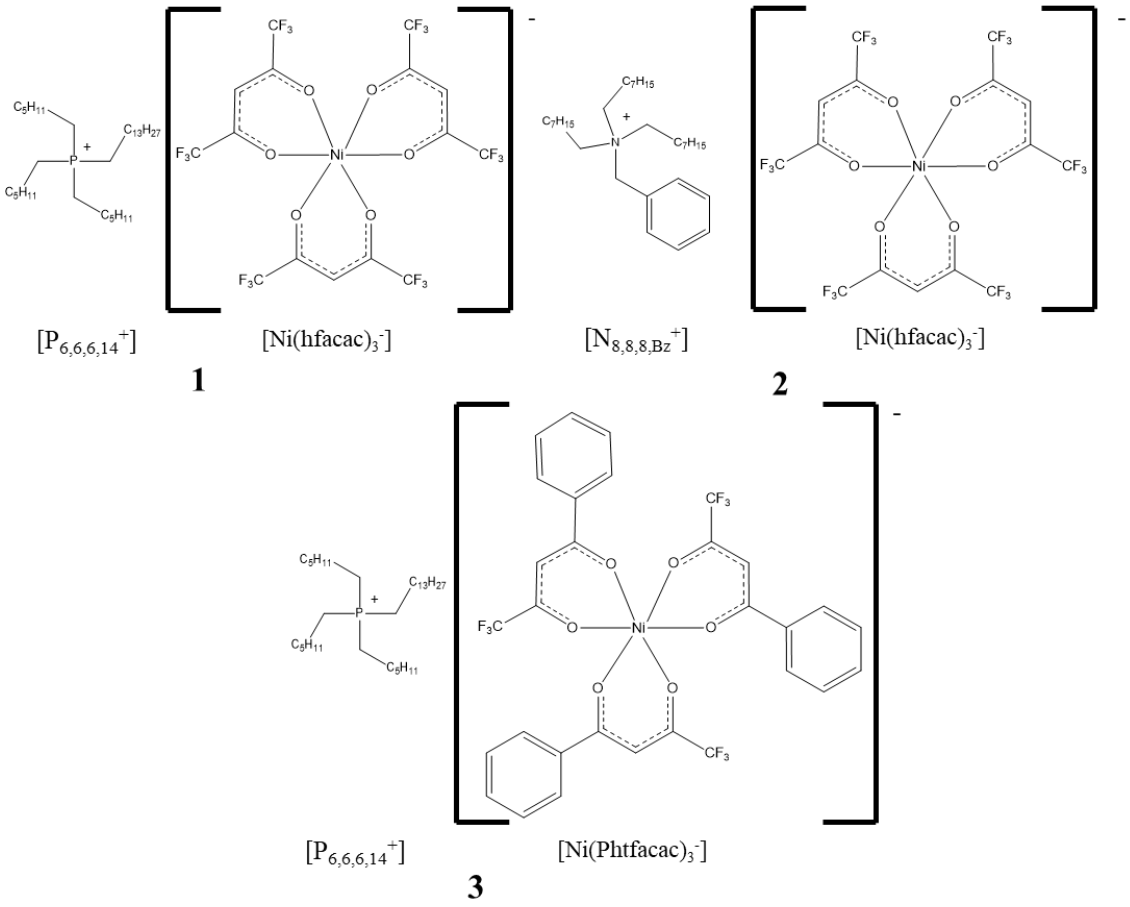

Figure 3-S1 Chemical structures of the $[P_{6,6,6,14}^{+}][Ni(hfacac)_3^{-}]$, $[P_{6,6,6,14}^{+}][Ni(Phtfacac)_3^{-}]$, and $[N_{8,8,8,Bz}^{+}][Ni(hfacac)_3^{-}]$ MILs examined in this study.

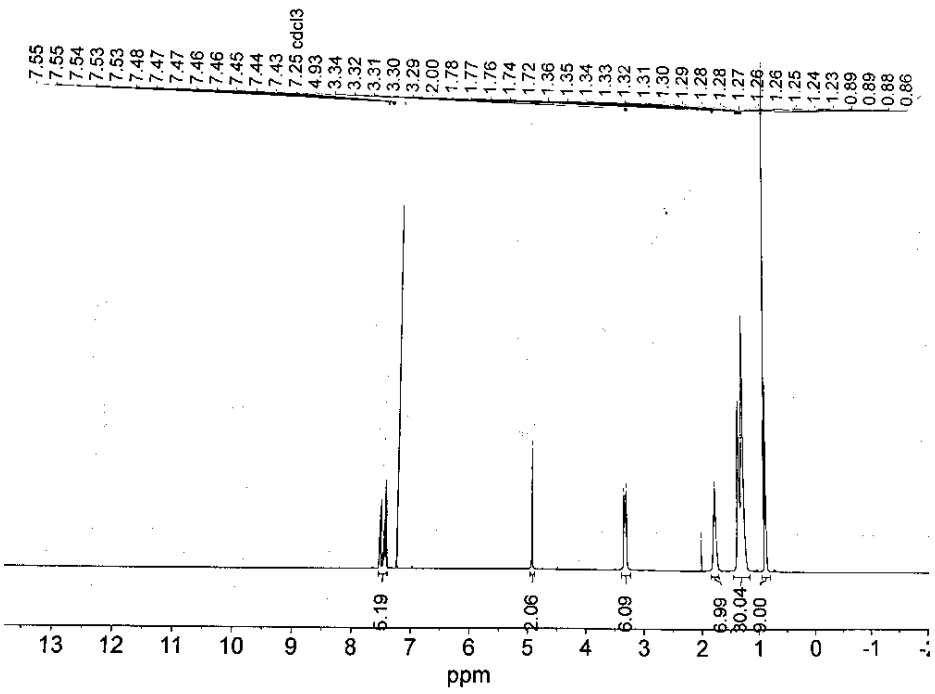

Figure 3-S2 H^1 NMR spectrum of the $[N_{8,8,8,Bz}^{+}][Br^{-}]$ salt.

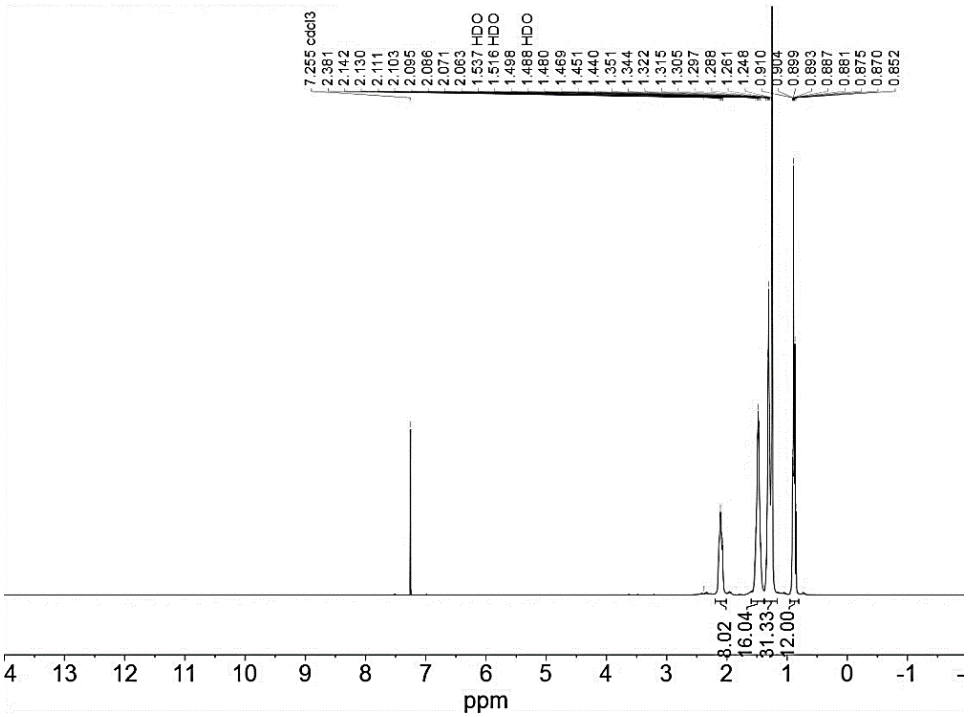

Figure 3-S3 H^1 NMR spectrum of the $[P_{6,6,6,14}^{+}][NTf_2^{-}]$ IL.

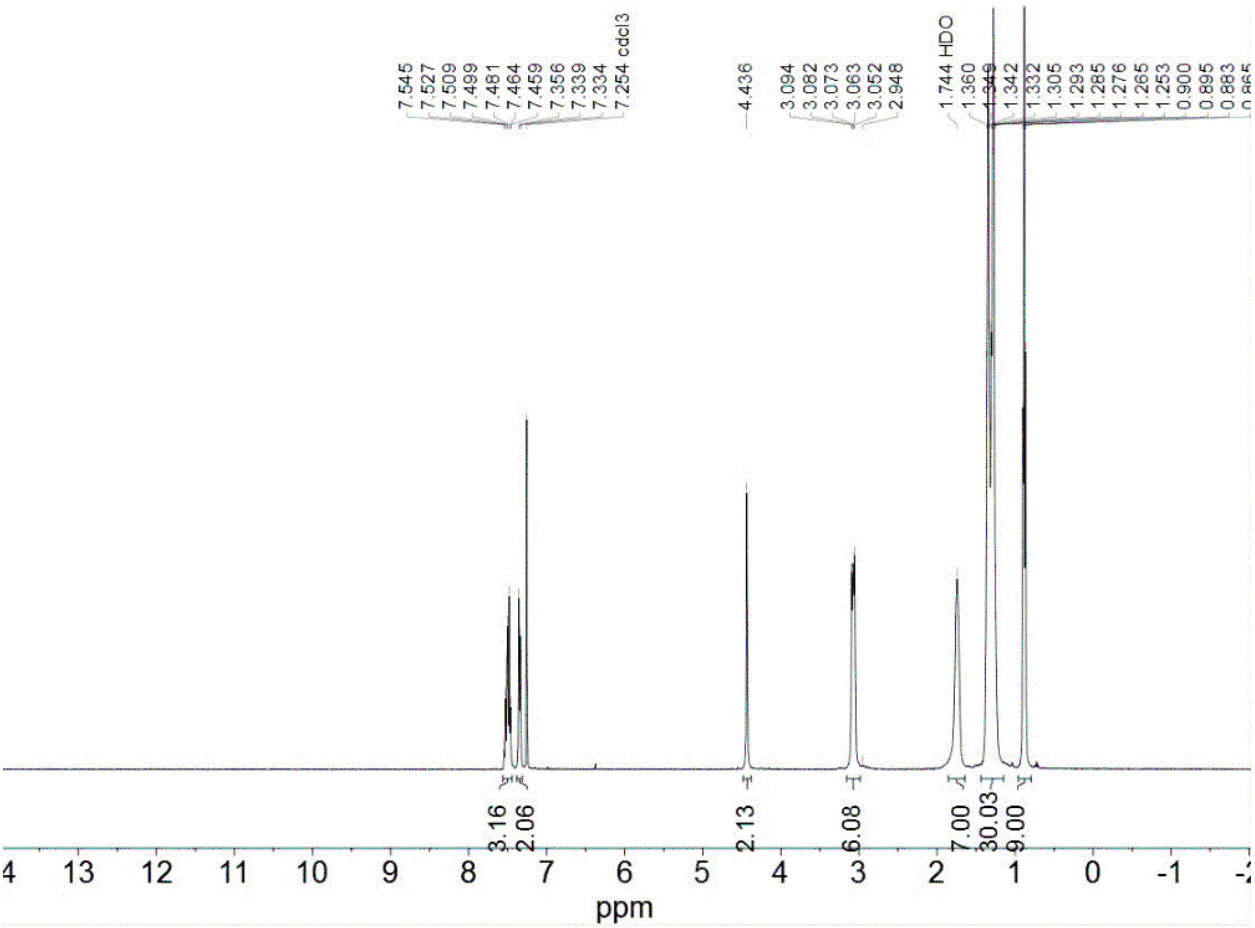

Figure 3-S4 H^1 NMR spectrum of the $[N_{8,8,8,Bz}^{+}][NTf_2^{-}]$ IL.

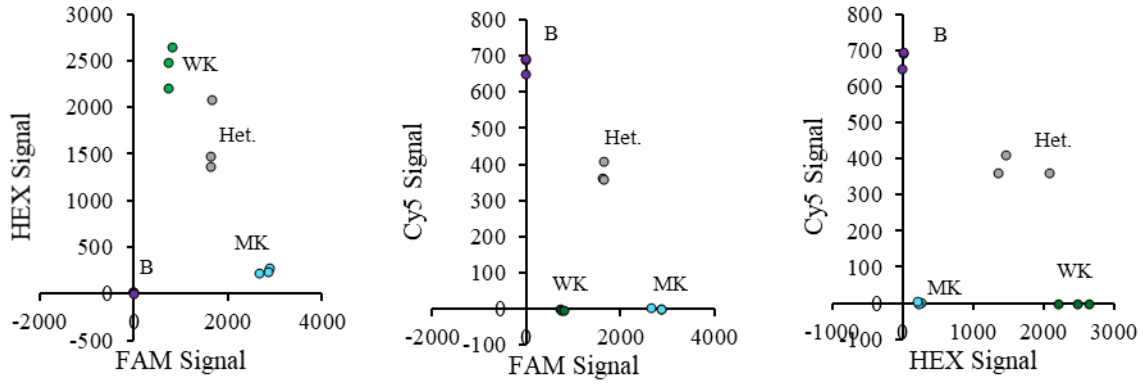

Figure 3-S5 Allelic discrimination between the wild-type *KRAS*, G12S *KRAS*, and wild-type *BRAF* targets using multiplex-qPCR. Het., heterozygous; B, wild-type *BRAF*; WK, wild-type *KRAS*; MK, G12S *KRAS*. Triplicate reactions were performed for each cluster.

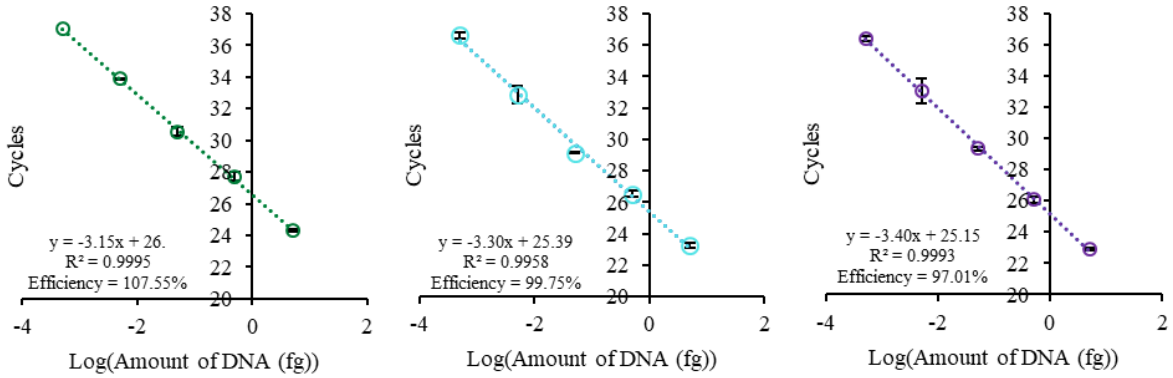

Figure 3-S6 Five-point standard curves generated for the (green) wild-type *KRAS*, (blue) G12S *KRAS*, and (violet) wild-type *BRAF*. Triplicate reactions were performed for each concentration.

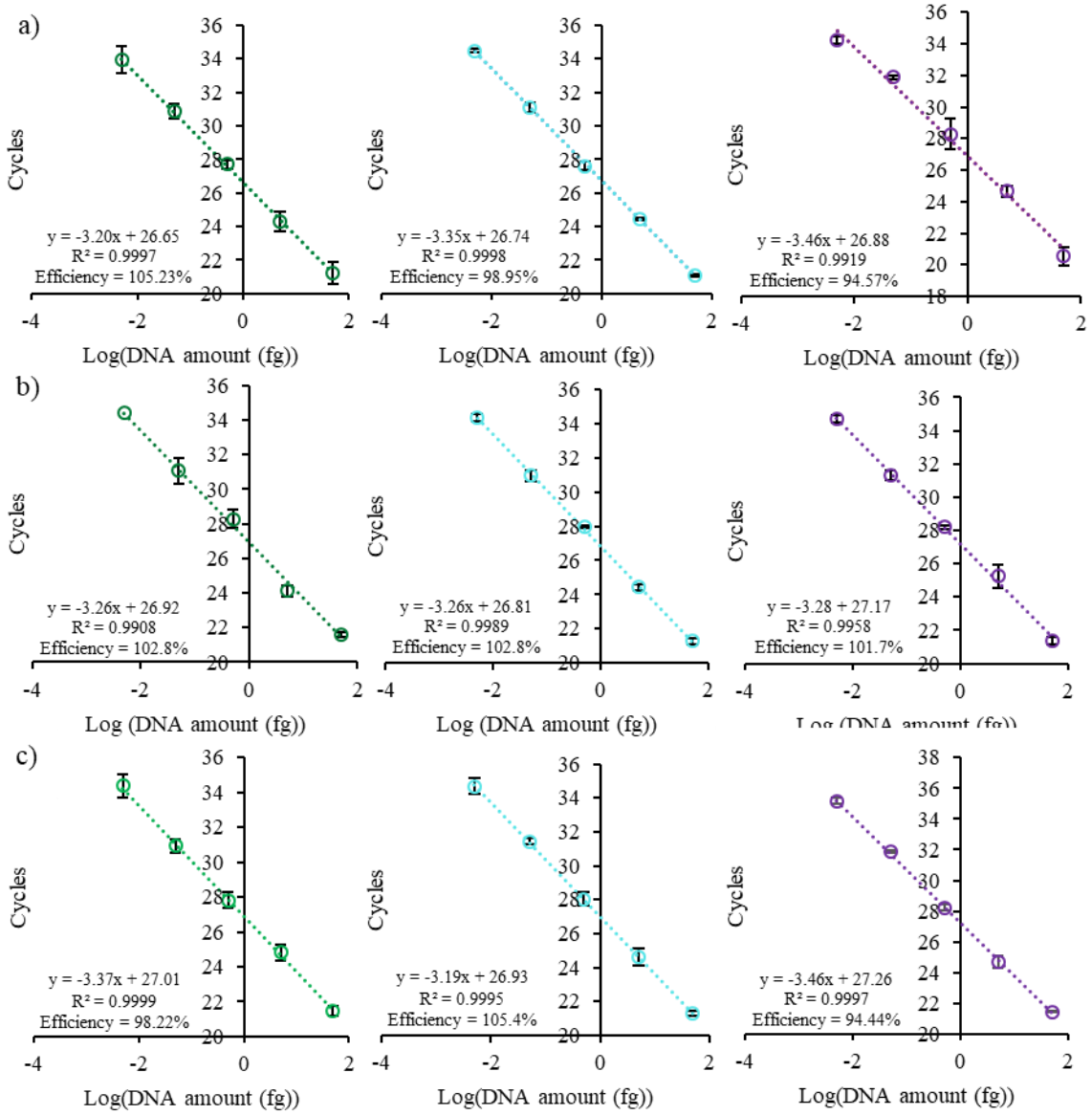

Figure 3-S7 Five-point standard curves generated for the (green) wild-type *KRAS*, (blue) G12S *KRAS*, and (violet) wild-type *BRAF* with the (a) $[P_{6,6,6,14}^{+}][Ni(hfacac)_3^{-}]$, (b) $[N_{8,8,8,Bz}^{+}][Ni(hfacac)_3^{-}]$, and (c) $[P_{6,6,6,14}^{+}][Ni(Phtfacac)_3^{-}]$ MILs in the buffer. Triplicate reactions were performed for each concentration.

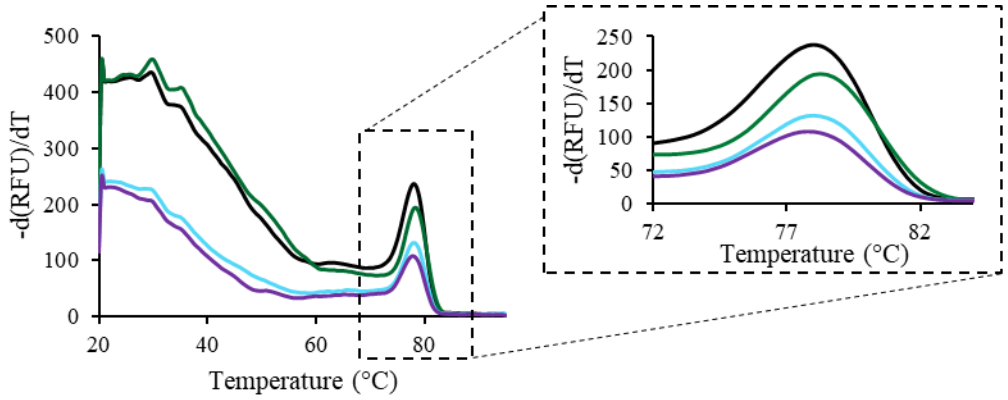

Figure 3-S8 Melt curves of the G12S *KRAS* amplicon with 0.3 µL of (green) $[P_{6,6,6,14}^{+}][Ni(hfacac)_3^{-}]$, (blue) $[N_{8,8,8,Bz}^{+}][Ni(hfacac)_3^{-}]$, and (violet) $[P_{6,6,6,14}^{+}][Ni(Phtfacac)_3^{-}]$ MILs spiked into the solution compared to a (black) standard.

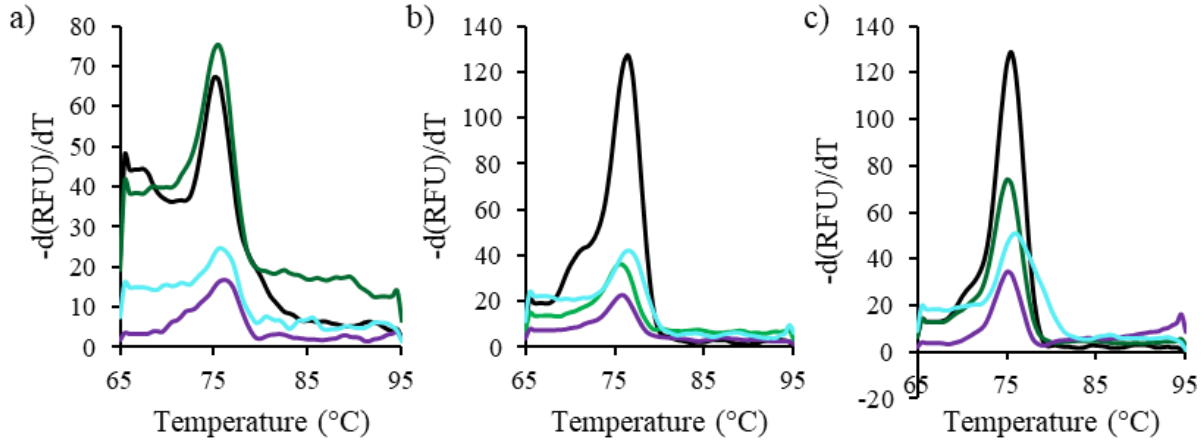

Figure 3-S9 Melt curves associated with (a) wild-type *KRAS*, (b) G12S *KRAS*, and (c) wild-type *BRAF* after extracting DNA using the (green) $[P_{6,6,6,14}^{+}][Ni(hfacac)_3^{-}]$ (blue) $[N_{8,8,8,Bz}^{+}][Ni(hfacac)_3^{-}]$, and (violet) $[P_{6,6,6,14}^{+}][Ni(Phtfacac)_3^{-}]$ MILs spiked into the solution compared to a (black) standard.

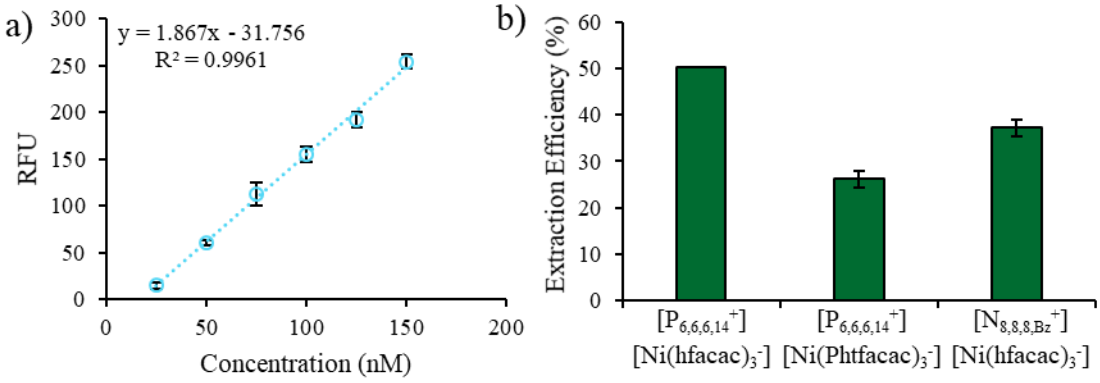

Figure 3-S10 (a) Six-point standard curve of Cy5. Slope = 1.867 ± 0.045, y-intercept = -31.76 ± 4.65, standard deviation of the regression = 8.651. All points were performed in triplicate. (b) Extraction of 150 nM Cy5 using four hydrophobic MILs. Sample volume: 20 µL; extraction time: 10 min; MIL volume: 0.3 µL. Each extraction was performed in triplicate.

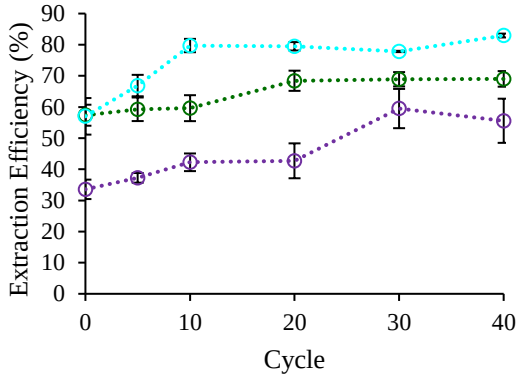

Figure 3-S11 Extraction of 150 nM Cy5 by the (green) $[P_{6,6,6,14}^+][Ni(hfacac)_3^-]$, (violet) $[P_{6,6,6,14}^+][Ni(Phtfacac)_3^-]$, and (blue) $[N_{8,8,8,Bz}^+][Ni(hfacac)_3^-]$ MILs. Sample volume: 20 µL; MIL volume: 0.3 µL. Initialization conditions: 2 min at 50 °C then 10 min at 90 °C. Cycling conditions for the $[P_{6,6,6,14}^+][Ni(hfacac)_3^-]$ and $[P_{6,6,6,14}^+][Ni(Phtfacac)_3^-]$ MILs: 15 s at 90 °C and 1 min at 59 °C. Cycling conditions for the $[N_{8,8,8,Bz}^+][Ni(hfacac)_3^-]$ MIL: 15 s at 90 °C and 1 min at 62 °C. All extractions were performed in triplicate.

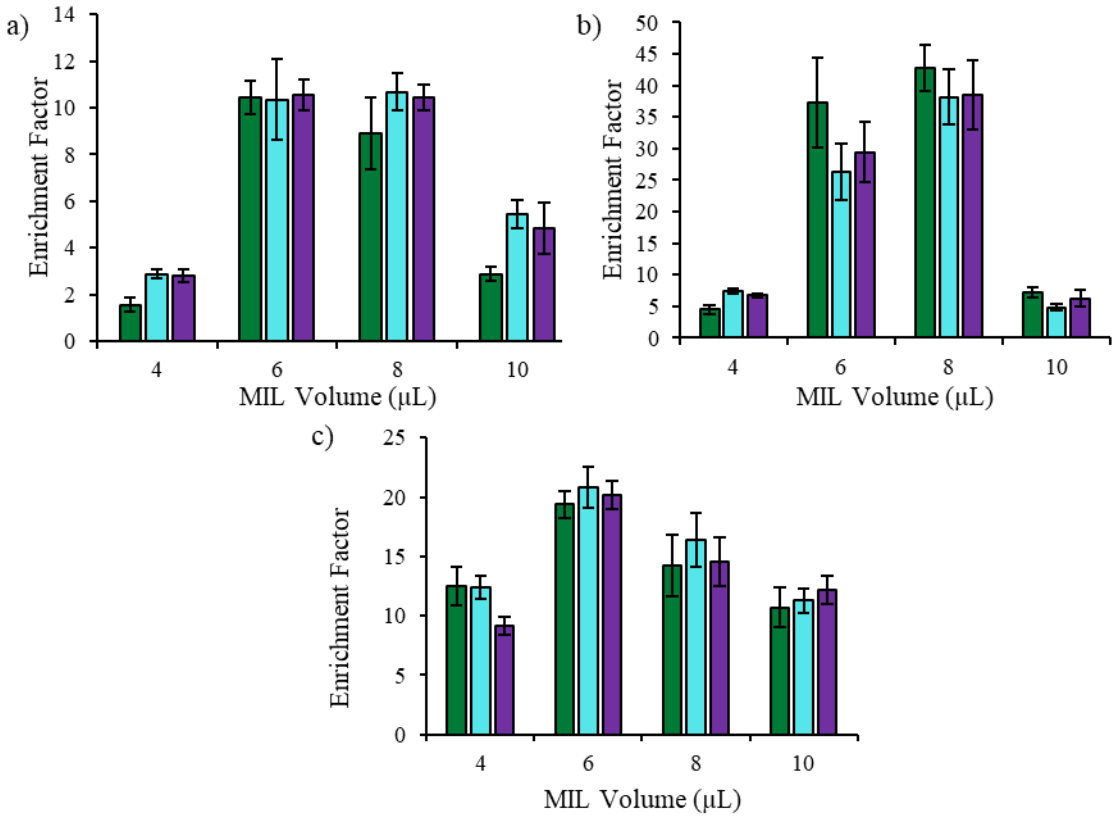

Figure 3-S12 Optimization of the amount of MIL dispersed using the (a) $[P_{6,6,6,14}^{+}]$ $[Ni(hfacac)_3^{-}]$, (b) $[N_{8,8,8,Bz}^{+}][Ni(hfacac)_3^{-}]$, and (c) $[P_{6,6,6,14}^{+}][Ni(Phtfacac)_3^{-}]$ MIL solvents to extract (green) wild-type *KRAS*, (blue) G12S *KRAS*, and (violet) wild-type *BRAF* DNA. Wild-type *KRAS*, G12S *KRAS*, and wild-type *BRAF* template concentration: 0.5 fg μL^{-1}, sample volume: 1.0 mL; extraction time: 2 min. Triplicate extractions were performed for each condition.

.

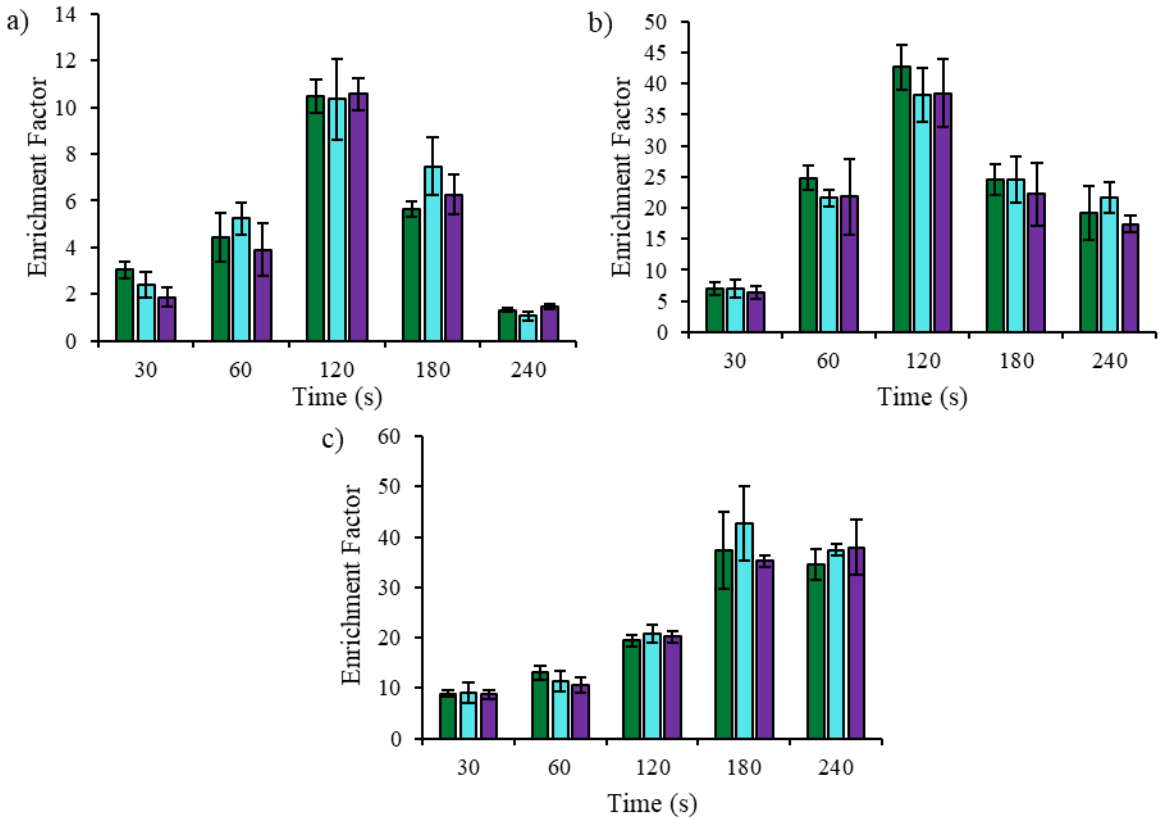

Figure 3-S13 Extraction time optimization of (green) wild-type *KRAS*, (blue) G12S *KRAS*, and (violet) wild-type *BRAF* using the (a) $[P_{6,6,6,14}^{+}][Ni(hfacac)_3^{-}]$, (b) $[N_{8,8,8,Bz}^{+}][Ni(hfacac)_3^{-}]$, and (c) $[P_{6,6,6,14}^{+}][Ni(Phtfacac)_3^{-}]$ MILs. Wild-type *KRAS*, G12S *KRAS*, and wild-type *BRAF* template concentration: 0.5 fg μL^{-1}, sample volume: 1.0 mL; $[P_{6,6,6,14}^{+}][Ni(hfacac)_3^{-}]$ volume: 6 µL; $[N_{8,8,8,Bz}^{+}][Ni(hfacac)_3^{-}]$ volume: 6 µL; $[P_{6,6,6,14}^{+}][Ni(Phtfacac)_3^{-}]$ volume: 8 µL. Triplicate extractions were performed for each condition.

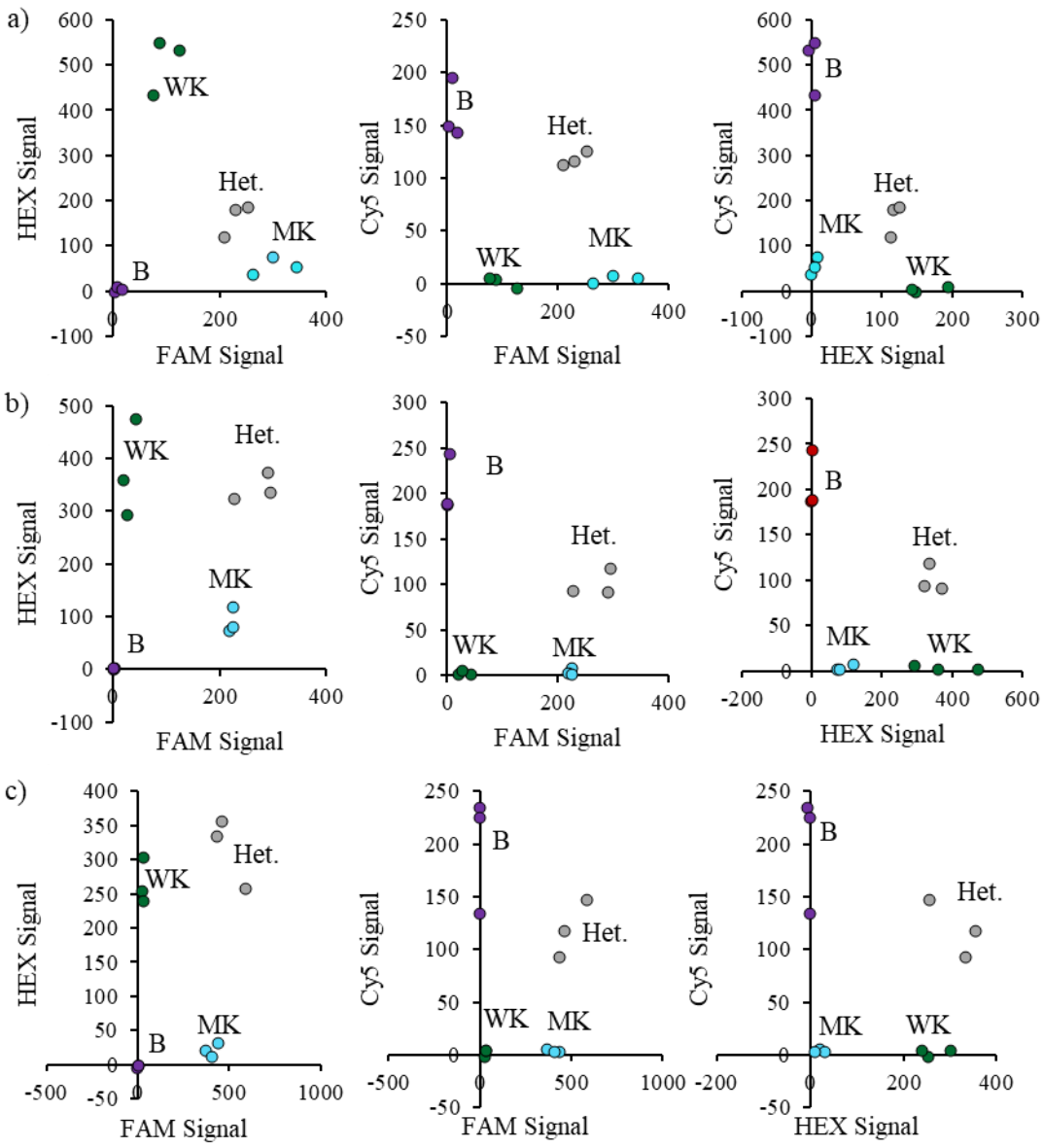

Figure 3-S14 Allelic discrimination plots developed after performing MIL-DLLME and desorbing DNA during multiplex-qPCR program with the (a) $[P_{6,6,6,14}^{+}][Ni(hfacac)_3^{-}]$, (b) $[N_{8,8,8,Bz}^{+}][Ni(hfacac)_3^{-}]$, and (c) $[P_{6,6,6,14}^{+}][Ni(Phtfacac)_3^{-}]$ MILs. DNA concentration: 0.5 fg μL^{-1}, sample volume: 1.0 mL; $[P_{6,6,6,14}^{+}][Ni(hfacac)_3^{-}]$ volume: 6 µL; $[N_{8,8,8,Bz}^{+}][Ni(hfacac)_3^{-}]$ volume: 6 µL; $[P_{6,6,6,14}^{+}][Ni(Phtfacac)_3^{-}]$ volume: 8 µL;$[P_{6,6,6,14}^{+}][Ni(hfacac)_3^{-}]$ extraction time: 2 min; $[N_{8,8,8,Bz}^{+}][Ni(hfacac)_3^{-}]$ extraction time: 2 min; $[P_{6,6,6,14}^{+}][Ni(Phtfacac)_3^{-}]$ extraction time: 3 min. Het., heterozygous; B, wild-type *BRAF*; WK, wild-type *KRAS*; MK, G12S *KRAS*. Triplicate extractions were performed for each cluster.

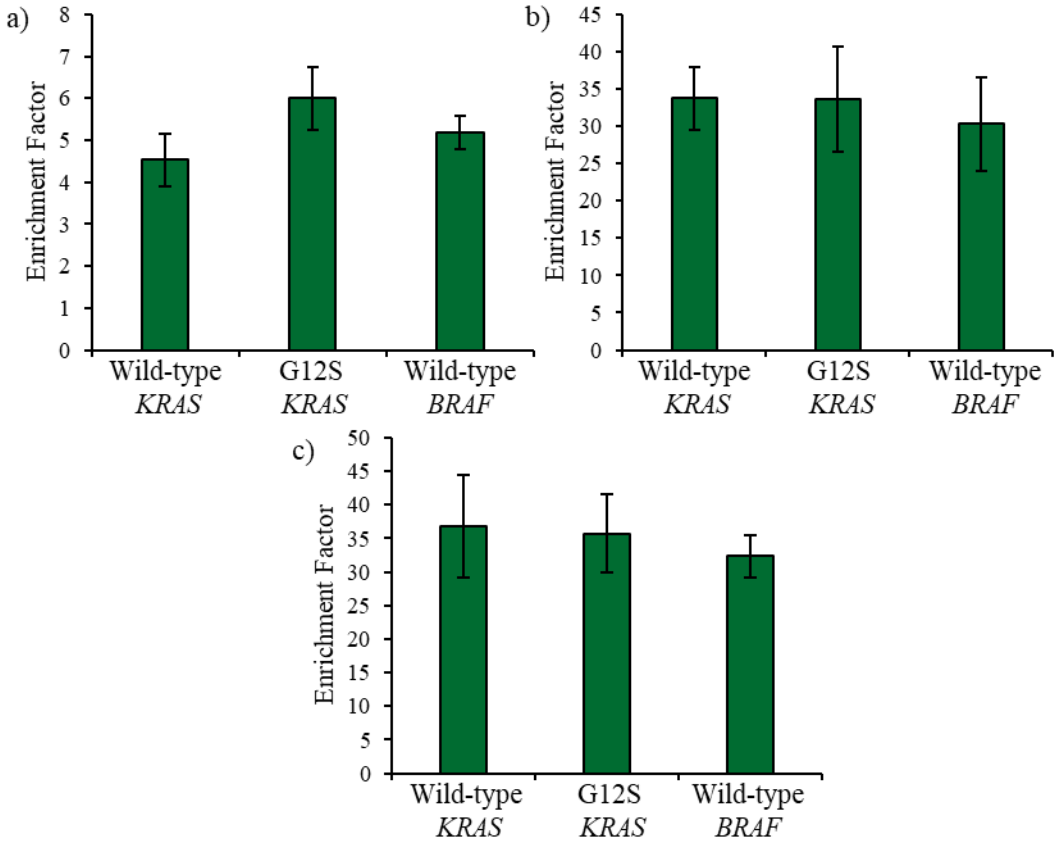

Figure 3-S15 Enrichment factors obtained when extracting only one of three DNA fragments using the (a) $[P_{6,6,6,14}^{+}][Ni(hfacac)_3^{-}]$, (b) $[N_{8,8,8,Bz}^{+}][Ni(hfacac)_3^{-}]$, and (c) $[P_{6,6,6,14}^{+}][Ni(Phtfacac)_3^{-}]$ MILs. DNA concentration: 0.5 fg μL^{-1}, sample volume: 1.0 mL; $[P_{6,6,6,14}^{+}][Ni(hfacac)_3^{-}]$ volume: 6 µL; $[N_{8,8,8,Bz}^{+}][Ni(hfacac)_3^{-}]$ volume: 6 µL; $[P_{6,6,6,14}^{+}][Ni(Phtfacac)_3^{-}]$ volume: 8 µL. $[P_{6,6,6,14}^{+}][Ni(hfacac)_3^{-}]$ extraction time: 2 min; $[N_{8,8,8,Bz}^{+}][Ni(hfacac)_3^{-}]$ extraction time: 2 min; $[P_{6,6,6,14}^{+}][Ni(Phtfacac)_3^{-}]$ extraction time: 3 min. Triplicate extractions were performed for each sequence.

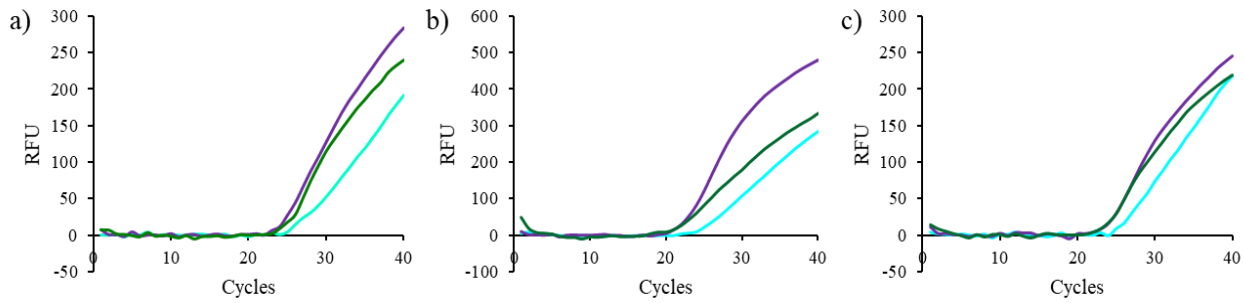

Figure 3-S16 Amplification curves of (green) wild-type *KRAS*, (blue) G12S *KRAS*, and (purple) wild-type *BRAF* associated with the MIL-multiplex-qPCR using the (a) $[P_{6,6,6,14}^{+}][Ni(hfacac)_3^{-}]$, (b) $[N_{8,8,8,Bz}^{+}][Ni(hfacac)_3^{-}]$, and (c) $[P_{6,6,6,14}^{+}][Ni(Phtfacac)_3^{-}]$ MILs. *KRAS* WT and *BRAF* template concentration: 5 fg μL^{-1}, G12S *KRAS* template concentration: 0.5 fg μL^{-1}; sample volume: 1.0 mL; $[P_{6,6,6,14}^{+}][Ni(hfacac)_3^{-}]$ volume: 6 µL; $[N_{8,8,8,Bz}^{+}][Ni(hfacac)_3^{-}]$ volume: 6 µL; $[P_{6,6,6,14}^{+}][Ni(Phtfacac)_3^{-}]$ volume: 8 µL. $[P_{6,6,6,14}^{+}][Ni(hfacac)_3^{-}]$ extraction time: 2 min; $[N_{8,8,8,Bz}^{+}][Ni(hfacac)_3^{-}]$ extraction time: 2 min; $[P_{6,6,6,14}^{+}][Ni(Phtfacac)_3^{-}]$ extraction time: 3 min.

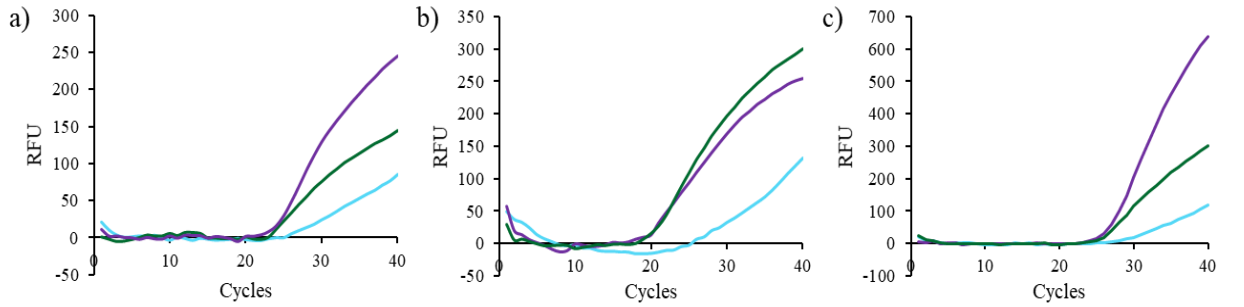

Figure 3-S17 Amplification curves of (green) wild-type *KRAS*, (blue) G12S *KRAS*, and (purple) wild-type *BRAF* associated with the MIL-multiplex-qPCR with the (a) $[P_{6,6,6,14}^{+}][Ni(hfacac)_3^{-}]$, (b) $[N_{8,8,8,Bz}^{+}][Ni(hfacac)_3^{-}]$, and (c) $[P_{6,6,6,14}^{+}][Ni(Phtfacac)_3^{-}]$ MILs. *KRAS* WT and *BRAF* template concentration: 5 fg μL^{-1}, G12S *KRAS* template concentration: 0.05 fg μL^{-1}; sample volume: 1.0 mL; $[P_{6,6,6,14}^{+}][Ni(hfacac)_3^{-}]$ volume: 6 µL; $[N_{8,8,8,Bz}^{+}][Ni(hfacac)_3^{-}]$ volume: 6 µL; $[P_{6,6,6,14}^{+}][Ni(Phtfacac)_3^{-}]$ volume: 8 µL. $[P_{6,6,6,14}^{+}][Ni(hfacac)_3^{-}]$ extraction time: 2 min; $[N_{8,8,8,Bz}^{+}][Ni(hfacac)_3^{-}]$ extraction time: 2 min; $[P_{6,6,6,14}^{+}][Ni(Phtfacac)_3^{-}]$ extraction time: 3 min.

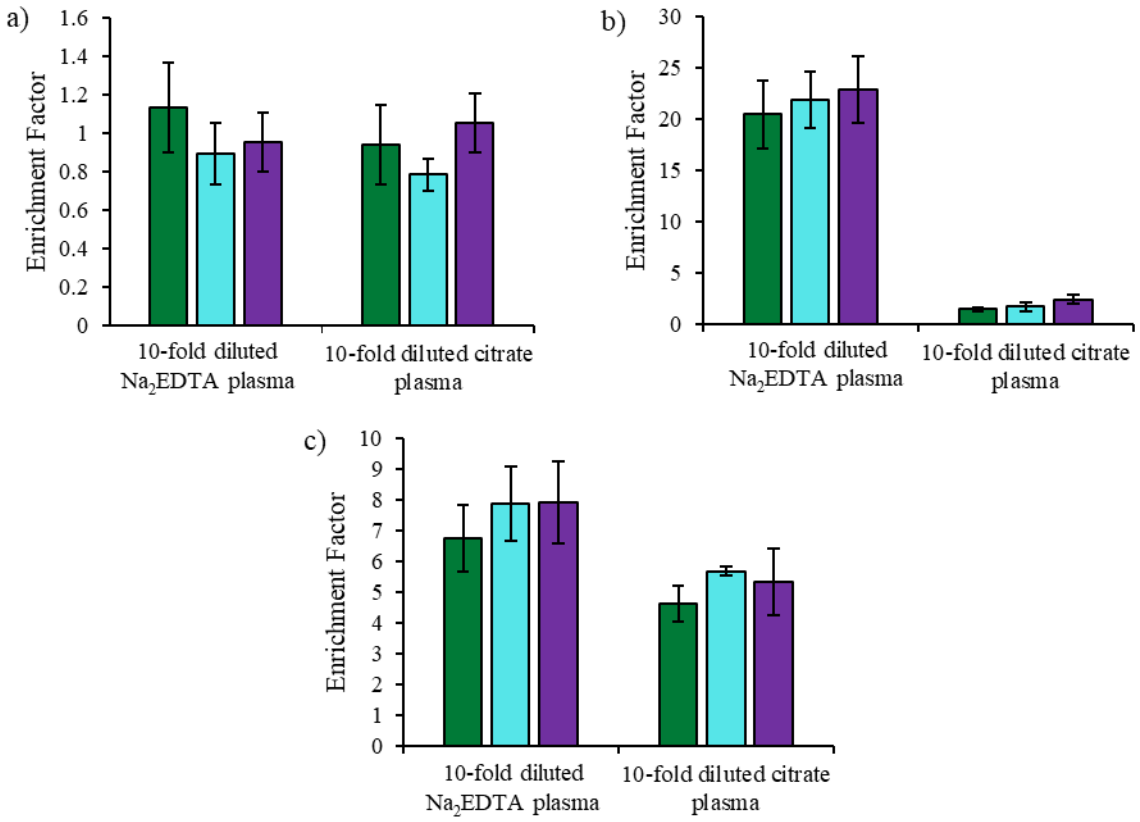

Figure 3-S18 MIL-DLLME from 10-fold diluted plasma containing either Na_2EDTA or citrate as an anticoagulant with the (a) $[P_{6,6,6,14}^+][Ni(hfacac)_3^-]$, (b) $[N_{8,8,8,Bz}^+][Ni(hfacac)_3^-]$, and (c) $[P_{6,6,6,14}^+][Ni(Phtfacac)_3^-]$ MILs. Wild-type *KRAS*, G12S *KRAS*, and wild-type *BRAF* template concentration: 0.5 fg μL^{-1}, sample volume: 1.0 mL; $[P_{6,6,6,14}^+][Ni(hfacac)_3^-]$ volume: 6 µL; $[N_{8,8,8,Bz}^+][Ni(hfacac)_3^-]$ volume: 6 µL; $[P_{6,6,6,14}^+][Ni(Phtfacac)_3^-]$ volume: 8 µL. $[P_{6,6,6,14}^+][Ni(hfacac)_3^-]$ extraction time: 2 min; $[N_{8,8,8,Bz}^+][Ni(hfacac)_3^-]$ extraction time: 2 min; $[P_{6,6,6,14}^+][Ni(Phtfacac)_3^-]$ extraction time: 3 min. Triplicate extractions were performed for all conditions.

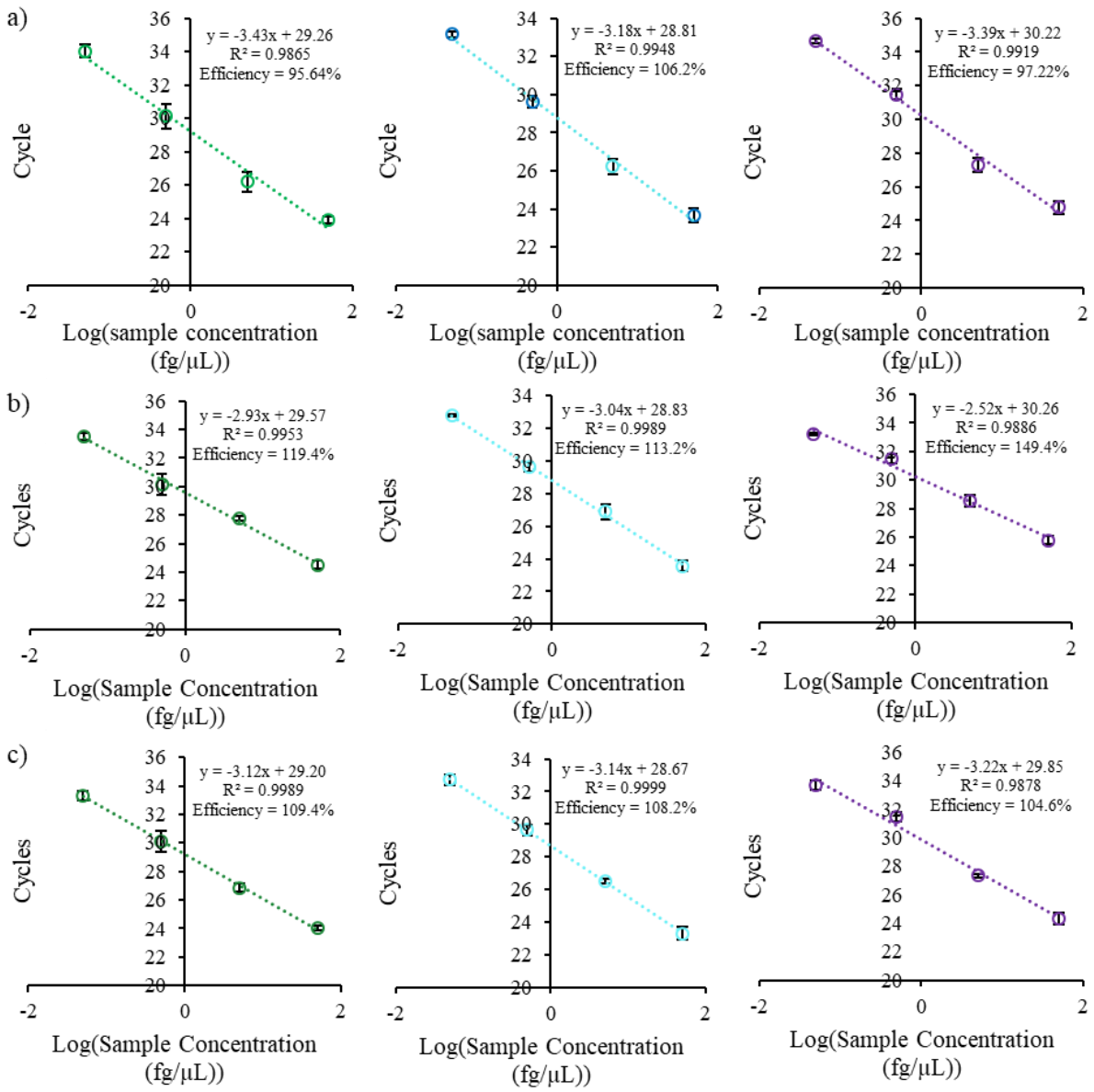

Figure 3-S19 Four-point standard curves generated for the (green) wild-type *KRAS*, (blue) G12S *KRAS*, and (violet) wild-type *BRAF* by performing extractions from 10-fold diluted plasma with the Na_2EDTA anticoagulant using the (a) $[P_{6,6,6,14}^+][Ni(hfacac)_3^-]$, (b) $[N_{8,8,8,Bz}^+][Ni(hfacac)_3^-]$ MIL, and (c) $[P_{6,6,6,14}^+][Ni(Phtfacac)_3^-]$ MILs. Wild-type *KRAS*, G12S *KRAS*, and wild-type *BRAF* template concentration: 0.5 fg μL^{-1}, sample volume: 1.0 mL; $[P_{6,6,6,14}^+][Ni(hfacac)_3^-]$ volume: 6 µL; $[N_{8,8,8,Bz}^+][Ni(hfacac)_3^-]$ volume: 8 µL; $[P_{6,6,6,14}^+][Ni(Phtfacac)_3^-]$ volume: 6 µL. $[P_{6,6,6,14}^+][Ni(hfacac)_3^-]$ extraction time: 2 min; $[N_{8,8,8,Bz}^+][Ni(hfacac)_3^-]$ extraction time: 2 min; $[P_{6,6,6,14}^+][Ni(Phtfacac)_3^-]$ extraction time: 3 min. Triplicate extractions were performed for each concentration.

APPENDIX C

SUPPORTING INFORMATION ACCOMPANYING CHAPTER 4

Table 4-S1 All oligo sequences examined in this study.

Name	Sequence
Thiolated *KRAS*	5' 5Thio-MC6-D/TTG AAC TAG CAA TGC CTG TG -3'
KRAS Complement	5' – CAC AGG CAT TGC TAG TTC AA -3'
Thiolated *KRAS* Single Nucleotide Variant	5' 5Thio-MC6-D/TTG AAC TAG GAA TGC CTG TG -3'
Biotinylated *KRAS*	5'-5Biosg/TTG AAC TAG CAA TGC CTG TG -3'
KRAS 1 nt mismatch	5' – CAC AGG CAT TCC TAG TTC AA -3'
KRAS 2 nt mismatch	5' – GAC AGG CAT TCC TAG TTC AA -3'

Table 4-S2 Calculated and observed masses for the ITOs synthesized in this study.

ITO	Exact Mass (monoisotopic)	m/z (Calculated) -4 Charged State	m/z (Observed) -4 Charged State
[AOIM$^+$]-*KRAS* [Br$^-$]	6549.6007	1636.4002	1635.8976
[AOIM$^+$]-*KRAS* [PF_6^-]	6549.6007	1636.4002	1635.8737
[ABzIM$^+$]-*KRAS* [Br$^-$]	6527.5097	1630.8774	1630.6268
[ABzIM$^+$]-*KRAS* [PF_6^-]	6527.5097	1630.8774	1630.0978

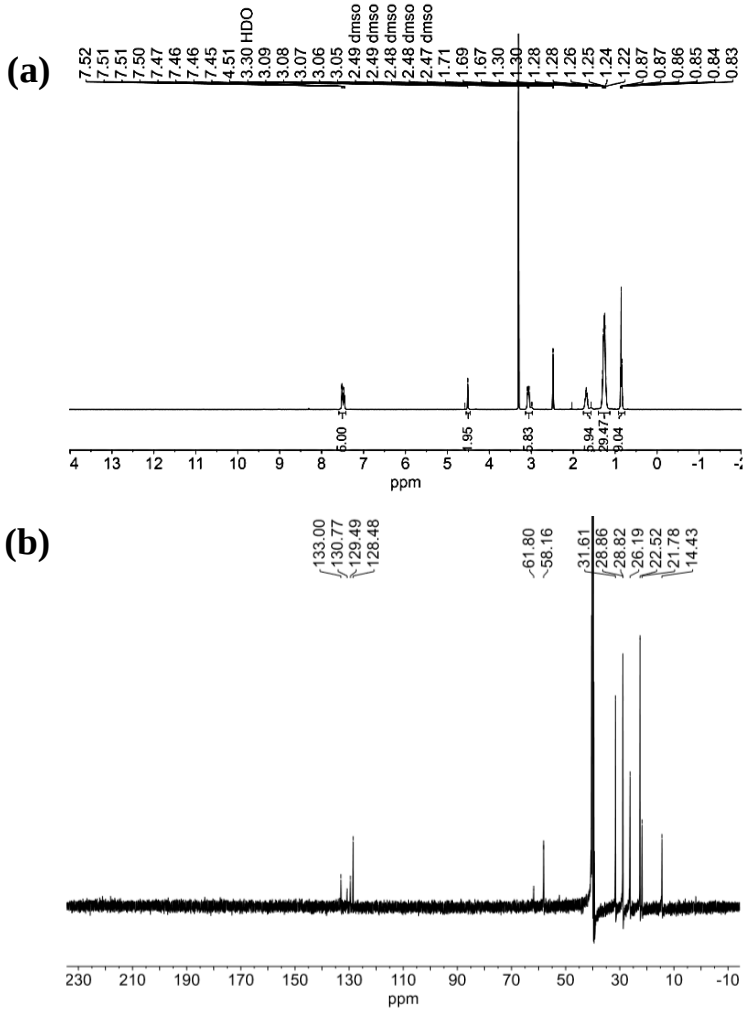

Figure 4-S1 ^{1}H NMR (a) and ^{13}C NMR (b) spectra of the $[N_{8,8,8,Bz}^{+}][Br^{-}]$ salt taken on a 400 MHz instrument.

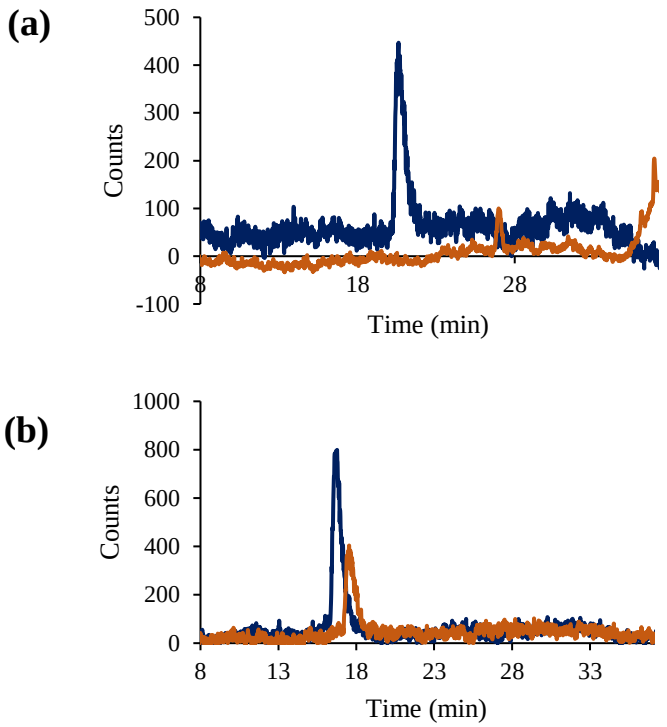

Figure 4-S2 Extracted ion chromatograms of the -4 charged state of the (a) [AOIM$^+$]-*KRAS* [Br$^-$] (blue) and [AOIM$^+$]-*KRAS* [PF_6^-] (orange) and (b) [AOIM$^+$]-*KRAS* [Br$^-$] (blue) and [AOIM$^+$]-*KRAS* [PF_6^-] (orange) ITOs.

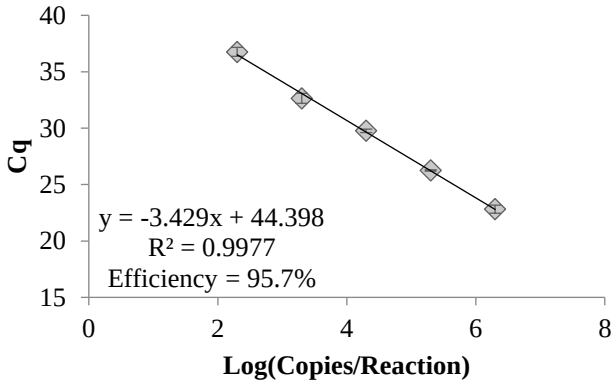

Figure 4-S3 Five-point standard curve with 10-fold dilution to determine the amplification efficiency of the *KRAS* template.

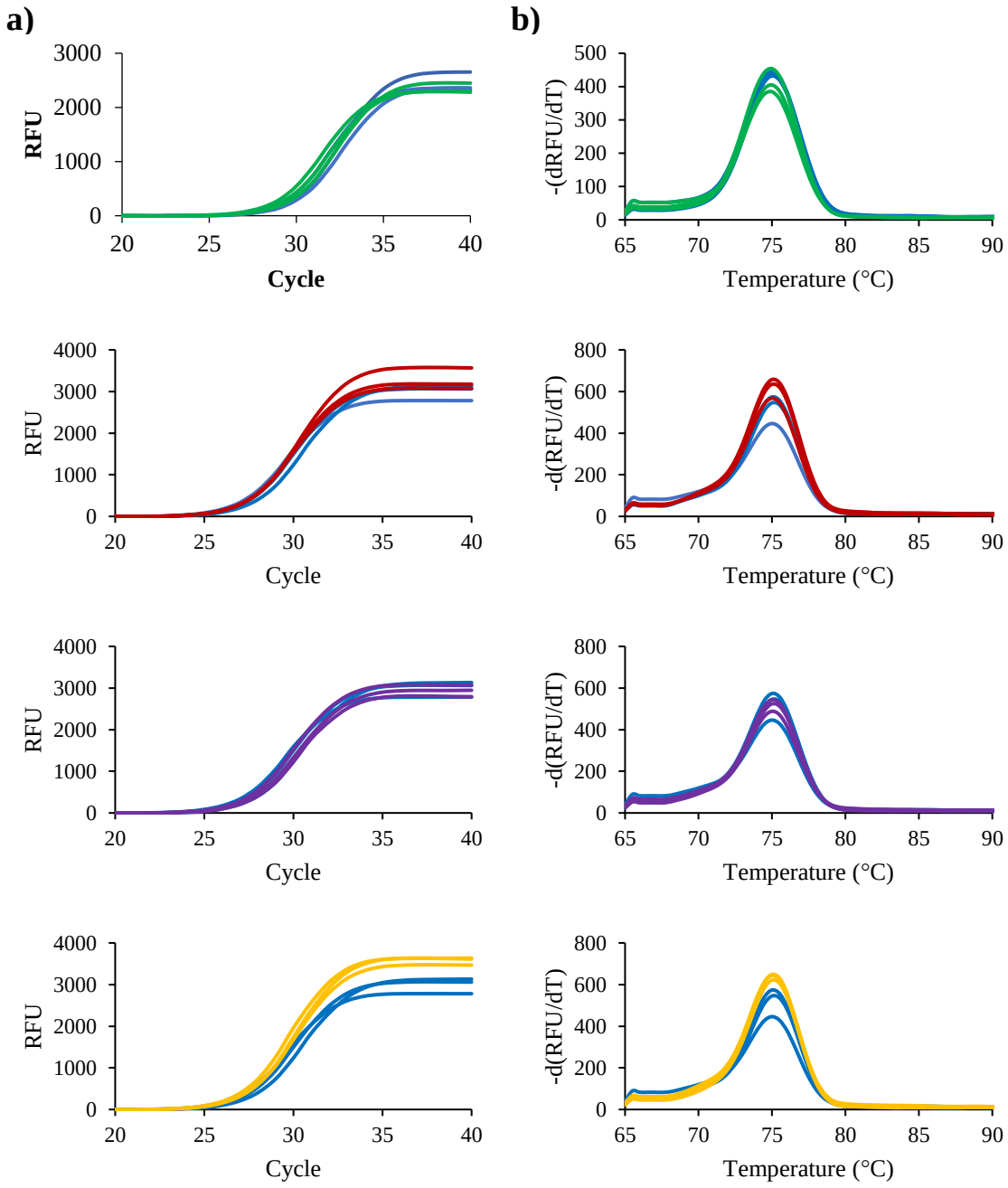

Figure 4-S4 (a) qPCR amplification curves with 2×10^5 copies μL^{-1} of [$AOIM^+$]-*KRAS* [Br^-] (green), [$AOIM^+$]-*KRAS* [PF_6^-] (red), [$ABzIM^+$]-*KRAS* [Br^-] (purple), and [$ABzIM^+$]-*KRAS* [PF_6^-] (orange) spiked into the buffer compared to a standard (blue). (b) Melt curves following qPCR amplification with 2×10^5 copies μL^{-1} of [$AOIM^+$]-*KRAS* [Br^-] (green), [$AOIM^+$]-*KRAS* [PF_6^-] (red), [$ABzIM^+$]-*KRAS* [Br^-] (purple), and [$ABzIM^+$]-*KRAS* [PF_6^-] (orange) spiked into the buffer compared to a standard (blue). Sample volume: 20 µL; SSO Supermix concentration: 1x; *KRAS* primer concentration: 1x; ITO concentration: 2×10^5 copies μL^{-1}; DNA concentration: 2×10^4 copies μL^{-1}.

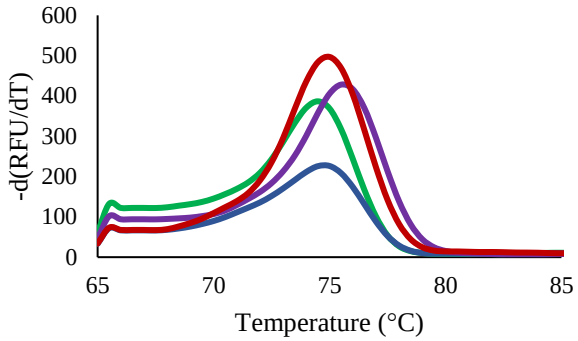

Figure 4-S5 Melt curves associated with *KRAS* template extracted using $[P_{6,6,6,14}^{+}][Mn(hfacac)_3^{-}]$ (green), $[N_{8,8,8,Bz}^{+}][Mn(hfacac)_3^{-}]$ (blue), and $[N_{8,8,8,Bz}^{+}][Mn(hfacac)_2(Phtfacac)^{-}]$ MIL (purple) compared against a *KRAS* standard (blue) following qPCR amplification.

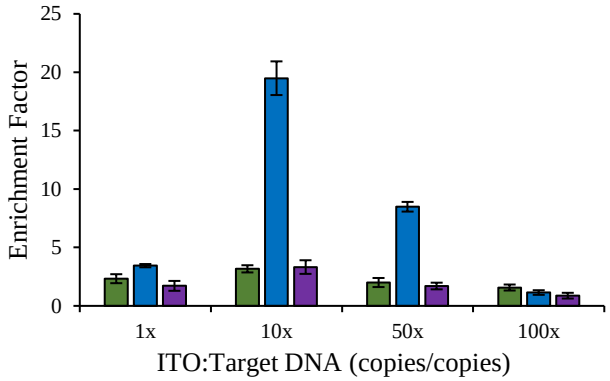

Figure 4-S6 Optimization of the amount of ITO relative to the amount of DNA using the $[P_{6,6,6,14}^{+}]$ $[Mn(hfacac)_3^{-}]$ (green), $[N_{8,8,8,Bz}^{+}][Mn(hfacac)_3^{-}]$ (blue), and $[N_{8,8,8,Bz}^{+}][Mn(hfacac)_2(Phtfacac)^{-}]$ MILs (purple). $[P_{6,6,6,14}+]$ $[Mn(hfacac)_3^{-}]$ MIL conditions: KRAS template concentration: 2×10^4 copies μL^{-1}, NaCl concentration: 25 mM, sample volume: 1.0 mL, MIL volume: 8 µL; extraction time: 3 min. $[N_{8,8,8,Bz}^{+}][Mn(hfacac)_3^{-}]$ MIL conditions: KRAS template concentration: 2×10^4 copies μL^{-1}, NaCl concentration: 25 mM, sample volume: 1.0 mL, MIL volume: 6 µL: extraction time: 1 min. $[N_{8,8,8,Bz}^{+}]$ $[Mn(hfacac)_2(Phtfacac)^{-}]$ MIL conditions: KRAS template concentration: 2×10^4 copies μL^{-1}, NaCl concentration: 25 mM, sample volume: 1.0 mL, MIL volume: 4 µL; extraction time: 1 min.

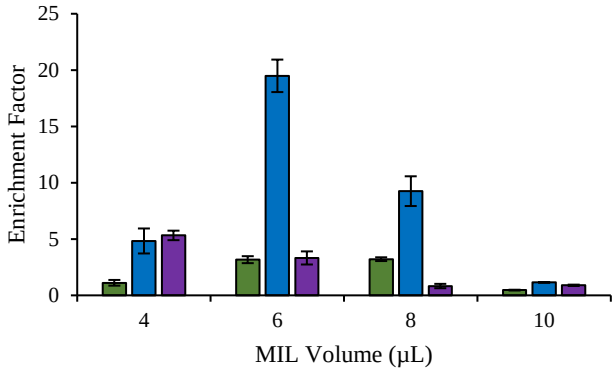

Figure 4-S7 Optimization of the amount of MIL dispersed using the [$P_{6,6,6,14}^{+}$] [$Mn(hfacac)_3^{-}$] (green), [$N_{8,8,8,Bz}^{+}$] [$Mn(hfacac)_3^{-}$] (blue), and [$N_{8,8,8,Bz}^{+}$][$Mn(hfacac)_2(Phtfacac)^{-}$] (purple) MILs. [$P_{6,6,6,14}^{+}$] [$Mn(hfacac)_3^{-}$] MIL conditions: *KRAS* template concentration: 2×10^4 copies μL^{-1}, amount of [$AOIM^{+}$]-*KRAS* [PF_6^{-}] ITO relative to DNA: 10x, NaCl concentration: 25 mM, sample volume: 1.0 mL, MIL volume: 8 µL; extraction time: 3 min. [$N_{8,8,8,Bz}^{+}$][$Mn(hfacac)_3^{-}$] MIL conditions: *KRAS* template concentration: 2×10^4 copies μL^{-1}, amount of [$ABzIM^{+}$]-*KRAS* [Br^{-}] ITO relative to DNA: 10x, NaCl concentration: 25 mM, sample volume: 1.0 mL, MIL volume: 6 µL: extraction time: 1 min. [$N_{8,8,8,Bz}^{+}$] [$Mn(hfacac)_2(Phtfacac)^{-}$] MIL conditions: *KRAS* template concentration: 2×10^4 copies μL^{-1}, amount of [$ABzIM^{+}$]-*KRAS* [Br^{-}] ITO relative to DNA: 10x, NaCl concentration: 25 mM, sample volume: 1.0 mL, MIL volume: 4 µL; extraction time: 1 min.

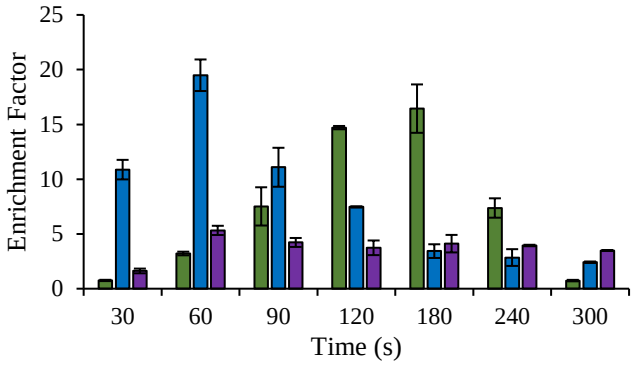

Figure 4-S8 Extraction time optimization using the [$P_{6,6,6,14}^{+}$] [$Mn(hfacac)_3^{-}$] (green), [$N_{8,8,8,Bz}^{+}$] [$Mn(hfacac)_3^{-}$] (blue), and [$N_{8,8,8,Bz}^{+}$] [$Mn(hfacac)_2(Phtfacac)^{-}$] (purple) MILs. [$P_{6,6,6,14}^{+}$] [$Mn(hfacac)_3^{-}$] MIL conditions: *KRAS* template concentration: 2×10^4 copies μL^{-1}, amount of [$AOIM^{+}$]-*KRAS* [PF_6^{-}] ITO relative to DNA: 10x, NaCl concentration: 25 mM, sample volume: 1.0 mL, MIL volume: 8 µL; extraction time: 3 min. [$N_{8,8,8,Bz}^{+}$][$Mn(hfacac)_3^{-}$] MIL conditions: *KRAS* template concentration: 2×10^4 copies μL^{-1}, amount of [$ABzIM^{+}$]-*KRAS* [Br^{-}] ITO relative to DNA: 10x, NaCl concentration: 25 mM, sample volume: 1.0 mL, MIL volume: 6 µL: extraction time: 1 min. [$N_{8,8,8,Bz}^{+}$] [$Mn(hfacac)_2(Phtfacac)^{-}$] MIL conditions: *KRAS* template concentration: 2×10^4 copies μL^{-1}, amount of [$ABzIM^{+}$]-*KRAS* [Br^{-}] ITO relative to DNA: 10x, NaCl concentration: 25 mM, sample volume: 1.0 mL, MIL volume: 4 µL; extraction time: 1 min.

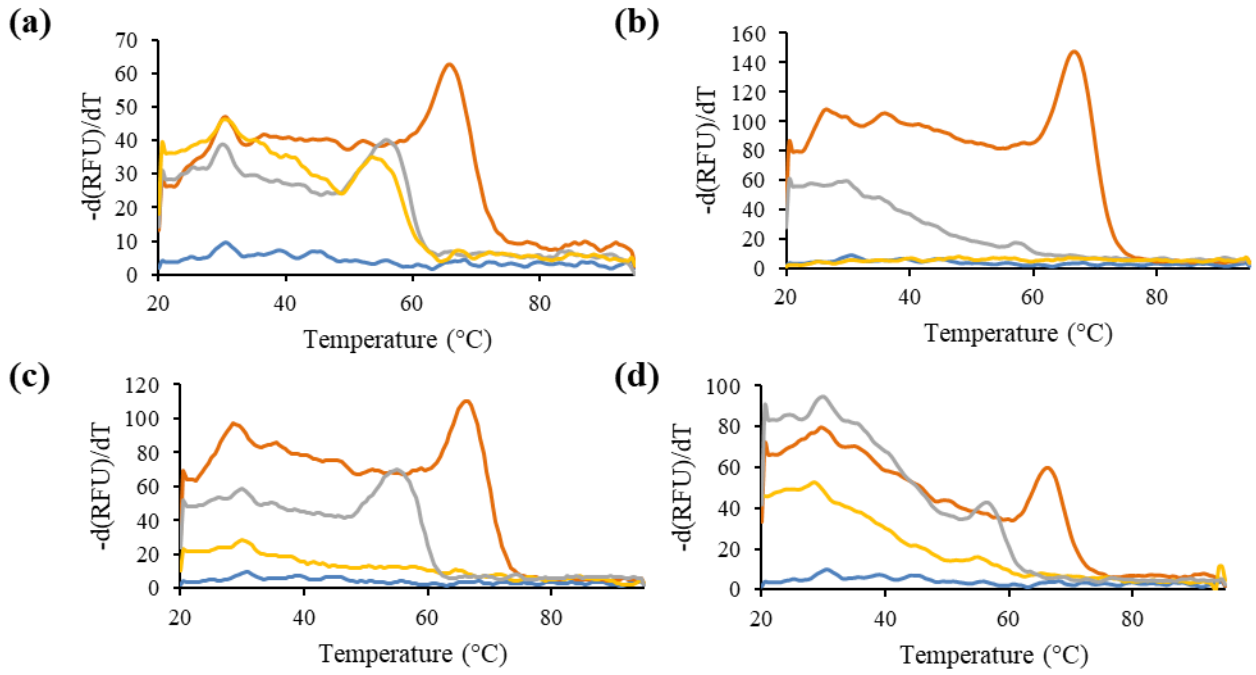

Figure 4-S9 Melt curves associated with the hybridization of a complimentary oligonucleotide (orange), 1 nt mismatch (grey), and 2 nt mismatch (yellow) to the [AOIM$^+$]-*KRAS* [Br$^-$] (a), [AOIM$^+$]-*KRAS* [PF_6^-] (b), [ABzIM$^+$]-*KRAS* [Br$^-$] (c), and [ABzIM$^+$]-*KRAS* [PF_6^-] ITOs (d). Sample volume: 20 µL; ITO concentration: 1 ppm; oligonucleotide concentration: 1 ppm; NaCl concentration: 50 mM; SYBR Green I concentration: 1x.

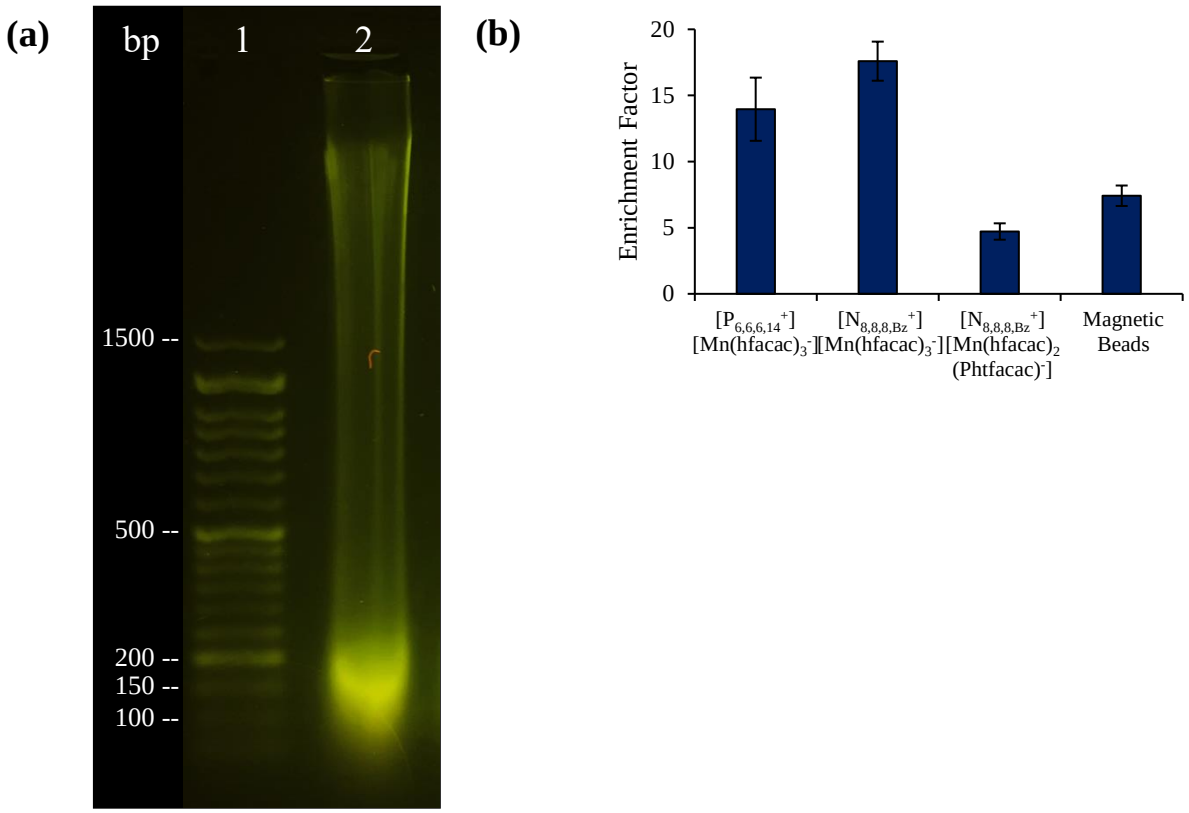

Figure 4-S10 (a) Agarose gel (1.5%) electrophoresis separation of sheared stDNA (lane 2) alongside a 50 bp DNA ladder (lane 1). (b) Extraction of *KRAS* fragments from a solution containing 1000 ng of sheared stDNA using steptavidin-coated magnetic beads and the $[P_{6,6,6,14}^{+}]$ $[Mn(hfacac)_3^{-}]$, $[N_{8,8,8,Bz}^{+}]$ $[Mn(hfacac)_3^{-}]$, and $[N_{8,8,8,Bz}^{+}]$ $[Mn(hfacac)_2(Phtfacac)^{-}]$ MILs. $[P_{6,6,6,14}^{+}]$ $[Mn(hfacac)_3^{-}]$ MIL conditions: stDNA concentration: 1000 ng/mL; *KRAS* template concentration: 2×10^4 copies μL^{-1}, amount of $[AOIM^{+}]$-*KRAS* $[PF_6^{-}]$ ITO relative to DNA: 10x, NaCl concentration: 25 mM, sample volume: 1.0 mL, MIL volume: 8 µL; extraction time: 3 min. $[N_{8,8,8,Bz}^{+}][Mn(hfacac)_3^{-}]$ MIL conditions: stDNA concentration: 1000 ng mL^{-1}; *KRAS* template concentration: 2×10^4 copies μL^{-1}, amount of $[ABzIM^{+}]$-*KRAS* $[Br^{-}]$ ITO relative to DNA: 10x, NaCl concentration: 25 mM, sample volume: 1.0 mL, MIL volume: 6 µL: extraction time: 1 min. $[N_{8,8,8,Bz}^{+}]$ $[Mn(hfacac)_2(Phtfacac)^{-}]$ MIL conditions: stDNA concentration: 1000 ng mL^{-1}; *KRAS* template concentration: 2×10^4 copies μL^{-1}, amount of $[ABzIM^{+}]$-*KRAS* $[Br^{-}]$ ITO relative to DNA: 10x, NaCl concentration: 25 mM, sample volume: 1.0 mL, MIL volume: 4 µL; extraction time: 1 min.

APPENDIX D

SUPPORTING INFORMATION ACCOMPANYING CHAPTER 5

Table 5-S1 Sequences of all oligonucleotides used in this study.

Name	Sequence
Thiolated *BRAF*	5'-/5ThioMC6-D/TAGCTACAGAGAAATCTCGA-3'
BRAF Forward Primer	5'-TTCATGAAGACCTCACAGTAAA-3'
BRAF Reverse Primer	5'-GGATCCAGACAACTGTTCAA-3'
WT *BRAF* Probe	5'-TGGTCTAGCTACAGTGAAATCTCGATG-3'
V600E *BRAF* Probe	5'-TGGTCTAGCTACAGAGAAATCTCGATG-3'
WT *BRAF* Insert	TATATTTCTTCATGAAGACCTCACAGTAAAAA TAGGTGATTTTGGTCTAGCTACAGTGAAATCTC GATGGAGTGGGTCCCATCAGTTTGAACAGTTG TCTGGATCCATTTTGTGGATGTAAGAATTGAGG CTATTTTTCCACTGATTAAATTTTTGGCCCTGAG ATGCTGCTGAGTTACTAGAAAGTCATTGAAGGT CTCAACTATAGT
V600E *BRAF* Insert	TATATTTCTTCATGAAGACCTCACAGTAAAAATA GGTGATTTTGGTCTAGCTACAGAGAAATCTCGAT GGAGTGGGTCCCATCAGTTTGAACAGTTGTCTG GATCCATTTTGTGGATGTAAGAATTGAGGCTATT TTTCCACTGATTAAATTTTTGGCCCTGAGATGCT GCTGAGTTACTAGAAAGTCATTGAAGGTCTCAAC TATAGT

Table 5-S2 Calculated and observed masses for the ITOs synthesized in this study.

ITO	Exact mass (monoisotopic)	m/z (calculated) -4 Charged state	m/z (observed) -4 Charged state
[AOIM$^+$]-*KRAS*	6548.3200	1636.0800	1630.5602
[ABzIM$^+$]-*KRAS*	6526.2408	1636.2681	1630.9911

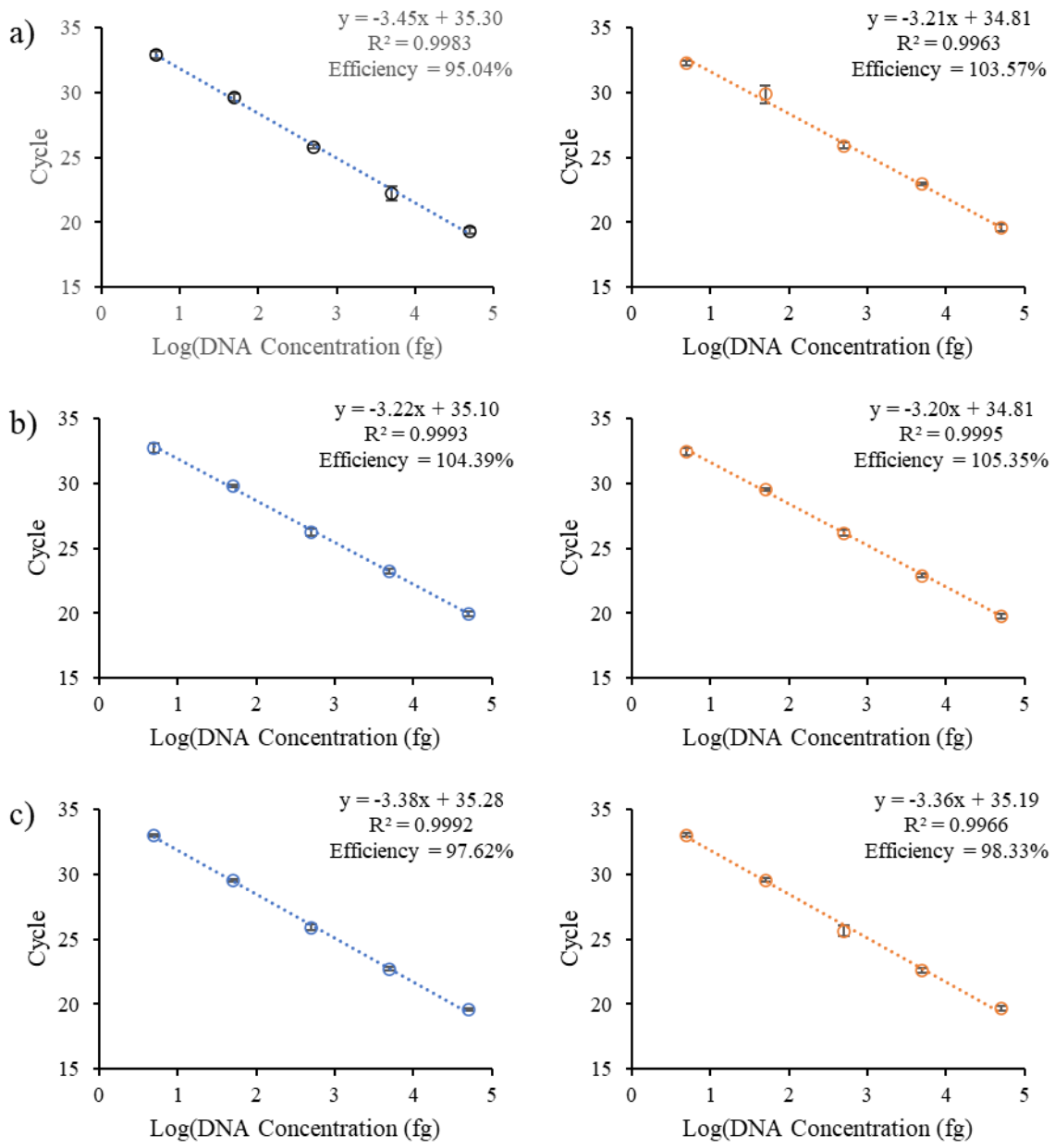

Figure 5-S1 Five-point standard curves generated for the (blue) V600E *BRAF* and (orange) WT *BRAF* associated with (a) standard reaction with out MIL, (b) reactions containing 0.3 µL of $[P_{6,6,6,14}^{+}][Ni(hfacac)_3^{-}]$, (c) and reactions containing the $[N_{8,8,8,Bz}^{+}][Ni(hfacac)_3^{-}]$ MIL.

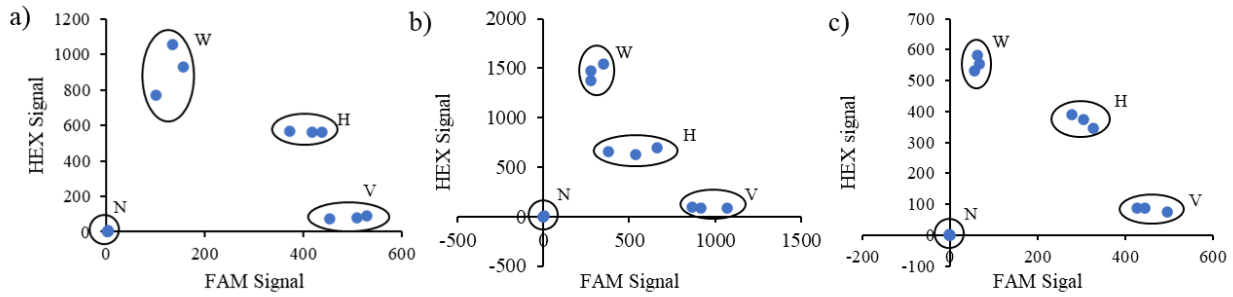

Figure 5-S2 Allelic discrimination plots for the (a) standard reaction, (b) reactions containing 0.3 µL of $[P_{6,6,6,14}^{+}][Mn(hfacac)_3^{-}]$ MIL, and (c) reactions containing 0.3 µL of $[N_{8,8,8,Bz}^{+}][Mn(hfacac)_3^{-}]$ MIL. N: NTC, W: 100% WT *BRAF*, V: 100% V600E *BRAF*; H: Heterozygous.

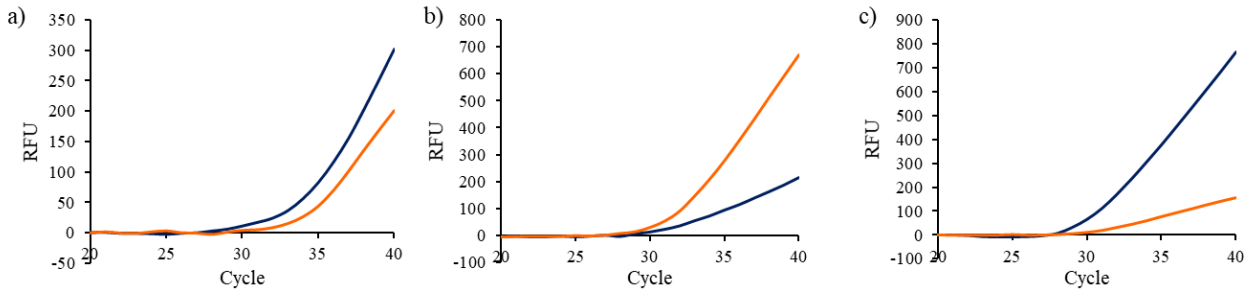

Figure 5-S3 Amplification curves associated with (green) WT *BRAF* and (blue) V600E *BRAF* associated with (a) the ITO extraction above the optimum annealing temperature (50°C), (b) the ITO-MIL extraction below the optimized annealing temperature (40°C), and (c) the ITO-MIL extraction at the optimum annealing temperature (45°C). Sample solution: 50 fg·µL^{-1} V600E *BRAF*, 50 fg·µL^{-1} WT *BRAF*, 178 pg·µL^{-1} ITO, 5% DMSO, 2 mM Tris; sample volume: 1 mL; extraction time: 2 min; volume of $[P_{6,6,6,14}^{+}][Mn(hfacac)_3^{-}]$: 6 µL.

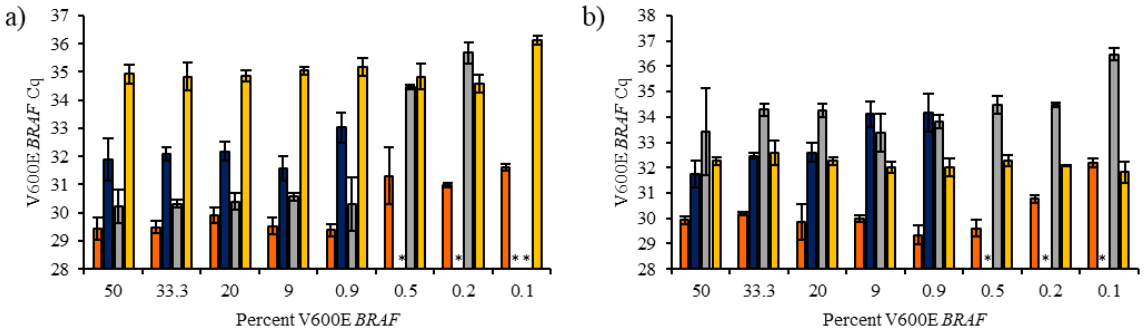

Figure 5-S4 Cq values associated with V600E *BRAF* extracted from (orange) 25 mM NaCl, (blue) 2-fold diluted plasma, (grey) artifical urine, (yellow) 4-fold diluted artificial sputum extracted with the (a) $[P_{6,6,6,14}^{+}][Mn(hfacac)_3^{-}]$ and (b) $[N_{8,8,8,Bz}^{+}][Mn(hfacac)_3^{-}]$ MIL. *Extraction was not performed.

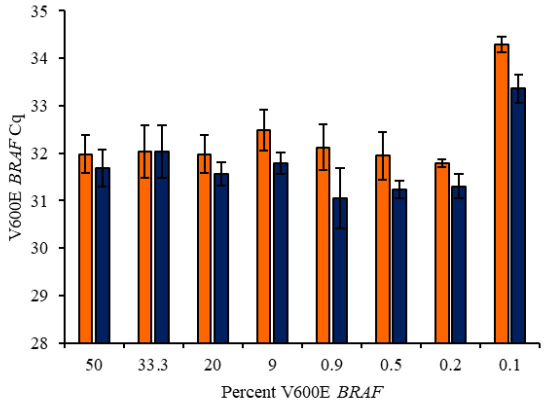

Figure 5-S5 Cq values associated with V600E *BRAF* extracted with 356 $pg \cdot \mu L^{-1}$ of ITO from 4-fold diluted plasma with (orange) $[P_{6,6,6,14}^{+}][Mn(hfacac)_3^{-}]$ and (blue) $[N_{8,8,8,Bz}^{+}][Mn(hfacac)_3^{-}]$ MIL.

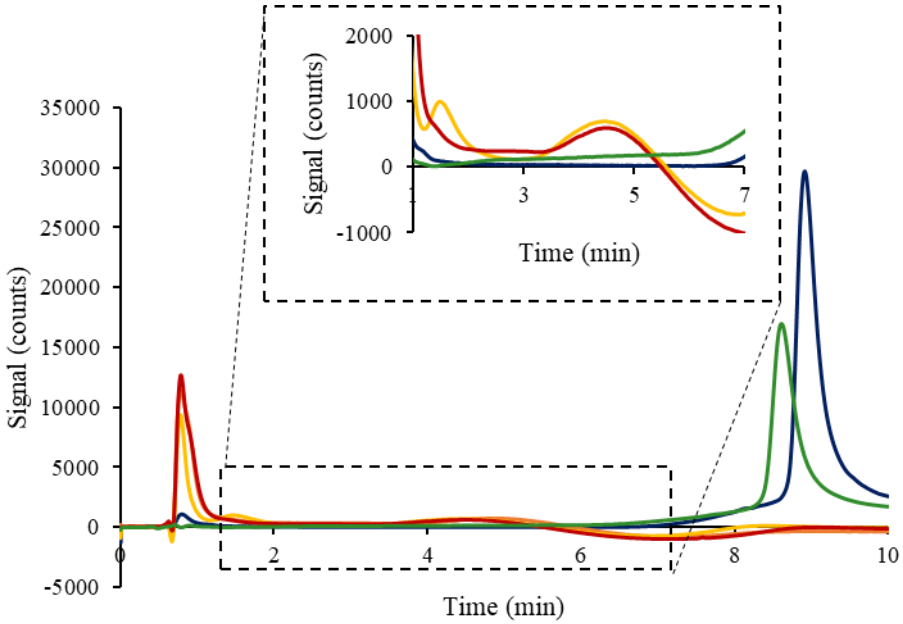

Figure 5-S6 Chromatogram displaying the separation of plasmids containing the (green) V600E *BRAF* and (blue) WT *BRAF* inserts and sheared plasmids containing the (red) V600E *BRAF* and (yellow) WT *BRAF* inserts.

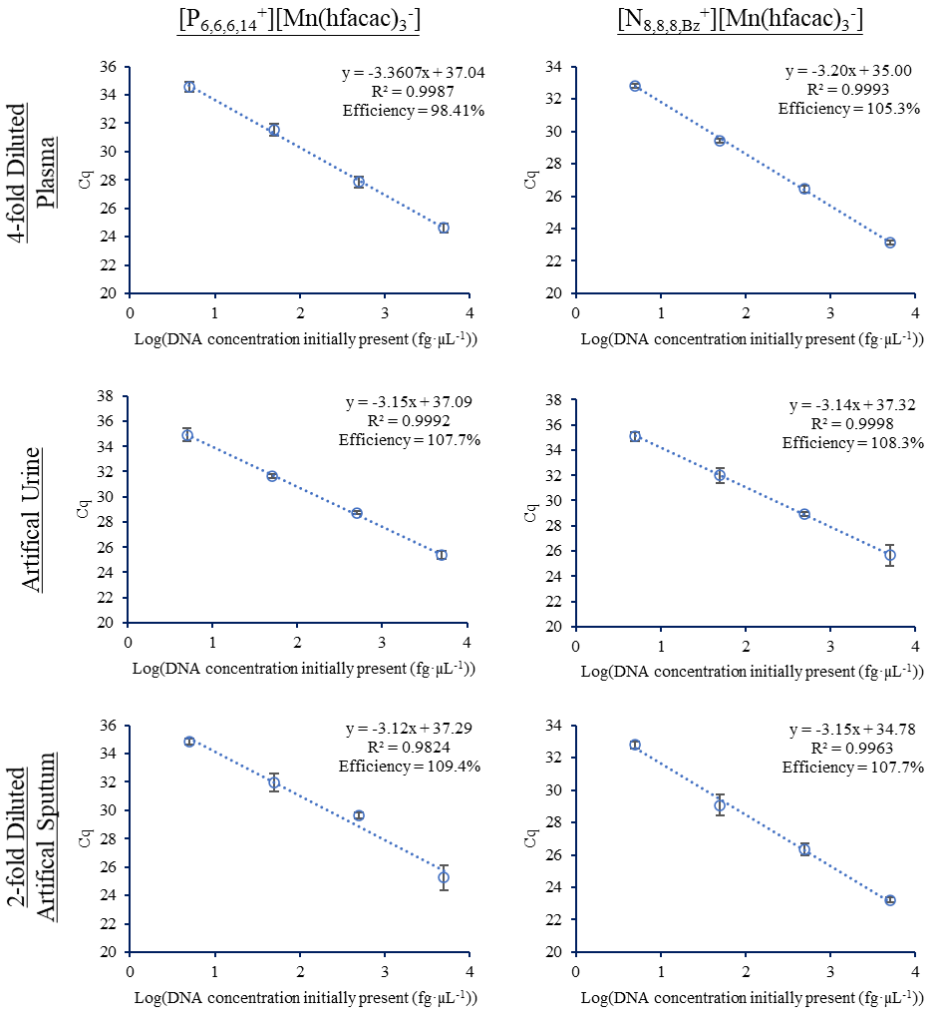

Figure 5-S7 Standard curves developed by extracting the V600E *BRAF* from 4-fold diluted human plasma, artificial urine, and 2-fold diluted artificial sputum using the ITO-MIL extraction method.

APPENDIX E

SUPPORTING INFORMATION ACCOMPANYING CHAPTER 6

Table 6-S1 Oligonucleotide sequences examined in this study.

Name	Sequence
Forward β-Actin Primer	5'-GGC GAC GAG GCC CAG A-3'
Reverse β-Actin Primer	5'-CGA TTT CCC GCT CGG C-3'
Forward Non-target Primer	5'-TTCATGAAGACCTCACAGTAAA-3'
Reverse Non-target Primer	5'-GGATCCAGACAACTGTTCAA-3'
98 bp Non-target Sequence	5'-TTCATGAAGACCTCACAGTAAAAATAGGTGAT TTTGGTCTAGCTACAGtGAAATCTCGATGGAGTGGG TCCCATCAGTTTGAACAGTTGTCTGGATCC-3'
210 bp Insert	5'-TATATTTCTTCATGAAGACCTCACAGTAAAAA TAGGTGATTTTGGTCTAGCTACAGTGAAATCT CGATGGAGTGGGTCCCATCAGTTTGAACAGT TGTCTGGATCCATTTTGTGGATGTAAGAATTG AGGCTATTTTTCCACTGATTAAATTTTTGGCCC TGAGATGCTGCTGAGTTACTAGAAAGTCATTG AAGGTCTCAACTATAGT-3'

Table 6-S2 Summary of the optimized concentrations of EDTA, $MgCl_2$, BSA, and additional SYBR Green 1 required for uninhibited amplification of human genomic DNA with 0.3 µL of MIL in the buffer.

MIL	EDTA Concentration (mM)	Additional $MgCl_2$ Concentration (mM)	BSA Concentration ($mg \cdot mL^{-1}$)	Additional SYBR Green I Concentration
$[P_{6,6,6,14}^+][Ni(hfacac)_3^-]$	0	0	0	1x
$[N_{8,8,8,Bz}^+][Ni(hfacac)_3^-]$	0	0	0	1x
$[OMIM^+][Ni(hfacac)_3^-]$	0	0	0	1x
$[C_{14}MIM^+][Ni(hfacac)_3^-]$	0	1.25	0	1x
$[P_{6,6,6,14}^+][Ni(Phfacac)_3^-]$	0	0	0	1x
$[P_{6,6,6,14}^+][Ni(tfacac)_3^-]$	0	0	0	0x
$[P_{6,6,6,14}^+][Co(hfacac)_3^-]$	0	0	0	2x
$[P_{6,6,6,14}^+][Dy(hfacac)_4^-]$	6	7.5	1.5	1x
$[P_{6,6,6,14}^+][Gd(hfacac)_4^-]$	6	6.5	1.5	1x

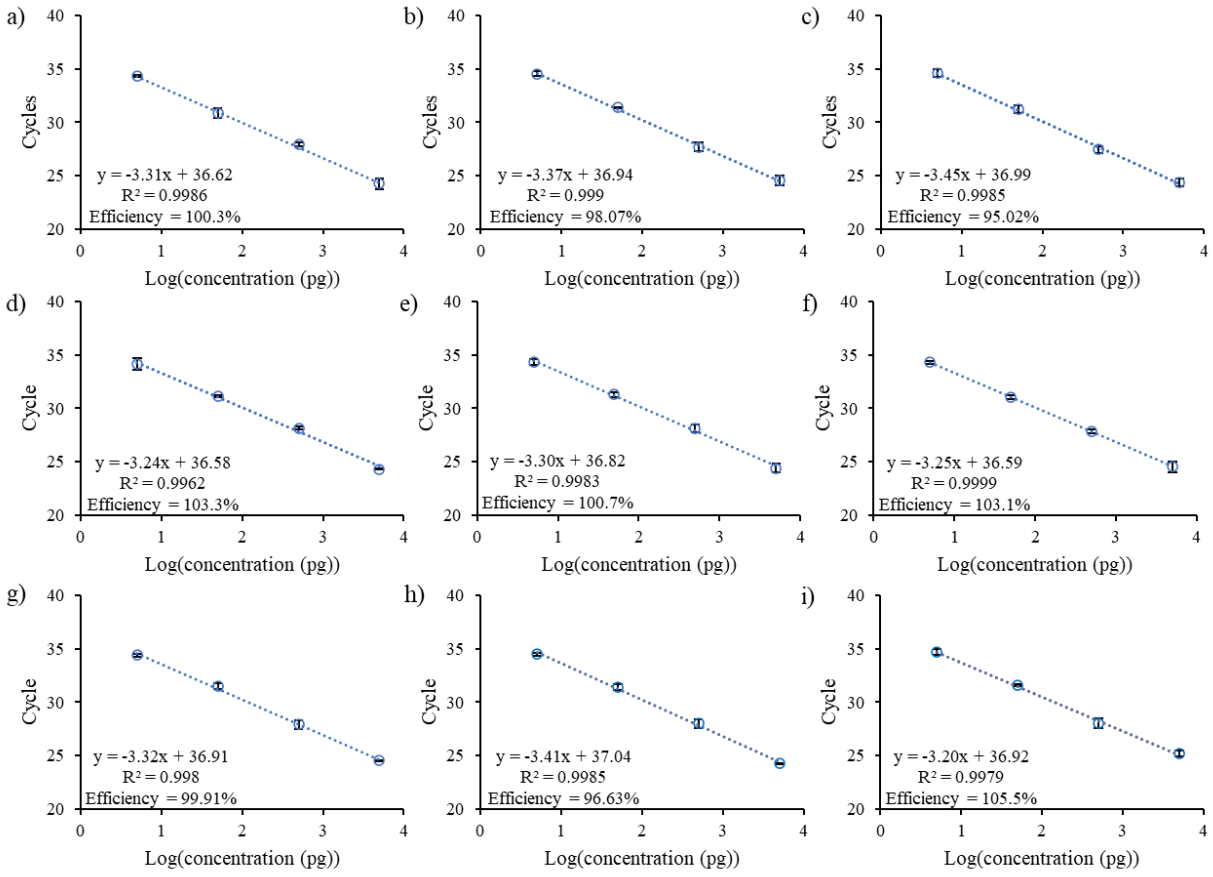

Figure 6-S1 Standard curves of human genomic DNA generated with 0.3 µL of the (a) $[P_{6,6,6,14}^+][Ni(hfacac)_3^-]$, (b) $[N_{8,8,8,Bz}^+][Ni(hfacac)_3^-]$, (c) $[OMIM^+][Ni(hfacac)_3^-]$, (d) $[C_{14}MIM^+][Ni(hfacac)_3^-]$, (e) $[P_{6,6,6,14}^+][Ni(Phtfacac)_3^-]$, (f) $[P_{6,6,6,14}^+][Ni(tfacac)_3^-]$, (g) $[P_{6,6,6,14}^+][Co(hfacac)_3^-]$, (h) $[P_{6,6,6,14}^+][Dy(hfacac)_4^-]$, and (i) $[P_{6,6,6,14}^+][Gd(hfacac)_4^-]$ MILs in the qPCR buffer.

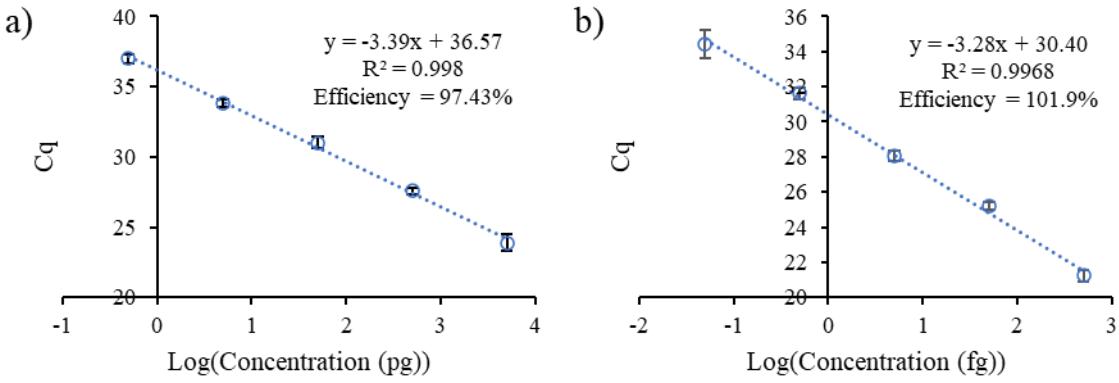

Figure 6-S2 Five-point standard curve for (a) human genomic DNA and (b) a 98 bp DNA fragment.

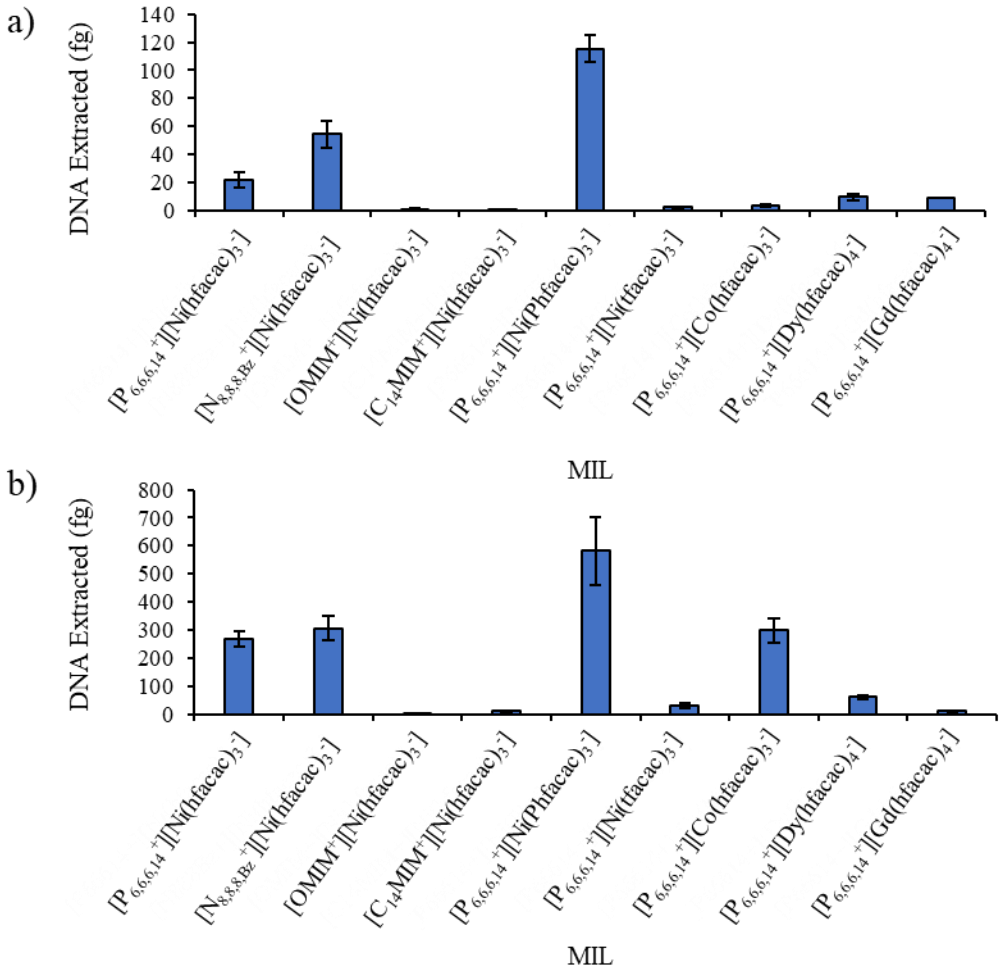

Figure 6-S3 Extraction of a non-targeted 98 bp DNA sequence from (a) whole blood and (b) 2 mM Tris buffer using MILs. Sample volume: 50 µL; DNA concentration: 50 fg·µL; MIL volume: 2 µL; extraction time: 1 min.

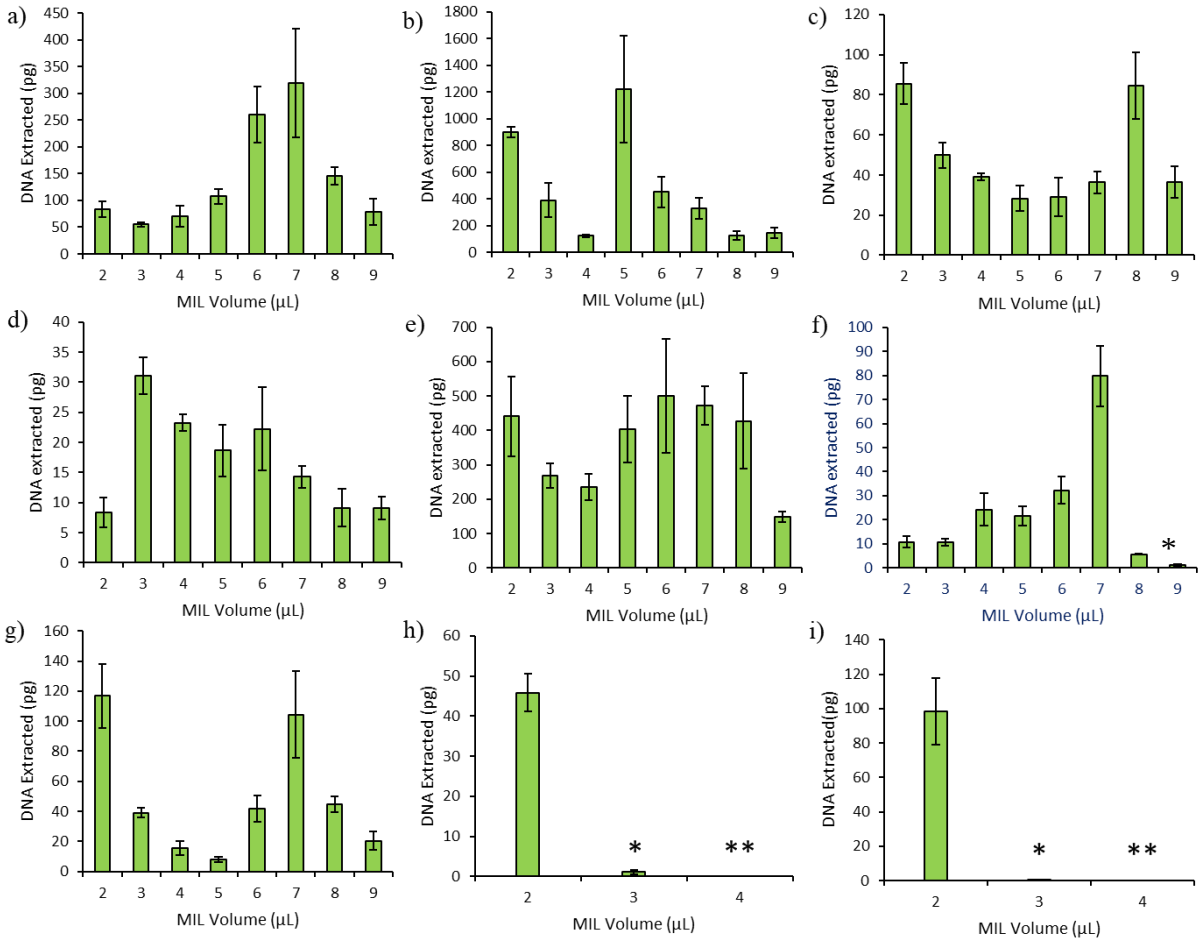

Figure 6-S4 Optimization of the volume of MIL dispersed in 2-fold diluted blood to lyse cells and extracted human genomic DNA for the (a) $[P_{6,6,6,14}^{+}][Ni(hfacac)_3^{-}]$, (b) $[N_{8,8,8,Bz}^{+}][Ni(hfacac)_3^{-}]$, (c) $[OMIM^{+}][Ni(hfacac)_3^{-}]$, (d) $[C_{14}MIM^{+}][Ni(hfacac)_3^{-}]$, (e) $[P_{6,6,6,14}^{+}][Ni(Phtfacac)_3^{-}]$, (f) $[P_{6,6,6,14}^{+}][Ni(tfacac)_3^{-}]$, (g) $[P_{6,6,6,14}^{+}][Co(hfacac)_3^{-}]$, (h) $[P_{6,6,6,14}^{+}][Dy(hfacac)_4^{-}]$, and (i) $[P_{6,6,6,14}^{+}][Gd(hfacac)_4^{-}]$ MILs. Sample volume: 50 µL; extraction time: 1 min. *Cq values fell outside the standard curve. **MIL could not be recovered.

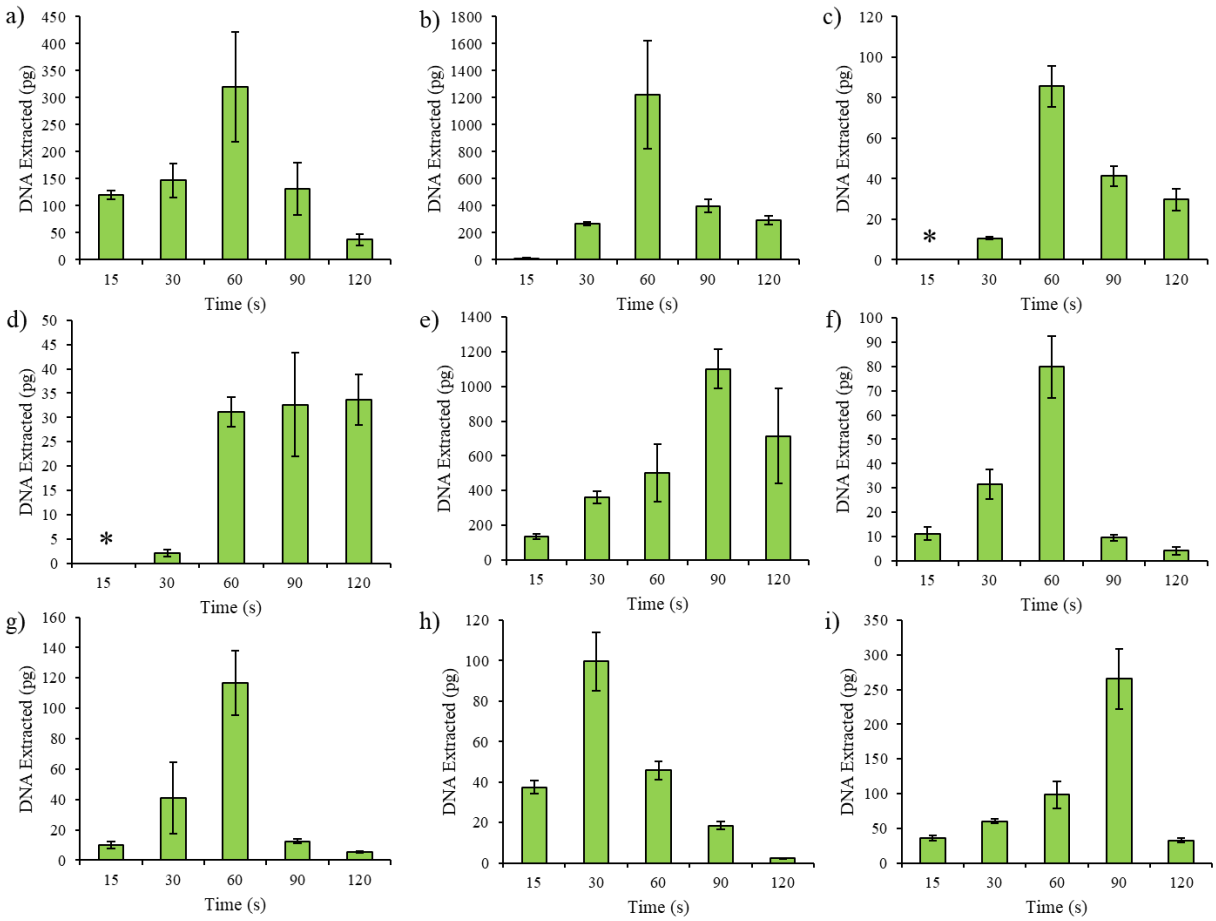

Figure 6-S5 Extraction time optimization for the (a) $[P_{6,6,6,14}^{+}][Ni(hfacac)_3^{-}]$, (b) $[N_{8,8,8,Bz}^{+}][Ni(hfacac)_3^{-}]$, (c) $[OMIM^{+}][Ni(hfacac)_3^{-}]$, (d) $[C_{14}MIM^{+}][Ni(hfacac)_3^{-}]$, (e) $[P_{6,6,6,14}^{+}][Ni(Phtfacac)_3^{-}]$, (f) $[P_{6,6,6,14}^{+}][Ni(tfacac)_3^{-}]$, (g) $[P_{6,6,6,14}^{+}][Co(hfacac)_3^{-}]$, (h) $[P_{6,6,6,14}^{+}][Dy(hfacac)_4^{-}]$, and (i) $[P_{6,6,6,14}^{+}][Gd(hfacac)_4^{-}]$ MILs. Sample volume: 50 µL; extraction time: 1 min. *Amplification did not occur.

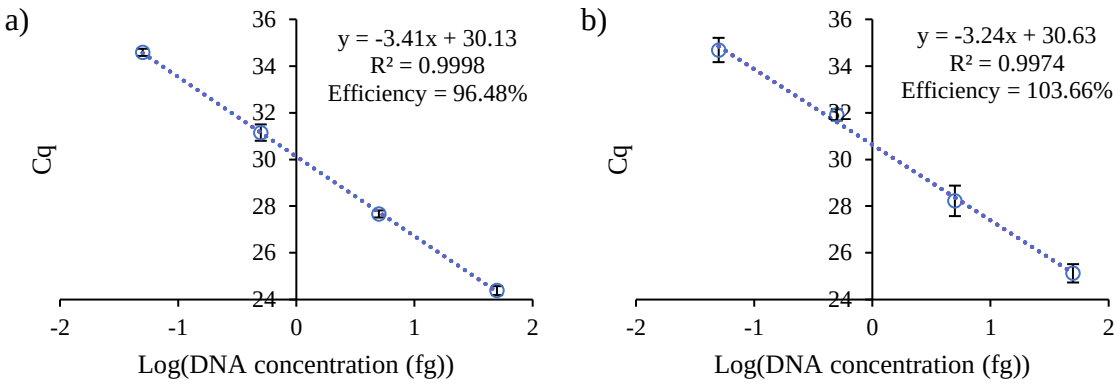

Figure 6-S6 Standard curves generated by spiking a 98 bp DNA sequence into the qPCR reaction after dispersing the (a) $[N_{8,8,8,Bz}^{+}][Ni(hfacac)_3^{-}]$ and (b) $[P_{6,6,6,14}^{+}][Ni(tfacac)_3^{-}]$ MILs in whole blood. Extraction time: 1 min; MIL volume: 2 µL.

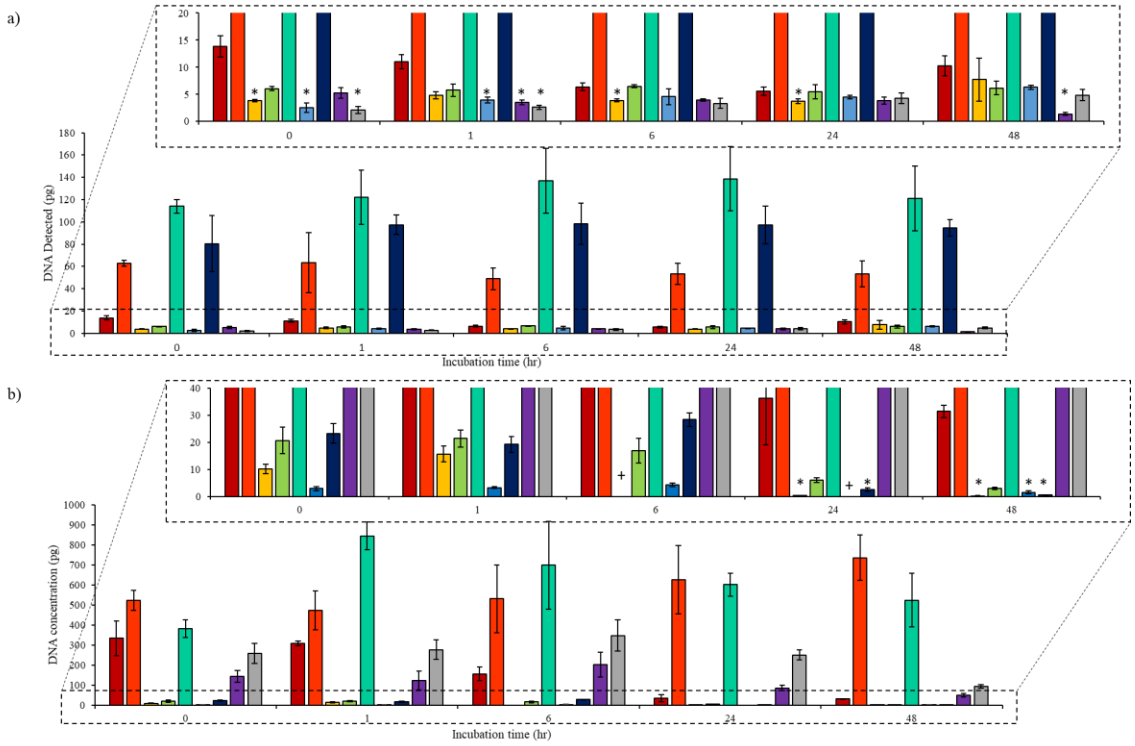

Figure 6-S7 DNA degradation in the MIL over time at 25 °C after dispersing the (red) $[P_{6,6,6,14}^{+}][Ni(hfacac)_3^{-}]$, (orange) $[N_{8,8,8,Bz}^{+}][Ni(hfacac)_3^{-}]$, (yellow) $[OMIM^{+}][Ni(hfacac)_3^{-}]$, (green) $[C_{14}MIM^{+}][Ni(hfacac)_3^{-}]$, (teal) $[P_{6,6,6,14}^{+}][Ni(Phtfacac)_3^{-}]$, (light blue) $[P_{6,6,6,14}^{+}][Ni(tfacac)_3^{-}]$, (navy blue) $[P_{6,6,6,14}^{+}][Co(hfacac)_3^{-}]$, (violet) $[P_{6,6,6,14}^{+}][Dy(hfacac)_4^{-}]$, and (grey) $[P_{6,6,6,14}^{+}][Gd(hfacac)_4^{-}]$ MILs in (a) a 50 pg·µL^{-1} human genomic DNA solution in 2 mM Tris buffer and (b) whole blood. *Cq values fell outside the standard curve. +Amplification did not occur.

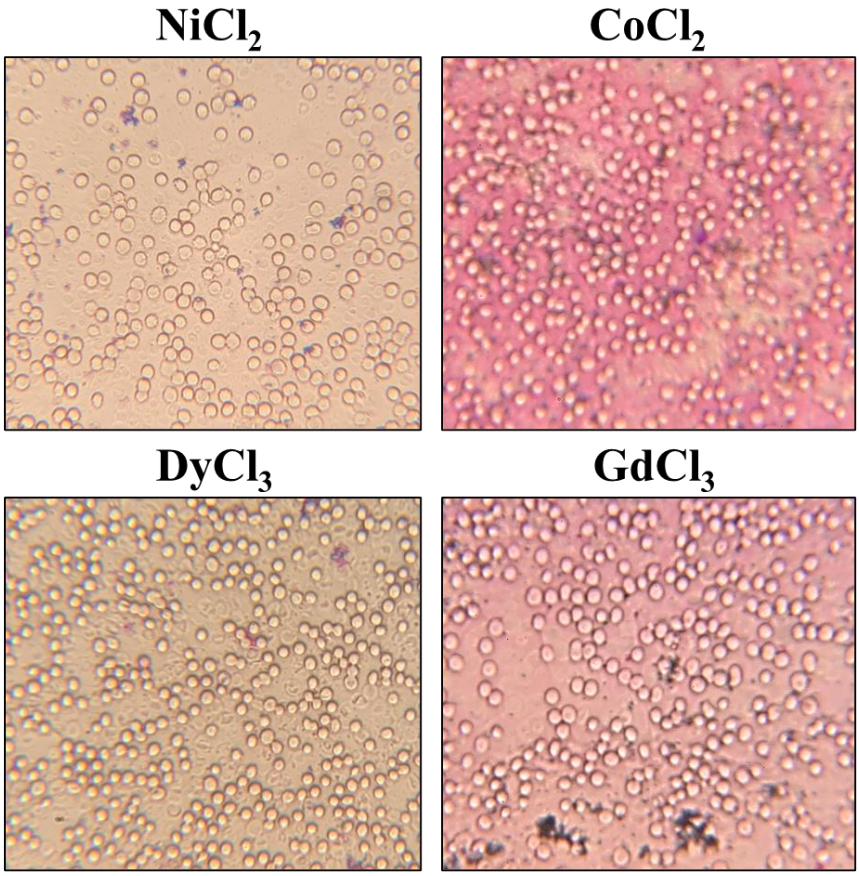

Figure 6-S8 Images showing the Wright stains of blood spiked with 2.2 µmol $NiCl_2$, 2.2 µmol $CoCl_2$, 1.8 µmol $DyCl_3$, and 1.8 µmol $GdCl_3$.

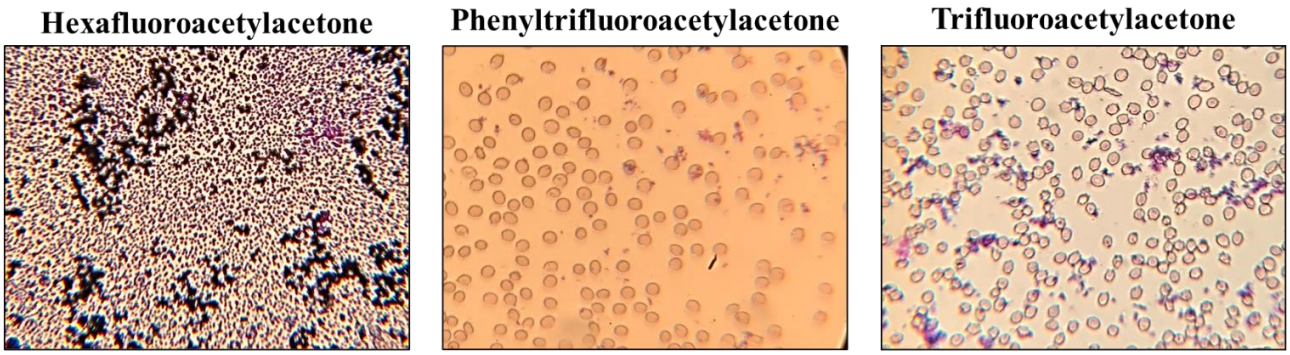

Figure 6-S9 Images of Wright stains of blood spiked with 6.7 µmol hexafluoroacetylacetone, 6.7 µmol phenyltrifluoroacetylacetone, and 6.7 µmol trifluoroacetylacetone.

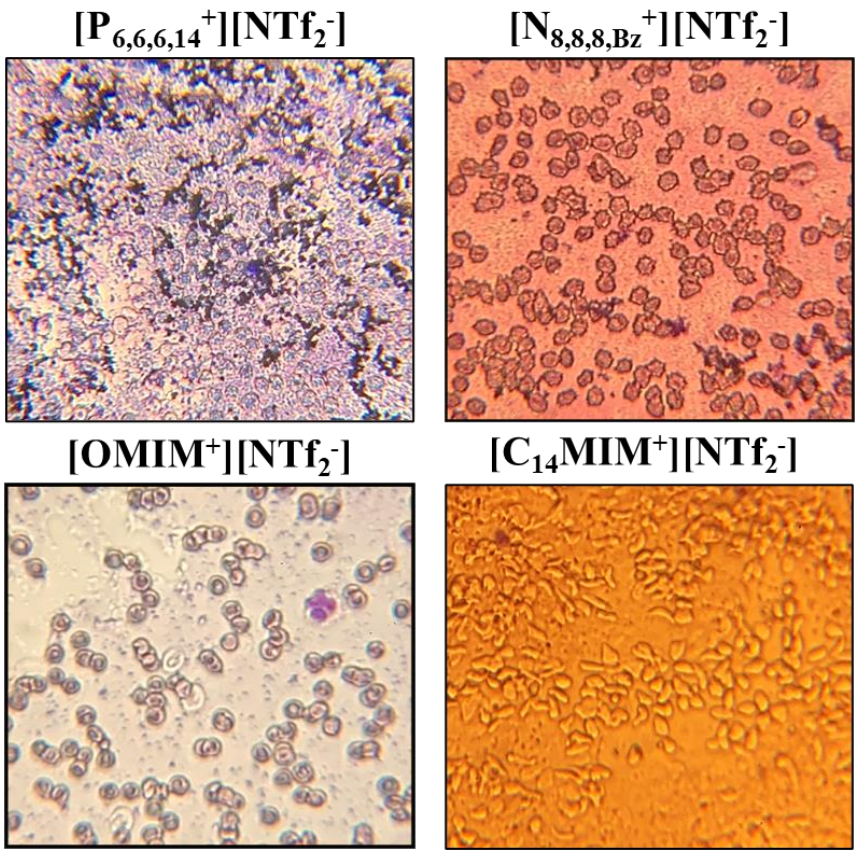

Figure 6-S10 Images revealing Wright stains of blood spiked with 1 µL [P6,6,6,14+][NTf2-], 1 µL [$N_{8,8,8,Bz}^{+}$][NTf_2^{-}], 1 µL [$OMIM^{+}$][NTf_2^{-}], and 1 µL [$C_{14}MIM^{+}$][NTf_2^{-}].